Reactive Halogen Compounds in the Marine Boundary Layer: Method Developments and Field Measurements

Dissertation zur Erlangung des Grades
„Doktor der Naturwissenschaften“

im Promotionsfach Chemie
am Fachbereich Chemie, Pharmazie und Geowissenschaften
der Johannes Gutenberg-Universität
in Mainz

vorgelegt von
M.Sc. Ru-Jin Huang
geb. in FuJian, China

Mainz, 2009

Declaration of Authorship

I, Ru-Jin Huang, declare that this thesis entitled "Reactive Halogen Compounds in the Marine Boundary Layer: Method Developments and Field Measurements" and the work presented in it are my own. I confirm that:

- This work was done wholly or mainly while in candidature for a research degree at this University;
- Where any part of this thesis has previously been submitted for a degree or any other qualification at this University or any other institution, this has been clearly stated;
- Where I have consulted the published work of others, this is always clearly attributed;
- Where I have quoted from the work of others, the source is always given. With the exception of such quotations, this thesis is entirely my own work;
- I have acknowledged all main sources of help;
- Where the thesis is based on work done by myself jointly with others, I have made clear exactly what was done by others and what I have contributed myself.

Declared by: Ru-Jin Huang

Signature:…………………………

Dated on…………………………Mainz

Summary

Reactive Halogen Species (RHSs, X, X_2, XY, XO, OXO, HOX, XNO_2, and $XONO_2$, where X, Y denotes different halogen atoms) are known to play an important role in a wide variety of atmospheric processes such as atmospheric oxidation capacity (e.g., catalytic destruction of ozone, altering the partitioning of NO_x and HO_x) and coastal new particle formation. Despite extensive efforts in the past 10 years a number of uncertainties about the sources, sinks, kinetic parameters as well as the recycling of RHSs remain, and the identification and quantification of certain key RHSs are still a challenging analytical problem. The aim of this work was, at first, to develop analytical approaches for measuring X_2, XY, and HOX and, secondly, to investigate the sources, atmospheric processes and impacts of RHSs in the marine boundary layer (MBL) by using the approaches developed here in conjunction with other related atmospheric measurements.

A readily accessible, straightforward impinger method based on in situ collection/derivatization followed by Gas Chromatography–Mass Spectrometry (GC–MS) determination was developed for measurement of gaseous iodine-containing halogen species. When an aqueous solution of 1,3,5-trimethoxybenzene (1,3,5-TMB) is used in the impinger, the total iodine of a mixture of ICl, IBr, and I_2 can be quantitatively determined with an error ranging between 2.6% and 11.2% as I. The differentiation between ICl, IBr, and I_2 prove to be possible by using different reaction mediums (i.e., CH_3OH, CCl_4, and H_2O), which provides an attractive protocol for iodine species analysis for laboratory-based atmospheric chemistry research. However, the impinger method is subjected to potential artifacts resulting from particulate halogens for field-based measurements. Therefore, diffusion denuder based approaches which can separate gases and particles present in the same air mass and quantitatively collect the gaseous targets were developed. Quantitative collection of I_2 with efficiency larger than 98% is realized when α-cyclodextrin (α-CD) spiked with a differentiable $^{129}I^-$ isotope (optimized molar ratio, ≥ 1:3 of I^-/I_2 and ≥ 950:1 of α-CD/I_2, respectively) is used as denuder coating materials. The entrapped $^{127}I_2$ together with the $^{129}I^-$ spike is subjected to postderivatization to convert inorganic $^{127}I_2$ and $^{129}I^-$ to

4-iodo-*N,N*-dimethylaniline for GC–MS analysis. A 1,3,5-TMB-coated denuder is demonstrated to be capable of quantitatively collecting gaseous Activated Halogen Compounds (AHCs, i.e., Activated Chlorine Compounds (AClCs, HOCl and Cl_2), Activated Bromine Compounds (ABrCs, HOBr, Br_2, BrCl, and IBr), and Activated Iodine Compounds (AICs, ICl and HOI)) based on in-situ selective derivatization. The respective derivatives of AClCs, ABrCs, and AICs are separated by GC and determined by MS. The 1,3,5-TMB-coated denuder is a very poor sink for gaseous I_2 collection with an efficiency being less than 1%. Consequently, the separation and quantitative collection of gaseous AHCs and I_2 can be achieved by coupling the 1,3,5-TMB-coated cylindrical tube upstream of an α-CD/$^{129}I^-$-coated tube. The limits of detection (LODs) of these halogen species are achieved at the sub-part-per-trillion (sub-ppt) level. Also the coupled denuder system is demonstrated to be applicable for field measurements.

The developed denuder methods have been used in three field campaigns, i.e., two carried out in the coastal MBL on the West Coast of Ireland (Mace Head and Mweenish Bay) in 2007 and 2009 and one in Antarctica in 2009. Extraordinarily high concentrations (of the order of 10^2 ppt) of AHCs and I_2 are observed for the first time in the coastal MBL in Ireland, which explains the ozone destruction observed at that site during day and night-time. Concurrent measurements show that the mixing ratios of I_2 are about 10^2–10^4 higher than the mixing ratios of the iodocarbons. The emission levels of I_2 are found to correlate inversely with tidal height and correlate positively with the concentration levels of O_3 in the surrounding air. In addition the release is found to be dominated by algal species compositions and biomass density, which proves the “hot-spot” hypothesis of atmospheric iodine chemistry. The observations of elevated concentration levels of I_2 substantially support the existence of higher concentrations of littoral iodine oxides and thus the connection to the strong ultra-fine particle formation events in the coastal MBL. Furthermore, the enhanced ozone destruction at night and the involvement of NO_3 radicals may stimulate future interest in night-time atmospheric halogen chemistry.

In conclusion, while considerable advances have been made in the past years in terms of a better understanding of the atmospheric processes of RHSs, considerably more work needs to be conducted to advance our knowledge of the impact of RHSs, in particular AHCs, on the marine atmosphere. With the increased scientific focus on this field it can be expected that the questions arising in this thesis can be answered in the near future.

Table of Contents

Chapter 1: Introduction

Chapter 1
Introduction

1.1 Current State of Knowledge

1.1.1 Halogen Chemistry in the Troposphere

Halogens are very reactive chemical compounds that are known to play an important role in a wide variety of atmospheric processes such as the well-known stratospheric ozone depletion [Molina and Rowland, 1974; Wofsy et al., 1975]. They are of special interest because they are also involved in many reaction cycles in tropospheric chemistry that can influence the atmospheric oxidation budget indirectly by effecting the concentration levels of O_3, HO_x (OH and HO_2), and NO_x (NO and NO_2) and directly by reactions of the halogen radicals with organic molecules. Halogens can also regulate the formation of cloud condensation nuclei (CCN) and thus influence the global radiation budget and climate.

Interest in halogen atmospheric chemistry was greatly stimulated after it was postulated that the release of industrially produced halocarbons, in particular the chlorofluorocarbons (CFCs), could lead to severe depletion of stratospheric ozone by reactions involving the CFC photolytic product radicals as catalysts [Molina and Rowland, 1974]. The involvement of halogens in tropospheric chemistry was first observed in the Arctic, where strong ozone depletion events (ODEs) were found to coincide with high concentration levels of bromine [Barrie et al., 1988]. Since then, the impact of halogens on tropospheric chemistry received increasing attention and became a growing active research field. Numerous tropospheric field measurements and modeling studies were realized within the past two decades. These studies mainly concentrated on chlorine (Cl), bromine (Br), and iodine (I) since these halogens proved to be of special importance.

In the following sub-sections, sources of halogens (i.e., Cl, Br, and I) in the troposphere and the impacts of halogens on tropospheric chemistry are described.

1.1.1.1 Sources of Halogens in the Troposphere

There are two predominant sources of halogens in the troposphere. First, emissions of halogenated organic compounds (halocarbons) from a variety of terrestrial and marine sources, and second, emissions/release of inorganic halogens from marine sources, volcanoes, and salt lakes. Once halogens are released into the atmosphere they undergo a series of reaction chains in the gas-phase, the particle-phase and at the interface (see Figure 1.1) [von Glasow and Crutzen, 2007], which results in the recycle of some halogen species and the formation of new halogen species.

1.1.1.1.1 Emissions of Halocarbons

Halocarbons are emitted from a range of natural sources, as well as from anthropogenic sources such as fossil fuel burning, biomass burning, and industrial emissions. The natural sources are mainly of marine origin (e.g., seawater, macroalgae, and phytoplankton). Over the past two decades a wide variety of halocarbons, such as CH_3Cl, $CHCl_3$, CH_3Br, $CHBr_3$, CH_2Br_2, CH_2BrCl, $CHBr_2Cl$, $CHBrCl_2$, CH_3I, CH_2I_2, C_2H_5I, C_3H_7I, CH_2ClI, and CH_2BrI, has been observed at a number of oceanic locations [Lovelock et al., 1973; Penkett et al., 1985; Khalil and Rasmussen, 1999a; Li et al., 1999; Carpenter, 2003; Carpenter et al., 2009]. Table 1.1 shows the typical atmospheric mixing ratios, estimated global annual emission rates, and atmospheric lifetimes of some important halocarbons. Some of the organic halogen compounds get photolyzed or react with OH radicals in the troposphere leading to the release of halogen atoms whose main fate is to react with ozone, forming the halogen oxide radicals (XO). The alkyl chlorides and bromides have longer atmospheric lifetimes, which leads to the transport of fractions of these compounds into the stratosphere and the destruction of stratospheric ozone. Since the absorption spectra of iodocarbons tend to be shifted to longer wavelengths than their chlorine- and bromine-containing counterparts, the photolysis of iodocarbons is much faster (see Table 1.1), which results in the occurrence of ozone depletion and new particle formation in the marine boundary layer (MBL) [O'Dowd et al., 2002; O'Dowd and Hoffmann, 2005; Read et al., 2008].

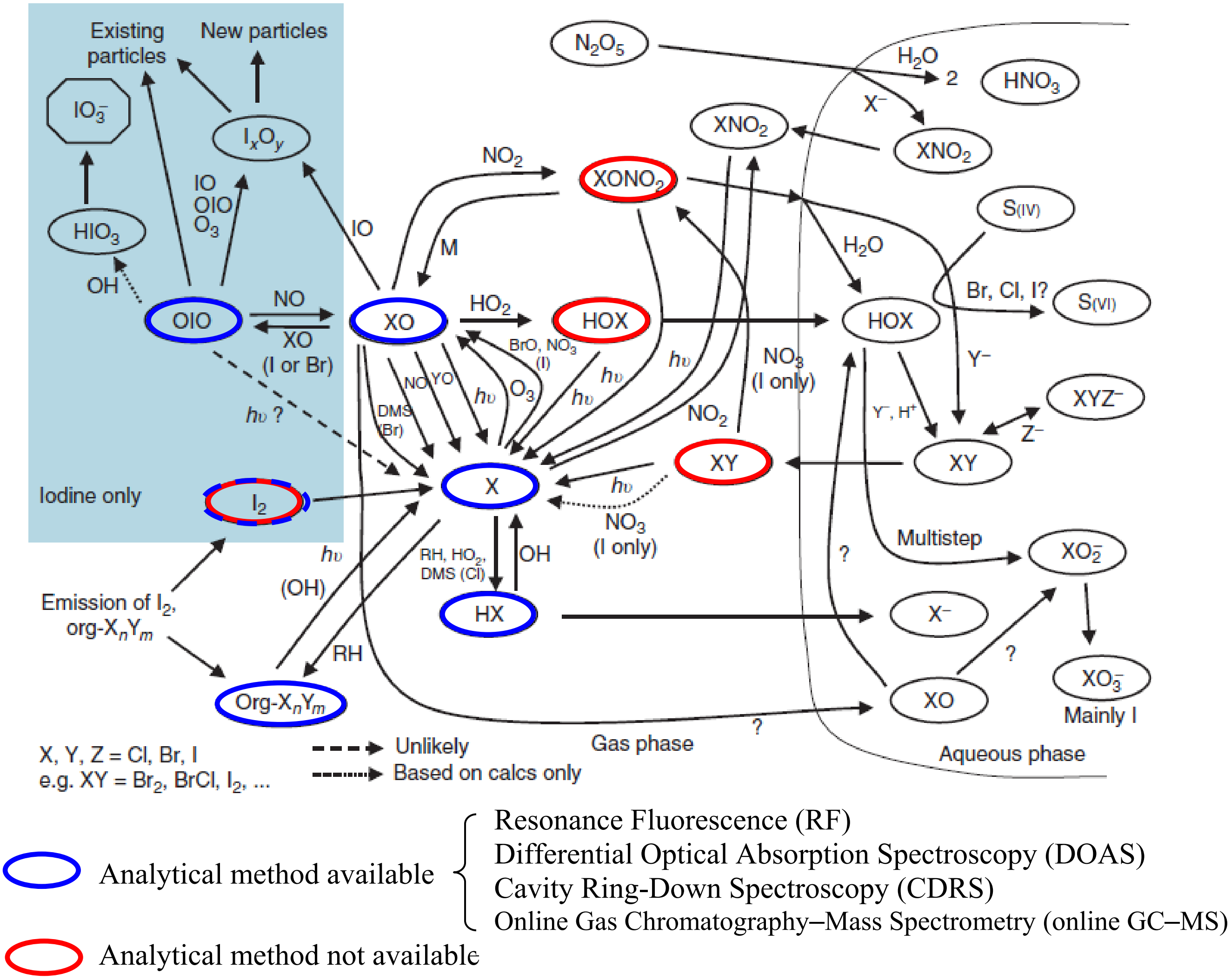

Figure 1.1 Schematic diagram of the major halogen-related reactions within the gas- and particle-phase and at the interface (modified from von Glasow and Crutzen, 2007).

1.1.1.1.2 *Emissions/Release of Inorganic Halogens*

Biogenic emission of inorganic halogens by seaweed has been recognized to be of importance for halogen chemistry on regional and global scales. About two decades ago, Wever [1988] and Wever et al. [1991] reported direct emission of HOBr and Br_2 from macroalgae. Recent field measurements and laboratory-based studies [Saiz-Lopez and Plane, 2004; McFiggans et al., 2004; Huang et al., 2009a; Palmer et al., 2005; Küpper et al., 2008; Dixneuf et al., 2009] also indicate that biogenic emission of I_2 by seaweed is one of the most important processes responsible for the observed tropospheric iodine levels in coastal locations. A possible mechanism for the release of I_2 from marine *Laminaria* macroalgal species was suggested as follows [Küpper et al., 2008]: Iodine is accumulated in kelp in form of iodide (I^-) that provides kelp with an antioxidant and can readily scavenge reactive oxygen species like O_3 on the thallus surface and in the apoplast of the kelp, leading to the release of I_2 when the plant is exposed to the atmosphere at low tide. However, whether seaweeds also release other inorganic halogen species is unclear.

Table 1.1 Typical mixing ratios, estimated global annual emission rates, and atmospheric lifetimes of some important halocarbons in the troposphere

Species	Mixing ratio (ppt)	Emission rate (10^9 kg yr^{-1})	Atmospheric lifetime
CH_3Cl	570–620[a]	3.7[a]	1.1–1.5 yr[b]
CH_3Br	10–20[c,d]	0.12[e]	~0.7 yr[f]
CH_3I	0.2–5.0[g]	2.1[h]	4 day[b]
$CHCl_3$	10–45[i]	0.4–0.6[i]	6 month[i]
$CHBr_3$	0.5–1.0[j]	0.25–1.86[j]	20 day[k]
CH_2Cl_2	20–40[l]	6.0[e]	5–6 month[b]
CH_2Br_2	0.5–4[m]	0.012–0.02[m]	0.2–0.5 yr[m]
CH_2I_2	<2[g]	1–2[n]	~5 min[g]
CH_2ICl	<1[g]	4.8[h]	100 min[b]
C_3H_7I	0.2–2[o]	0.003[g]	40 h[o]

[a]Khalil and Rasmussen, 1999a; [b]Keene et al., 1999; [c]Li et al., 1999; [d]Lobert et al., 1995; [e]Kurylo et al., 1999; [f]Yvon et al., 1996; [g]Carpenter, 2003, and references therein; [h]Baker et al., 2001, and references therein; [i]Khalil and Rasmussen, 1999b; [j]Quack and Wallace, 2003; [k]Bilde et al., 1998; [l]Khalil et al., 1999; [m]Carpenter and Liss, 2000; [n]Klick and Abrahamsson, 1992; [o]von Glasow and Crutzen, 2007.

Besides biogenic emissions, there are other possibilities for the release of iodine from the sea surface. One might be the direct photochemical oxidation of iodide at the sea-air interface suggested by Miyake and Tsunogai [1963]

$$4I^- + O_2 + 2H_2O + h\nu \rightarrow 2I_2\uparrow + 4OH^- \qquad (R1.1)$$

However, the relevance and chemical mechanism of such photochemically induced I_2 release from sea surface under real ambient conditions is still unclear. Another possible release mechanism of I_2 is the oxidation of iodide at the sea surface by atmospheric ozone followed by the release of I_2 into the atmosphere [Garland and Curtis, 1981]

$$2I^- + O_3 + 2H^+ \rightarrow I_2\uparrow + O_2 + H_2O \qquad (R1.2)$$

From this iodine release mechanism, it is obvious that the I_2 release is directly connected to the dry deposition of ozone to the sea surface. These abiotic release processes of I_2 might occur not only at the open sea/atmosphere interface but also at the surface of sea-salt particles [Mochida et al., 2000]. Actually, the release mechanisms of inorganic halogens from sea-salt aerosols have been the subject of a number of modeling and field investigations. The most important reservoirs for inorganic halogen species are supposed to be HX, HOX and $XONO_2$ [Platt and Hönninger, 2003]. The release occurs through heterogeneous reactions involving hypohalous acids HOX (X= Cl, Br, or I), strong acids, and nitrogen oxides.

Halogen release via reactions with HOX

Gaseous HOX can be produced via the reactions of XO with HO_2 or organic peroxy radicals (RO_2) such as CH_3O_2 [Aranda et al., 1997]

$$XO + HO_2 \rightarrow HOX + O_2 \qquad \text{(R1.3)}$$

$$XO + CH_3O_2 \rightarrow HOX + CH_2O \qquad \text{(R1.4)}$$

HOX could also be a direct emission from seaweeds [Wever, 1998]. The reactive uptake of gaseous HOX onto the surfaces of acidic salt aerosols can lead to the release of the corresponding dihalogen XY (e.g., Br_2, IBr, ICl, I_2, and BrCl) [Fan and Jacob, 1992; Tang and McConnell, 1996; Vogt et al., 1996; Vogt et al., 1999; McFiggans et al., 2002; Braban et al., 2007]

$$HOX + Y^- + H^+ \rightarrow XY + H_2O \qquad \text{(R1.5)}$$

This process has been proposed to initiate both chlorine and bromine activation in aerosols and is of particular importance in remote marine locations. In the case of uptake of HOBr onto sea-salt aerosols, it is found that the ratio of $[Cl^-]/[Br^-]$ in sea-salt influences the halogen species produced. In seawater the $[Cl^-]/[Br^-]$ ratio is about 650, but in experiments the $[Cl^-]/[Br^-]$ ratios are varied to elucidate the release mechanism of halogen species. When the concentration of Br is decreased below the sea-salt ratio, an increasing fraction of BrCl is produced; however at high relative Br/Cl ratios, the predominant product released into the gas phase is Br_2 rather than BrCl [Adams et al., 2002] because a substantial fraction of the resulting BrCl reacts further with Br^- leading to autocatalytic Br activation [Vogt et al., 1996]. This mechanism has been supported by field observation that both BrCl and Br_2 are produced from snow pack [Foster et al., 2001]. The $[Cl^-]/[Br^-]$ ratio in snow is found to be very variable, possibly because Br^- is removed from snow by Br_2 release and uptake of gas-phase HBr can add Br^- back to the snow [Simpson et al., 2005]. When all Br^- is used up, BrCl can escape from the surface. Also, the uptake of HOBr and HOI onto frozen and dry NaCl/NaBr surfaces has been investigated in the laboratory [Holmes et al., 2001; Adams et al., 2002]. The relative percentage of the dihalogens released to the gas phase is found to be strongly dependent on the ratio of Cl^- to Br^-, with Br_2 and IBr being the predominant products for HOBr and HOI uptake, respectively. Further studies in terms of the reactive uptake of HOI on sea-salt and sea-salt proxies show that the release of IBr may dominate ICl production since the resulting ICl reacts further with Br^- [Braban et al., 2007].

The H^+ required in reaction R1.5 (the reaction appears to occur at appreciable rates only at $pH < 6.5$ [Fickert et al., 1999]) could be supplied by strong acids such as H_2SO_4 and HNO_3 originating from anthropogenic or natural sources (see below). The bromide-containing aerosol could be sufficiently acidified by HBr. In the case of X=Y, the reaction (R1.5) sequence followed by photolysis of X_2, oxidation of X by O_3 and the conversion of XO to HOX by HO_2 or CH_3O_2 (R1.3 and R1.4), leads the reaction cycle to the net result

$$XO + X^- + H^+ + HO_2 + 2O_3 \rightarrow 2XO + H_2O + 3O_2 \qquad \text{(R1.6)}$$

In the case of X=Br the BrO radical acts like a catalyst promoting the oxidation of Br^- by O_3. As a consequence, one BrO radical is converted into two by oxidizing bromide at the surface of brine or dry sea salt on sea ice or aerosol. This process leads to an exponential growth of the BrO concentration in the atmosphere, which results in the “Bromine Explosion” [Platt and Janssen, 1995; Wennberg, 1999]. The current knowledge shows that bromine is released by the autocatalytic process while chlorine is a byproduct [Fickert et al., 1999]. Indeed, severe depletions of Br^- in sea-salt aerosol are observed in oceanic locations such as Southern Ocean. Br^- deficits are typically greater than 40% (occasionally over 90%) compared with only about 5% for Cl^-.

Halogen release via reaction with strong acids

The action of strong acids on sea-salt aerosols can lead not only to the acidification of the aerosol particles but also to the release of hydrogen halides (HX)

$$H_2SO_4 + 2(NaX)_{aerosol} \rightarrow 2HX + (Na_2SO_4)_{aerosol} \qquad \text{(R1.7)}$$

$$HNO_3 + (NaX)_{aerosol} \rightarrow HX + (NaNO_3)_{aerosol} \qquad \text{(R1.8)}$$

Since HX is highly water soluble it is likely to be irreversibly removed from the atmosphere by wet or dry deposition. Also the recycling of gaseous HX via heterogeneous reactions is possible and is supposed to be of significant importance in the polar region and in the remote marine boundary layer [McFiggans et al., 2000; Sander et al., 1999; Vogt et al., 1999]. On the surface of sea-salt aerosols the reaction of HOX with HX leads to the release of X_2 to the gas phase, as suggested by Fan and Jacob [1992].

Halogen release via reaction with NO_x

The uptake of NO_x like NO_2 and N_2O_5 on sea-salt aerosols has been found to lead to the release of halogens. Under the conditions of high NO_x (e.g., at polluted or semi-polluted environments) halogen release can occur via the reactions [Finlayson-Pitts et al., 1989; Schweitzer et al., 1999; McFiggans et al., 2002]

$$N_2O_5 + (NaX)_{aerosol} \rightarrow (NaNO_3)_{aerosol} + XNO_2 \qquad (R1.9)$$

$$2NO_2 + (NaX)_{aerosol} \rightarrow (NaNO_3)_{aerosol} + XNO \qquad (R1.10)$$

The XNO_2 formed in the above reaction may photolyze to release a halogen atom or possibly further react with sea-salt [Schweitzer et al., 1999]

$$XNO_2 + (NaX)_{aerosol} \rightarrow (NaNO_2)_{aerosol} + X_2 \qquad (R1.11)$$

The formation of XNO_2 and X_2 can occur without light, leading to an accumulation of these photolabile species before sunrise. Another possible night-time source of halogenated nitrogen oxides is the uptake of NO_3 [Gershenzon et al., 1999]

$$NO_3 + (NaX)_{aerosol} \rightarrow (NaNO_3)_{aerosol} + X \qquad (R1.12)$$

The halogen release can also occur by uptake of $XONO_2$ that is formed by the reaction of XO with NO_2 in the gas phase. On the aqueous surface of aerosol particles $XONO_2$ can be converted to HOX by hydrolysis [Sander et al., 1999; Holmes et al., 2001]

$$XONO_2 + H_2O \rightarrow HNO_3 + HOX \qquad (R1.13)$$

or to (inter)halogen molecules by heterogeneous reaction with HY

$$XONO_2 + HY \rightarrow HNO_3 + XY \qquad (R1.14)$$

For the clean marine boundary layer (MBL), the above reactions involving N_2O_5, $XONO_2$, and XNO_2 are expected to play a minor role because of the low NO_x concentrations. In coastal regions or over salt lakes with elevated NO_x, these reactions are more likely to be of importance [von Glasow and Crutzen, 2007].

Halogen release via other potential processes

Under freezing conditions frost flowers may directly release gaseous halogens to the atmosphere or they may produce aerosol particles that carry halide ions into the atmosphere, where they then undergo halogen activation. Brine derived aerosol particles or brine wicking may contaminate snow with halide ions that are then activated and emitted to the atmosphere [Simpson et al., 2007]. Halogens may also be released into the atmosphere when ice freezes, since the freeze-concentrated solutions have different reactivity compared with the unfrozen solution [O'Driscoll et al., 2006]. The release of halogens under freezing conditions is of critical importance, especially in Antarctica. More details about these processes are discussed by Simpson et al. [2007].

1.1.1.2 Impacts of Halogen Species on Tropospheric Chemistry

1.1.1.2.1 Ozone Depletion

Halogen radicals are formed in the troposphere by the photolysis of dihalogens (X_2 or XY), other inorganic compounds like HOX, $XONO_2$, and XNO_2, or organic halogen precursors. The resulting halogen atoms react with ozone thereby producing halogen oxides (XO) within a second. If the XO species photolyze, both ozone and the halogen radical are reformed and no net reaction occurs. This photolysis process is of importance for X=I, Br and to a minor extent Cl.

$$O_3 + X \rightarrow XO + O_2 \qquad \text{(R1.15)}$$

$$XO + O_2 (+M) + h\nu \rightarrow X + O_3 \qquad \text{(R1.16)}$$

For bromine in the polar region, during the day and at a high ozone level BrO is the prevalent species, however, at low ozone levels (<1 ppb) calculations suggest that Br can become more abundant than BrO. Therfore, the partitioning of X/XO is controlled by the balance of reactions R1.15 and R1.16. For the catalytic destruction of ozone to occur, the XO must recycle to X atoms without production of ozone. This can be realized by self-reaction (XO +

XO), cross-reaction (XO + YO), XO + HO_2, and XO + NO_2. The self-reaction of halogen oxides reforms halogen atoms or dihalogens, which rapidly photolyze leading again to two X atoms

$$\begin{aligned} XO + XO &\rightarrow 2X + O_2 \\ &\rightarrow X_2 + O_2 \qquad \text{(R1.17)} \end{aligned}$$

In the case of X=Br, the reaction sequence that combines R1.15 and R1.17 represents a strong catalytic ozone destruction cycle

$$2(BrO + O_3 \rightarrow BrO + O_2) \qquad \text{(R1.18)}$$
$$BrO + BrO \rightarrow 2Br + O_2 \qquad \text{(R1.19)}$$
$$\rightarrow Br_2 + O_2 \xrightarrow{hv} 2Br + O_2 \qquad \text{(R1.20)}$$

net: $2O_3 \rightarrow 3O_2$

This reaction cycle was proposed by Barrie et al. [1988] to explain Arctic ozone depletion episodes.

XO may also react with a different halogen oxide YO

$$X + O_3 \rightarrow XO + O_2$$
$$Y + O_3 \rightarrow YO + O_2 \qquad \text{(R1.15)}$$
$$XO + YO \rightarrow X + Y + O_2 \qquad \text{(R1.21)}$$
$$\rightarrow XY + O_2 \xrightarrow{hv} X + Y + O_2 \qquad \text{(R1.22)}$$

net: $2O_3 \rightarrow 3O_2$

Cross-reactions, e.g., ClO + BrO and IO + BrO, are about one order of magnitude faster than the self-reaction of BrO + BrO [LeBras and Platt, 1995; Solomon et al., 1994]. In a model study by Sander et al. [1997] the presence of about 1 ppt of IO leads to an increase in the O_3 destruction rate of about 20% mainly via the reaction BrO + IO. The self-reaction and cross-reaction of halogen oxides dominate O_3 destruction when relatively high mixing ratios of halogen oxides are present [Saiz-Lopez et al., 2004]. At lower concentrations of halogen oxides, reaction with HO_2 radicals becomes important [Adams and Cox, 2002].

$$\mathrm{X+O_3 \rightarrow XO+O_2} \qquad \text{(R1.15)}$$
$$\mathrm{XO+HO_2 \rightarrow HOX+O_2} \qquad \text{(R1.3)}$$
$$\mathrm{HOX+}h\nu \mathrm{\rightarrow X+OH} \qquad \text{(R1.23)}$$
$$\mathrm{OH+CO+O_2 \rightarrow CO_2+HO_2} \qquad \text{(R1.24)}$$

net: $\mathrm{CO+O_3 \rightarrow CO_2+O_2}$

Note that instead of CO some other reduced compounds like CH_4 could also be oxidized.

In the polluted or the semi-polluted atmosphere the formation of halogen nitrate can also lead to O_3 depletion

$$\mathrm{XO+NO_2\,(+M) \rightarrow XONO_2} \qquad \text{(R1.25)}$$
$$\mathrm{XONO_2+}h\nu \mathrm{\rightarrow X+NO_3} \qquad \text{(R1.26)}$$
$$\mathrm{NO_3+}h\nu \mathrm{\rightarrow NO+O_2} \qquad \text{(R1.27)}$$
$$\mathrm{X+O_3 \rightarrow XO+O_2} \qquad \text{(R1.15)}$$
$$\mathrm{NO+O_3 \rightarrow NO_2+O_2} \qquad \text{(R1.28)}$$

net: $\mathrm{2O_3 \rightarrow 3O_2}$

However, the efficiency of this reaction cycle might be small since $XONO_2$ and NO_3 can also photolyze to XO + NO_2 and NO_2 + O, respectively. Furthermore, $XONO_2$ formed in R1.25 can also be removed by uptake onto aerosol surfaces.

More recent model study [Saiz-Lopez et al., 2006a] and field measurements [Huang et al., 2009a] suggest that the production of atomic iodine radicals from the reaction of NO_3 with I_2 in the coastal MBL can lead to elevated O_3 depletion at night.

1.1.1.2.2 Modulating Atmospheric NO_x and HO_x

The ratio of [NO_2]/[NO] and [HO_2]/[OH] as well as their absolute concentrations are affected by the presence of halogen species, leading to a change of atmospheric photooxidation potential. In the absence of halogen species, the ratio of [NO_2]/[NO] is controlled by the reaction of NO with O_3 and the photolysis ($\lambda < 400$ nm) of the resulting NO_2. In the presence of elevated halogen species, however, the ratio of [NO_2]/[NO] increases based on the following reaction [Platt and Janssen, 1995; McFiggans et al., 2000]

$$\mathrm{XO+NO \rightarrow X+NO_2} \qquad \text{(R1.29)}$$

Note that the resulting X will consume an O_3 (R1.15); but the photolysis of NO_2 will produce an O_3. Thus, the overall effect of R1.29 is a null cycle in terms of O_3. However, the reaction of XO with NO bypasses oxidation of NO by other oxidant, such as HO_2 to NO_2, therefore reducing the production of ozone, which can only happen by photolysis of NO_2 in the throposphere.

The main sources of HO_x are photolysis of O_3 and HCHO, with potentially important but uncertain contributions from HONO and higher aldehydes [Bloss et al., 2007]. The reaction of XO with HO_2 (R1.3) can lead to the reduction of the $[HO_2]/[OH]$ ratio since the resulting HOX acts as a (short-lived) HO_x reservoir that delays the reformation of OH. The HO_2 loss via reaction with XO is noticeable under low NO_x conditions. Bloss et al. [2005] reported that the reaction of IO with HO_2 accounts for up to 40% of the total HO_2 radical sink. Further reduction of the $[HO_2]/[OH]$ ratio can be expected if HOX is taken up by aerosol particles instead of being photolyzed. In this case, HO_2 is lost from the gas phase and cannot be reformed (R1.23 and R1.24). It should be noted that due to the reaction of XO with HO_2 ozone production is reduced since HO_2 is no longer available for the oxidation of NO.

1.1.1.2.3 Impact on Organic Compounds

Halogens also have a significant impact on the photochemistry of volatile organic compounds (VOC). Some light alkanes can be readily consumed (mostly by Cl atoms) by hydrogen abstraction (producing HCl) during ozone depletion events (ODEs). The lifetime of propane under normal conditions for example is about 14 days, however, reduced to about 8 hours during ODEs due to the high concentration of Cl atoms (up to 7.5×10^4 cm^{-3} during ODEs) [Boudries and Bottenheim, 2000] and the high rate constant of Cl with propane (8800 times larger with Cl than OH). Jobson et al. [1994] and Yokouchi et al. [1994] showed that reactive alkanes, such as butane and n- and isopentane, are nearly completely removed during ODEs. The main sink for Cl is the reaction with hydrocarbons and especially with CH_4. In the cases of alkenes and most aromatics, the production of oxygenated products is more important in the polar marine boundary layer. For example, during ODEs, there is substantial consumption of propane, and a concomitant increase in acetone [Guimbaud et al., 2002]. Also, the link between organic and inorganic halogen may offer an explanation for the abiotic sources of halocarbons. The reaction of extremely reactive HOI and /or HOBr with organic compounds in the quasi-liquid layer has been proposed to explain high concentrations of the short-lived di- and tri-halomethanes (e.g., CH_2I_2, $CHBr_3$) observed in Hudson Bay, Arctic [Carpenter et al., 2005]. In a more recent study in our laboratory, it is found that some inorganic halogen molecules, such as dihalogens, are very reactive towards aromatic compounds [Huang and Hoffmann, 2009]. Therefore, the impact of inorganic halogen molecules on the atmospheric photochemistry might be smaller than expected in polluted environments.

Dimethyl sulfide (DMS) is the most important gaseous precursor for sulfate aerosol in the MBL. OH and NO_3 are assumed to be the main oxidants for DMS, leading to the formation of gaseous SO_2 whose main fate is to react with OH, forming new sulfate particles. However, an alternate pathway is provided by BrO + DMS and IO + DMS (although there are uncertainties about the rate coefficient for the reaction of IO with DMS) [Dillon et al., 2006]. Since the product of these reactions is methane sulfonic acid rather than SO_2, it is speculated that the formation of new sulfate particles in the marine troposphere could be decreased.

1.1.1.2.4 Other Important Impacts

The impact of halogen on the mercury (Hg) cycle in the polar boundary layer has been realized [Steffen et al., 2007 and references therein]. Schroeder et al. [1998] were the first to report rapid depletion of gaseous element mercury (GEM) in the polar boundary layer during ODEs (“mercury depletion events”, MDEs). The typical GEM atmospheric residence time is in the range of 6 to 24 months. However, during MDEs, GEM is converted to reactive gaseous meucury (RGM) within a few hours, leading to lower GEM and enhanced particulate Hg concentrations and increased deposition of mercury. This may have consequences for the health of the aboriginal population and the Arctic ecosystems following flushing of the RGM which is more bioavailable than GEM. It has been realized that atomic bromine plays an essential role in MDEs since most MDEs are observed during nearly complete depletion of ozone when a higher number of bromine atoms are available. Reactions of Cl, Cl_2, and Br_2 are too slow to be responsible for MDEs (e.g., Ariya et al., 2002).

Over the past few years, studies at mid-latitude sites have shown that new particles can be produced very efficiently under iodine-rich conditions [O’Dowd et al., 2002; O’Dowd and Hoffmann, 2005]. It is proposed that coastal nucleation events are driven by biogenic emissions of iodine vapors that undergo rapid chemical reactions to produce condensable iodine oxides [Hoffmann et al. 2001], leading to nucleation and growth of new particles. The primary source of the condensable iodine vapors is thought to be molecular iodine [McFiggans et al., 2004; Saiz-Lopez et al., 2006b; Huang et al, 2009b]. Although the formation of iodine oxide particles is easy to reproduce in the laboratory, the mechanism whereby iodine species such as IO, OIO, and I_2O_2 are oxidized to the higher oxides such as I_2O_3, I_2O_4, and I_2O_5 which are likely to be highly condensable because of their large dipole moments, are not well understood. Also the role of iodine oxides in open-ocean new particle production still remains an open question.

1.1.1.3 Observations of Reactive Halogen Species and the Approaches Used

In recent years it became clear that reactive halogen species (RHSs = X, X_2, XY, XO, OXO, HOX, XNO_2 and $XONO_2$, where X, Y denotes a halogen atom) play a significant role in tropospheric chemistry, as described above. Numerous tropospheric field measurements have been realized, and some RHSs have been detected by several direct or indirect techniques. A summary is shown below.

Differential optical absorption spectroscopy (DOAS)

Differential optical absorption spectroscopy (DOAS) is one of the most widely used techniques for the field observations of RHSs. The principle of DOAS is the identification and quantification of atmospheric trace gases by their specific narrow (<5 nm) band optical absorption structure in the open atmosphere, separating trace gas absorption from broad band molecule and aerosol extinction processes, thus allowing very sensitive detection of many molecular species. The identification of the gases is unambiguous since their specific absorption structure is, similar to a fingerprint, unique. Calibration of the instrument is not necessary as long as the absorption cross section is known. The light source of DOAS can be artificial (active DOAS) such as Xe-arc lamp, or natural (passive DOAS) such as zenith scattered sunlight, moon or stars. Active DOAS has been used for ground-based measurements of ClO, BrO, IO, OIO, and I_2 [Platt and Janssen, 1995; Hebestreit et al., 1999; Saiz-Lopez et al., 2004; Saiz-Lopez and Plane, 2004; Saiz-Lopez et al., 2007b], and passive DOAS for ground-, balloon-, and satellite-based measurements [Wagner and Platt, 1998; Hönninger et al., 2004; Saiz-Lopez et al., 2007a].

The observations of ambient iodine species (I_2, IO, and OIO) are realized only within the past few years [Alicke et al., 1999; Saiz-Lopez and Plane, 2004; Stutz et al., 2007]. A maximum I_2 mixing ratio of 93 parts per trillion by volume (pptv) at night and of 25 pptv during the day was observed during the NAMBLEX field campaign at Mace Head, Ireland using LP-DOAS [Saiz-Lopez and Plane, 2004], and the concentration levels of I_2 were found to correlate inversely with tidal height [Saiz-Lopez, et al., 2006a], suggesting that local algae could be the emission source of I_2. During daylight I_2 molecules released will photolyze rapidly to form I atoms that then react with O_3 to yield IO, which explains the clear anti-correlation between IO and tidal height and a correlation between IO and solar irradiation observed at Mace Head and Mweenish Bay, Ireland [Saiz-Lopez, et al., 2006a; Huang et al., 2009a]. However, the main precursors of IO could be other iodine species than I_2 at certain coasts. Peters et al. [2005] found that IO (up to 7.7 ppt) exhibited a clear anti-correlation with the presence of CH_2I_2 (at levels of up to 20 ppt) during a field campaign at the coastal line of Brittany, France. The absence of some Laminaria species could be the reason why I_2 could not be detected in Brittany since the biogenic emissions of I_2 could be algae species dependent [Huang et al., 2009a]. In a field campaign at the Isles of Shoals, Gulf of Maine, IO was identified on 19 out of 23 days; but no correlation with tidal height could be observed, suggesting an unknown source of IO [Stutz et al., 2007]. Besides measurements in the coastal MBL, observations of IO at levels of about 1 ppt at Tenerife indicate that IO is probably present in much of the open ocean boundary layer, at levels where it may cause significant ozone destruction [Allan et al., 2000; Read et al., 2008]. In addition, IO was occasionally observed during night-time. A maximum mixing ratio of 2.5 ppt was observed at Mace Head [Saiz-Lopez and Plane, 2004] and of 4.7 ppt at Mweenish Bay [Huang et al., 2009a]. The source of night-time IO could be related to the reaction of I_2 with NO_3 to form iodine atoms which then rapidly combines with O_3 [Chambers et al., 1992; Kaltsoyannis and Plane, 2008; Huang et al., 2009a].

OIO observations are still quite scarce so far and were realized in the remote MBL at Mace Head [Saiz-Lopez and Plane, 2004; Peters et al., 2005] and Cape Grim (Tasmania) [Allan et al., 2001] at night. During the day the mixing ratios of OIO observed were mostly below the limit of detection of the DOAS instruments, probably due to the rapid photolysis and the high detection limit of DOAS. An exception daytime OIO observation was realized in the polluted Gulf of Maine [Stutz et al., 2007]. However, models predict that significantly higher OIO levels could exist in a clean environment than in the polluted atmosphere. Our recent field measurements at Mace Head and Mweenish Bay also showed that OIO mixing ratios were above the DOAS detection limit several times during the day [Huang et al., 2009a]. However, these elevated daytime OIO cannot be explained by the currently known iodine chemistry. Certainly, more detailed measurements of OIO and its photolysis rate are required to clarify the importance of OIO for the atmospheric iodine chemistry in the MBL (e.g., the impact on new particle formation process).

In addition to the RHSs, DOAS techniques can also be used for the measurements of other key atmospheric constituents such as O_3, NO_x, and HO_x, which facilitates a better understanding of the impacts of halogen species on atmospheric processes. Nevertheless, considering the low mixing ratios of the RHSs in the boundary layer, atmospheric spectra are usually recorded over a light-path of several kilometers within tens of minutes when working with the active DOAS, to enhance the optical absorption and therefore the limits of detection. In such case, however, DOAS can just provide spatial and temporal average levels of the RHSs, thus is incapable of resolving inhomogenous distributions of the trace gases and the identification of potential sources and sinks. In addition, the limits of detection of DOAS are somewhat high for certain halogen species like I_2 and OIO and are affected by weather conditions, which makes the clear identification still difficult when the compounds of interest are present at low concentration levels.

Resonance fluorescence method

Resonance fluorescence combined with chemical conversion (RF/CC) is another approach for halogen oxides ClO and BrO measurements. Nitric oxide (NO) is added to the airstream upstream of the detection region, converting halogen oxides to atoms ($XO + NO \rightarrow X + NO_2$, where X= Br or Cl). The resulting atoms are subsequently detected by resonance fluorescence in the vacuum ultraviolet, at about 131 nm for Br and 119 nm for Cl. This technique has been used extensively in the stratosphere on balloons and aircrafts. For tropospheric measurements, however, a modified sampling system is required to achieve an internal pressure low enough that losses of signal resulting from quenching and absorption by water vapor and oxygen are minimal. This technique provides in situ measurements for halogen oxides and has been used for BrO measurements at two high-latitude boundary layer sites (i.e., Ny Ålesund and Alert) [Avallone et al., 2003]. However, the overall accuracy of the RF/CC technique is limited by the knowledge of the atomic absorption cross-sections, the accuracy of laboratory calibrations, and the accuracy of the rate constants in the $BrO/Br/NO/O_3$ system.

More recently, a vacuum UV RF system was developed and employed to detect atomic iodine at around 178–184 nm [Bale et al., 2008]. The system can be operated either to directly measure ambient iodine atoms or to measure the total photolabile iodine loading of ambient air through broadband visible photolysis of photolabile iodine-containing species with subsequent RF detection of the resulting iodine atoms. The instrument provides in situ measurements with relatively high time resolution and a relatively low limit of detection (5.3 ppt for iodine atom). The system has been used for the first time in August 2007 at the Mace Head Atmospheric Research Station, Ireland. Ambient iodine atoms were measured at levels up to 22 ppt during the day. The total photolabile iodine loading was also measured during several night-time and daytime periods and was found to correlate inversely with tidal height.

"Hydrocarbon clock" method

Estimates of enhanced levels of chlorine and bromine atoms during ODEs can be obtained from measurements of changes of the ratio of different nonmethane hydrocarbons (NMHCs)—the so called "hydrocarbon clock" method [Jobson et al., 1994]. The basic assumption for this estimation is that the difference between the mixing ratios of selected NMHCs in ozone-depleted air masses and during "normal" ozone conditions is caused solely by chlorine/bromine atoms because the reaction rates for some NMHCs with Cl/Br are much higher than those with OH radicals [Ramacher et al., 1999]. Time integrated chlorine atom concentrations can be calculated from the changes in mixing ratios of substituted alkanes such as C_2Cl_4, and the bromine atom concentrations can be calculated from the change in the real concentration of ethyne after correction for the Cl-atom-induced change. Wingenter et al. [1996] estimated midnight to 11:00 am and noontime concentrations of 3.3×10^4 and 6.5×10^4 Cl-atoms cm^{-3}, respectively, in the North Atlantic. Singh et al. [1996] used measurements of five different species to estimate early-morning Cl concentrations in the remote tropical MBL in the Pacific and inferred from these different compounds a range of 1.8×0^4 to 7.6×10^5 Cl-atoms cm^{-3}. Other published data show average Cl-atom concentrations in the MBL around 10^3 atoms cm^{-3} [Rudolph et al., 1997; Wingenter et al., 1999]. Solberg et al. [1996] estimated the Br-atom concentrations of 5×10^7–1×10^8, which was about 1000 times higher than Cl-atom concentrations. This ratio is very similar to the findings of Jobson et al. [1994] and Ramacher et al. [1999].

It should be noted that the "hydrocarbon clock" method can only provide the upper limits of Cl- and Br-atom mixing ratios. The major part of the uncertainty of the estimation of Cl- and Br-atom concentrations results from errors in the rate constants for the reaction of the NMHCs with OH radicals as well as the initial concentrations of the investigated NMHCs, i.e., the concentrations of these compounds before halogen atoms are injected into the air masses. Certainly, a careful selection of suitable NMHCs sets and a reliable and consistent set of the relevant rate constants would further improve the accuracy of the halogen atom concentration estimations.

Measurements of $^{13}C/^{12}C$ in CH_4 and CO

In contrast to NMHCs, the typical consumption of CH_4 by Cl during ODEs is only about 1 out of 1850 ppb. Such a small deviation from ambient levels will be masked by natural variations in CH_4 mixing ratios in the order of several ppb. Also the change of CO produced via CH_4 + Cl is much smaller than the natural variability. Therefore, variations in CH_4 or CO cannot provide a signal for the presence of Cl radicals. However, it should be noted that Cl atoms react slower with $^{13}CH_4$ than with $^{12}CH_4$. The CO produced via CH_4 + Cl is about 90% less ^{13}C than ambient CO. This addition of heavily depleted CO is measurable. Therefore, measurement of the $^{13}C/^{12}C$ ratio in atmospheric CO is a sensitive indirect method to detect relatively low levels of Cl. This isotopic signature of CO has been used to estimate the time-integrated amount of Cl atoms encountered by the O_3 depleted air mass in the Arctic [Röckmann et al., 1999]. Also, the measurements of "apparent kinetic isotopic effect" of CH_4 imply a kinetic isotope fractionation, which is inconsistent with OH being the only sink of CH_4, and suggests a competitive removal of CH_4 by Cl atoms. The summer maximum and the seasonal mean Cl concentrations inferred were 7.1×10^3 and 2.6×10^3 atoms cm^{-3} in the Southern Hemisphere [Allan et al., 2001]. A more recent work showed that a seasonal and interannual variability in Cl, i.e., 3×10^4 atoms cm^{-3} in 1994–1996 and $\sim 10^4$ atoms cm^{-3} in 1998–2000, is needed to explain the observed kinetic isotope effect [Allan et al., 2005].

Chemical amplification combined with chemiluminescence

Chemical amplification is a method commonly used for the detection of peroxy radicals (HO_2 and RO_2). However, Perner et al. [1999] found that chemical amplification is also sensitive towards ClO_x (Cl+ClO+OClO). ClO_x is recduced by NO to Cl atoms which then react with CO in the presence of O_2. The efficiency of the chain reaction (chain length), i.e., the number of NO_2 molecules produced from one primary radical, was estimated to be 300 ± 60 for ClO_x and 160 ± 15 for peroxy radicals by measuring the product NO_2. This allows the atmospheric ClO_x to be measured under ambient conditions with a detection limit of better than 1 ppt. During the Arctic Tropospheric Ozone Chemistry campaigns at Ny-Ålesund, Spitsbergen,

ClO_x was found at night during low ozone events at mixing ratios of up to 2 ppt. Unfortunately, the chemical amplification is not specific, and both peroxy radicals and ClO_x can contribute to a combined amplification signal, especially during daytime when large HO_x/RO_x concentrations are present. In addition, water vapor proved to affect the chain length for peroxy radical measurements, however, the influence on the chain length of ClO_x is not clear [Martinz et al., 1999]. This could result in large uncertainty of the ClO_x measurements.

Based on the theory of chemical amplification, Impey et al. [1999] developed an approach for BrO_x (Br+BrO). In this system, BrO_x reacts with an added hydrocarbon (e.g., propene) in the presence of NO to form a peroxy radical. The resulting HO_2 is then chemically amplified in the presence of NO, CO and O_2. BrO_x can finally be measured by the determination of NO_2 formed in the reaction chains. The interferences from RO_2, HO_2, ClO_x, and the reaction of O_3 with the added NO could be minimized by modulating the production of the HO_2 radicals from BrO_x. The detection limit is about 4 ppt.

Photoactive halogen detector

A photoactive halogen detector (PHD) was developed by Impey et al. [1997a], to distinguish between photolyzable chlorine (Cl_2 and HOCl) and bromine (Br_2 and HOBr). In this analytical system ambient air is drawn through a cylindrical flow cell (with a Xe arc lamp), where the photoactive halogen molecules are photolyzed. The resulting chlorine and bromine atoms then react with propene in the presence of O_2 and NO. The chloroacetone and bromoacetone formed are subsequently measured with a gas chromatographic method. This method has been used for total photolyzable chlorine and bromine measurements at Alert during the Polar Sunrise Experiment 1995 [Impey et al., 1997b]. The mixing ratios of the photolyzable chlorine observed were typically below 20 ppt as Cl_2, with several events as high as 40 and one 100 ppt as Cl_2. The measured photolyzable bromine ranged from a few to 20 ppt as Br_2, with one event up to 40 ppt. Subsequent developments of the PHD system [Impey et al., 1999] allow the differentiation between the two photolyzable molecules, i.e., X_2 and HOX, due to their significantly different photolysis rates. The detection limits are 14 ppt for Cl_2 and 10 ppt for Br_2, with higher values of 45 ppt for HOCl and 25 ppt for HOBr. Although the PHD method provides a potentially useful technique for detecting the presence of photolyzable chlorine and bromine, it should be noted that the PHD can also respond to other photoactive halogen species, such as XNO, XNO_2, $XONO_2$, XY, and some organic halogens [Impey et al., 1997a; Impey et al., 1999]. Therefore, the systematic errors in the determination of an absolute concentration could be significant.

Filter–adsorbent method

The filter–adsorbent technique is one of the most widely used methods for the sampling of gaseous halogen species, which typically involves a front filter to remove particles followed by an impregnated filter or alternative aqueous solution that captures gaseous analytes. Keene et al. [1993] developed a tandem mist chamber to sample chlorine gases in the MBL. In this system, both coarse and fine aerosol particles are removed in the inlet. A trace gas concentrator positioned downstream incorporates an acidic mist chamber (pH> 1.0) and an alkaline mist chamber in series. Gaseous HCl^* (including HCl, NOCl, $ClNO_2$, and $ClNO_3$) and Cl^* (including Cl_2 and a portion of HOCl) are collected in the acidic and alkaline mist chambers, respectively. Mist solutions are analyzed by ion chromatography by measuring the resulting Cl^-. However, in this tandem mist chambers, about 7–10% Cl_2 are collected in the acidic chamber. Also if significant amounts of HOCl are present in ambient MBL air, reported HCl^* are overestimated by about 10% of corresponding Cl^*, and reported Cl_2 + HOCl are underestimated by the unknown fraction of HOCl sampled in the acidic mist chamber. This technique has been employed at different locations. The observed mixing ratios of HCl^* and Cl^* were < 38–268 ppt and < 26–254 ppt, respectively, in coastal air near Miami, FL, USA [Pszenny et al., 1993], 27–263 ppt and < 6–38 ppt in Hawaii in September 1999 under clean conditions [Pszenny et al., 2004], 133–883 ppt and < 30–258 in Bermuda in Spring 1996 under moderately polluted conditions [Keene and Savoie, 1998], and < 48–5727 ppt and < 20–421 ppt in New England under polluted conditions [Keene et al., 2007]. Alternatively, a NaOH (or LiOH)/glycerin impregnated filter paper positioned downstream of the pre-filter can be used to collect inorganic gaseous chlorine, bromine, and iodine [Rahn et al., 1976; Gäbler and Heumann, 1993]. Although the filter–adsorbent technique provides an useful approach for the differentiation between particulate associated, inorganic and organic gaseous halogen, this technique is subjected to many artifacts resulting from particle-to-gas and gas-to-particle conversion reactions as well as the retention of gaseous halogen species on the pre-filter either directly on the filter material or on concurrently collected particulate matter.

Atmospheric pressure chemical ionization with tandem mass spectrometry

Species-specific measurements of dihalogen molecules can be achieved by an atmospheric pressure chemical ionization with a triple quadrupole mass spectrometer (APCI/MS/MS). The instrument provides high selectivity by using two stages of mass analysis: the parent ion—a negatively charged molecular ion selected in the first mass analyser—undergoes collisionally activated dissociation to yield fragments (daughter ions) whose mass-to-charge ratios (*m*/*z*) can be determined by the second mass analyzer. Highly selective monitoring then can be performed by using the two mass filters to pass only the parent and daughter ions related to the species of interest. For example, Br_2 can be measured as the ion pairs 158/79, 160/79, 160/81, and 162/81; Cl_2 as 70/35, 72/35, 72/37, and 74/37; BrCl as 114/35, 116/35, 116/37, and 118/37; and I_2 as 254/127. Since dihalogen molecules (e.g., Cl_2) are highly surface active, a laminar flow and multi-stage inlet is used to minimize wall interactions during transit of the ambient air to the instrument. The sample line loss was estimated to be 10% for Cl_2, 9% for Br_2, and 13% for I_2, respectively [Finley and Saltzman, 2008]. The measurements suffer from some potential interference such as the aerosol remaining in the air stream.

The APCI/MS/MS technique has been used for dihalogens measurements by several groups. Spicer et al. [1998] observed up to 150 ppt Cl_2 at a coastal site in Long Island, NY, USA, during night-time. Finley and Saltzman [2006] detected the mixing ratios of Cl_2 ranging from < 2.5–20 ppt with a 2-month mean of 3.5 ppt in urban air in Irvine, CA, USA. Unlike Spicer et al. [1998], they also measured Cl_2 during daylight, typically below 5 ppt but with a maximum mixing ratio of 15 ppt, which implies a likely marine source. More recent measurements [Lawler et al., 2009] at Cape Verde in the eastern tropical Atlantic showed that the Cl_2 levels ranged between < 2 and 30 ppt and that elevated Cl_2 was associated with aged polluted air, most likely as a result of aerosol acidification. The measurements at Alert, Canada, during polar sunrise in Febuary/March, 2000 [Foster et al., 2001; Spicer et al., 2002] showed mixing ratios of up to 35 ppt BrCl and of up to 25 ppt Br_2, however for Cl_2 values below the detection limit. The measured BrCl and Br_2 concentrations were inversely correlated with those of ozone. Concurrent observations of Cl_2, Br_2, and I_2 were made in a coastal Pacific site (La Jolla, CA) in January 2006 [Finley and Saltzman, 2008]. The observed concentration levels of Cl_2, Br_2, and I_2 ranged from below detection limits of 1.0, 0.5, and 0.2 ppt, respectively, to maxima of 26, 19, and 8 ppt, respectively. The authors concluded that these dihalogens were present at significant and highly variable levels in polluted coastal air and that the halogen atoms resulting from the photolysis of Cl_2 caused a net production of ozone, while those from Br_2 and I_2 destroyed ozone.

In general, approaches to species-specific identification and quantification of RHSs in the troposphere are still quite scarce (see also Figure 1.1). This makes the identification of the sources and sinks difficult, especially under certain environmental conditions when, for example, halogen species deplete rapidly or in certain regions, where some key RHSs are present at relatively low concentrations. In addition, most of the current techniques just provide temporal and/or spatial averaging, which does not facilitate a better understanding of the halogen recycling. However, it should be noted that efforts have been made to develop highly sensitive and selective techniques for in situ "single-point" measurements. For example, a laser induced fluorescence spectrometer for IO [Whalley et al., 2007], a cavity ring-down spectrometer for IO [Wada et al., 2007], a broadband cavity ring-down spectrometer (BBCRDS) for I_2 [Bitter et al., 2005], an incoherent broadband cavity-enhanced absorption spectroscopy (IBBCEAS) for I_2, OI, and OIO [Vaughan et al., 2008], and the APCI equipped with an ion trap mass spectrometer [Ivey and Foster, 2005] or a triple quadrupole mass spectrometer (see above) for dihalogens have been developed in the past few years.

1.2 Aims of this Work

The first aim of this work was to develop new analytical approaches for certain key RHSs such as HOX, XY, and X_2. Time resolved concentration data on these key species are still quite scarce or even not available so far. As described above, the measurements of RHSs are still a challenging analytical problem, mostly because

- they are present at ppt or sub-ppt concentration levels in most cases;
- the lifetime of most of RHSs is short;
- some RHSs have very similar chemical properties, which leads to difficulties in species-specific differentiation;
- other constituents in the atmosphere could also interfere in the RHSs measurements.

The currently available methods for RHSs are still few and therefore a number of uncertainties about the sources, sinks, and the recycling of halogen remains open questions.

Nevertheless, it should be noted that several analytical methods were improved or newly developed during the three years of this study. Several methods regarding “single-point” in situ measurements of certain RHSs (XY, HOX, and X_2) have been successfully developed. These novel measurement techniques allow a much deeper understanding of the atmospheric processes in terms of sources identification and evaluation of atmospheric implications of RHSs.

The second aim of this work was to investigate the mixing ratios of XY, HOX, and X_2 in the coastal MBL using the methods developed in the first part. The field measurements performed—for the first time—at the west coastal of Ireland (Mace Head and Mweenish Bay) in 2007 provide “single-point” in situ concentration levels of these key halogen species, which favors a better understanding of the sources and the impact of these halogen species on the regional atmosphere. To get a better understanding about the sources and the cycling of these halogen species, a more intensive field campaign was carried out in Ireland (at the same measurement locations) in 2009. In addition, field measurements were also carried out during an Antarctic cruise in early 2009 to investigate the concentrations of these halogen species and to better understand their impact on the polar boundary layer. Unfortunately, laboratory measurements of the samples from 2009-Ireland and 2009-Antarctica campaign have not finished yet. Thus, these data will not be discussed in this thesis.

The results presented in the thesis are broken into two primary parts, i.e., Chapter 2 and 3. Each part consists of 2–4 sub-chapters which have been published in or have been submitted to internationally recognized journals:

- Chapter 2—Method developments
  - 2.1 Diffusion technique for the generation of gaseous halogen standards (Submitted to *Journal of Chromatography A*, 2009)
  - 2.2 A denuder–impinger system with in situ derivatization followed by gas chromatography–mass spectrometry for the determination of gaseous iodine-containing halogen species (Published in *Journal of Chromatography A*, 2008)
  - 2.3 Extensive evaluation of a diffusion denuder for the quantification of atmospheric stable and radioactive molecular iodine (Submitted to *Environmental Science & Technology*, 2009)

- 2.4 Development of a coupled diffusion denuder system combined with gas chromatography/mass spectrometry for the separation and quantification of molecular iodine and the activated iodine compounds iodine monochloride and hypoiodous acid in the marine atmosphere (Published in *Analytical Chemistry*, 2009)

- Chapter 3—Field measurements
  - 3.1 Observations of high concentrations of I_2 and IO in coastal air supporting iodine-oxide driven coastal new particle formation (Accepted by *Geophysical Research Letters*, 2009)
  - 3.2 In situ measurements of molecular iodine in the marine boundary layer: the link to macroalgal species and the implications for O_3, IO, OIO and NO_x (Accepted by *Atmospheric Chemistry and Physics*, 2009)

1.2.1 Technique—Diffusion Denuder

Denuders were used for the first time as gas collection device in 1979. Since then, intensive studies on the utilization of denuders for the measurements of gaseous constituents in the atmosphere have been conducted, and the collection of ambient ammonia, nitrate, and sulphur species by this technique are becoming routine analytical approaches for atmospheric research [Kloskowski et al., 2002]. However, little attention is paid to date to atmospheric halogen species.

Currently, theoretical principles governing the operation of denuders have been elaborated. The phenomenon of denudation (see Figure 1.2) involves the movement of molecules and/or particles being as a result of two forces: (1) a force vectored in accordance with the direction of the gas stream, resulting from the forced flow of gas, and (2) a force perpendicular to the longitudinal axis of the denuder (and its inner walls), resulting from the radial diffusion. As such, the combined process of isolation and enrichment of analytes can proceed directly from the primary matrix, that is, analytes present in the gas phase are retained by the active collection surfaces of the denuder by either physical adsorption or chemical bonding, due to their high diffusion coefficients, while aerosol particles can pass through the denuder tube practically avoiding any contact with the walls of the device. In practice, to achieve excellent performance with high collection efficiencies, a series of criteria must be met for the proper operation of the denuder: (1) the sampled gas flow must be stable and laminar, (2) the temperature and viscosity must be uniform within the gas stream, (3) any axial diffusion of the sampled gas must be insignificant compared to the linear velocity of the gas flow, (4) the coating materials should behave as perfect sinks for the analytes in question (one of the most important items), and (5) the adsorbate species should be neither created nor destroyed in the gas phase within the denuder tube.

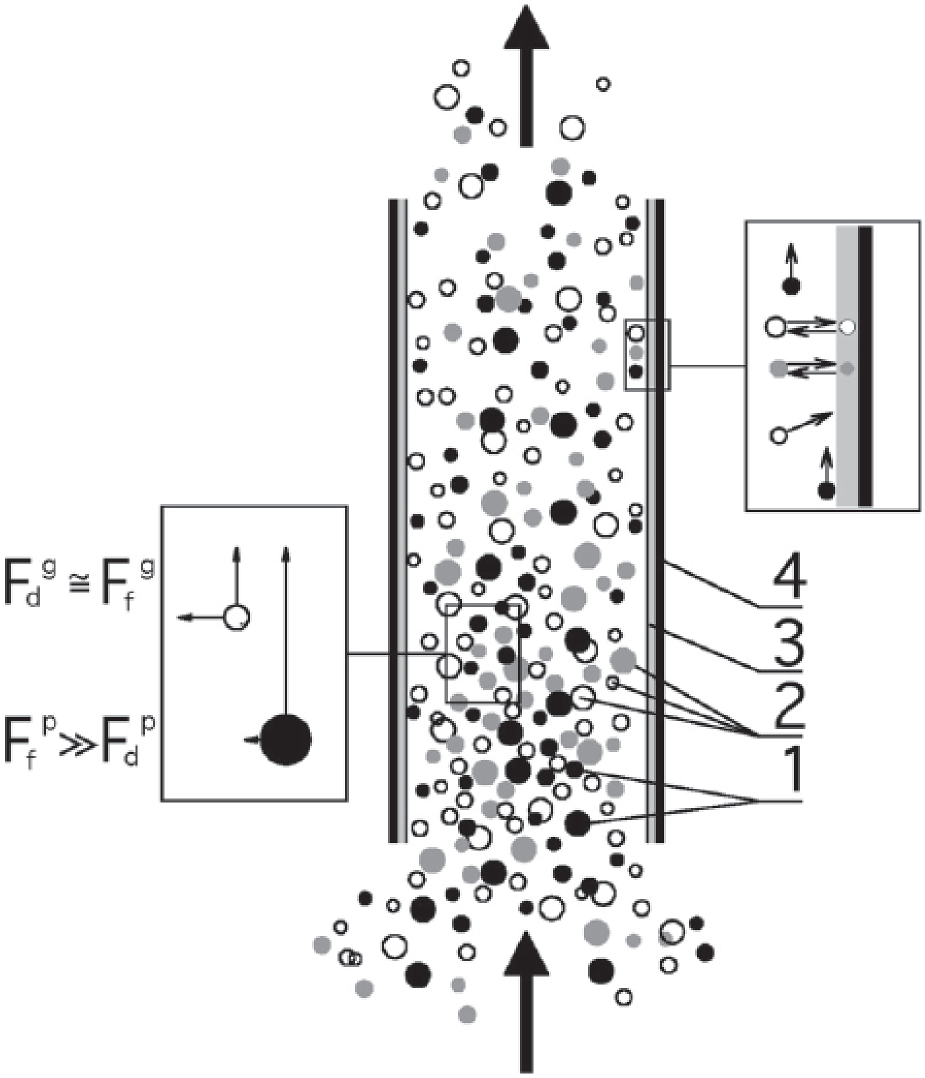

Figure 1.2 Schematic diagram of the separation of gaseous molecules from particles in the denuder: 1, particle; 2, gas molecules; 3, denuder coatings; 4, denuder wall. F-force, indices: g–gas; p–particle; d–diffusion; f–gas flow [Kloskowski et al., 2002].

A wide variety of denuder constructions such as cylindrical denuders, annular denuders, parallel plate denuders, and multiple channel denuders, are currently available [Dasgupta, 2002]. In this study, the cylindrical type was used since it has the advantages of being less laborious to prepare and of ease of operation. A brief description of the theoretical background of the cylindrical denuder is given as follows [Kloskowski et al., 2002].

In general, the balance of component A in the cylindrical denuder is given by the following differential equation:

$$\frac{\partial c_A}{\partial t}=-v\frac{\partial c_A}{\partial x}+D_A\frac{\partial^2 c_A}{\partial x^2}+D_A\left(\frac{\partial^2 c_A}{\partial r^2}+\frac{1}{r}\frac{\partial c_A}{\partial r}\right)-r_A \qquad \text{(Eqn.1)}$$

where C_A is the concentration of component A in air (mol cm^{-3}), t is the time (s), x is the longitudinal coordinate (cm), r is the distance from the longitudinal axis of the cylinder (cm), v is the actual linear velocity of air flow (cm s^{-1}) for a laminar flow given by $v = 2\ v_{\mathrm{av}}\ (1\text{-}r^2/R^2)$, v_{av} is the linear velocity of air flow (cm s^{-1}), R is the internal radius of the denuder (cm), D_A is the diffusion coefficient of component A in air (cm^2 s^{-1}), and r_A is the gas-phase reaction rate of component A (mol cm^{-3} s^{-1}). The equation describes the rate of change in the concentration of component A in the cylindrical denuder, composed of the forced movement of the air along the denuder (first term), longitudinal diffusion (second term), radial diffusion (third term), and the homogenous chemical reaction (fourth term). Obviously, the solution of the equation depends on the assumed initial conditions ($t = 0$) and the boundary conditions with respect to x (from $x = 0$ to $x = L$, where L is the denuder length (cm)) and r (from $r = 0$ to $r = R$). It should be noted that in the case of $r = R$ any heterogenous chemical reaction between component A and the coating should be included.

Besides the boundary conditions, some additional assumptions have to be made to solve Eqn. 1. The first, also the most commonly used one, is the assumption that the composition of the sampled air dose not change during its flow along the denuder, i.e., $\partial c_A/\partial x = 0$. The second term of the equation, $D_A(\partial^2 c_A/\partial x^2)$, can also be omitted since the linear velocity of molecules of component A resulting from longitudinal diffusion is negligible compared with linear velocity of the air stream passed through the denuder (this situation exists when $2Rv/D_A > 10$). The last approximation lies in assuming that no homogenous reactions occur in the denuder ($r_A = 0$). Based on these reasonable assumptions, Eqn. 1 can be rewritten as

$$\frac{\partial c_A}{\partial t}=D_A\left(\frac{\partial^2 c_A}{\partial r^2}+\frac{1}{r}\frac{\partial c_A}{\partial r}\right) \qquad \text{(Eqn.2)}$$

Assuming that the component A is present in trace concentrations, the flow is laminar, the temperature is constant, and the amount of retained component A is small compared with the capacity of the coating, the solution of Eqn. 2 is the well-known Gormley–Kennedy equation [Gormley and Kennedy, 1949]:

$$\frac{C_{av}}{C_0}=0.819\exp(-7.314\Delta_c)+0.0975\exp(-44.6\Delta_c)+0.0325\exp(-212\Delta_c)+\cdots \quad \text{(Eqn. 3)}$$

$$\Delta_c=\frac{\pi D_A L}{2F} \quad \text{(Eqn.4)}$$

where C_{av} is the mean concentration of the gaseous analyte leaving the denuder, C_0 is the concentration of gaseous analyte entering the denuder, and F is the volume air flow rate (cm^3 s^{-1}). It is noted that Eqn. 3 is valid only if the value of Δ_c is greater than 0.01. However, for most sampling applications, Δ_c is of the order of magnitude of 0.1, so that only the first term on the right side of Eqn. 3 will be significant. Obviously, in such cases, the collection efficiency ($1-C_{av}/C_0$) of a cylindrical denuder increases with an increase in the length of the denuder and the diffusion coefficient of the analyte, and with a decrease in the gas flow rate. The collection efficiency can be enhanced further by decreasing the radius of the tube.

Given that the diffusion coefficients of particles are substantially low, the values of Δ_c are in general lower than 0.01 and the Gormley–Kennedy equation is rewritten as

$$\frac{C_{av}}{C_0}=1-4.06\Delta_c^{2/3}+1.9\Delta_c+0.28\Delta_c^{4/3} \quad \text{(Eqn.5)}$$

The diffusion coefficient of gas molecules can be estimated either by the experiential Fuller–Schettler–Giddings method [Fuller et al., 1966] or by experimental determination [Karaiskakis and Gavril, 2004]. The diffusion coefficients of particles can be obtained in Seinfeld and Pandis [2006] and Hinds [1999]. Therefore, the theoretical (maximum) collection efficiency of gas molecules and of fine particles can be estimated by Eqn. 3 and 5. Figure 1.3 shows the theoretically calculated collection efficiency (for a denuder of 6 mm i.d. × 50 cm length, and a gas flow rate of 500 mL min^{-1} which is a typical value used in this work) as a function of the size of particle and halogen molecules. It can be seen from the figure that for particles with the diameter of > 10 nm they pass through the denuder, whereas, for smaller particles with the diameter of ≤ 10 nm a certain amount of which can diffuse to the inner wall of the denuder.

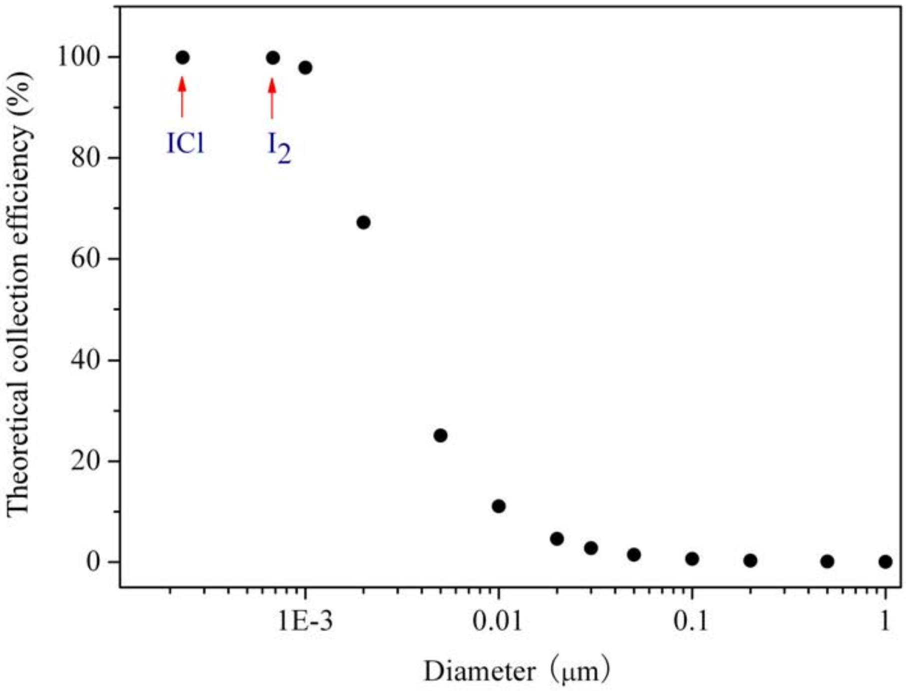

Figure 1.3 Theoretically calculated collection efficiency (maximum) as a function of the size of particle and halogen molecules.

1.3 Summary of the Work

1.3.1 Diffusion Technique for the Generation of Gaseous Halogen Standards

One of the most critical steps associated with the development of analytical procedures to measure gaseous compounds in air is the generation of know and reproducible gaseous standards at typical ambient mixing ratios since gaseous standards are essential for the verification of reliability of either sampling methods, multi-step analytical procedures or online instruments. The first paper describes for the first time the generation of inorganic gaseous standards of halogens based on a capillary diffusion device. Compared to static methods (involving the dilution of a concentrated standard or a pure compound to a defined gas volume) the capillary-based device (dynamic method) provides more reliable concentrations of the compounds of interest over a large concentration range by simply changing the capillary dimension (i.e., length and inner diameter) or temperature used. When diffusion capillaries with relatively large inner diameters (i.e., > 1–2 mm i.d.) are used the experimentally measured output rates of ICl, IBr, Br_2 and I_2 are in close agreements with their respective theoretical predictions calculated by the diffusion equation, which is consistent with a previous work focussing on semi-volatile organic compounds [Possanzini et al., 2000] in which a good agreement is also found when larger capillaries are applied. When smaller capillaries are used the actual test gas output can be elevated by up to two orders of magnitude compared to their respective calculated values and the output rates significantly depend on the headspace volume of the diffusion vessel. This phenomenon can be attributed to the influence of ambient pressure variation on the test gas output. During an ambient pressure drop (e.g., by metorological variations) the resulting volume variations within the diffusion device will force a certain amount of saturated vapour to leave the test gas vessel (in this case, the output will not only be governed by diffusion). However, despite the increasing discrepancies between theoretical and practical output rates, diffusion capillaries with longer length and smaller diameter are still useful for the generation of gaseous standards because low concentrations can be achieved without sequential large-volume dilution. It is found that the output rates decrease with the decrease of capillary dimension (i.e., increasing length and decreasing inner diameter) (see Figure 1.4, results from ICl testing for example).

In addition, it is found that in the case of using capillaries with extremely small dimensions (e.g., 0.10 mm i.d. × length 5–20 cm) relatively poor reproducibility occurs (R.S.D. (Relative Standard Deviation) = 6.0%–13.5%). In addition to the measurements of the test gas output by a gravimetric method (i.e., by periodically measuring the mass loss of the analyte vessel), the paper demonstrates that a diffusion denuder method (e.g., the method described in the second paper) to measure the test gas output is suitable and can even be beneficial since it is less time-consuming than the gravimetric method.

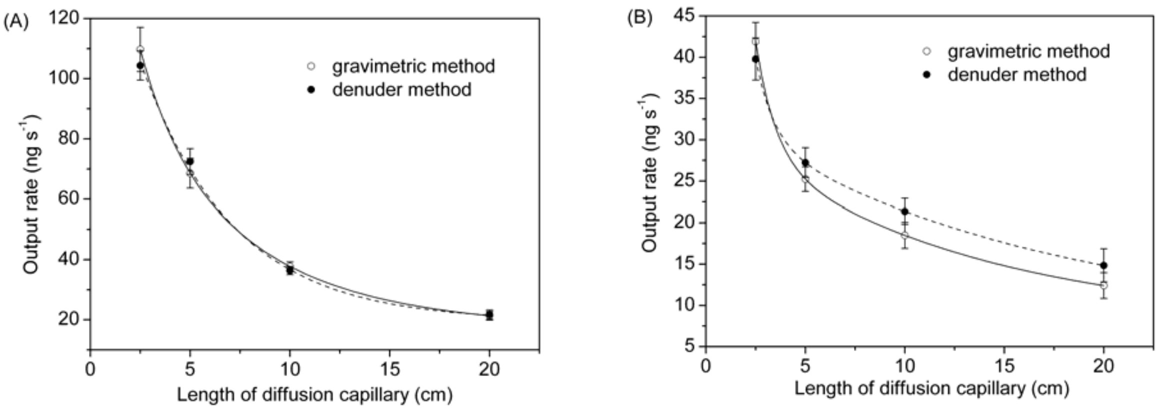

Figure 1.4 Measured output rate of ICl from the diffusion based capillary device, as a function of the capillary dimension. (a) capillary inner diameter 0.53 mm, and (b) capillary inner diameter 0.1 mm.

1.3.2 A Denuder–Impinger System with in situ Derivatization Followed by Gas Chromatography–Mass Spectrometry for the Determination of Gaseous Iodine-Containing Halogen Species

After the generation of gaseous halogen standards the aim was to develop a reliable analytical technique for the measurements of these gaseous halogens. The basis of the approach is in situ derivatization (collection) of inorganic halogens to form organic halogen compounds followed by a gas chromatography–mass spectrometry (GC–MS) method. Two totally different sampling techniques, i.e., impinger and denuder, are investigated. For the measurements taken by the impinger the respective collection efficiency obtained is 90.3% for ICl, 95.7% for IBr, and 88.8% for I_2 (see Figure 1.5a), when an aqueous solution of 1,3,5-trimethoxybenzene (1,3,5-TMB) is used. All three iodine species form the same iodination derivative 1-iodo-2,4,6-trimethoxybenzene (1-iodo-2,4,6-TMB) in 1,3,5-TMB aqueous solution.

$$\mathrm{IX(X=Cl,Br,I)+H_2O \rightarrow HOI+HX} \qquad \text{(R1.30)}$$

$$\mathrm{HOI+ArH \rightarrow ArI+H_2O} \qquad \text{(R1.31)}$$

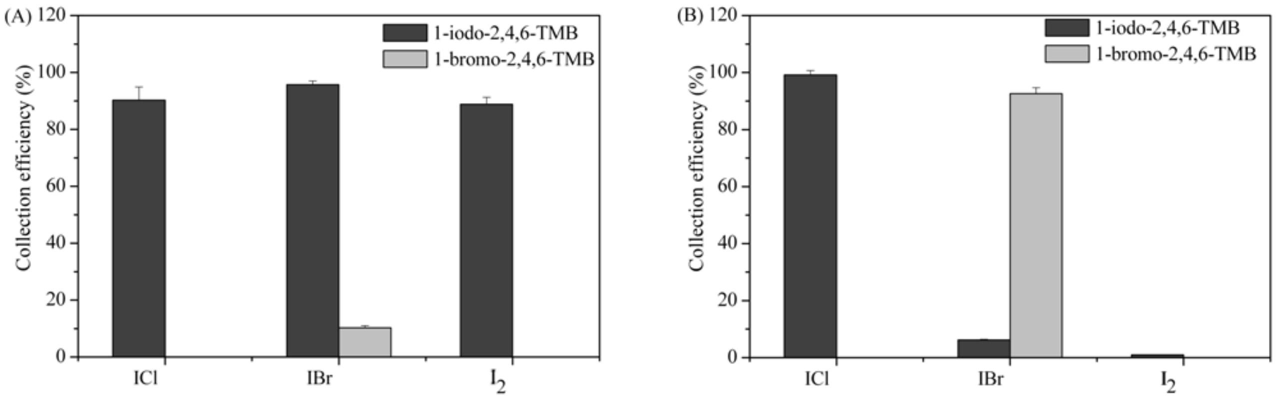

Figure 1.5 Collection efficiency of ICl, IBr, and I_2 by aqueous 1,3,5-TMB-loaded impinger (a) and by 1,3,5-TMB-coated denuder (b).

As such, this method can be used for total iodine measurements of a mixture of the three iodine species (2.6–11.2% error as I). However, the aim was to differentiate and quantify these species since the potential influences of iodine on tropospheric processes are species dependent. Therefore, other reaction media were investigated. In methanolic solution of 1,3,5-TMB the collection efficiency of IBr and I_2 decrease to 21.5% and 6.93%, respectively;

whereas a relatively high efficiency of 78.7% is maintained for ICl. In CCl_4 solution of 1,3,5-TMB the iodination yields drop further; however, IBr delivers bromination derivative 1-bromo-2,4,6-trimethoxybenzene (1-bromo-2,4,6-TMB) with an efficiency as high as 88.2%. Therefore, it is possible to directly measure individual iodine species ICl and IBr and to calculate the I_2 concentration as the difference between total iodine (ICl +IBr + I_2) and ICl + IBr by the use of different reaction media for impinger operation.

However, it should be noted that ICl can be overestimated when either IBr or I_2 is present in significant higher concentrations than ICl since both IBr and I_2 also moderately deliver the same iodination derivative in methanolic solution of 1,3,5-TMB. As a consequence, the concentration of I_2 will be underestimated. To address this issue in this paper we use a denuder–impinger coupled system (see Figure 1.6). ICl and IBr are quantitatively collected in the front denuder based on in situ selective derivatization (i.e., ICl and IBr are converted into 1-iodo-2,4,6-TMB and 1-bromo-2,4,6-TMB, respectively), with respective collection efficiencies of 99.2% for ICl and 92.6% for IBr at 500 mL min^{-1} gas flow rate. The collection efficiency for I_2 is lower than 1% in the same denuder system (see Figure 1.5b). Therefore, I_2 will pass through the denuder tube and will be collected by the aqueous 1,3,5-TMB loaded impinger downstream of the denuder.

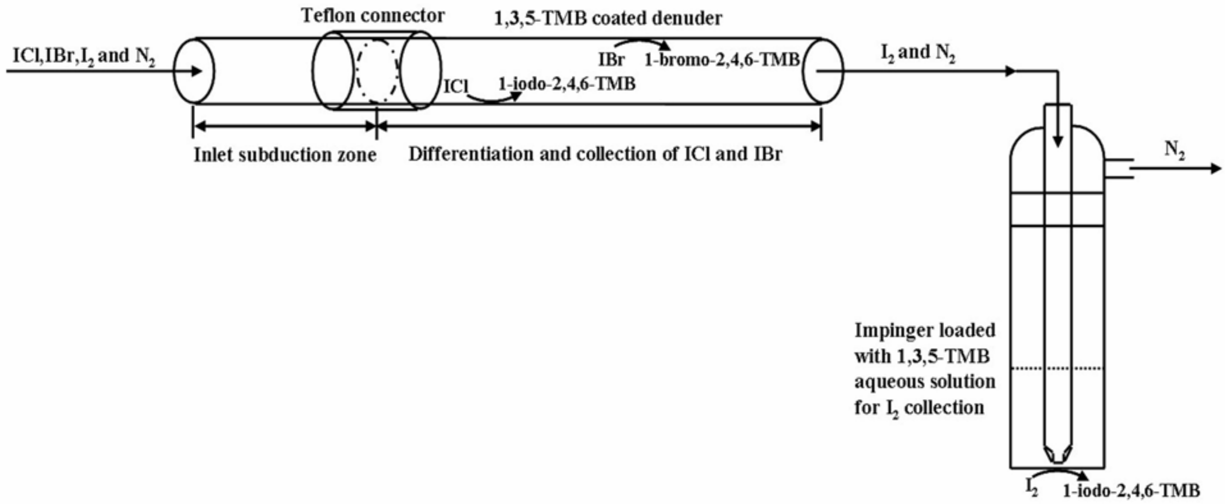

Figure 1.6 Schematic diagram of the denuder–impinger coupling system.

1.3.3 Extensive Evaluation of a Diffusion Denuder for the Quantification of Atmospheric Stable and Radioactive Molecular Iodine

Interest in iodine atmospheric chemistry has been greatly stimulated in the past few years by the suggestion that I_2 rather than iodocarbons is the most important precursor for coast new particle formation and also the dominant source of coastal reactive iodine in the MBL [O'Dowd and Hoffmann, 2005; Saiz-Lopez and Plane, 2004; McFiggans et al., 2004]. Although some progress has been made, a number of uncertainties about the sources, sinks, and the recycling of iodine remain. One of the problems in this field is the lack of a readily accessible, straightforward and robust technique to measure gaseous I_2 at low concentrations approaching those encountered in the atmosphere. Typically, atmospheric measurements of molecular iodine are made by the use of LP-DOAS [Saiz-Lopez and Plane, 2004; Peters et al., 2005] or BBCRDS [Saiz-Lopez et al., 2006b]. However, the limits of detection of these spectrometric methods are in general relatively high (~ 20 ppt), which makes the accurate quantification of daytime I_2 still difficult and therefore obscures our understanding on the atmospheric processes of iodine (for example, the process of coastal new particle bursts), since models have predicted that even very small amount of I_2 under daytime conditions could strongly affect the marine atmosphere [Peters et al., 2005]. Although the impinger-based method [Huang and Hoffmann, 2009] provides an alternative for the "single-point" in situ measurements of molecular iodine, a front filter (upstream of the impinger) is typically required to remove particulate iodine, which is then subjected to the potential artifacts resulting from particle-to-gas and gas-to-particle conversion reactions as well as the retention of gaseous I_2 on the prefilter either directly on the filter material or on concurrently collected particulate matter.

The aims of this paper were to develop a denuder-based method for gaseous I_2 measurements since denuders can separate gaseous compounds from their particulate counterparts. At first, in situ derivatization chemicals such as nitrobenzene, phenol, salicylic acid, and *N,N*-dialkylaniline are used for the sampling of gaseous I_2. However, quantitative collection is not achieved, even in combination with glycerol. α-cyclodextrin (α-CD), which is well-known to form inclusion complex with iodine in aqueous solution, is then tried as denuder coating for gaseous I_2 collection. However, the collection efficiencies vary widely with the sources of α-CD delivered by different chemical companies (ranging from about 40% to 87%). The value drops further to 30% when anhydrous α-CD is applied but increases to 94% in the case of additional water present in the inner wall of denuder, indicating that water molecules, which could lead to the hydrolysis of a small fraction of entrapped gaseous I_2 to form I^-, play an active role in such inclusion complex formation. We therefore use trace of iodide ions as α-CD coating spike to improve the collection efficiency (see Figure 1.7).

A collection efficiency larger than 98% is obtained at a molar ratio of 1:3 of I^- to I_2 and 950:1 of α-CD to I_2. After sample collection and subsequent water extraction the collected inorganic iodine is converted to organic species by reaction with an organic derivatization reagent for GC–MS measurement. Quantitative release/derivatization is observed after about 120 min. Since both the entrapped I_2 and spiked I^- deliver the same derivative the isotopic iodide $^{129}I^-$ is used to differentiate the entrapped I_2 from the spiked I^-. It is found that no isotopic effect takes place during the derivatization process and that the derivatives of ^{127}I and their isotopic analogues have the same retention behavior in GC separation and experience the same degree of ionization in MS analysis.

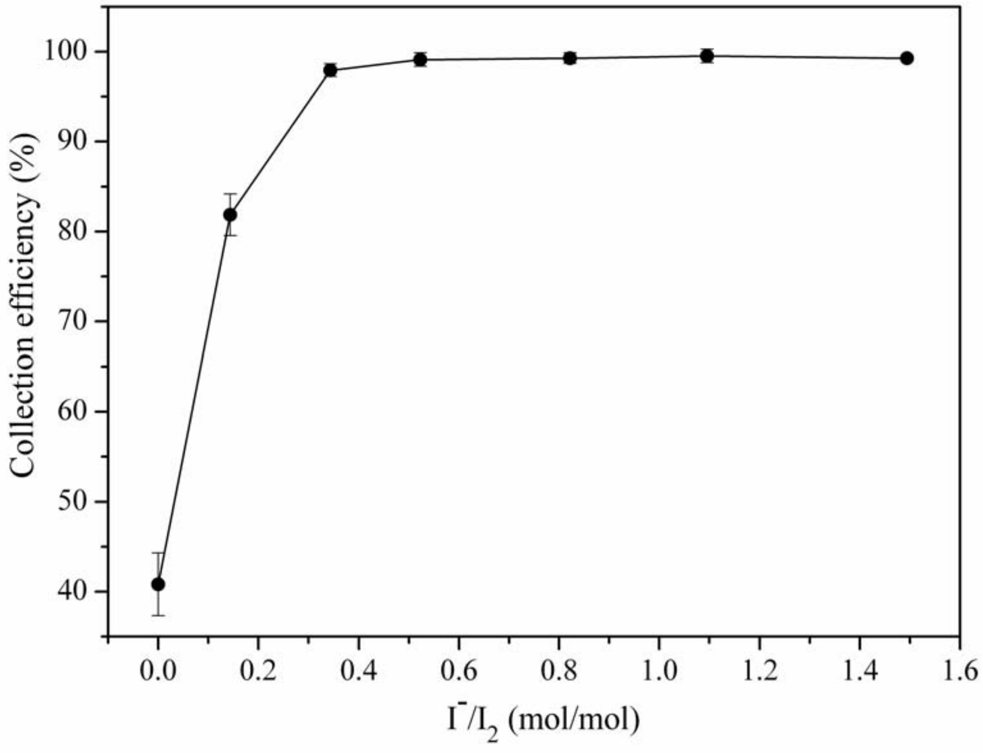

Figure 1.7 Effect of I^- on the gaseous I_2 collection by α-CD-coated denuder.

The potential use of this denuder sampling system in the collection and differentiation of radioactive I_2 is a straightforward variation of the technique if $^{127}I^-$ instead of $^{129}I^-$ is spiked into the coatings. The capability of this technique to measure radioactive I_2 is of special interest because the urgency of radioactive molecular iodine for environmental and human health has arisen due to increasing human nuclear activities. In view of the ultra-low concentration levels of radioactive I_2 in the atmosphere, we use 12 individual denuder tubes in parallel to compensate for the low sampling flow rate. An exemplary measurement of ambient $^{129}I_2$ (for the first time) has been carried out at Mainz, Germany.

1.3.4 Development of a Coupled Diffusion Denuder System Combined with Gas Chromatography/Mass Spectrometry for the Separation and Quantification of Molecular Iodine and the Activated Iodine Compounds Iodine Monochloride and Hypoiodous Acid in the Marine Atmosphere

As described above, 1,3,5-TMB coating is suitable for the collection of gaseous ICl and IBr in the denuder with a very satisfactory efficiency but a very poor sink for gaseous I_2 collection. On the other hand, the α-CD/$^{129}I^-$ coating is a very efficient coating material for gaseous I_2 collection. Therefore, in this work, we use a coupled denuder system which consists of a 1,3,5-TMB-coated denuder as front-denuder coupled upstream of an α-CD/$^{129}I^-$-coated denuder to separate and quantitatively collect gaseous activated iodine compounds (AICs; ICl and HOI) and I_2 in combination with a GC–MS method. In the paper, we use ICl as a surrogate for AICs since HOI possess a positively polarized iodine atom which enhances its electrophilic character and makes the molecule, like ICl, very reactive toward organic materials (what is demonstrated to be true by further experiments, see below). The experimental collection efficiencies for AICs and I_2 are tested and the results show close agreements between experimental and theoretical values at a gas flow rate between 300 and 1800 mL min^{-1}. The operation of both denuder systems is demonstrated to be independent of relative humidity and storage period (at least 2 weeks prior to and after sampling). The gas mixture of ICl and I_2 at different mixing ratio is well separated and quantitatively collected by the coupled system. The precision and accuracy range from 1.8% to 7.9% and from 1.5% to 6.8%, respectively. The sampling time can be as long as 180 min at a flow rate of 500 mL min^{-1} and the detection limits are achieved at sub-ppt level. Such low detection limits are beneficial for the measurements of gaseous iodine species in some atmospheric domains with rather low iodine fluxes such as open sea and polar regions. Also we discuss the potential interference species and document that volatile organohalogens, IO, and OIO will not contribute to the AICs and I_2 measurements.

In addition, the results of the first application of the method for field measurements at the Mace Head Atmospheric Research Station (Ireland), carried out between 29 August and 2 September, 2007, are presented. Details about the diurnal variations of I_2 and their implication to the atmosphere are discussed in another paper. It is found that the mixing ratios of AICs during the period of 5 days are correlated with the levels of I_2 with a maximum value up to 30.2 ppt at night and 6.0 ppt during the day. However, the formation pathways and concentrations of AICs are not well-known up to now. HOI is believed to be formed by the reaction of I atoms with HO_2 radicals and therefore is expected to be present during the day. The formation of gaseous interhalogens including ICl is currently believed to be linked to the release from sea salt particles following uptake and heterogeneous chemistry of HOI [Vogt et al., 1999; McFiggans et al., 2002]. It is apparent that a better understanding of the AICs chemistry could be achieved by further laboratory experiments and field measurements using the method developed here.

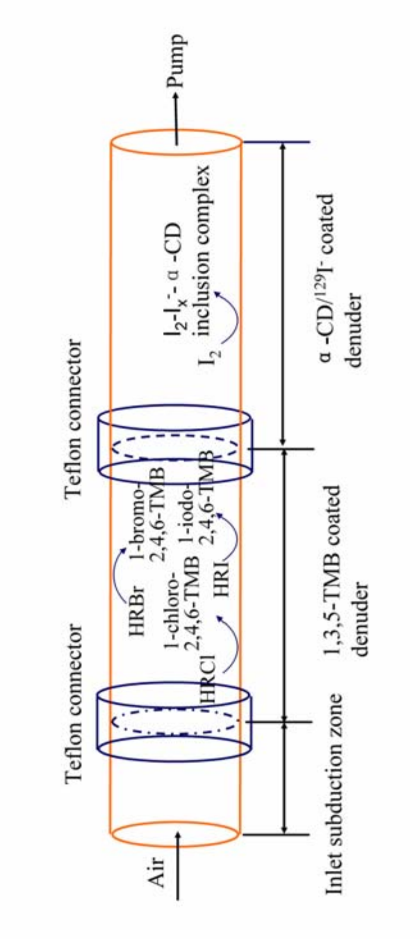

Figure 1.8 Schematic diagram of the coupled denuder system and the reaction scheme occurred.

Beside the quantification for ICl and HOI (AICs, also termed Highly Reactive Iodine, HRI) which has been presented in this paper, we further test and demonstrate that the 1,3,5-TMB-coated denuder is capable of quantitatively collecting Cl_2, HOCl (termed hereafter Highly Reactive Chlorine, HRCl), Br_2, BrCl, IBr, HOBr (termed hereafter Highly Reactive Bromine, HRBr). HRCl and HRBr, like HRI, are converted in situ to 1-chloro-2,4,6-trimethoxybenzene (1-chloro-2,4,6-TMB) and 1-bromo-2,4,6-trimethoxybenzene (1-bromo-2,4,6-TMB), respectively (see Figure 1.8). The chlorination, bromination, and iodination derivatives can be separated by GC and determined by MS. Figure 1.9 shows a representative chromatogram for these halogen species measurements and Figure 1.10 shows the concentration levels of HRCl, HRBr, and HRI for two selected days.

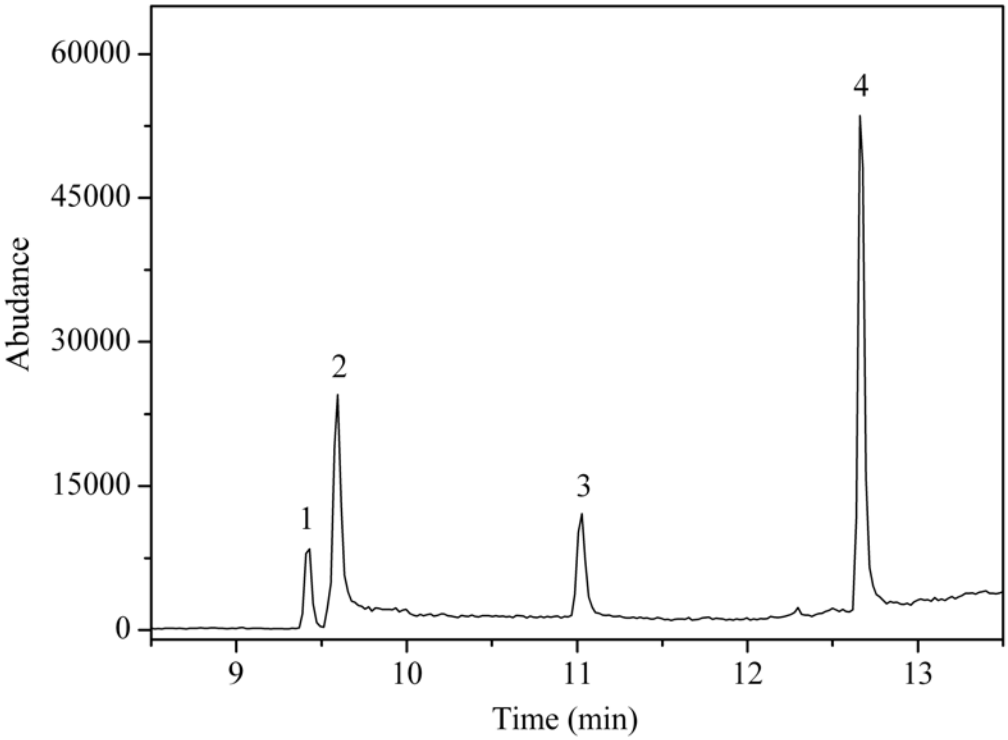

Figure 1.9 Typical chromatogram obtained by GC–MS under selective ion monitoring model. Peak assignments: (1) 2,4,6-tribromoanisole, internal standard, (2) 1-chloro-2,4,6-TMB, (3) 1-bromo-2,4,6-TMB, and (4) 1-iodo-2,4,6-TMB.

The denuder/GC–MS method developed in this work, therefore, provides an attractive protocol for halogen species analysis for atmospheric chemistry research. Besides the field measurements at the west coast of Ireland in 2007, an intensive field campaign has been carried out at the same location in 2009 to get a better understanding on the source and cycling of these highly reactive halogen species. Furthermore, in cooperation with the British Antarctica Survey the presented method has been used—for the first time—in Antarctica in early 2009. The samples of these field measurements still have to be analyzed and—if appropriate—the results will be presented separately in the near future.

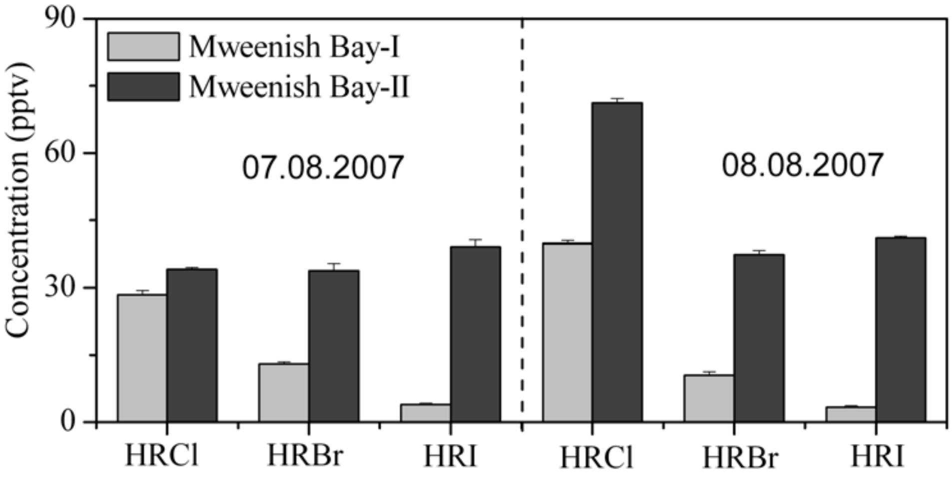

Figure 1.10 Exemplary concentration of HRCl, HRBr, and HRI in the coastal MBL.

1.3.5 Observations of High Concentrations of I_2 and IO in Coastal Air Supporting Iodine-oxide Driven Coastal New Particle Formation

Coastal new particle formation events are of particular concern since these processes could affect the earth's radiative budget, climate change and air quality levels. Interest in this field has been greatly stimulated in the past few years by the observation of iodine induced new particle bursts [O'Dowd and Hoffmann, 2005]. The current consensus is that coastal nucleation events are driven by iodine vapours that undergo rapid chemical reactions to produce condensable iodine oxides leading to nucleation and growth of new particles. The primary source of the condensable iodine vapours is suggested to be molecular iodine and theoretical studies have predicted that the concentrations of gaseous I_2 and IO of the order of 80–100 ppt and 40–50 ppt, respectively, are required in coastal air to account for iodine-oxide driven coastal new particle formation events to occur [Saiz-Lopez et al., 2006b]; . However, measurements reported to date (i.e., ~20 ppt I_2, $\leq$ 10 ppt IO) have not supported the required model predictions, mostly because these measurements are carried out by LP-DOAS which provides distance-averaged measurements and therefore can not reveal the real concentrations of these species in the coastal atmosphere.

The aim was to get a better understanding of the impact of iodine species on new particle formation by taking measurements during the periods of low tidal seaweed exposure at the local shoreline. The ambient measurements are carried out in N. E. Atlantic marine air on the west coast of Ireland. Gaseous I_2 is measured by the coupled denuder system in combination with a GC–MS method developed in this work, which provides "single-point" in situ I_2 concentration levels at the coastal site. IO is measured by LP-DOAS with some additional measurements being taken above the exposed seaweed beds at low tide. Extraordinarily high concentrations of I_2 and IO are observed. The maximum mixing ratios of daytime I_2 and IO over the seaweed beds during low tide are 302 ppt and 35 ppt, respectively. The IO diurnal profile is well consistent with the characteristics of I_2 emission at the local shoreline. I_2 distribution is found to be rather inhomogeneous, even at the inter-tidal zone, but closely related to the macroalgae biomass abundance. New particle formation bursts are frequently observed during daytime hours with the concentrations up to 4.5×10^5 particles cm^{-3} during low-tide conditions, and the concentrations of ultra-fine particles are positively correlated with the IO concentrations. Considering the constraints set out in theoretical studies for new particle formation *via* condensation of condensable iodine oxide vapours, our results clearly demonstrate that the molecular iodine and iodine monoxide concentrations in coastal air are sufficient to meet the theoretical precursor concentrations required to drive intensive coastal new-particle formation from higher order condensable iodine oxides.

1.3.6 In Situ Measurements of Molecular Iodine in the Marine Boundary Layer: The Link to Macroalgal Species and the Implications for O_3, IO, OIO and NO_x

Since molecular iodine was suggested to be the dominant source of coastal reactive iodine in the MBL during the 2002 NAMBLEX field campaign at Mace Head (Ireland) [Saiz-Lopez and Plane, 2004], it has become well-established by laboratory studies that the emission of this molecular iodine from low tidal macroalgal exposure is indeed a most important process responsible for the observed tropospheric iodine level [McFiggans et al., 2004; Küpper et al., 2008; Dixneuf et al., 2009]. However, evidence from field measurements (i.e., "hot spots") is still not quite clear, nor is the source strength, since most of the current data are observed by LP-DOAS which provides only spatial mean values of molecular iodine. Also uncertainties about the impact of molecular iodine on the atmosphere and the linkage between molecular iodine and other atmospheric constituents are not clear so far, especially for the nighttime episode.

One of the aims of this work was to demonstrate the “hot-spot” theory of the atmospheric iodine chemistry and to reveal the real source strength of molecular iodine. When measurements are taken directly above the seaweed beds the mixing ratios of daytime I_2 are as high as 302 ppt (which could be treated as source strength since the inlet of denuder is only about 5 cm above the seaweed beds); however, shortly beyond the seaweed beds (about 100–150 m downwind of the seaweed beds) the concentration levels decrease significantly due to the rapid photolysis and the dilution effect during convection (see Figure 1.11). The results substantially support that I_2 release from seaweeds is really one of the most important sources. By taking comparison measurements we see that the mixing ratios of I_2 at Mace Head are much lower than that at Mweenish Bay. The difference of I_2 levels between these two sites could be attributed to the higher biomass density at Mweenish Bay than at Mace Head and the difference on algae species present at these two locations. Furthermore, the emission levels of I_2 are found to correlate inversely with tidal height and correlate positively with the concentration levels of O_3 in the surrounding air. The concurrent measurements show that the mixing ratios of I_2 are of the order of 10^2–10^4 higher than organic iodine such as CH_3I, CH_2I_2, C_2H_5I, CH_2BrI, and CH_2ClI.

The second aim of this work was to try to investigate the relations between molecular iodine and other gaseous constituents like ozone and iodine oxides. Over the course of the field measurements, the average and maximum values of daytime IO are 3.4 ± 1.0 and 9.5 ± 0.8 ppt for consecutive 30-day measurements at Mweenish Bay, and 1.1 ± 0.3 and 4.4 ± 0.6 ppt for consecutive 9-day measurements at Mace Head, respectively. The daytime IO concentrations are found to increase with the increase of I_2 concentrations and of the solar irradiation, suggesting the photochemical production of IO from coastal emissions of I_2. The observed maximum levels of OIO are 29.3 ppt at Mweenish Bay and 10.1 ppt at Mace Head for night-time measurements, and 38.2 ppt at Mweenish Bay and 6.5 ppt at Mace Head for daytime measurements. The processes of photochemical production of these iodine oxides could lead to tropospheric ozone destruction, which has been predicted by recent model experiments [von Glasow et al., 2004]. However, reduction in the tropospheric ozone burden through iodine released from coastal marine sources has not been verified by observations so far. During the 5-week field observations at Mweenish Bay the mixing ratios of ozone decrease during several days from the normal levels of ~40 ppt down to as low as 12 ppt and are anti-correlated with the I_2 concentrations (see Figure 1.12).

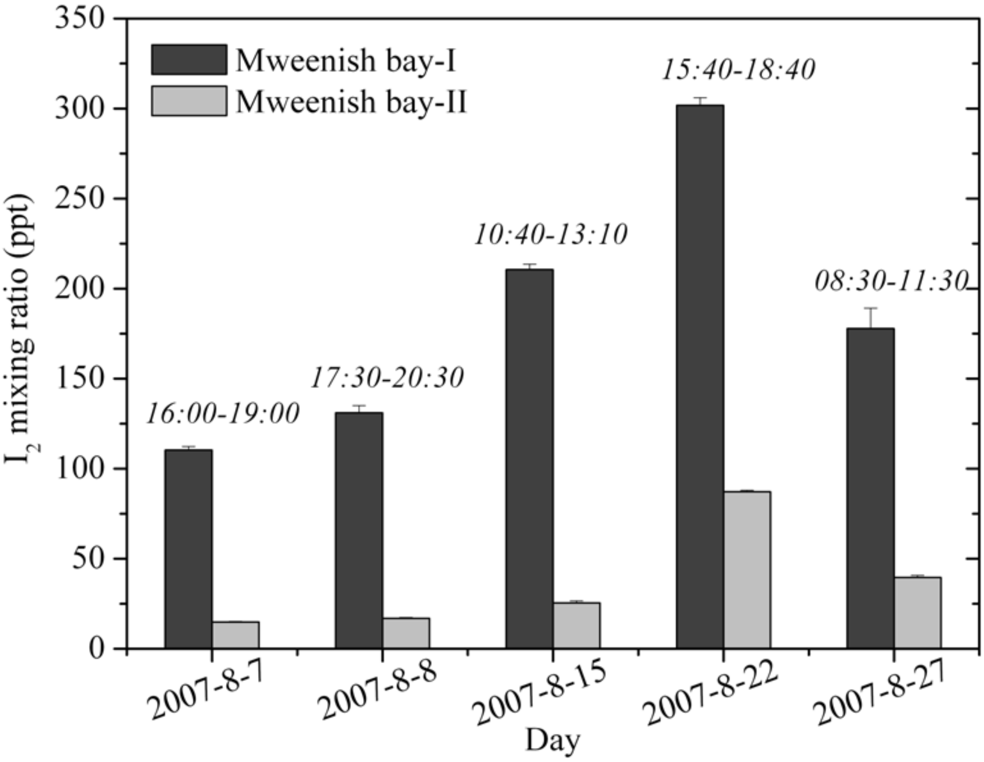

Figure 1.11 Comparison of the mixing ratio of I_2 between Mweenish Bay-I and Mweenish Bay-II. Note Mweenish Bay-I represents the measurements taken above the seaweed beds and Mweenish Bay-II represents the downwind measurements.

For daytime measurements, it strongly supports the viewpoint that photochemical production of daytime IO is related to concentration levels of O_3. For night-time observations, however, the reaction suggested below could be responsible for the night-time IO production and O_3 destruction.

$I_2 + NO_3 \rightarrow I + IONO_2$ (R1.32)

$I + O_3 \rightarrow IO + O_2$ (R1.33)

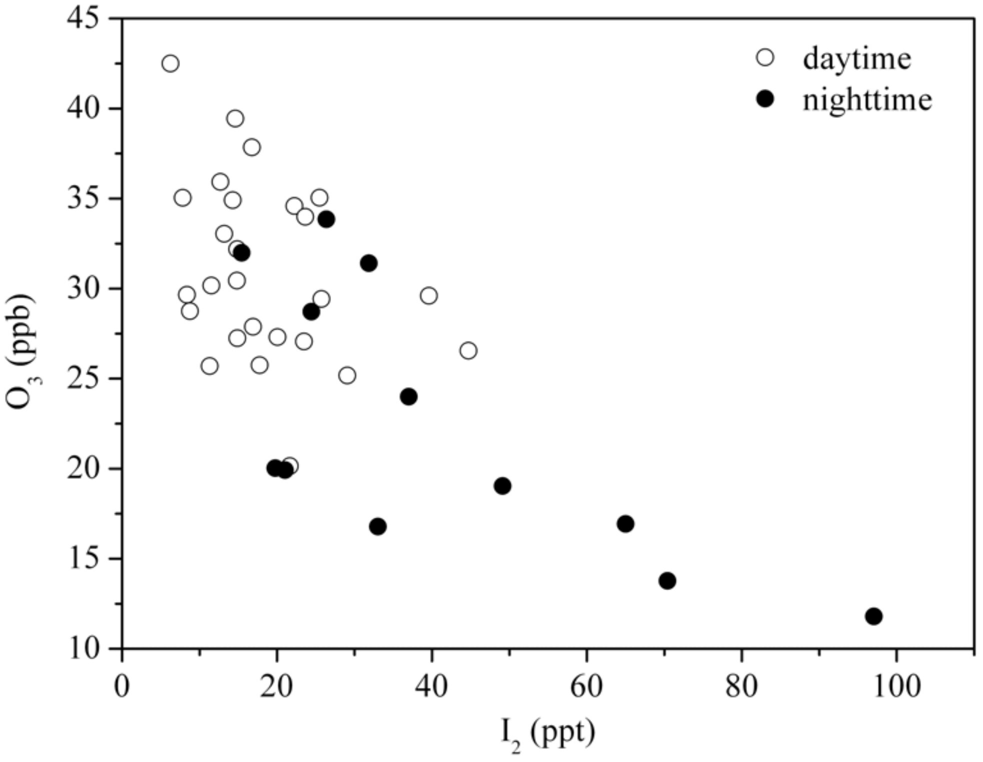

Figure 1.12 Plot of O_3 versus I_2 during ozone destruction events at Mweenish Bay.

In this work, we also take concurrent I_2 measurements by the denuder/GC–MS and the LP-DOAS technique. The results show that the denuder method records much higher concentrations of I_2 than the LP-DOAS method, for both daytime and night-time measurements. The denuder method provides the concentration levels at a single point; however, the LP-DOAS technique provides the average mixing ratios of a rather inhomogeneous distribution along the light-path of several kilometers extending over open sea (i.e., 4–14 km). These results further demonstrate that the local seaweed sources dominate the inorganic iodine chemistry in the coastal MBL.

1.4 Conclusions and Outlook

Reactive halogen species are important gaseous constituents in the atmosphere and play a key role in many aspects of tropospheric chemistry, such as oxidative capacity, ozone destruction, and particle nucleation and growth. A multitude of gas-phase reactions and gas-particle interactions occur, including participation in the cycles of sulfur and nitrogen and reactions with hydrocarbons. One of the keys to better understand these processes is to quantify HRCl, HRBr, HRI, as well as I_2, which are predicted by atmospheric numerical models to be the most important species. In this thesis, the impinger- and denuder-based sampling techniques in combination with a GC–MS method for the determination of these key species have been successfully developed. The method has been used for the first time for field measurements at the west coast of Ireland in 2007, followed by 2009-Ireland and 2009-Antarctica campaigns. A series of important and interesting results have been found, namely that in addition to I_2 high concentration levels of HRCl, HRBr and HRI are also present in the coastal MBL, that seaweeds are the local source of iodine, that the local source strength of iodine supports the observed new particle formation events in the coastal MBL, and that the presence of halogens in the coastal MBL indeed leads to ozone destruction. However, there remain many uncertainties in this field that need to be elucidated. Certainly, more laboratory studies and field measurements are required. The methods developed in this thesis will be attractive tools for laboratory- and field-based halogen-related atmospheric research, in particular (1) in the chamber-based quantification of halogens, especially interhalogens, recycling from particle-phase to gas-phase which has been predicted by models, (2) in the sources identification and source strength measurements in the field, especially in the coastal MBL and polar regions, (3) in the investigation of halogens concentration levels and their distribution over the open sea by research vessel based measurements, (4) in the investigation of vertical distribution of halogens from the lower troposphere up to the stratosphere by taking airborne measurements (e.g., aircraft or balloon), and (5) in a better understanding of coastal new particle formation process by concurrent measurements of iodine species, sulfur species, ammonia and amine compounds to determine which constituents are the precursor vapors for nucleation.

In general, it could be expected that, with the current interest in halogen chemistry, more techniques will be developed to better identify and quantify these key atmospheric halogen species (e.g., “single-point” in situ on-line measurement technique with better time resolution, the differentiation of individual highly reactive halogen species) and that our understanding about the halogen atmospheric chemistry will become clearer in the near future.

1.5 References

Adams, J. W., and Cox, R. A.: Halogen chemistry of the marine boundary layer, *J. Phys. IV*, 12, 105–124, **2002**.

Adams, J. W., Holmes, N. S., and Crowley, J. N.: Uptake and reaction of HOBr on frozen and dry NaCl/NaBr surfaces between 253 and 233 K, *Atmos. Chem. Phys.*, 2, 79–91, **2002**.

Alicke, B., Hebestreit, K., Stutz, J., and Platt, U.: Iodine oxide in the marine boundary layer, *Nature*, 397, 572–573, **1999**.

Allan, B. J., McFiggans, G., Plane, J. M. C., and Coe, H.: Observations of iodine monoxide in the remote marine boundary layer, *J. Geophys. Res.-Atmos.*, 105, 14363–14369, **2000**.

Allan, B. J., Plane, J. M. C., and McFiggans, G.: Observations of OIO in the remote marine boundary layer, *Geophys. Res. Lett.*, 28, 1945–1948, **2001**.

Allan, W., Lowe, D. C., and Cainey, J. M.: Active chlorine in the remote marine boundary layer: Modeling anomalous measurements of $\delta^{13}C$ in methane, *Geophys. Res. Lett.*, 28, 3239–3242, **2001**.

Allan, W., Lowe, D. C., Gomez, A. J., Struthers, H., and Brailsford, G. W.: Interannual variation of ^{13}C in tropospheric methane: Implications for a possible atomic chlorine sink in the marine boundary layer, *J. Geophys. Res.-Atmos.*, 110, D11306, doi:10.1029/2004JD005650, **2005**.

Aranda, A., Bras, G. L., Verdet, G. L., and Poulet, G.: The BrO + CH_3O_2 reaction: kinetics and role in the atmospheric ozone budget, *Geophys. Res. Lett.*, *24*, 2745–2748, **1997**.

Ariya, P. A., Khalizov, A., and Gidas, A.: Reactions of gaseous mercury with atomic and molecular halogens: kinetics, product studies, and atmospheric implications, *J. Phys. Chem. A*, 106, 7310–7320, **2002**.

Avallone, L. M., Toohey, D. W., Fortin, T. J., McKinney, K. A., and Fuentes, J. D.: In situ measurements of bromine oxide at two high-latitude boundary layer sites: Implications of variability, *J. Geophys. Res.-Atmos.*, 108, D34089, doi: 10.1029/2002JD002843, **2003**.

Baker, J. M., Sturges, W. T., Sugier, J., Sunnenberg, G., Lovett, A. A., Reeves, C. E., Nightingale, P. D., and Penkett, S. A.: Emissions of CH_3Br, organochlorines, and organoiodines from temperate macroalgae, *Chemosphere*, 3, 93–106, **2001**.

Bale, C. S. E., Ingham, T., Commane, R., Heard, D. E., and Bloss, W. J.: Novel measurements of atmospheric iodine species by resonance fluorescence, *J. Atmos. Chem.*, 60, 51–70, **2008**.

Barrie, L. A., Bottenheim, J. W., Schnell, R. C., Crutzen, P. J., and Rasmussen, R. A.: Ozone destruction and photochemical reactions at polar sunrise in the lower Arctic atmosphere, *Nature*, 334, 138–141, **1988**.

Bilde, M., Wallington, T. J., Ferronato, C., Orlando, J. J., Tyndall, G. S., Estupinan, E., and Haberkorn, S.: Atmospheric chemistry of CH_2BrCl, $CHBrCl_2$, $CHBr_2Cl$, $CF_3CHBrCl$, and CBr_2Cl_2, *J. Phys. Chem. A*, 102, 1976–1986, **1998**.

Bitter, M., Ball, S. M., Povey, I. M., and Jones, R. L.: A broadband cavity ringdown spectrometer for in-situ measurements of atmospheric trace gases, *Atmos. Chem. Phys.*, 5, 2547–2560, **2005**.

Bloss, W. J., Lee, J. D., Johnson, G. P., Sommariva, R., Heard, D. E., Saiz-Lopez, A., Plane,

J. M. C., McFiggans, G., Coe, H., Flynn, M., Williams, P., Rickard, A. R., and Fleming, Z. L.: Impact of halogen monoxide chemistry upon boundary layer OH and HO_2 concentrations at a coastal site, *Geophys. Res. Lett.*, 32, L06814, **2005**.

Bloss, W. J., Lee, J. D., Heard, D. E., Salmon, R. A., Bauguitte, S. J.-B., Roscoe, H. K., and Jones, A. E.: Observations of OH and HO_2 radicals in coastal Antarctica, *Atmos. Chem. Phys.*, 7, 4171–4185, **2007**.

Boudries, H., and Bottenheim, J. W.: Cl and Br atom concentrations during a surface boundary layer ozone depletion event in the Canadian High Arctic, *Geophys. Res. Lett.*, 27, 517–520, **2000**.

Braban, C. F., Adams, J. W., Rodriguez, D., Cox, R. A., Crowley, J. N., and Schuster, G.: Heterogeneous reactions of HOI, ICl and IBr on sea salt and sea salt proxies, *Phys. Chem. Chem. Phys.*, 9, 3136–3148, **2007**.

Burkholder, J. B., Curtius, J., Ravishankara, A. R., and Lovejoy, E. R.: Laboratory studies of the homogeneous nucleation of iodine oxides, *Atmos. Chem. Phys.*, *4*, 19–34, **2004**.

Carpenter, L. J.: Iodine in the marine boundary layer, *Chem. Rev.*, 103, 4953–4962, **2003**.

Carpenter, L. J., and Liss, P. S.: On temperate sources of bromoform and other reactive organic bromine gases, *J. Geophys. Res.-Atmos.,* 105, 20539–20547, **2000**.

Carpenter, L. J., Jones, C. E., Dunk, R. M., Hornsby, K. E., and Woeltjen, J.: Air-sea fluxes of biogenic bromine from the tropical and North Atlantic Ocean, *Atmos. Chem. Phys.*, 9, 1805–1816, **2009**.

Chambers, R. M., Heard, A. C., and Wayne, R. P.: Inorganic gas-phase reactions of the nitrate radical: I_2+NO_3 and I+NO_3, *J. Phys. Chem.*, 96, 3321–3331, **1992**.

Dasgupta, P. K., In *Sampling and sample preparation techniques in field and laboratory*; Pawliszyn, J., Ed.; Elsevier: Amsterdam, The Netherlands, pp 97–160, **2002**.

Dillon, T. J., Karunanandan, R., and Crowley, J. N.: The reaction of IO with CH_3SCH_3: products and temperature dependent rate coefficients by laser induced fluorescence, *Phys. Chem. Chem. Phys.*, 8, 847–855, **2006**.

Dixneuf, S., Ruth, A. A., Vaughan, S., Varma, R. M., and Orphal, J.: The time dependence of molecular iodine emission from Laminaria digitata, *Atmos. Chem. Phys.*, *9*, 823–829, **2009**.

Fan, S. M., and Jacob, D. J.: Surface ozone depletion in Arctic spring sustained by bromine reactions on aerosols, *Nature*, 359, 522–524, **1992**.

Fickert, S., Adams, J. W., and Crowley, J. N.: Activation of Br_2 and BrCl via uptake of HOBr onto aqueous salt solutions. *J. Geophys. Res.-Atmos.*, 104, 23719–23728, **1999**.

Finlayson-Pitts, B. J., Ezell, M. J., and Pitts, J. N.: Formation of chemically active chlorine compounds by reactions of atmospheric NaCl particles with gaseous N_2O_5 and $ClONO_2$, *Nature*, 337**,** 241–244, **1989**.

Finley, B. D., and Saltzman, E. S.: Measurement of Cl_2 in coastal urban air, *Geophys. Res. Lett.*, 33, L11809, doi:10.1029/2006GL025799, **2006**.

Finley, B. D., and Saltzman, E. S.: Observations of Cl_2, Br_2, and I_2 in coastal marine air, *J. Geophys. Res.-Atmos.*, 113, D21301, doi:10.1029/2008JD010269, **2008**.

Foster, K. L., Plastridge, R. A., Bottenheim, J. W., Shepson, P. B., Finlayson-Pitts, B. J., and Spicer, C. W.: The role of Br_2 and BrCl in surface ozone destruction at Polar sunrise, *Science*, 291, 471–474, **2001**.

Fuller, E. N., Schettler, P. D., and Giddings, J. C.: A new method for prediction of binary gas-phase diffusion coefficients, *Ind. Eng. Chem.*, 58, 19–27, **1966**.

Gäbler, H.-E., and Heumann, K. G.: Determination of atmospheric iodine species using a system of specifically prepared filters and IDMS, *Fresenius J. Anal. Chem.*, 345, 53–59, **1993**.

Garland, J. A., and Curtis, H.: Emission of iodine from the sea surface in the presence of ozone, *J. Geophys. Res.-Atmos.*, 86, 3183–3186, **1981**.

Gershenzon, M. Y., Il'in, S., Fedetov, N. G., Gershenzon, Y. M., Aparina, E. V., and Zelenov, W.: The mechanism of reactive NO_3 uptake on dry NaX (X=Cl, Br), *J. Atmos. Chem.*, 34, 119–135, **1999**.

Gormley, P. G., and Kennedy, M.: Diffusion from a stream flowing through a cylindrical tube, *Proc. Roy. Irish. Acad. A*, 52, 163–169, **1949**.

Guimbaud, C., Grannas, A. M., Shepson, P. B., Fuentes, J. D., Boudries, H., Bottenheim, J. W., Domine, F., Houdier, S., Perrier, S., Biesenthal, T. B., and Splawn, B. G.: Snowpack processing of acetaldehyde and acetone in the Arctic atmospheric boundary layer, *Atmos. Environ.*, 36, 2743–2752, **2002**.

Hebestreit, K., Stutz, J., Rosen, D., Matveiv, V., Peleg, M., Luria, M., and Platt, U.: DOAS measurements of tropospheric bromine oxide in mid-latitudes, *Science*, 283, 55–57, **1999**.

Hinds, W. C., Aerosol Technology: Properties, behavior, and measurement of airborne particles, send edition, John Wiley & Sons, Hoboken, New Jersey, **1999**.

Hoffmann, T., O'Dowd, C. D., and Seinfeld, J. H.: Iodine oxide homogeneous nucleation: An explanation for coastal new particle production, *Geophys. Res. Lett.*, 28, 1949–1952, **2001**.

Holmes, N., Adams, J. W., and Crowley, J. N.: Uptake and reaction of HOI and $IONO_2$ on frozen and dry NaCl/NaBr surfaces and H_2SO_4, *Phys. Chem. Chem. Phys.*, 3, 1679–1687, **2001**.

Hönninger, G., Leser, H., Sebastián, O., and Platt, U.: Ground-based measurements of halogen oxides at the Hudson Bay by active longpath DOAS and passive MAX-DOAS, *Geophys. Res. Lett.*, 31, L04111, doi:10.1029/2003GL018982, **2004**.

Huang, R.-J., and Hoffmann, T.: A denuder–impinger system with in situ derivatization followed by gas chromatography–mass spectrometry for the determination of gaseous iodine-containing halogen species, *J. Chromatogr. A.*, 1210, 135–141, **2008**.

Huang, R.-J., and Hoffmann, T.: Development of a coupled diffusion denuder system combined with gas chromatography/mass spectrometry for the separation and quantification of molecular iodine and the activated iodine compounds iodine monochloride and hypoiodous acid in the marine atmosphere, *Anal. Chem.*, 81, 1777–1783, **2009**.

Huang, R.-J., Seitz, K., Buxmann, J., Hornsby, K. E., Carpenter, L. J., Platt, U., and Hoffmann, T.: In situ measurements of molecular iodine in the marine boundary layer: the link to macroalgal species and the implications for O_3, IO, OIO and NO_x, *Atmos. Chem. Phys. Discuss.*, accepted, **2009a**.

Huang, R.-J., Seitz, K., O'Dowd, C. D., Platt, U., and Hoffmann T.: Observations of high concentrations of I_2 and IO in coastal air supporting iodine-oxide driven coastal new particle formation, *Geophys. Res. Lett.*, accepted, **2009b**.

Impey, G. A., Shepson, P. B., Hastie, D. R., and Barrie, L. A.: Measurement technique for the determination of photolyzable chlorine and bromine in the atmosphere, *J. Geophys.*

Res.-Atmos., 102, 15999–16004, **1997a**.

Impey, G. A., Shepson, P. B., Hastie, D. R., Barrie, L. A., and Anlauf, K. G.: Measurements of photolyzable chlorine and bromine during the Polar Sunrise Experiment 1995, *J. Geophys. Res.-Atmos.*, 102, 16005–16010, **1997b**.

Impey, G. A., Mihele, C. M., Anlauf, K. G., Barrie, L. A., Hastie, D. R., and Shepson, P. B.: Measurements of photolyzable halogen compounds and bromine radicals during the Polar Sunrise Experiment 1997, *J. Atmos. Chem.*, 34, 21–37, **1999**.

Ivey, M. M., and Foster, K.: Mass spectrometer characterization of halogen gases in air at atmospheric pressure, *Anal. Chem.*, 77, 1467–1472, **2005**.

Jobson, B. T., Niki, H., Yokouchi, Y., Bottenheim, J., Hopper, F., and Leaitch, R.: Measurements of C_2–C_6 hydrocarbons during the Polar Sunrise 1992 Experiment: Evidence for Cl atom and Br atom chemistry, *J. Geophys. Res.-Atmos*, 99, 25355–25368, **1994**.

Kaltsoyannis, N., and Plane, J. M. C.: Quantum chemical calculations on a selection of iodine-containing species (IO, OIO, INO_3, $(IO)_2$, I_2O_3, I_2O_4 and I_2O_5) of importance in the atmosphere, *Phys. Chem. Chem. Phys.*, 10, 1723–1733, **2008**.

Karaiskakis, G., and Gavril, D.: Determination of diffusion coefficients by gas chromatography, *J. Chromatogr. A*, 1037, 147–189, **2004**.

Keene, W. C., and Savoie, D. L.: The pH of deliquesced sea-salt aerosol in polluted marine air, *Geophys. Res. Lett.*, 25, 2181–2184, **1998**.

Keene, W. C., Maben, J. R., Pszenny, A. A. P., and Galloway, J. N.: Measurement technique for inorganic chlorine gases in the marine boundary layer, *Environ. Sci. Technol.*, 27, 866–847, **1993**.

Keene, W. C., Khalil, M. A. K., Erickson, D. J., McCulloch, A., Graedel, T. E., Lobert, J. M., Aucott, M. L., Gong, S.-L., Harper, D. B., Kleimen, G., Midgley, P., Moore, R. M., Seuzaret, C., Sturges, W. T., Benkovitz, C. M., Koropalov, V., Barrie, L. A., and Li, Y.-F.: Composite global emissions of reactive chlorine from anthropogenic and natural sources: reactive chlorine emissions inventory. *J. Geophys. Res.-Atmos.*, 104, 8429–8440, **1999**.

Keene, W. C., Stutz, J., Pszenny, A. A. P., Maben, J. R., Fischer, E. V., Smith, A. M., von Glasow, R., Pechtl, S., Sive, B. C., and Varner, R. K.: Inorganic chlorine and bromine in coastal New England air during summer, *J. Geophys. Res.-Atmos.*, 112, D10S12, doi:10.1029/2006JD007689, **2007**.

Khalil, M. A. K., and Rasmussen, R. A.: Atmospheric methyl chloride, *Atmos. Environ.*, 33, 1305–1321,**1999a**.

Khalil, M. A. K., and Rasmussen, R. A.: Atmospheric chloroform, *Atmos. Environ.*, 33, 1151–1158, **1999b**.

Khalil, M. A. K., Moore, R. M., Harper, D. B., Lobert, J. M., Erickson, D. J., Koropalov, V., Sturges, W. T., and Keene, W. C.: Natural emissions of chlorine-containing gases: Reactive Chlorine Emissions Inventory, *Geophys. Res.-Atmos.*, 104**,** 8333–8346, **1999**.

Klick, S., and Abrahamsson, K. J.: Biogenic volatile iodated hydrocarbons in the ocean, *J. Geophys. Res.-Oceans.*, 97, 12683–12687, **1992**.

Kloskowski, A., Pilarczyk, M., and Namiesnik, J.: Denudation—a convenient method of isolation and enrichment of analytes, *Crit. Rev. Anal. Chem.*, 32, 301–335, **2002**.

Küpper, F. C., Carpenter, L. J., McFiggans, G. B., Palmer, C. J., Waite, T. J., Boneberg, E.

M., Woitsch, S., Weiller, M., Abela, R., Grolimund, D., Potin, P., Butler, A., Luther, G. W., Kroneck, P. M. H., Meyer-Klaucke, W., and Feiters, M. C.: Iodide accumulation provides kelp with an inorganic antioxidant impacting atmospheric chemistry. *Proc. Natl. Acad. Sci. U.S.A.*, 105, 6954–6958, **2008**.

Kurylo, M. J., Rodriguez, J. M., Andrea, M. O., Atlas, E. L., Blake, D. R., Butler, J. H., Lal, S., Lary, D. J., Midgley, P. M., Montzka, S. A., Novelli, P. C., Reeves, C. E., Simmonds, P. G., Steele, L. P., Sturges, W. T., Weiss, R. F., and Yokouchi, Y., Chapter 2: Short-lived ozone-related compounds. In: Scientific Assessment of Ozone Depletion: UNEP/WMO, Geneva, **1999**.

Lawler, M. J., Finley, B. D., Keene, W. C., Pszenny, A. A. P., Read, K. A., von Glasow, R., and Saltzman, E. S.: Pollution-enhanced reactive chlorine chemistry in the eastern tropical Atlantic boundary layer, *Geophys. Res. Lett.*, 36, L08810, doi:10.1029/2008GL036666, **2009**.

LeBras, G., and Platt, U.: A possible mechanism for combined chlorine and bromine catalyzed destruction of tropospheric ozone in the Arctic, *Geophys. Res. Lett.*, 22, 599–602, **1995**.

Li H.-J., Yokouchi, Y., and Akimoto, H.: Measurement of methyl halides in the marine atmosphere, *Atmos. Environ.*, 33, 1881–1887, **1999**.

Lobert, J. M., Butler, J. H., Montzka, S. A., Geller, L. S., Myers, R. C., and Elkins, J. W.: A net sink for atmospheric CH_3Br in the East Pacific Ocean, *Science*, 267, 1002–1005, **1995**.

Lovelock, J. E., Maggs, R. J., and Wade, R. J.: Halogenated hydrocarbons in and over the Atlantic, *Nature*, 241, 194–196, **1973**.

Martinez, T., Arnold, T., and Perner, D.: The role of bromine and chlorine chemistry for arctic ozone depletion events in Ny- Ålesund and comparison with model calculations, *Ann. Geophysicae*, 17, 941–956, **1999**.

McFiggans, G., Plane, J. M. C., Allen, B., Carpenter, L. J., Coe, H., and O'Dowd, C. D.: A modeling study of iodine chemistry in the marine boundary layer, *J. Geophys. Res.-Atmos.*, 105, 14371–14385, **2000**.

McFiggans, G., Cox, R. A., Mossinger, J. C., Allan, B. J., and Plane, J. M. C.: Active chlorine release from marine aerosols: Roles for reactive iodine and nitrogen species, *J. Geophys. Res.-Atmos.*, 107(D15), 4271, doi:10.1029/2001JD000383, **2002**.

McFiggans, G., Coe, H., Burgess, R., Allan, J., Cubison, M., Alfarra, M. R., Saunders, R., Saiz-Lopez, A., Plane, J. M. C., Wevill, D. J., Carpenter, L. J., Rickard, A. R., and Monks, P. S.: Direct evidence for coastal iodine particles from Laminaria macroalgae–linkage to emissions of molecular iodine, *Atmos. Chem. Phys.*, 4, 701–713, **2004**.

Miyake, Y., and Tsunogai, S.: Evaporation of iodine from ocean, *J. Geophys. Res.-Atmos.*, 68, 3989–3993, **1963**.

Mochida, M., Hirokawa, J., and Akimoto, H.: Unexpected large uptake of O_3 on sea salts and the observed Br_2 formation, *Geophys. Res. Lett.*, 27, 2629–2632, **2000**.

Molina, M. J., and Rowland, F. S.: Stratospheric sink for chlorofluoromethanes-chlorine atom-catalysed destruction of ozone, *Nature*, 249, 810–812, **1974**.

O’Dowd, C. D., and Hoffmann T.: Coastal new particle formation: A review of the current state-of-the-art, *Environ. Chem.*, 2, 245–255, **2005**.

O’Dowd, C. D., Jimenez, J. L., Bahreini, R., Flagan, R. C., Seinfeld, J. H., Hämer, K., Pirjola, L., Kulmala, M., Jennings, S. G., and Hoffmann, T.: Marine aerosol formation from biogenic iodine emissions, *Nature*, 417, 632–636, **2002**.

O'Driscoll, P., Lang, K., Minogue, N., and Sodeau, J.: Freezing halide ion solutions and the release of interhalogens to the atmosphere, *J. Chem. Phys. A*, 110, 4615–4618, **2006**.

Palmer, C. J., Anders, T. L., Carpenter, L. J., Küpper, F. C., and McFiggans, G. B.: Iodine and halocarbon response of Laminaria digitata to oxidative stress and links to atmospheric new particle production, *Environ. Chem.*, 2, 282–290, **2005**.

Penkett, S. A.; Jones, B. M. R.; Rycroft, M. J.; and Simmons, D. A.: An interhemispheric comparison of the concentrations of bromine compounds in the atmosphere, *Nature*, 318, 550–553, **1985**.

Perner, D., Arnold, T., Crowley, J., Klupfel, T., Martinez, M., and Seuwen, R.: The measurement of active chlorine in the atmosphere by chemical amplification, *J. Atmos. Chem.*, 34, 9–20, **1999**.

Peters, C., Pechtl, S., Stutz, J., Hebestreit, K., Hönninger, G., Heumann, K. G., Schwarz, A., Winterlik, J., and Platt, U.: Reactive and organic halogen species in three different European coastal environments, *Atmos. Chem. Phys.*, 5, 3357–3375, **2005**.

Platt, U., and Hönninger, G. H.: The role of halogen species in the troposphere, *Chemosphere*, 52, 325–338, **2003**.

Platt, U., and Janssen, C.: Observation and role of the free radicals NO_3, ClO, BrO and IO in the troposphere, *Faraday Discuss.*, 100, 175–198, **1995**.

Possanzini, M., Di Palo, V., Brancaleoni, E., Frattoni, M., and Ciccioli, P.: Dynamic system for the calibration of semi-volatile carbonyl compounds in air, *J. Chromatogr. A*, 883, 171-183, **2000**.

Pszenny, A. A. P., Keene, W. C., Jacob, D. J., Fan, S., Maben, J. R., Zetwo, M. P., Springer-Young, M., and Galloway, J. N.: Evidence of inorganic chlorine gases other than hydrogen chloride in marine surface air, *Geophys. Res. Lett.*, 20, 699–702, **1993**.

Pszenny, A. A. P., Moldanova, J., Keene, W. C., Sander, R., Maben, J. R., Martinez, M., Crutzen, P. J., Perner, D., and Prinn, R. G.: Halogen cycling and aerosol pH in the Hawaiian marine boundary layer, *Atmos. Chem. Phys.*, 4, 147–168, **2004**.

Quack, B., and Wallace, D. W. R.: Air-sea flux of bromoform: Controls, rates, and implications, *Global Biogeochem. Cycles*, 17, 1023, doi:10.1029/2002GB001890, **2003**.

Rahn, K. A., Borys, R. D., and Duce, R. A.: Tropospheric halogen gases: Inorganic and organic components, *Science*, 192, 549–550, **1976**.

Ramacher, B., Rudolph, J., and Koppmann, R.: Hydrocarbon measurements during tropospheric ozone depletion events: Evidence for halogen atom chemistry, *J. Geophys. Res.-Atmos.*, 104, 3633–3653, **1999**.

Read, K. A., Mahajan, A. S., Carpenter, L. J., Evans, M. J., Faria, B. V. E., Heard, D. E., Hopkins, J. R., Lee, J. D., Moller, S. J., Lewis, A. C., Mendes, L., McQuaid, J. B., Oetjen, H., Saiz-Lopez, A., Pilling, M. J., and Plane, J. M. C.: Extensive halogen-mediated ozone destruction over the tropical Atlantic Ocean, *Nature*, 453, 1232–1235, **2008**.

Röckmann, T., Brenninkmeijer, C. A. M., Crutzen, P. J., and Platt, U.: Short-term variations in the $^{13}C/^{12}C$ ratio of CO as a measure of Cl activation during tropospheric ozone depletion events in the Arctic, *J. Geophys. Res.-Atmos.*, 104, 1691–1697, **1999**.

Rudolph, J., Ramacher, B., Plass-Dulmer, C., Muller, K. P., and Koppmann, R.: The indirect determination of chlorine atom concentration in the troposphere from changes in the patterns of non-methane hydrocarbons, *Tellus*, 49B, 592–601, **1997**.

Saiz-Lopez, A., and Plane, J. M. C.: Novel iodine chemistry in the marine boundary layer, *Geophys. Res. Lett.*, 31, L04112, doi:10.1029/2003GL019215, **2004**.

Saiz-Lopez, A, Plane, J. M. C., and Shillito, J. A.: Bromine oxide in the mid-latitude marine boundary layer, *Geophys. Res. Lett.*, 31, L03111, **2004**.

Saiz-Lopez, A., Shillito, J. A., Coe, H., and Plane, J. M. C.: Measurements and modelling of I_2, IO, OIO, BrO and NO_3 in the mid-latitude marine boundary layer, *Atmos. Chem. Phys.*, 6, 1513–1528, **2006a**.

Saiz-Lopez, A., Plane, J. M. C., McFiggans, G., Williams, P. I., Ball, S., M., Bitter, M., Jones, R. L., Hongwei, C., and Hoffmann, T.: Modelling molecular iodine emission in a coastal marine environment: the link to new particle formation, *Atmos. Chem. Phys.*, 6, 883–895, **2006b**.

Saiz-Lopez, A., Chance, K., Liu, X., Kurosu, T. P., and Sander S. P.: First observations of iodine oxide from space, *Geophys. Res. Lett.*, 34, L12812, doi:10.1029/2007GL030111, **2007a**.

Saiz-Lopez, A., Mahajan, A. S., Salmon, R. A., Bauguitte S. J. B., Jones, A. E., Roscoe, H. K., and Plane, J. M. C.: Boundary layer halogens in coastal Antarctica, *Science*, 317, 348–351, **2007b**.

Sander, R., Vogt, R., Harris, G. W., and Crutzen, P. J.: Modeling the chemistry of ozone, halogen compounds, and hydrocarbons in the arctic troposphere during spring, *Tellus*, 49B, 522–532, **1997**.

Sander, R., Rudich, Y., von Glasow, R., and Crutzen, P. J.: The role of $BrNO_3$ in marine tropospheric chemistry: A model study, *Geophys. Res. Lett.*, 26, 2857–2860, **1999**.

Schroeder,W. H., Anlauf, K. G., Barrie, L. A., Lu, J. Y., Steffen, A., Schneeberger, D. R., and Berg, T.: Arctic springtime depletion of mercury, *Nature*, 394, 331–332, **1998**.

Schweitzer, F., Mirabel, P., and George, C.: Heterogeneous chemistry of nitryl halides in relation to tropospheric halogen activation, *J. Atmos. Chem.*, 34**,** 101–117, **1999**.

Seinfeld, J. H., and Pandis, S. N., Atmospheric chemistry and physics: From air pollution to climate change, second edition, John Wiley & Sons, Hoboken, New Jersey, **2006**.

Simpson, W. R., Alvarez-Aviles, L., Douglas, T. A., Sturm, M., and Domine, F.: Halogens in the coastal snow pack near Barrow, Alaska: Evidence for active bromine air-snow chemistry during springtime, *Geophys. Res. Lett.*, 32, L04811, doi:10.1029/2004GL021748, **2005**.

Simpson, W. R., von Glasow, R., Riedel, K., Anderson, P.,Ariya, P., Bottenheim, J., Burrows, J., Carpenter, L. J., Friess, U., Goodsite, M. E., Heard, D., Hutterli, M., Jacobi, H. W., Kaleschke, L., Neff, B., Plane, J., Platt, U., Richter, A., Roscoe, H., Sander, R., Shepson, P., Sodeau, J., Steffen, A., Wagner, T., Wolff, E.: Halogens and their role in polar boundary-layer ozone depletion, *Atmos. Chem. Phys.*, 7, 4375–4418, **2007**.

Singh, H. B., Gregory, G. L., Anderson, B., Browell, E., Sachse, G. W., Davis, D. D., Crawford, J., Bradshaw, J. D., Talbot, R., Blake, D. R., Thornton, D., Newell, R., and Merrill, J.: Low ozone in the marine boundary layer of the tropical Pacific Ocean: Photochemical loss, chlorine atoms, and entrainment, *J. Geophys. Res.-Atmos.*, 101, 1907–1917, **1996**.

Solberg, S., Schmidbauer, N., Semb, A., Stordal, F., and Hov, Ø.: Boundary layer ozone depletion as seen in the Norwegian Arcitc in Spring, *J. Atmos. Chem.*, 23, 301–332, **1996**.

Solomon, S., Garcia, R. R., and Ravishankara, A. R.: On the role of iodine in ozone depletion, *J. Geophys. Res.-Atmos.*, 99, 20 491–20 499, **1994**.

Spicer, C. W., Chapman, E. G., Finlayson-Pitts, B. J., Plastrdge, R. A., Hubbe, J. M., Fast, J. D., and Berkowitz, C. M.: Unexpectedly high concentrations of molecular chlorine in coastal air, *Nature*, 394, 353–356, **1998**.

Spicer, C. W., Plastridge, R. A., Foster, K. L., Finlayson-Pitts, B. J., Bottenheim, J. W., Grannas, A. M., and Shepson, P. B.: Molecular halogens before and during ozone depletion events in the Arctic at polar sunrise: concentrations and sources, *Atmos. Environ.*, 36, 2721–2731, **2002**.

Steffen, A., Douglas, T., Amyot, M., Ariya, P., Aspmo, K., Berg, T., Bottenheim, J., Brooks, S., Cobbett, F., Dastoor, A., Dommergue, A., Ebinghaus, R., Ferrari, C., Gardfeldt, K., Goodsite, M. E., Lean, D., Poulain, A. J., Scherz, C., Skov, H., Sommar, J., and Temme, C.: A synthesis of atmospheric mercury depletion event chemistry in the atmosphere and snow, *Atmos. Chem. Phys.*, 8, 1445–1482, **2008**.

Stutz, J., Pikelnaya, O., Hurlock, S. C., Trick, S., Pechtl, S., and von Glasow, R.: Daytime OIO in the Gulf of Maine, *Geophys. Res. Lett.*, 34, L22816, dio: 10.1029/2007GL031332, **2007**.

Tang, T., and McConnell, J. C.: Autocatalytic release of bromine from Arctic snow pack during polar sunrise, *Geophys. Res. Lett.*, 23, 2633–2636, **1996**.

Vaughan, S., Gherman, T., Ruth, A. A., and Orphal, J.: Incoherent broad-band cavity-enhanced absorption spectroscopy of the marine boundary layer species I_2, IO and OIO, *Phys. Chem. Chem. Phys.*, 10, 4471–4477, **2008**.

Vogt, R., Crutzen, P. J., and Sander, R.: A mechanism for halogen release from sea-salt aerosol in the remote marine boundary layer, *Nature*, 383, 327–330, **1996**.

Vogt, R., Sander, R., von Glasow, R., and Crutzen, P. J.: Iodine chemistry and its role in halogen activation and ozone loss in the marine boundary layer: A model study, *J. Atmos. Chem.*, 32, 375–395, **1999**.

von Glasow, R., and Crutzen, P. J., Tropospheric halogen chemistry, in: Treatise on Geochemistry Update 1, edited by: Holland, H. D., Turekian, K. K., Eleviser, Amsterdam, The Netherlands, Vol. 4.02, pp 1-67, **2007**.

Wada, R., Beames, J. M., and Orr-Ewing, A. J.: Measurement of IO radical concentrations in the marine boundary layer using a cavity ring-down spectrometer, *J. Atmos. Chem.*, 58, 69–87, **2007**.

Wagner, T., and Platt, U.: Satellite mapping of enhanced BrO concentrations in the troposphere, *Nature*, 395, 486–490, **1998**.

Wennberg, P. O.: Bromine explosion, *Nature*, 397, 299–301, **1999**.

Wever, R.: Ozone destruction by algae in the Arctic atmosphere, *Nature*, 335, 501–501, **1988**.

Wever, R., Tromp, M. G. M., Krenn, B. E., Marjani, A., van Tol, M.: Brominating activity of the seaweed *Ascophyllum nodosum*: Impact on the biosphere, *Environ. Sci. Technol.*, 25, 446–449, **1991**.

Whalley, L. K., Furneaux, K. L., Gravestock, T., Atkinson, H. M., Bale, C. S. E., Ingham, T., Bloss, W. J., and Heard, D. E.: Detection of iodine monoxide radicals in the marine boundary layer using laser induced fluorescence spectroscopy, *J. Atoms. Chem.*, 58, 19–39, **2007**.

Wingenter, O. W., Kubo, M. K., Blake, N. J., Smith Jr., T. W., Blake, D. R., and Rowland, F. S.: Hydrocarbon and halocarbon measurements as photochemical and dynamical indicators of atmospheric hydroxyl, atomic chlorine, and vertical mixing obtained during Lagrangian flights, *J. Geophys. Res.-Atmos.*, 101, 4331–4340, **1996**.

Wingenter, O. W., Blake, D. R., Blake, N. J., Sive, B. C., and Rowland, F. S.: Tropospheric hydroxyl and atomic chlorine concentrations, and mixing timescales determined from hydrocarbon and halocarbon measurements made over the Southern Ocean, *J. Geophys. Res.-Atmos.*, 104, 21819–21828, **1999**.

Wofsy, S. C., McElroy, M. B., and Yung, Y. L.: The chemistry of atmospheric bromine, *Geophys. Res. Lett.*, 2, 215–218, **1975**.

Yokouchi, Y., Akimoto, H., Barrie, L. A., Bottenheim, J. W., Anlauf, K., and Jobson, B. T.: Serial gas-chromatographic mass-spectrometric measurements of some volatile organic compounds in the Arctic atmosphere during the 1992 Polar Sunrise Experiment, *J. Geophys. Res.-Atmos.*, 99, 25379–25389, **1994**.

Yvon, S. A., and Butler, J. H.: An improved estimate of the oceanic lifetime of atmospheric CH_3Br, *Geophys. Res. Lett.*, 23, 53–56, **1996**.

Chapter 2

Method Developments

2.1 Diffusion technique for the generation of gaseous halogen standards

Ru-Jin Huang, Thorsten Hoffmann*

Institute of Inorganic and Analytical Chemistry, Johannes Gutenberg-University of Mainz, Duesbergweg 10-14, D-55128 Mainz, Germany

Status: Under review in Journal of Chromatography A

Abstract

Halogens are known to play an important role in the tropospheric ozone-depletion chemistry and are of special interest because of their influence on the atmospheric oxidation capacity. In this paper, we investigate the application of a capillary diffusion technique for the generation of gaseous halogen standards like Br_2, IBr, ICl and I_2. The influence of capillary dimension (i.e. length and inner diameter), ambient pressure and headspace volume of the diffusion vessel on the test gas output has been evaluated. The experimental output rates are determined from the mass loss of the analyte vessel on a regular schedule and compared with their respective theoretical predictions. We also demonstrate that a 1,3,5-trimethoxybenzene-coated diffusion denuder is capable of collecting gaseous ICl quantitatively, which provides an attractive alternative for the rapid determination of the output of test gas devices. The output rates of ICl measured by the denuder method are in close agreements with the data obtained by the gravimetric method.

Keywords: Gas standard generation; Denuder; Gas chromatography–mass spectrometry; Atmospheric halogens

1. Introduction

Halogens are very reactive chemical compounds that are known to play an important role in a wide variety of atmospheric processes such as ozone depletion in the polar boundary layer and new particle formation in the coastal boundary layer ([1–4] and references therein). Of special interest in this field is the photolysis of halogen atom precursors (e.g. dihalogens X_2 or XY, where X, Y denotes different halogen atoms), which leads to rapid production of halogen atoms whose main fate is to react with ozone, forming XO radicals and consequently influencing the atmospheric photooxidant budget as well as the formation of cloud condensation nuclei by chain reactions involving halogen atoms [1]. The atmospheric mixing ratios of most of these dihalogens vary widely throughout coastal areas and polar regions and the typical values are supposed to be at the level of parts-per-trillion (ppt) or sub-ppt ([1] and references therein). However, still concentration data on the dihalogens are rare (even unavailable for ICl and IBr so far), which leaves many key processes related to atmospheric halogen chemistry open [1–3].

One of the critical steps associated with the development of analytical procedures to measure gaseous compounds in air is the generation of known and reproducible gaseous standards at typical ambient mixing ratios. Gaseous standards are essential for the verification of reliability of either sampling methods, multistep analytical procedures or online instruments. Therefore, it is desirable to have a highly precise gas generation source to minimize potential analytical errors. Several techniques are currently available for the preparation of gaseous standards and these are generally classified as static and dynamic methods [5–11]. The former [5–7], which involves the dilution of a concentrated standard or a pure compound to a defined gas volume, has the advantage of ease of operation; however, for certain compounds it lacks reliability mainly due to the possible adsorption or reaction of constituents on the container walls, especially at low concentration levels [5]. For these compounds dynamic methods [8–11], including permeation and diffusion techniques, provide more reliable concentrations of the compounds of interest. In these techniques the test gas concentration is controlled by the constant diffusion or permeation of the compound of interest into a diluting gas flow. By selecting suitable diffusion (i.e. capillaries) or permeation barriers (i.e. membranes) a low concentration of the gaseous standard with a wide concentration range is attainable. Especially the capillary diffusion-based method has often been used for the production of gaseous standards of volatile and semi-volatile organic compounds [9–11]. An overview of the different methods is given by Namiesnik [12].

In this work, we describe for the first time the generation of inorganic gaseous standards of halogens based on a capillary diffusion device. The stability of the gas source and the effects of capillary dimensions and headspace volume of the diffusion vessel on the output rates of different halogens are evaluated. Besides gravimetric determination of the test gas output from the capillary device a diffusion denuder sampling system combined with gas chromatography–mass spectrometry (GC–MS) [13] is used for the rapid determination of the output rate of ICl.

2. Experimental

2.1. Reagents and materials

ICl, IBr, I_2, Br_2, 1,3,5-trimethoxybenzene (1,3,5-TMB), and 2,4,6-tribromoanisole were obtained from Aldrich (Steinheim, Germany). Ethyl acetate was obtained from Fluka (Steinheim, Germany). All other chemicals were of analytical reagent grade. 1-iodo-2,4,6-trimethoxybenzene (1-iodo-2,4,6-TMB) was not commercially available and has been synthesized for the purpose of quantification [14]. The synthetic procedure was as follows: to 15 mL of 0.2 mol L^{-1} 1,3,5-TMB aqueous solution, 381 mg of finely powdered I_2 was added. After the mixture was stirred at 50 ^{o}C for a few minutes, 30% aqueous solution of

H_2O_2 (1.8 mmol) and a drop of 40% H_2SO_4 were introduced. The reaction mixture was stirred at 50 ^oC until iodine consumption. The product was extracted with 30-mL CH_2Cl_2 and then washed with an aqueous solution of $Na_2S_2O_3$ (5%, 40 mL), and dried over anhydrous $MgSO_4$. Pure products were isolated by SiO_2 column chromatography using CH_2Cl_2 as mobile phase. The purity of 1-iodo-2,4,6-TMB was 99.3% detected by GC–MS.

2.2. Construction, operation and evaluation of the gas standard source

The design of the assembled diffusion devices (V = 2.24 mL) used in this study is shown in Fig. 1A. A certain amount of halogen compounds of interest was filled into the vessel to which a deactivated fused capillary was connected. The length and inner diameter of the diffusion capillaries ranged from 1.0 to 20.0 cm and from 0.1 to 2.15 mm, respectively. The diffusion device was placed at the bottom of a double-walled glass chamber (Fig. 1B). The temperature in this diffusion chamber was kept at 25.0 ± 0.1 ^oC using thermostated water. Nitrogen gas was flushed continuously through the diffusion chamber from the bottom to the top at a constant flow rate. The outlet of the diffusion chamber was connected to a split valve. Therefore, only part of the gaseous compound was fed into a 500-mL three-neck dilution chamber. Here, another nitrogen flow was introduced for dilution of the analyte to the concentration range needed. The whole experimental system was protected from any light by aluminium foil to avoid complications from the photodissociation of halogen compounds.

The output of the test gas (output or loss rate) was determined by periodically measuring the mass loss of the analyte vessel on a microbalance (Precisa XB120A, Switzerland). In addition to this gravimetric approach, a denuder-based method [13] was also used for the measurements of output rate of the halogen compounds.

2.3. Sample collection and preparation (denuder method)

Brown borosilicate glass tubes (6 mm i.d.) with a length of 50 cm were used for the preparation of denuders. 1.5 mmol L^{-1} 1,3,5-TMB dissolved in methanol was used as coating solution. Six 500 μL-portions of the solution were alternately pipetted into both openings of the glass tube. During the coating procedure the tubes were rotated and flushed with nitrogen for drying (flow rate 0.5 L min^{-1}). Afterwards, the coated denuders were sealed with polypropylene (PP) end-caps and stored in the refrigerator until sampling.

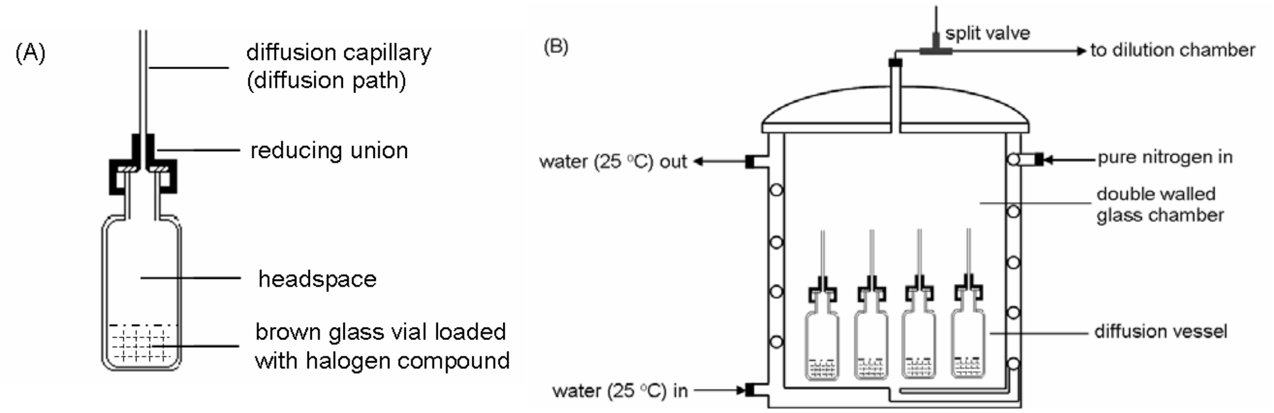

Fig. 1. Schematic diagram of the design of capillary diffusion vessel (A) (modified from [13]) and the gas standard generation system (B).

The sampled gas entered the denuder through a subduction zone (uncoated glass tube, 6 mm i.d × length 3–18 cm depending on the gas flow) which ensured laminar flow conditions. A membrane pump was located downstream of the denuder to adjust the sampling flow rate. The sampling time was 10–20 min at a typical flow rate of 500 mL min^{-1}. Three to five samples were taken for each measurement.

After sampling the coatings were eluted with five 2.0 mL-portions ethanol/ethyl acetate (1:1, v/v). Afterwards, 100 μL of 2,4,6-tribromoanisole (internal standard, 6.0 mg L^{-1} in ethyl acetate) was added into the eluate. The mixture was concentrated almost to dryness with a gentle stream of purified nitrogen (99.999%) and then redissolved in 100 μL ethyl acetate.

2.4. GC–MS analysis

For the chromatographic analysis a Finnigan GC–MS (Trace GC/PolarisQ, Rodano, Italy) with a fused-silica capillary column (30 m × 0.25 mm i.d., d_f: 0.25 μm, Rtx®-5MS, Restek Co., Bad Homburg, Germany) was used. High-purity helium (99.999%) was used as a carrier gas at a constant flow of 1.0 mL min^{-1}. One μL of sample solution was introduced and the injection was done in the splitless mode (splitless time, 1.0 min) with a deactivated splitless injection glass liner that contained no glass wool. The temperature of the injector was set to 250 °C and the transfer line was set to 300 °C. The GC oven was programmed as follows: initial temperature 90 °C (hold 3 min), 30 °C min^{-1} to 220 °C (hold 3 min). The mass spectrometer was operated in the electron impact (EI) mode (70-eV). A solvent delay of 4.5 min preceded the MS spectra acquisition and acquisition was in full scan mode at a mass range of 45–450 amu.

3. Results and discussion

3.1. Test gas output

The diffusion process in the assembled diffusion device involves the evaporation of analyte of interest from a liquid (or solid) reservoir into the headspace volume followed by the diffusion of the vapor through the capillary into the double-walled glass chamber. The output rate can be controlled by the length and diameter of the capillary as well as the temperature in the capillary diffusion device and is given by [15, 16]

$$r = \frac{D_0 P_0 M}{RT} \times \frac{A}{l} \times \ln \frac{P}{P-p} \qquad (1)$$

where r (g s^{-1}) is the output rate; D_0 ($\text{cm}^2\ \text{s}^{-1}$) is the diffusion coefficient at standard pressure P_0 (101 kPa); M (g mol^{-1}) is the molecular weight of vapor; P (kPa) is the total pressure in the double-walled glass chamber; p (kPa) is the partial pressure of the diffusing vapor at the absolute temperature T (K); R (cm^3 kPa $\text{mol}^{-1}\ \text{K}^{-1}$) is the gas constant; A (cm^2) and l (cm) are the cross-sectional area and length of the diffusion capillary, respectively. The diffusion coefficient of individual compounds can be either calculated by using the Fuller–Schettler–Giddings method [17–19] or experimentally determined. Also the values of the vapour pressures of the compounds of interest can be obtained by either the Antoine equation estimation [20] or by experimental measurements.

3.1.1. Comparison of measured and theoretical output rates

The diffusion equation (Eq. (1)) is valid only if the partial pressure of the analyte is low in the dilution gas and that the saturation partial pressure in the capillary diffusion vessel is maintained constant. In practice, the variation of the total pressure, which cannot be controlled in an open system as used here, has an additional effect on the actual test gas output and might result in differences between the theoretical predictions and practical observations. Therefore, the output rate *r* has to be determined by monitoring the mass loss of the analyte vessel on a regular schedule (namely, by a gravimetric method). Table 1 lists the measured and calculated output rates of ICl, IBr, Br_2, and I_2. It can be seen from this table that the experimental values are in close agreements with their respective theoretical predictions with a factor of 1.02–1.07 when diffusion capillaries with large inner diameters are used (i.e. 1.15 mm i.d. for ICl, IBr, and I_2, and 2.15 mm i.d. for Br_2). In a previous work focussing on semi-volatile organic compounds by Possanzini et al.[10], a good agreement was also found between the calculated and tested output rates when capillaries with an inner diameter of 0.7–1.0 mm were used. However, when smaller capillaries (e.g. 0.53 mm i.d.) were applied to the halogen species investigated here, the measured test gas output was much greater than the theoretical value (see Table 1). This phenomenon can be attributed to the influence of ambient pressure variation on the test gas output. During an ambient pressure drop (e.g. by meteorological variations) the output of the test gas will not only be governed by diffusion of the test gas through the capillary, but the resulting volume variations within the diffusion device will force a certain amount of saturated vapour to leave the test gas vessel, i.e., the saturated vapor will eject through the capillary leading to enhanced output. Obviously, this effect has a larger influence on smaller test gas output; however, the inner volume of the capillary (or more precisely the ratio of the capillary volume to the headspace volume of the capillary diffusion vessel (see below)) also plays a role.

The effect of the headspace volume of the diffusion vessel on the output rate was also investigated. This set of experiments was focused on ICl and I_2, representing one more volatile and one less volatile analyte. As can be seen in Table 2, the output rates of both ICl and I_2 are independent of the headspace volume when a 1.15 mm i.d. capillary is used. However, when a 0.53 mm i.d. capillary is used the output rate obtained from 1.5-mL headspace volume is higher than the value obtained from 0.5-mL headspace volume for both ICl and I_2. This observation is in agreement with the influence of ambient pressure variations on the test gas output as discussed above.

Table 1
Difference between calculated and measured output rate of different halogen species: dependence of capillary dimension[a]

Analyst	Saturation vapor pressure (kPa)	Capillary length (cm)	Capillary inner diameter (mm)	Calculated output rate[e] (ng s^{-1})	Measured output rate[g] (ng s^{-1})	Factor (measured/ calculated output)
Br_2	28.69[b]	2.5	0.53	209	1639 ± 116 (9)	7.84
		2.5	2.15	3438	3571 ± 202 (6)	1.04
ICl	4.05[c]	2.5	0.10	0.83[f]	41.9 ± 2.3 (6)	50.5
		5.0	0.10	0.42[f]	25.2 ± 1.5 (9)	60.8
		10.0	0.10	0.21[f]	18.5 ± 1.6 (12)	89.0
		20.0	0.10	0.10[f]	12.4 ± 1.6 (6)	119
		2.5	0.53	23.3[f]	109 ± 7 (12)	4.70
		5.0	0.53	11.7[f]	68.6 ± 4.9 (6)	5.88
		10.0	0.53	5.83[f]	37.7 ± 1.5 (8)	6.47
		20.0	0.53	2.92[f]	21.4 ± 1.4 (8)	7.32
		2.5	1.15	110[f]	117 ± 4 (6)	1.07
IBr	1.01[c]	2.5	0.53	7.59	22.2 ± 1.1 (6)	2.92
		2.5	1.15	35.7	38.2 ± 1.5 (6)	1.07
I_2	0.041[d]	4.5	0.32	0.0705	0.867 ± 0.075 (9)	12.3
		2.0	0.53	0.435	0.996 ± 0.052 (21)	2.29
		1.0	0.53	0.87	1.21 ± 0.05 (21)	1.39
		2.5	1.15	1.64	1.67 ± 0.04 (6)	1.02

[a] Headspace volume ~1.5 mL.
[b] Calculated by the Antoine equation using the Antoine coefficients published in [21].
[c] Obtained from [22].
[d] Obtained from [23]
[e] Diffusion coefficients calculated by Fuller–Schettler–Giddings method (except ICl) and saturation vapour pressure listed in the table are used for the theoretical calculation of output rate.
[f] Average of calculated and measured (0.103 cm^2 s^{-1}, this work) diffusion coefficient is used.
[g] Mean ± SD, data in the bracket indicates the number of replicates.

3.1.2. Effect of capillary length on the output rate and the stability of the gas source

Based on these results, it is obvious that a test gas output close to the theoretically calculated value can be achieved only if a diffusion capillary with relatively large dimensions is applied. In such case, however, the output of the gaseous standards of halogens is relatively high. A sequential large-volume dilution of the gaseous standards produced is therefore required to get low concentrations and to match the typical ambient mixing ratios of halogens. Therefore, despite the increasing differences between theoretical and practical output rates, diffusion capillaries with longer length and smaller diameter are still useful for the generation of standard gas mixtures. Consequently, we further tested the output rate of ICl (whose vapor pressure is in the median among the halogen compounds investigated here) using 0.53 mm i.d. and 0.10 mm i.d. capillaries with different lengths. The output rates were measured by both methods (gravimetric and denuder method). For the measurements by the denuder method, samples were collected in the regular intervals between weighings. Fig 2A shows the output rate of ICl as a function of the length of a 0.53 mm i.d. capillary. With the increase of capillary length from 2.5 cm to 20 cm, the output rate decreased significantly. The measured values by the gravimetric method are very close to the values by denuder measurements with differences ranging from 1.7% to 5.5%, indicating that both gravimetric and denuder methods are effective approaches for the determination of output rates of gaseous standard produced by the capillary diffusion technique. However, it should be noted that gravimetry is a more time-consuming method compared with the denuder method because longer weighing intervals are necessary to get a quantifiable loss of mass when lower output rates are adjusted. Certainly, for the denuder method, an effective coating material towards the target analyte collection is necessary to guarantee the accuracy of output rate measurement.

Table 2

Effect of headspace volume of the diffusion vessel on the output rate

Analyt	Capillary inner diameter (mm)	Capillary length (cm)	Measured output rate (ng s^{-1})		Difference (%)
			Headspace volume ~1.5 mL	Headspace volume ~0.5 mL	
ICl	0.53	10.0	37.7	22.6	66.7
	1.15	2.5	117	113	3.4
I_2	0.53	2.0	0.996	0.796	25.1
	1.15	2.5	1.67	1.63	2.4

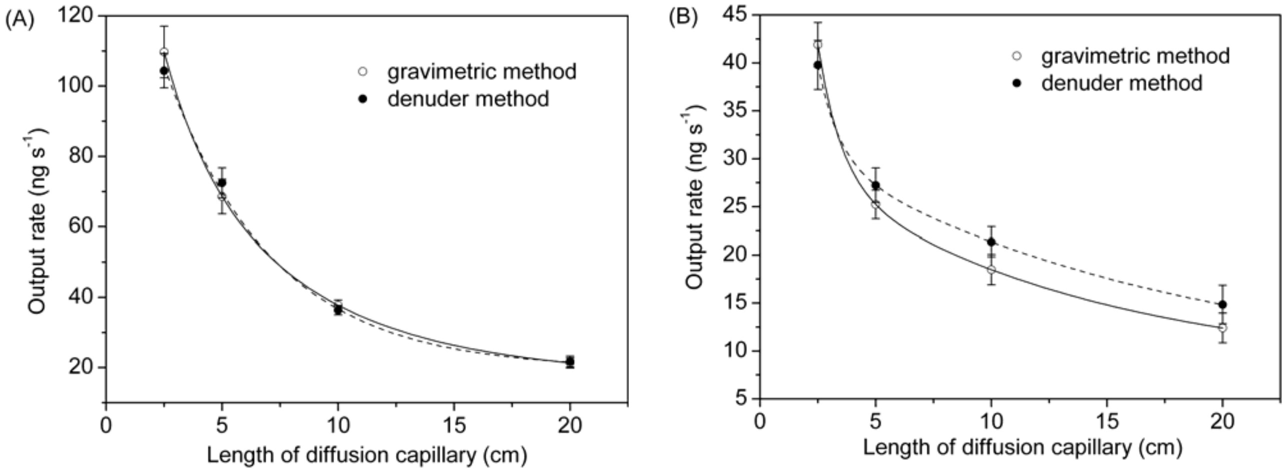

Fig. 2. The output rate of ICl as a function of length of capillary with 0.53 mm i.d (A) and 0.10 mm i.d. (B).

The effect of the length of a smaller capillary (0.10 mm i.d.) on the test gas output of ICl is shown in Fig. 2B. As before, the output rate decreases with an increase of capillary length. The data obtained by the gravimetric method and denuder method were again very similar when a capillary length of 2.5 cm was used, however, with the increase of the capillary length significant differences (7.6%–17.9%) were observed between these two sets of data (Fig. 2B). Furthermore, in such cases, the precisions of the gas sources (R.S.D. (Relative Standard Deviation) = 6.0%–13.5%) were worse than the data obtained by using 0.53 mm i.d. capillaries (R.S.D. = 3.6%–7.1%). These results indicate that the test gas source might be more and more unstable when smaller and longer capillaries (0.10 mm i.d. × length 5–20 cm) are used for the generation of highly volatile gases, such as ICl. Actually, one major problem using smaller capillaries was the formation of liquid droplets of ICl inside the diffusion capillary tube (0.10 mm i.d. × length 5–20 cm), which certainly affects dramatically the output rate and the stability of the gas source [10].

4. Conclusions

This paper shows that capillary diffusion devices are an effective approach for the generation of gaseous standards of halogens. However, the experimental output rate matches the theoretical prediction only if a capillary with relatively large dimension (>1–2 mm i.d.) is applied. When a capillary with smaller dimension is used, the actual test gas output can be elevated by up to two orders of magnitude compared to their respective theoretical values. Moreover, relatively poor reproducibility is observed for the standard gas source when capillaries with small inner diameter and larger length are used (i.e. 0.10 mm i.d. × length 5–20 cm). In addition, the paper demonstrates that a suitable diffusion denuder method to measure the test gas output can be beneficial, since it is less time-consuming than the gravimetric method.

Acknowledgements

The authors gratefully acknowledge the financial support of the German Research Foundation (Deutsche Forschungsgemeinschaft, DFG) within the graduate program "Trace Analysis of Elemental Species: Methods Developments and Applications". The authors also acknowledge additional support from the EU project MAP (Marine Aerosol Production).

References

[1] R. von Glasow, P.J. Crutzen, in H.D. Holland, K.K. Turekian (Editors), Treatise on Geochemistry Update 1, Eleviser, Amsterdam, 2007, vol. 4.02, pp 1–67.

[2] W.R. Simpson, R. von Glasow, K. Riedel, P. Anderson, P. Ariya, J. Bottenheim, J. Burrows, L.J. Carpenter, U. Friess, M.E. Goodsite, D. Heard, M. Hutterli, H.W. Jacobi, L. Kaleschke, B. Neff, J. Plane, U. Platt, A. Richter, H. Roscoe, R. Sander, P. Shepson, J. Sodeau, A. Steffen, T. Wagner, E. Wolff, Atmos. Chem. Phys. 7 (2007) 4375.

[3] C.D. O'Dowd, T. Hoffmann, Environ. Chem. 2 (2005) 245.

[4] L.J. Carpenter, Chem. Rev. 103 (2003) 4953.

[5] G.C. Rhoderick, W.R. Miller, J. Chromatogr. A 653 (1993) 71.

[6] G.C. Rhoderick, J. Chromatogr. A 1187 (2008) 226.

[7] G.C. Rhoderick, J.H. Yen, Anal. Chem. 78 (2006) 3125.

[8] S. Tumbiolo, L. Vincent, J.F. Gal, P.C. Maria, Analyst 130 (2005) 1369.

[9] M. Gautrois, R. Koppmann, J. Chromatogr. A 848 (1999) 239.

[10] M. Possanzini, V. Di Palo, E. Brancaleoni, M. Frattoni, P. Ciccioli, J. Chromatogr. A

883 (2000) 171-183.

[11] D. Helmig, T. Revermann, J. Pollmann, O. Kaltschmidt, A.J. Hernandez, F. Bocquet, D. David, J. Chromatogr. A 1002 (2003) 193-211.

[12] J. Namiesnik, J. Chromatogr. 300 (1984) 79.

[13] R.-J. Huang, T. Hoffmann, J. Chromatogr. A 1210 (2008) 135.

[14] M. Jereb, M. Zupan, S. Stavber, Chem. Commun. 22 (2004) 2614.

[15] A.P. Altshuller, I.R. Cohen, Anal. Chem. 32 (1960) 802.

[16] J.M. McKelvey, H.E. Hoelscher, Anal. Chem. 29 (1957) 123.

[17] G. Karaiskakis, D. Gavril, J. Chromatogr. A 1037 (2004) 147.

[18] E.N. Fuller, P.D. Schettler, J.C. Giddings, Ind. Eng. Chem. 58 (1966) 19.

[19] E.N. Fuller, K. Ensley, J.C. Giddings, J. Phys. Chem. 73 (1969) 3679.

[20] R.H. Perry, D.W. Green, J.O. Maloney, Perry's Chemical Engineers Handbook, McGraw-Hill, 6th edition, New York, 1984.

[21] NIST Standard Reference Database Number 69, June 2005 release, http://webbook.nist.gov/chemistry/

[22] J. McMorris, D.M. Yost, J. Am. Chem. Soc. 53 (1931) 2625.

[23] G.P. Baxter, C.H. Hickey, W.C. Holmes, J. Am. Chem. Soc. 29 (1907) 127.


Journal of Chromatography A, 1210 (2008) 135–141

Contents lists available at ScienceDirect

Journal of Chromatography A

journal homepage: www.elsevier.com/locate/chroma

A denuder–impinger system with in situ derivatization followed by gas chromatography–mass spectrometry for the determination of gaseous iodine-containing halogen species

Ru-Jin Huang, Thorsten Hoffmann*

Institute of Inorganic and Analytical Chemistry, Johannes Gutenberg-University of Mainz, Duesbergweg 10-14, D-55128 Mainz, Germany

2.2 A denuder–impinger system with in situ derivatization followed by gas chromatography–mass spectrometry for the determination of gaseous iodine-containing halogen species

Ru-Jin Huang, Thorsten Hoffmann*

Institute of Inorganic and Analytical Chemistry, Johannes Gutenberg-University of Mainz, Duesbergweg 10-14, D-55128 Mainz, Germany

Status: Published in Journal of Chromatography A

Abstract

Reactive iodine species have been suggested to play an important role in the atmosphere (e.g. tropospheric ozone depletion, coastal new particle formation). However, there still exist major uncertainties about their atmospheric chemistry, mostly due to the lack of analytical approaches for the accurate speciation of certain key compounds. In this study, 1,3,5-trimethoxybenzene (1,3,5-TMB)-coated denuder proved to be suitable for the differentiation between gaseous interhalogens (iodine monochloride (ICl), iodine monobromide (IBr)) and molecular iodine (I_2) based on a selective collection/derivatization method. The results of the denuder sampling were compared with the results of impinger sampling in water, methanol and carbon tetrachloride solutions of 1,3,5-TMB. ICl and IBr are converted into 1-iodo-2,4,6-trimethoxybenzene (1-iodo-2,4,6-TMB) and

1-bromo-2,4,6-trimethoxybenzene (1-bromo-2,4,6-TMB), respectively, in the denuder systems. The respective collection efficiency is 99.2% for ICl and 92.6% for IBr, at 500 mL min^{-1} gas flow rate. The collection efficiency for I_2 is lower than 1% in the same denuder system, but significantly increases to about 90% in the aqueous 1,3,5-TMB loaded impinger. The denuder–impinger coupled system was then used to differentiate and to collect the ICl, IBr and I_2 gas mixtures, followed by gas chromatography–ion trap mass spectrometry (GC–MS) determination. The precision of the method is in general better than 9.1%. The parameters affecting denuder operation including sampling flow rate, sampling duration, and relative humidity have been evaluated. The presented method provides an attractive protocol for iodine species analysis for atmospheric chemistry research.

Keywords: Gaseous iodine-containing halogens; 1,3,5-Trimethoxybenzene; Derivatization; GC–MS; Diffusion denuder; Impinger; Atmospheric chemistry

1. Introduction

Reactive halogen compounds are present in various domains throughout the troposphere and play a key role for several atmospheric processes ([1–3], and references therein). Of major interest in this regard is the catalytic destruction of ozone. The suggested mechanism mostly involves the bromine and chlorine cycles. However, recent measurements of free IO radicals [4–6], an unambiguous product of iodine atom reaction with ozone, lead to renewed interest in the tropospheric iodine chemistry. The assumption is that iodine is capable of triggering the chlorine and bromine release. The reactive uptake of inorganic iodine species by sea-salt aerosol has been proposed to initiate both chlorine and bromine activation in marine aerosol [7,8]. The subsequently released gaseous products, iodine monochloride (ICl) and iodine monobromide (IBr), are believed to contribute to an additional depletion of ozone. In a theoretical study, Calvert and Lindberg [9] found that relatively small inputs of ICl, IBr and I_2 to a Br_2/BrCl mixture could cause a significant enhancement of the ozone depletion relative to that from Br_2 and BrCl alone. In contrast to the frequent measurement of BrCl in the field campaigns [10,11], to the authors' knowledge, data on the source strength or concentrations of the other two important interhalogen precursors (ICl and IBr) are still not available and therefore their potential influences on tropospheric processes are not well understood. The key to elucidate the chemistry leading to the ozone depletion in the troposphere is the measurement of specific gaseous reactive halogen compounds present before and during ozone depletion episode. Thus, the identification and quantification of ICl and IBr are important analytical tasks.

For the determination of gaseous compounds in air the diffusion denuder technique [12], designed to differentiate gaseous analytes from their particulate counterparts, is substantially superior to the often used prefilter−filter/impinger methods. The latter techniques are subjected to a series of artifacts associated with undesirable sample modifications (positive or negative artifacts). Since gaseous analytes can be preconcentrated inside the denuder, denuder-based techniques are preferred for the measurement of trace gaseous analytes and has been widely utilized for the sampling of organic acids [13,14], nitric and nitrous acids [15−17], mercuric chloride [18], polynuclear aromatic hydrocarbons [19], diisocyanates [20,21], formaldehyde [22], and other inorganic and organic compounds [23−26]. Although numerous papers related to denuder techniques have been published, little attention was given to the analysis of reactive halogen species. To achieve excellent performance with a high collection efficiency, the selection of an effective sorption material to the target analyte is of crucial importance. Here, we report an efficient denuder technique for the quantitative analysis of gaseous iodine interhalogens (ICl and IBr) based on in situ selective derivatization with 1,3,5-TMB, followed by GC−MS determination. We also report results of impinger experiments for ICl, IBr and I_2 collection.

2. Experimental

2.1. Reagents and materials

ICl, IBr, I_2, 1,3,5-TMB, and 2,4,6-tribromoanisole were purchased from Aldrich (Steinheim, Germany). *N*,*N*-Dimethylaniline was purchased from Acros Organics (Geel, Belgium).

Cyclohexane was obtained from Fisher (Loughborough, UK). Ethyl acetate was from Fluka (Steinheim, Germany). H_2O_2 aqueous solution (30%, wt.%), nitrobenzene, phenol, and salicylic acid were purchased from Sigma-Aldrich (Steinheim, Germany). 1-Bromo-2,4,6-TMB was purchased from CHESS (purity≥98%, CHESS GmbH, Mannheim, Germany). All other chemicals were of analytical reagent grade. Deionized water (18 MΩ cm) was used for the preparation of all aqueous solutions. 1-Iodo-2,4,6-TMB was not commercially available and has been synthesized [27], for the purpose of quantification. The synthesis procedure was as follows: to 15 mL of 0.2 mol L^{-1} 1,3,5-TMB aqueous solution, 381 mg of finely powdered I_2 was added. After the mixture was stirred at 50 °C for a few minutes, 30% aqueous solution of H_2O_2 (1.8 mmol) and a drop of 40% H_2SO_4 were introduced. The reaction mixture was stirred at 50 °C until iodine consumption. The product was extracted with 30-mL CH_2Cl_2 and then washed with an aqueous solution of $Na_2S_2O_3$ (5%, 40 mL), and dried over anhydrous $MgSO_4$. Pure products were isolated by SiO_2 column chromatography using CH_2Cl_2 as mobile phase. The purity of 1-iodo-2,4,6-TMB was 99.3% detected by GC–MS. The stock standard solutions of 1-iodo-2,4,6-TMB (4.0 mg mL^{-1}) and 1-bromo-2,4,6-TMB (2.5 mg mL^{-1}) were prepared in ethyl acetate separately. A series of working standard solutions was prepared by sequential dilution of the stock standard solutions with ethyl acetate.

2.2. Installation and calibration of test gas sources

Gaseous ICl, IBr and I_2 were generated from home-made gas sources based on controlled evaporation of the analytes. To get low concentration levels of the individual test gas, a capillary diffusiontype device (see Fig. 1) was used. A certain amount of analyte of interest was filled into a bottom-sealed vessel with an exposed surface area of 0.78 cm^2, and a 530 μm internal diameter deactivated fused silica capillary (CS-Chromatographie Service GmbH, Langerwehe, Germany) was installed on the top end of the vessel. The length of capillary was 15.3 cm for the ICl (liquid) source, 4 cm for the IBr (solid) source, and 2 cm for the I_2 (solid) source. This capillary diffusion-type device was placed at the bottom of a double walled glass chamber. The temperature in this glass chamber, which affects the vapor pressure and the subsequent evaporation of the analyte, was thermostated to 25 ± 0.1 °C. A nitrogen gas flow was continuously flushed through the glass chamber from the bottom to the top at a constant flow rate and transported the gaseous analyte into a 500-mL five-neck round bottom flask. Here, another nitrogen flow was introduced for dilution of the analytes to the concentration range needed. When lower concentrations of the gaseous analyte were necessary, a split valve was connected to the outlet of the double walled glass chamber and only a defined fraction of the analyte containing nitrogen stream was transferred into the flask for dilution. The whole experimental system was protected from any adventitious light by aluminium foil to avoid complications from the photodissociation of ICl, IBr and I_2. All different glass parts were connected by Teflon-tubing. The source output was calibrated by regularly monitoring the weight loss of the capillary sealed test gas source.

Safety caution: the gaseous halogen species are strong irritant, corrosive and poisonous, so proper ventilation is necessary to avoid inhalation and direct contact.

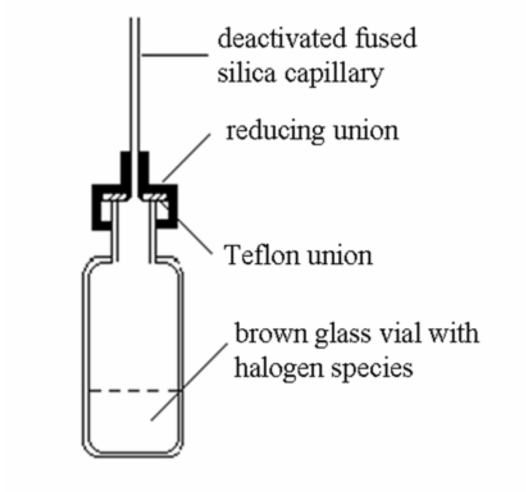

Fig. 1. Schematic diagram of the capillary diffusion vessel for test gas generation.

2.3. Preparation of denuder samplers

Brown borosilicate glass tubes (6mm i.d., length 50 cm) were used for the preparation of denuders. *N*,*N*-Dimethylaniline (1.5 mmol L^{-1}), nitrobenzene (1.5 mmol L^{-1}), phenol (1.5 mmol L^{-1}), salicylic acid (1.5 mmol L^{-1}) and 1,3,5-TMB (1.5 mmol L^{-1}) in methanol were tested as coating solutions. The concentration selected here ensured that the resulting amount of coating material is present in large excess over the analyte of interest. To obtain a uniform coating of the denuder tubes with the reagents, six 0.5 mL-portions of the individual solution were alternately pipetted into both openings of the slightly sloped glass tube. During the coating procedure the tubes were rotated and flushed with nitrogen for drying (flow rate 0.5 L min^{-1}). Afterwards, the coated denuders were sealed with polypropylene (PP) end-caps and stored in the refrigerator until sampling. For the different sampling flow rates used for this study untreated glass tubes of defined length (3–18 cm) with the same diameter as the denuder tubes were coupled to the denuder inlet, employed as subduction zones to adjust the laminar flow of sampled gas into the denuder [28].

2.4. Denuder and impinger sampling

The test gas was sucked into the denuder tube by a flow adjustable membrane pump located downstream of the denuder. The sampling time was 10–20 min with a typical flow rate of 500 mL min^{-1}. Three to five samples were taken for each measurement. After sampling the coatings were eluted five times with 2.0 mL ethanol/ethyl acetate (1:1, v/v). Afterwards, 100 µL of 2,4,6-tribromoanisole (internal standard, 6.0 mg L^{-1} in ethyl acetate) was added into the eluate. The mixture was concentrated almost to dryness with a gentle stream of purified nitrogen (99.999%) and then redissolved in 100 µL ethyl acetate. No detectable derivatives of ICl, IBr or I_2 were found in the sixth eluate of the denuder tubes. Therefore, the five-time eluting procedure was applied in all cases. An inter-method comparison was made between the denuder and impinger sampling. The midget impinger flasks (Duran®, Schott AG, Mainz, Germany) containing a derivatization solution of 25 mL 1,3,5-TMB (5 mg L^{-1}) in three different solvents (water, methanol and CCl_4) were used. The sampling flow rate was 500 mL min^{-1} and the same type of membrane pump was used as for the denuder sampling. After termination of sampling 100 µL (6.0 mg L^{-1}) of 2,4,6-tribromoanisole (internal standard) was added to the sample. The samples with water as solvent were extracted with cyclohexane (1.0 + 0.5 + 0.5 + 0.5 mL), concentrated almost to dryness with purified nitrogen flow and finally dissolved in 100 µL ethyl acetate. The samples with organic solvents were directly concentrated by purified nitrogen and then redissolved in 100 µL ethyl acetate.

2.5. Chromatographic separation and detection

For the chromatographic analysis a Finnigan GC–MS (Trace GC/PolarisQ, Rodano, Italy) with a fused-silica capillary column (30m × 0.25 mm i.d., d_f: 0.25 μm, Rtx®-5MS, Restek Co. Bad Homburg, Germany) was used. High-purity helium (99.999%) was used as a carrier gas at a constant pressure of 100 kPa. 1.0 μL of sample solution was introduced and the injection was done in the splitless mode (splitless time, 1.0 min) with a splitless injection glass liner that was deactivated and contained no glass wool. The temperature of the injector was set to 250 °C and the transfer line was set to 300 °C. The GC oven was programmed as follows: initial temperature 90 °C (hold 3 min), 30 °C min^{-1} to 210 °C, 7 °C min^{-1} to 235 °C, 20 °C min^{-1} to 250 °C (hold 1 min). A solvent delay of 4.5 min preceded the MS spectra acquisition was chosen and a mass range of 45–450 amu was selected (70-eV electron impact (EI) mode). The integrated ion currents (total ion current, TIC) were used to display the chromatograms, however, only the most abundant ion was used for quantification, i.e. *m/z* 294 for 1-iodo-2,4,6-TMB, *m/z* 246 for 1-bromo-2,4,6-TMB, and *m/z* 344 for 2,4,6-tribromoanisole.

3. Results and discussion

3.1. Test gas source evaluation and validation

The capillary diffusion-type test gas source is useful to produce low vapor concentrations. The output of the individual compounds could easily be increased or decreased by changing the length or the internal diameter of the capillary tube. However, when lower output rates were adjusted longer weighing periods were necessary to get a quantifiable loss of mass. In this study, 530 μm i.d., capillaries with a length of 15.3 cm for ICl, 4 cm for IBr and 2 cm for I_2, were chosen. The source output was periodically measured every week. After 2 weeks of initial equilibrium time, a stable output was observed and the mean output from the test gas source was 1609 ng min^{-1} (R.S.D. (Relative Standard Deviation) = 2.8%, $n = 20$), 1850 ng min^{-1} (R.S.D. = 6.6%, $n = 15$) and 61 ng min^{-1} (R.S.D. = 4.3%, $n = 9$) of ICl, IBr and I_2, respectively.

3.2. Selection of derivatizing reagent

The selection of derivatizing agents is based on three major considerations: (i) the derivatizing substrate should possess an enhanced reaction rate with the gaseous analyte (thus guaranteeing a sufficient collection efficiency), (ii) the derivatizing agent should be suitable for the coating procedure without additional pH control for the derivatization reaction, and (iii) the derivatizing substrate should deliver just one product after reaction with the analytes (no isomers, e.g. ortho- or para-products). Aromatic compounds can react with iodine or interhalogens to form halogenated aromatics [29]. We therefore tested the collection efficiencies of nitrobenzene, phenol, salicylic acid, and *N*,*N*-dialkylaniline as coating material for ICl collection (the most reactive species studied here). The results showed that the rates of these reactions are reasonably low, despite the fact that all of these compounds possess substituent at the aromatic ring which activates the halogenation step. To achieve better collection efficiency in principle an increasing reaction time would be required. However, for very low flow rates (increasing reaction time) the denuder would lose its ability to separate gaseous and particulate iodine. Our results indicate that for example *N*,*N*-dimethylaniline is an appropriate electrophilic reagent for iodination in slightly acidic aqueous solution (efficiency ~97.9%) within about 1min, but not suitable as denuder coating to collect gaseous I_2 (efficiency ~0.4%) and even not suited for the collection of the most polar interhalogen investigated here (ICl, collection efficiency $\leqslant$2.1%). Thus, a more reactive derivatizing reagent is required to get a higher collection efficiency. Since methoxy substituents enhance aromatic donors toward electrophilic aromatic substitution, 1,3,5-TMB, the most reactive substrate in the class of methoxy-substituted benzene derivatives, was selected as derivatizing reagent. In this case, excellent collection efficiency was observed with a respective difference of 0.7% for ICl and 7.6% for IBr, between the tested value and the theoretically calculated one (see Section 3.4). Consequently, 1,3,5-TMB was further investigated as coating reagent.

Table 1

Comparison of sampling systems: Denuder vs. Impinger[a]

	Denuder						Impinger with different solvent								
	Theoretical value			Tested value			Water			Methanol			CCl_4		
	ICl	IBr	I_2	ICl	IBr	I_2	ICl	IBr	I_2	ICl	IBr	I_2	ICl	IBr	I_2
Collection efficiency[b] (%)	99.93	99.91	99.86	99.2	6.23 92.6[c]	0.98	90.3	95.7 10.3[c]	88.8	78.7	21.5 16.7[c]	6.93	51.5	7.52 88.2[c]	15.8
S.D. (%) (*n* = 3)				1.5	0.19 2.1[c]	0.02	4.6	1.3 0.7[c]	2.5	1.3	0.9 0.7[c]	0.20	3.9	0.59 1.9[c]	0.4
R.S.D. (%) (*n* = 3)				1.6	3.1 2.3[c]	2.5	5.1	1.3 6.6[c]	2.8	1.6	5.0 3.8[c]	2.9	7.6	7.8 2.2[c]	2.6
Differences between tested and theoretical data[e] (%)				0.7	7.6[c]	196	10.1	4.3	11.7	23.7	89.4[d]	174	63.9	4.3[d]	145

[a] The listed experimental values without special explanation are based on 1-iodo-2,4,6-TMB.

[b] Gas flow rate: 500 mL min^{-1}.

[c] Tested based on 1-bromo-2,4,6-TMB.

[d] Based on the total amounts of 1-iodo-2,4,6-TMB and 1-bromo-2,4,6-TMB.

[e] Since there is no theoretical collection efficiency available for impinger tests, the theoretical values for denuder, based on Gormley–Kennedy equation, are assumed as the maximum for impinger tests for comparison purpose.

3.3. Differentiation between ICl, IBr and I_2

The 1,3,5-TMB coating within the denuder was present in large excess over the gaseous halogen analytes in all cases. Due to the differences in the composition and polarity of the three analytes, not only the individual derivatives formed are different but also their collection efficiencies vary with the tested halogen species. Typical chromatograms (Fig. 2A –C) and mass spectra (Fig. 2D–F) obtained for the analysis of gaseous ICl, IBr and I_2 after in situ derivatization within the denuders at a gas flow rate of 500 mL min^{-1} are shown in Fig. 2. As can be seen in Fig. 2, ICl is derivatized exclusively to 1-iodo-2,4,6-TMB as anticipated with an excellent efficiency of 99.2%. However, in the case of IBr, 92.6% of IBr is converted into 1-bromo-2,4,6-TMB, and the proportion of iodinated derivative drops to 6.23%. To our knowledge, the mechanism for aromatic bromination with iodine monobromide in vapor phase is still unclear. A possible explanation involves an initial electron transfer to generate the aromatic cation radical ($ArH^{\bullet +}$) as the reactive intermediate followed by bromide ion attack at the $ArH^{\bullet +}$ [29,30]. An alternative mechanism to explain the formation of the bromo-compound as major product could be that 1,3,5-TMB is brominated by either bromine radicals produced by homolytic cleavage of IBr or by molecular bromine formed by recombination of bromine radicals [31]. In the case of gaseous I_2 measurements using 1,3,5-TMB-coated denuders the results show that the collection efficiency is only about 1% due to the lower reactivity of iodine compared to the other halogen species. As mentioned above, both ICl and I_2 do not interfere in IBr measurements due to their differentiable derivatives; and the interference of IBr and I_2 in ICl measurement is less than 4.89% and 0.63%, respectively. Therefore, gaseous ICl, IBr and I_2 could be differentiated when 1,3,5-TMB is applied as denuder coating.

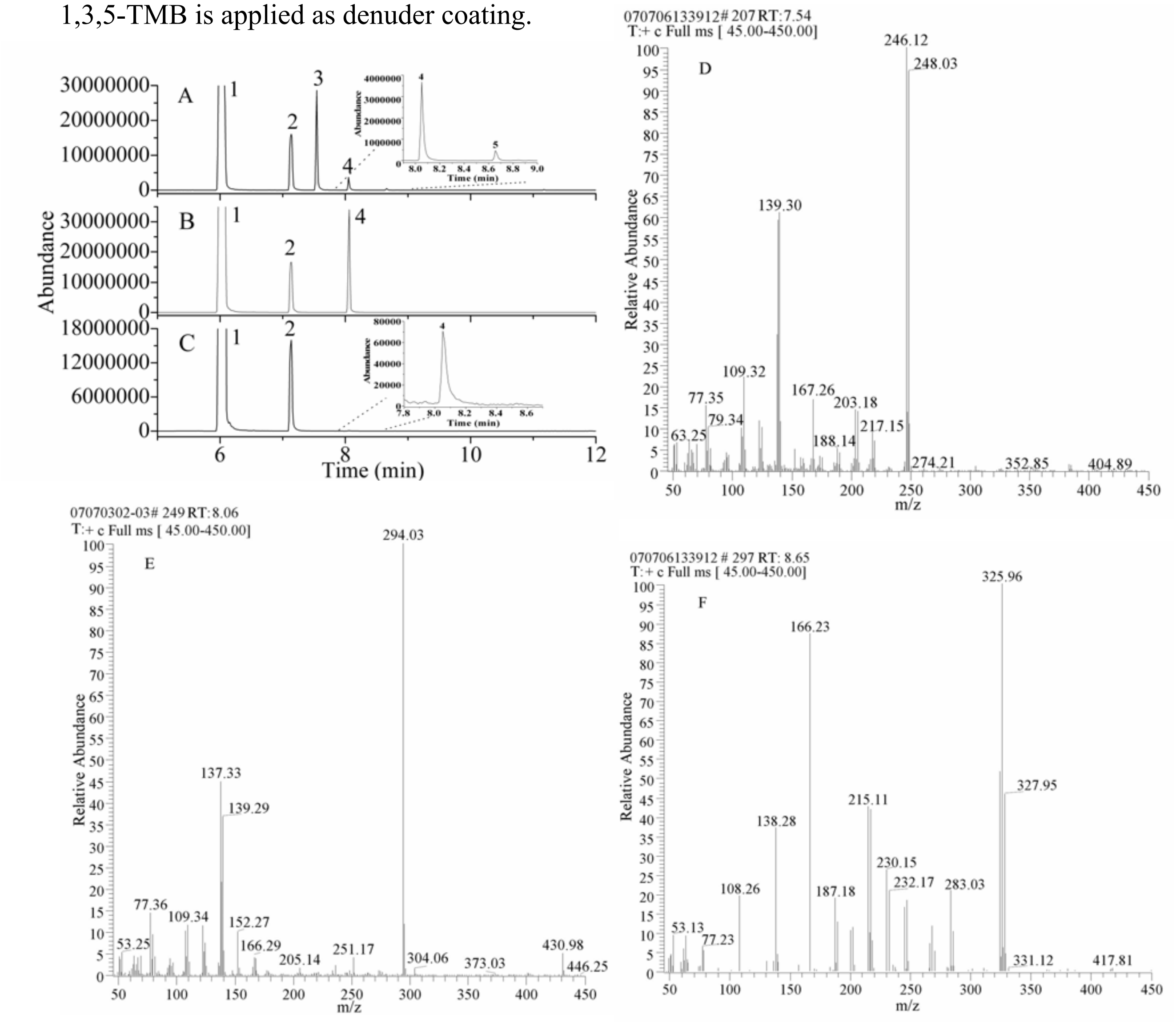

Fig. 2. Total ion chromatogram obtained by GC-MS of the derivatives of: (A) gaseous IBr; (B) gaseous ICl; (C) gaseous I_2, and the EI mass spectra of: (D) peak 3; (E) peak 4; and (F) peak 5. Peak assignments: (1) 1,3,5-TMB, (2) 2,4,6-tribromoanisole, internal standard, (3) 1-bromo-2,4,6-TMB, (4) 1-iodo-2,4,6-TMB, (5) 1,3-dibromo-2,4,6-TMB.

3.4. Comparison between denuder and impinger methods

The collection efficiency, which is defined as the ratio between the analyte amount found in the sampler and its known amount entering into the sampler, is a crucial factor for evaluation of the sampling methods. The efficiencies (see Table 1) of both the denuder and impinger methods for gaseous ICl, IBr and I_2 were tested and compared with the theoretical values (E) calculated according to the Gormley–Kennedy equation [32] (Eq. (1))

$$E(\%) = \left(1 - \frac{C}{C_0}\right) \times 100 = \left(1 - 0.819\, exp\left(-7.314 \frac{\pi DL}{2F}\right)\right) \times 100 \qquad (1)$$

where C is the mean concentration of the gaseous analyte leaving the denuder, C_0 is the concentration of gaseous analyte entering the denuder, D is the gas diffusion coefficient, L is the length of denuder and F is the flowrate. For ICl and IBr, the collection efficiencies obtained by the denuder method are in close agreements with their respective theoretical values with differences between measured and calculated values ranging from 0.7% to 7.6%. In general the collection efficiencies obtained by the impinger methods are lower than that obtained by the denuder method and vary widely with the reaction solvents used. The relatively high collection efficiency indicates that in aqueous solution both ICl and IBr rapidly hydrolyze to form HOI [33,34] (Eq. (2)) and the highly reactive HOI reacts further with 1,3,5-TMB to give the iodinated aromatic derivative (Eq. (3)).

$$\mathrm{IX\ (X = Cl, Br, I) + H_2O \rightarrow HOI + HX} \qquad (2)$$

$$\mathrm{HOI + ArH \rightarrow ArI + H_2O} \qquad (3)$$

Therefore, it is difficult to differentiate ICl and IBr from each other in aqueous solution since both deliver the same derivative with high collection efficiency (>90%, see Table 1). The iodination yields decrease as the polarities of the solvents decrease. The values drop to 78.7% for ICl and to 21.5% for IBr in methanol, and drop further to 51.5% for ICl and 7.52% for IBr in carbon tetrachloride. On the contrary, the bromination yields for IBr increase with the decrease of solvent polarity. The values increase extensively from 10.3% in aqueous solution to 88.2% in carbon tetrachloride. For less reactive molecular iodine, the presented denuder method provides extremely low yield. About 99% I_2 molecules did not react with the coating material and finally escaped from the denuder tube with the gas flow, suggesting this denuder method is unsuitable for gaseous I_2 analysis. Nevertheless, the values by impinger method in both methanol and carbon tetrachloride solutions of 1,3,5-TMB rise slightly, with a respective efficiency of 6.93% and 15.8%, and increase dramatically to about 90% in 1,3,5-TMB aqueous solution, mostly because of the rapid hydrolysis of I_2 to form HOI [35], followed by reaction with 1,3,5-TMB (Eqs. (2) and (3)). Obviously, for impinger method the selection of reaction medium is a crucial factor to improve reaction yields and to avoid undesired side reaction which lowers the sensitivity of the method and makes the trace analysis more difficult.

Table 2

Collection efficiency for ICl and IBr as a function of the test gas flow rate

Flow rate	ICl			IBr		
	Theoretical result (%)	Measured result[a] (%) (*n* =3)	Difference (%)	Theoretical result (%)	Measured result[b] (%) (*n* =3)	Difference (%)
300	99.99	99.67	0.3	99.99	94.26	5.9
600	99.77	99.13	0.6	99.72	91.87	8.2
1200	95.63	94.67	1.0	95.23	83.79	12.8
1800	88.38	88.09	0.4	87.70	75.32	15.2

[a] Tested based on 1-iodo-2,4,6-TMB.

[b] Tested based on 1-bromo-2,4,6-TMB.

3.5. Analytical performance of the denuder

The analytical performance of the denuder was further evaluated by examining the gas flow rate dependence of the collection efficiency. The data of both ICl and IBr were tested within the gas flow range between 300 and 1800 mL min^{-1} were compared with those calculated by the Gormley–Kennedy equation [32], as listed in Table 2. This equation calculates the theoretical efficiency assuming the surface to be a perfect sink of the gaseous analytes. It can be seen from the table that the experimental collection efficiencies for ICl are very close to the theoretical predictions, with differences ranging from 0.3% to 1.0%, indicating the absence of any significant losses during sampling. The experimental results for IBr comply with the theoretical predictions at lower gas flow rates, however, decrease strongly with increased gas flow rate with differences more than 10% lower than the theoretical values at gas flow rate above 1000 mL min^{-1}. The reasons for the decreased efficiencies could be manifold: (i) the decreased reaction time at higher flow rates (0.5 s, at 1800 mL min^{-1}) as well as the slightly lower reaction rate of the formation of 1-bromo-2,4,6-TMB result in the breakthrough of some gaseous IBr from the denuder before it can react with the coating material and (ii) the iodinated product was observed in all tested flow rates (e.g. 6.23% at 500 mL min^{-1}; 4.2% at 1800 mL min^{-1}). It is rationalized that a fraction of gaseous IBr, like gaseous ICl, undertakes an electrophilic attack on 1,3,5-TMB to form 1-iodo-2,4,6-TMB, which therefore reduces the efficiency in respect to the formation of 1-bromo-2,4,6-TMB.

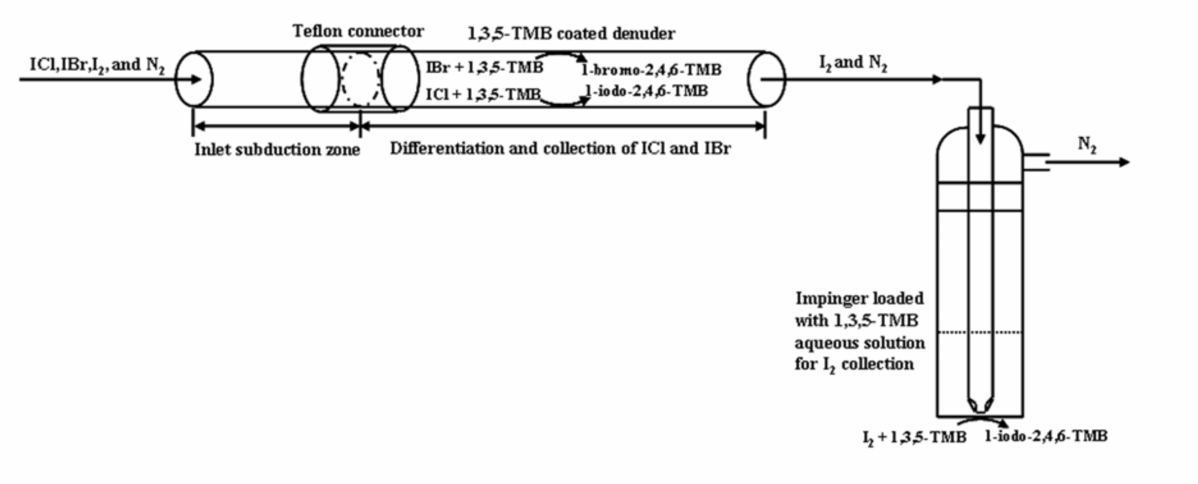

Fig. 3. Schematic diagram of denuder–impinger coupled system designed for the differentiation and collection of ICl, IBr and I_2 gas mixtures.

The potential influence of water vapor on the analytical performance of the denuder was evaluated by examining the collection efficiencies at 30%, 60% and 90% relative humidity. No significant differences of the collection efficiencies were observed. Due to the much lower reactivity of gaseous molecular halogens (e.g. Br_2) and especially organic halogens with the coating material, also interferences from these compounds for the determination of ICl and IBr are unlikely, except perhaps in cases when the molecular halogen concentrations are exceptionally high. One possible species which is expected to rapidly react with the coating material would be HOI or HOBr. However, due to the difficulties for generation of stable gas standards of these two species, it is still not clear whether, and if so, to what extent, HOI and HOBr interfere in the determination of halogen species studied here.

3.6. Analysis of ICl, IBr and I_2 gas mixtures

Gaseous mixtures of ICl, IBr and I_2 cannot be differentiated by the impinger method using 1,3,5-TMB aqueous solution because of the formation of same iodination derivative (see Table. 1). Instead, the total iodine concentration of a mixture of the three species can be measured with satisfactory accuracy (2.6 − 11.2% error as I). However, the potential influences of iodine on the tropospheric processes are species dependent. Therefore, it is of significant importance to speciate iodine in the atmosphere. In this study, a 1,3,5-TMB-coated denuder was coupled upstream of an impinger loaded with aqueous 1,3,5-TMB and this system was used for the pre-concentration and differentiation of gaseous ICl, IBr and I_2. As described above and shown in Fig. 3, ICl and IBr are collected from the gas mixture when it passes through the denuder system, whereby I_2 molecules pass through the denuder tube and are collected by the impinger system. The differentiation between IBr and ICl can then be done based on the different derivatives formed. The linearity of the analytical procedure was tested by sampling different mixtures of ICl, IBr and I_2 (ICl (0.409 ppbv to 9.95 ppbv) and IBr (0.405 ppbv to 12.15 ppbv) and I_2 (49.17 pptv to 14.8 ppbv)) at a gas flow rate 500 mL min^{-1}. The correlation coefficients (r^2) of the calibration lines are 0.9984 (n = 5) for ICl, 0.9786 (n = 5) for IBr and 0.9902 (n = 6) for I_2. The results shown in Table 3 indicate that the denuder–impinger coupled system is reliable and practical for the differentiation of ICl, IBr and I_2 gas mixtures. The precision (R.S.D. = 3.6–9.1%), can be considered to be very satisfactory in view of other potential sources of error, such as errors in connection with the GC–MS detection (R.S.D. = 2.5% and 2.0% for 1-iodo-2,4,6-TMB and 1-bromo-2,4,6-TMB, respectively). The measured ICl, IBr and I_2 concentrations for the different mixtures investigated agree well with the calibrated values from single component analysis with differences ranging from 3.1% to 8.6%.

Table 3

Differentiation and analysis of ICl, IBr and I_2 in gaseous mixtures[a]

Concentration of the test gas source (ppbv)			Measured concentration by present method[b] (ppbv)			Differences between test gas concentration and measured concentration (%)		
ICl	IBr	I_2	ICl	IBr	I_2	ICl	IBr	I_2
3.98 ± 0.11	4.86 ± 0.32	1.04 ± 0.04	4.19 ± 0.15	4.71 ± 0.29	0.99 ± 0.06	5.2	3.1	4.9
1.21 ± 0.03	1.16 ± 0.08	0.35 ± 0.02	1.31 ± 0.06	1.22 ± 0.09	0.37 ± 0.01	7.9	5.0	5.7
0.81 ± 0.02	0.77 ± 0.05	0.12 ± 0.01	0.87 ± 0.08	0.79 ± 0.05	0.13 ± 0.01	5.1	2.6	8.6

[a] Gas flow rate: 500 mL min^{-1}.

[b] Mean ± S.D. (n = 3).

It is noted that the concentrations of halogen species tested here could be somewhat higher than the typical ambient concentration levels. Thus, for field measurements, the extension of sampling time might be necessary to collect a sufficient analyte mass for subsequent GC–MS analysis. Therefore, additional experiments were carried out by increasing the sampling time to 180 min at a flow rate of 500 mL min^{-1}. The differences of collection efficiencies were less than 4.8%. This result is not surprising because 1,3,5-TMB is present in excess and highly reactive towards the target analytes. The limit of detection (LOD, S/N = 3) from the instrument under full-scan mode was 0.12 ng for 1-iodo-2,4,6-TMB and 0.69 ng for 1-bromo-2,4,6-TMB, respectively. On the basis of 90 L sample volume, the LOD for ICl, IBr and I_2 was 0.11 pptv, 0.76 pptv and 0.11 pptv, respectively.

4. Conclusions

1,3,5-TMB has been successfully applied as a selective derivatization agent for the determination of gaseous ICl, IBr and I_2. Gaseous ICl and IBr are quantitatively collected in a denuder system with satisfactory collection efficiencies (i.e. 99.2% for ICl and 92.6% for IBr, at 500 mL min^{-1} gas flow rate), which is close to the maximum collection efficiency calculated based on theoretical considerations. However, the collection efficiency for I_2 is lower than 1% in the same denuder system, but significantly increases to about 90% when an aqueous 1,3,5-TMB loaded impinger is used. Mixtures of ICl, IBr and I_2 can be differentiated using a coupled denuder–impinger system, in which ICl and IBr are converted in the front denuder into 1-iodo-2,4,6-TMB and 1-bromo-2,4,6-TMB, respectively, and I_2 passes through the denuder and is collected and converted into 1-iodo-2,4,6-TMB in the impinger system.

Acknowledgements

This work was carried out within the DFG Graduiertenkolleg 826 "Trace analysis of elemental species: Method developments and applications". The authors thank the Deutsche Forschungsgemeinschaft (German Research Foundation) for financial support. The authors also acknowledge additional support from the EU project MAP (Marine Aerosol Production).

References

[1] U. Platt, G. Hönninger, Chemosphere 52 (2003) 325.

[2] C.D. O'Dowd, T. Hoffmann, Environ. Chem. 2 (2005) 245.

[3] A. Saiz-Lopez, J.M.C. Plane, J. Phys. IV 121 (2004) 223.

[4] B. Alicke, K. Hebestreit, J. Stutz, U. Platt, Nature 397 (1999) 572.

[5] L.J. Carpenter, K. Hebestreit, U. Platt, P.S. Liss, Atmos. Chem. Phys. 1 (2001) 9.

[6] A. Saiz-Lopez, A.S. Mahajan, R.A. Salmon, S.J.B. Bauguitte, A.E. Jones, H.K. Roscoe, J.M.C. Plane, Science 317 (2007) 348.

[7] R. Vogt, R. Sander, R. von Glasow, P.J. Crutzen, J. Atmos. Chem. 32 (1999) 375.

[8] G. McFiggans, R.A. Cox, J.C. Mössinger, B.J. Allan, J.M.C. Plane, J. Geophys. Res. 107 (2002) D154271.

[9] J.G. Calvert, S.E. Lindberg, Atmos. Environ. 38 (2004) 5087.

[10] K.L. Foster, R.A. Plastridge, J.W. Bottenheim, P.B. Shepson, B.J. Finlayson-Pitts, C.W. Spicer, Science 291 (2001) 471.

[11] C.W. Spicer, R.A. Plastridge, K.L. Foster, B.J. Finlayson-Pitts, J.W. Bottenheim, A.M. Grannas, P.B. Shepson, Atmos. Environ. 36 (2002) 2721.

[12] A. Kloskowski, M. Pilarczyk, J. Namiesnik, Crit. Rev. Anal. Chem. 32 (2002) 301.

[13] R. Fisseha, J. Dommen, M. Sax, D. Paulsen, M. Kalberer, R. Maurer, F. Hofler, E. Weingartner, U. Baltensperger, Anal. Chem. 76 (2004) 6535.

[14] R. Zanella, M. Schilling, D. Klockow J. Environ. Monit. 1 (1999) 441.

[15] Z. Vecera, P. Dasgupta, Anal. Chem. 63 (1991) 2210.

[16] C. Perrino, M. Concetta, T. Sciano, I. Allegrini, J. Chromatogr. A 846 (1999) 269.

[17] N. Takenaka, H. Terada, Y. Oro, M. Hiroi, H. Yoshikawa, K. Okitsu, H. Bandow, Analyst 129 (2004) 1130.

[18] X.B. Feng, J.Y. Lu, Y.J. Hao, C. Banic, W.H. Schroeder, Anal. Bioanal. Chem. 376 (2003) 1137.

[19] B. Temime-Roussel, A. Monod, C. Massiani, H. Wortham, Atmos. Environ. 38 (2004) 1913.

[20] Y. Nordqvist, U. Nilsson, A. Colmsjo, Anal. Bioanal. Chem. 375 (2003) 786.

[21] Y. Nordqvist, J. Melin, U. Nilsson, R. Johansson, A. Colmsjo, Fresen. J. Anal. Chem. 371 (2001) 39.

[22] K. Motyka, P. Mikuska, Anal. Chim. Acta 518 (2004) 51.

[23] Y.C. Lin, M.T. Cheng, W.Y. Ting, C.R. Yeh, Atmos. Environ. 40 (2006) 4725.

[24] J. Peskova, P. Parizek, Z. Vecera, J. Chromatogr. A 918 (2001) 153.

[25] J. Sklenska, A. Broskovicova, Z.Vecera, J. Chromatogr. A 973 (2002) 211.

[26] D.E. Tobias, J.A. Perlinger, P.S. Morrow, P.V. Doskey, D.L. Perram, J. Chromatogr. A 1140 (2007) 1.

[27] J. Pavlinac, M. Zupan, S. Stavber, Synthesis-Stuttgart 15 (2006) 2603.

[28] Z. Ali, C.L.P. Thomas, J.F. Alder, Analyst 114 (1989) 759.

[29] S.M. Hubig, W. Jung, J.K. Kochi, J. Org. Chem. 59 (1994) 6233.

[30] D.E. Turner, R.F. O´Malley, D.J. Sardella, L.S. Barinelli, P. Kaul, J. Org. Chem. 59 (1994) 7335.

[31] A.F. Holleman, E. Wiberg, N. Wiberg, Lehrbuch der Anorganischen Chemie, Walter de Gruyter, Berlin·New York, 1985, p. 415 (in German).

[32] P.G. Gormley, M. Kennedy, Proc. R. Ir. Acad. Sect. A 52 (1949) 163.

[33] Y.L. Wang, J.C. Nagy, D.W. Margerum, J. Am. Chem. Soc. 111 (1989) 7838.

[34] R.C. Troy, M.D. Kelley, J.C. Nagy, D.W. Margerum, Inorg. Chem. 30 (1991) 4838.

[35] I. Lengyel, I.R. Epstein, K. Kustin, Inorg. Chem. 32 (1993) 5880.

2.3 Extensive Evaluation of a Diffusion Denuder for the Quantification of Atmospheric Stable and Radioactive Molecular Iodine

RU-JIN HUANG,[†] XIAOLIN HOU,[‡] AND THORSTEN HOFFMANN[*,†]

Institute of Inorganic and Analytical Chemistry, Johannes Gutenberg-University of Mainz, Duesbergweg 10-14, D-55128 Mainz, Germany, Radiation Research Department, Risø National Laboratory, NUK-202, Technical University of Denmark, DK-4000 Roskilde, Denmark

[*] Corresponding author e-mail: hoffmant@uni-mainz.de.
[†] Johannes Gutenberg-University of Mainz.
[‡] Technical University of Denmark.

Status: Submitted to Environmental Sciences & Technology

In this paper, we present a new approach for the quantification of gaseous molecular iodine (I_2) for laboratory- and field-based studies. α-cyclodextrin (α-CD) in combination with $^{129}I^-$ is shown to be an effective denuder coating for the sampling of gaseous I_2 by the formation of an inclusion complex. The entrapped $^{127}I_2$ together with the $^{129}I^-$ spike in the coating is then released and derivatized to 4-iodo-*N*,*N*-dimethylaniline (4-I-DMA) for gas chromatography–mass spectrometry (GC–MS) analysis. The $^{127}I_2$ collected can be differentiated from the $^{129}I^-$ spike by the MS. A set of parameters affecting the analytical performances of this approach, including amounts of α-CD and $^{129}I^-$ applied, denuder length, sampling gas flow rate and sampling duration, relative humidity, sample storage period, and condition of release and derivatization of iodine, is extensively evaluated and optimized. The collection efficiency is larger than 98% and the limit of detection (LOD) obtained is 0.17 pptv for a sampling duration of 30 min at 500 mL min^{-1}. Furthermore, the potential use of this protocol for the determination of radioactive I_2 at ultra trace level is also demonstrated when $^{129}I^-$ used in the coating is replaced by $^{127}I^-$ and a multiple denuder system is used. The developed method provides a reliable and attractive alternative in “single-point” in situ gaseous I_2 measurement for atmospheric chemistry research and has been used to measure ambient $^{127}I_2$ at a coastal site in Ireland and ambient $^{129}I_2$ at Mainz, Germany.

Introduction

Iodine is a biophilic trace element with one stable isotope (^{127}I), one long-lived isotope (^{129}I, $t_{1/2}$ = 15.7 million years), and several short-lived isotopes (e.g., ^{131}I, $t_{1/2}$ = 8 days). The impact of this element on the human health, such as iodine deficiency disorders and radioactive iodine-induced thyroid cancer, has been well documented. However, only in the past few years has particular attention been given to the potential atmospheric significance of iodine photochemistry (*1–7*) and iodine-related new particle formation (*8–11*). In these atmospheric processes molecular iodine (I_2) (*6*,*7*,*10*,*11*), rather than iodocarbons, was recently proposed to be the dominant source of coastal reactive iodine. A possible mechanism for the release of I_2 from marine Laminaria macroalgal species was suggested as follows (*12*): iodide (I^-) accumulated by kelp is well suited as a versatile antioxidant and can readily scavenge a variety of reactive oxygen species (e.g., H_2O_2, O_3, O_2^-, $^1O_2$, and $HO_2^{\cdot}$) on the thallus surface and in the apoplast of the kelp, leading to the release of I_2 at low tide. During daytime, the released I_2 molecules photolyse readily to form iodine atoms that react rapidly with atmospheric O_3 leading to the formation of iodine monoxide (IO). The self-reaction of IO yields higher oxides, which is probably responsible for the formation of iodine-containing new particles in the marine boundary layer (*4*,*8*,*9*,*13*).

The environmental levels of ^{129}I have been dramatically elevated by several orders of magnitude by human nuclear activities over the past 50 years (*14*). The major pathway of anthropogenic ^{129}I into the environment is through direct gaseous releases (mainly as $CH_3{}^{129}I$ and $^{129}I_2$ (*15*)) and marine discharges from nuclear facilities, wherein the nuclear reprocessing facilities at La Hague (France) and Sellafield (England) are responsible for about 90% of the anthropogenic ^{129}I releases (*16*). Recently, Hou *et al.* (*17*) found that the ^{129}I levels in the seaweeds investigated rise to 10–10^3 higher than the fall-out background and are dominated strongly by the marine discharges from nuclear reprocessing facilities. Considering the I_2 release mechanism described above, ^{129}I accumulated in the seaweeds can also be released into the atmosphere and then transported to the continent. Although there is no significant radiation risk for human health at the present $^{129}I_2$ level, with the increasing number of nuclear power plants and nuclear reprocessing facilities, more and more $^{129}I_2$ will be produced and released into the atmosphere. Nevertheless, because of the difficulties for accurate identification and quantification $^{129}I_2$ at ultra trace level a complete record of global atmospheric $^{129}I_2$ variability has not been available so far, nor have the direct gaseous $^{129}I_2$ release levels from nuclear reprocessing plants. Like other elements, the atmospheric behavior of iodine is species dependent. The specific physico-chemical properties of various iodine species result in differences in lifetime, phase partitioning, transportation, biogeochemical cycling, and environmental impacts. Therefore, a method development for qualification and quantification of radioactive molecular iodine is necessary, especially in the cases of nuclear accidents such as the Chernobyl accident in 1986, the Windscale (Sellafield's previous name) accident in 1957, and the Sellafield radioactive leak in 2005 (*18*).

Approaches to gaseous I_2 measurement are still scarce. For laboratory-based studies, an indirect detection method (*12*,*19*) is frequently used—in which gaseous I_2 is collected by an ethanol trap and quantified as I^- using a UV/Vis absorption spectrometer calibrated with standard solutions. I^- is produced through the rapid disproportionation of I_2 in alkaline solution. Although this indirect method provides excellent collection efficiency for gaseous I_2, the hydrolysis of I_2 in alkaline solution involves multiple equilibrium processes and the relevant products could be IO^-, HOI, and I_2OH^- besides I^- (*20*) of which the proportion is pH dependent. These co-produced hydrolysis species might effect the accuracy of the UV/Vis determination and thus strict pH control is necessary. For field-based measurements of I_2, differential optical absorption spectroscopy (DOAS) is currently the most widespread measurement technique (*6*,*7*). However, this technique can only provide the distance-average concentration of I_2 along the light-path (e.g., 8.4 km) and thus can not identify the so-called "hot spots"(*7*). Efforts have been made in the use of broadband cavity ring-down spectrometry (BBCRDS) (*6*) and incoherent broad-band cavity-enhanced absorption spectroscopy (IBBCEAS) (*21*) to provide "single-point" in situ measurements of I_2. However, the limit of detections (LODs) of these spectrometric methods are relatively high (~ 20 ppt), which would not be sufficient for some atmospheric domains with rather low I_2 fluxes such as open sea—not even for the daytime I_2 measurement in the intertidal zones. On the basis of the above discussions, it is obvious that an approach for “single-point” in situ gaseous I_2 measurement at low concentration level is required for both laboratory- and field-based consideration. Here, we present further improvements of a newly developed denuder system (*22*) in combination with postderivatization and gas chromatography–mass spectrometry (GC–MS) determination for the qualification and quantification of gaseous I_2. The parameters affecting the analytical performances of this method are extensively evaluated and optimized. Especially the molar ratios between I_2 and α-cyclodextrin (α-CD) and the spiked iodide, which can significantly affect the collection efficiency of denuder, are optimized. In addition, we demonstrate for the first time that this approach can be extended to measurements of radioactive I_2 in the gas phase by using a differentiable isotopic iodide as coating spike.

Experimental Section

Chemicals and Materials. Iodine (99.999% purity) was purchased from Aldrich (Steinheim, Germany) and used for both gas calibration source and the synthesis of 4-iodo-*N*,*N*-dimethylaniline (4-I-DMA). α-CD obtained from four chemical companies, i.e., Fluka (Steinheim, Germany), Sigma (Steinheim, Germany), Acros Organics (Geel, Belgium), and Alta Aesar (Karlsruhe, Germany), was used as coating material. *N*,*N*-dimethylaniline (DMA) and 2,4,6-tribromoaniline (2,4,6-TBA) were purchased from Across Organics (Geel, Belgium). Cyclohexane and anhydrous glycerin were obtained from Fluka (Steinheim, Germany). KI (99.995% purity) was purchased from Merck (Darmstadt, Germany). Iodide-129 standard solution (SRM 4949C) purchased from the National Institute of Standards and Technology (Gaithersburg, MD, USA) was diluted and used in concentration lower than 100 $\mu g\ L^{-1}$, which refers to a radioactivity lower than 0.65 $Bq\ g^{-1}$. Anhydrous α-CD was prepared by dehydration under vacuum ($\approx 10^{-2}$ Pa) at 110 ^{o}C for 24 h and used immediately. Sodium 2-iodosobenzoate was prepared by stirring 1 g of 2-iodosobenzoic acid (Sigma) with a slight molar excess of NaOH (0.2 $mol\ L^{-1}$, 20 mL) and diluting to 250 mL with ultrapure water (Milli-Q Water Purification System, Millipore, Bedford, MA). It was filtered with 0.45 μm membrane filter and kept in the dark. 4-I-DMA was not commercially available and was synthesized for the purpose of quantitation. The synthesis and isolation procedures are described in the Supporting Information. Purity of the synthetic 4-I-DMA was 98.9% measured by GC–MS. The concentration of stock standard solution of 4-I-DMA was 2.5 mg mL^{-1} in cyclohexane. A series of working standard solutions was prepared by sequential dilution of the stock standard solution with cyclohexane.

Laboratory Test. I_2 test gas in nitrogen was generated from a capillary diffusion based device. Details of the test gas source are described elsewhere (*22*). The output of the test gas was determined by periodically measuring the mass loss of the analyte vessel. Where required, a needle valve and dilution chamber were used to get the desired final concentration (ranging from 49 ppt to 15.6 ppb).

Brown borosilicate glass tubes (6 mm i.d.) were used for the preparation of denuder samplers. A length of 50 cm was chosen to attain satisfactory collection efficiency (see below). DMA (1.5 mmol L^{-1}), DMA/glycerin (containing 1.5 mmol L^{-1} DMA and 0.8%–8% glycerin), α-CD (2.5 mg mL^{-1}), and α-CD/I^- (containing 2.5 mg mL^{-1} α-CD and trace $^{129}I^-$ or $^{127}I^-$) in methanol, were tested as coating solutions. A similar coating procedure as described in literature (*22*) was used to obtain a denuder coated uniformly with the reagents. Untreated glass tubes of specific length (3–18 cm) with the same diameter as the denuder tube were coupled to the denuder inlet, acting as laminar flow subduction zone. The typical sampling period was 10–45 min at a flow rate of 500 mL min^{-1}, controlled by a flow-adjustable membrane pump located downstream of the denuder tube. Three to five samples were taken for each measurement.

The collection efficiency of an individual denuder was determined by calculating the proportion between analyte found in the denuder elution and its known amount entering into the denuder.

Field Sampling. Gaseous I_2 in the marine boundary layer was measured at Mweenish bay (53.32° N, 9.73° W) located at the west coast of Ireland in September 2007. Samples were taken by sampling the ambient air through the α-CD/$^{129}I^-$-coated denuder tubes for 30–180 min at a flow rate of 500 mL min^{-1}. Gaseous $^{129}I_2$ samples were consecutively collected on the roof of the Max Planck Institute for Chemistry (49.98^o N, 8.23^o E) in May–July 2008 (46 days, in total). A multiple denuder system consisting of 12 α-CD/$^{127}I^-$-coated denuder tubes (6 mm i.d. × length 50 cm each) in a circle in parallel was used and the denuder tubes were renewed every 14–16 days. The total sampling flow rate was increased to 14.4 L min^{-1} (1.2 L min^{-1} for each denuder). Finally, all these $^{129}I_2$ samples were combined to form a single sample to increase the sensitivity of analysis. At the measuring site, the denuders were set vertically to eliminate the particle deposition due to gravitational effect. Once the sampling was completed, the open ends of the denuder tubes were again sealed with PP end caps and kept in refrigeration.

Sample Preparation and Analysis. Two different sample preparation procedures were applied. The samples collected directly with DMA-related coatings were eluted with five 1.0 mL-portions ethanol into a vessel in which 100 µL of 2,4,6-TBA (2.5 mg L^{-1} in cyclohexane) was then added as internal standard. The mixture was concentrated almost to dryness with a gentle stream of purified nitrogen and then dissolved in 100 µL of cyclohexane. The samples collected with α-CD-related coatings (for both test gas experiments and ambient $^{127}I_2$ measurements) were eluted with five 2.0 mL-portions of ultrapure water into a 25-mL calibrated flask. 500 µL of phosphate buffer (pH 6.4), 100 µL of 2,4,6-TBA (2.5 mg L^{-1}, internal standard), 400 µL of sodium 2-iodosobenzoate, and 300 µL of DMA were then added. The solution was diluted to about 23 mL with ultrapure water and subsequently shaken at room temperature for about 120 min. 2.0 mL of sodium acetate solution (20% m/v) was then introduced and the solution was diluted to the mark with ultrapure water. Finally, the solution was extracted with 100 µL of cyclohexane. For ambient $^{129}I_2$ measurements, the samples collected were eluted into a 100-mL calibrated flask and then subjected to derivatization as described above. The solution was then extracted with 1.0 mL of cyclohexane. The extract was concentrated to 25 µL with a gentle stream of purified nitrogen. 1.0 µL of the solution was injected into a gas chromatography with an ion-trap mass spectrometer (Trace GC/PolarisQ, Thermo Finnigan Italia S.p.A., Rodano, Italy). A fused-silica capillary column (30 m × 0.25 mm i.d., d_f: 0.25 µm, Rtx-5MS, Restek Co., Bad Homburg, Germany) was used for chromatographic separation. High-purity helium (99.999%) was used as a carrier gas at a constant flow of 1.0 mL min^{-1}. The temperature of the injector was set to 250 ^{o}C and the transfer line was 300 ^{o}C. The temperature of the GC oven was programmed as follows: initial temperature 50 ^{o}C (hold 3 min), 30 ^{o}C min^{-1} to 220 ^{o}C (hold 3 min). The MS was operated in the electron impact (EI) ionization mode with an acceleration energy of 70 eV. A solvent delay of 4.5 min preceded the MS spectra acquisition in the full-scan mode (in the range *m/z* 45–450) or in the selected ion monitoring (SIM) mode in the following sequence: 4.50–6.00 min, *m/z*: 77, 121; 6.00–7.50 min, *m/z*: 119, 247 (or 249); 7.50–11.67 min, *m/z*: 250, 329, 331.

Results and Discussion

Sampling Optimization. A diffusion denuder is a sampling device that can separate gases and particles present in the same air mass and quantitatively collect the gaseous target by either physical adsorption/absorption or chemical bonds when the coating represents an ideal sink towards the analyte. Therefore, coating selection is a crucial factor determining the performances of denuder samplers. Quantitative collection was not achieved using in situ derivatization chemicals (*22*), even in combination with glycerol (see Table 1), which has been frequently used as a binding coating agent (*23*,*24*) to improve the residence of gaseous analyte on the coating layer.

The capability of α-CD to form inclusion complexes with iodine has been briefly investigated (*22*). Our further studies, however, show that when α-CD is used as a sole denuder coating the collection efficiencies of I_2 can vary widely (ranging from 40% to 87%) with the sources of α-CD delivered by different chemical companies. Interestingly, the collection efficiency dropped close to 30% when anhydrous α-CD was applied; however increased to 93.4% in the case of additional water present in the inner wall of denuder (Table 1). It is apparent that water molecules play an active role in such inclusion complex formation, probably by hydrolysis of a small fraction of entrapped gaseous I_2. The resulting I^- was proved to facilitate the gas-solid complexation of I_2 with α-CD (see below). Thus, the observed difference of collection efficiencies of α-CD might be attributed to the difference in the content of water molecules included in the commercially available α-CD (*25*).

TABLE 1. The Coated Absorption Materials Examined for Gaseous Molecular Iodine[a]

coating material	mass of solute in 100 ml methanol	volume of the coating solution introduced into denuder (ml)	collection efficiency (%)	RSD[b] (%)
DMA	19.1 mg	3.0	< 1.0	
DMA/glycerol	19.1 mg/1.0 g	3.0	27.1	19.3
DMA/glycerol	38.2 mg/10.0 g	3.0	53.9	14.5
α-CD	250.0 mg	4.5	40.8–86.7 [c]	6.1–9.3[c]
anhydrous α-CD	250.0 mg	4.5	31.9	5.2
α-CD/water	275.0 mg/10.0 g	4.5	93.4	2.6
α-CD/I^-	350.0 mg/50.0 µg	3.0	98.5	0.8

[a] gas flow rate: 500 mL min^{-1}. [b] *n* = 9 (RSDs were determined from triplicate runs of three samples in each case). [c] the range obtained indicates different sources of α-CD.

Although additional water molecules improve the performance of α-CD-coated denuder for gaseous I_2 collection, it is unfavorable for long-term sampling and storage because the potential water loss during such processes could lead to unpredictable artifacts. The alternative is to add iodide ions to the α-CD coating because iodide is assumed to be able to initiate the inclusion complexation between α-CD and I_2 in aqueous solution (22,*26*). However, attention should be paid to the amounts of iodide ions added because the spiked iodide finally deliver the same derivative as the trapped I_2 and therefore interfere in ambient I_2 measurement at trace concentration levels. This problem was addressed by selecting differentiable $^{129}I^-$ isotope rather than $^{127}I^-$ as spike. Figure 1 shows that the collection efficiency increases with the increasing iodide spike and reaches a maximum value at a molar ratio of 1:3 of I^- to I_2. Furthermore, it is found that compared to a required molar ratio of 2:1 of α-CD/I_2 to form inclusion complexes in aqueous solution a much higher ratio (≥ 950:1) is needed to ensure sufficient collection efficiency, as shown in Figure 2.

Figure 3 shows the effect of sampling flow rat and denuder length on the collection efficiency of I_2. At a flow rate of 100 mL min^{-1}, 96.1% efficiency was obtained using a 20-cm-long denuder. To get increased sensitivity, higher sample volumes are frequently required in view of the low concentration level of ambient I_2. This aim can be achieved by either increasing sampling time or increasing sampling gas flow. Obviously, higher sampling gas flow improves the time resolution of the sampling technique; however, with the increase of sampling gas flow the length of denuder should correspondingly be increased to guarantee satisfactory collection efficiency. As can be seen in Figure 3, at a flow rate of 500 mL min^{-1}, the collection efficiency was lower than 70% for a 20-cm-long denuder but increased to 97.1% for a 40-cm-long denuder.

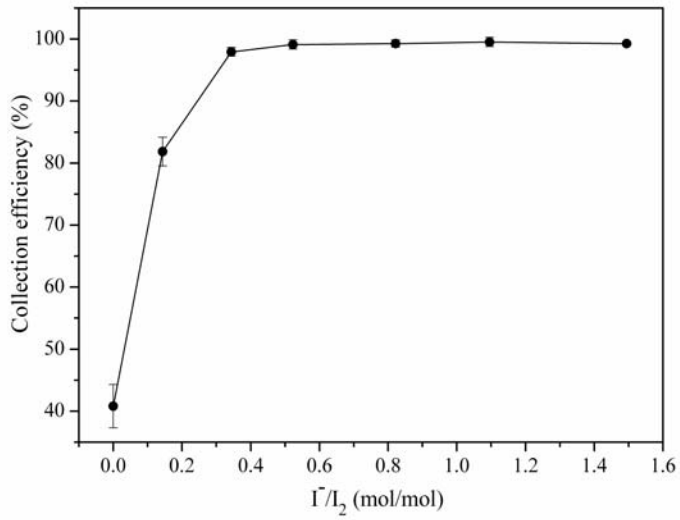

FIGURE 1. Effect of I^- on the gaseous I_2 collection by α-CD-coated denuder. The points represent mean values of five measurements.

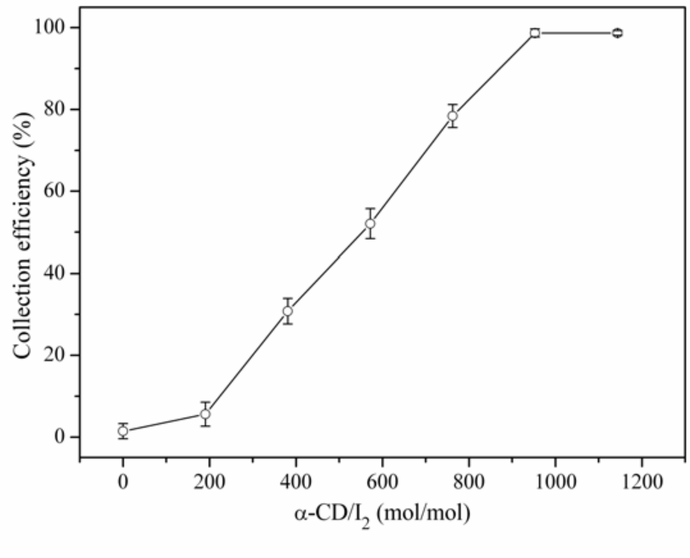

FIGURE 2. Effect of α-CD amount on the collection efficiency of gaseous I_2 by denuder in which sufficient I^- was presented. The points represent mean values of five measurements.

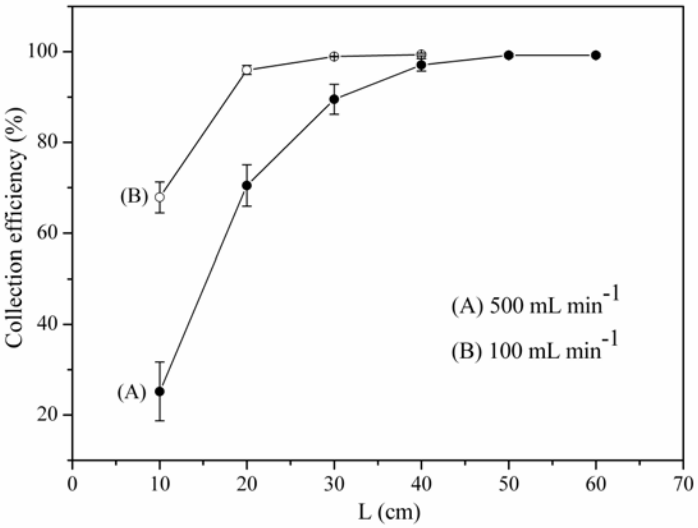

FIGURE 3. The denuder length-dependent collection efficiency at a gas flow rate of (A) 500 mL min^{-1} and (B) 100 mL min^{-1}. The points represent mean values of three measurements.

Postderivatization and Analysis. Because the complex formation (R1) between α-CD and iodine takes place based on non-covalent bonding, the entrapped iodine can be released relatively easy. After water extraction the released inorganic iodine species have to be converted to organic species for GC–MS measurement. Therefore, DMA and 2-iodosobenzoate (*27*) were added into the eluate of the coating. I_2 released from α-CD was converted rapidly into 4-iodo-*N,N*-dimethylaniline (4-I-DMA) *via* R2. The iodide ions liberated in R2 and those added in the coating were oxidized by 2-iodosobenzoate to molecular iodine (R3), followed by R2 until all iodide was converted into 4-I-DMA. As a consequence, 2 mol of 4-I-DMA were formed for each mole of molecular iodine, and 1 mol of 4-I-DMA was formed for each mole of spike iodide. The temporal behavior of the I_2 release from α-CD is shown in Figure 4. Quantitative release was observed after about 120 min. The derivative was then extracted into the cyclohexane solvent.

$$\alpha\text{-cyclodextrin} + I_2 + n\,I^- \leftrightarrow \alpha\text{-cyclodextrin}\cdot I_2 \cdot I_n^- \qquad \text{(R1)}$$

$$I_2 + N,N\text{-dimethylaniline} \rightarrow 4\text{-iodo-}N,N\text{-dimethylaniline} + H^+ + I^- \qquad \text{(R2)}$$

$$2\,I^- + 2\,H^+ + 2\text{-iodosobenzoate} \rightarrow I_2 + H_2O + 2\text{-iodobenzoate} \qquad \text{(R3)}$$

It should be noted that a certain fraction of ^{127}I coexists with ^{129}I in the iodide used here, which formed the same derivative as the entrapped gaseous $^{127}I_2$ and thus had to be subtracted for $^{127}I_2$ quantification. The isotopic composition of the radioactive iodide standard was measured by GC–MS following derivitization reactions and found to consist of 14.4% ^{127}I and 85.6% ^{129}I, corresponding to a constant $^{127}I/^{129}I$ ratio of 0.17. This isotopic ratio is consistent with a reported value of 0.16 (*28*). The result indicates that no isotopic effect takes place during the derivatization process and that the derivatives of ^{127}I and their isotopic analogues experience the same degree of ionization in MS analysis. These features are important for accurate quantification. From the total ion chromatogram of the iodinated derivatives (Figure S1A), it can be seen that the derivatives of ^{127}I and their isotopic counterparts have the same retention behavior in GC separation, however, produce a 2-Da mass difference between their respective base peaks (molecular ion peaks, *m/z* 247 and *m/z* 249) in the subsequent MS determination. Therefore, the amounts of total ^{127}I (sum of the collected gaseous $^{127}I_2$ and the small fraction of $^{127}I^-$ coexisted with $^{129}I^-$) and ^{129}I spike can be determined by measuring the signal area in the extracted ion chromatogram (Figure S1B and C) or in the SIM chromatogram (Figure S2). The amounts of collected $^{127}I_2$ (n, mol) were calculated according to equation 1

$$n\,(^{127}\mathrm{I}_2) = \frac{n\,(^{127}\mathrm{I}_{\mathrm{total}}) - 0.17 \times n\,(^{129}\mathrm{I})}{2} \qquad \text{(eqn.1)}$$

As the collection of molecular iodine is based on inclusion complex formation with the assistance of iodide and does not depend on the isotopic species, the potential use of this denuder sampling system in the collection and differentiation of radioactive I_2 is a straightforward variation of the technique if $^{127}I^-$ instead of $^{129}I^-$ is added to the coating. In view of the ultra-low concentration levels of radioactive I_2 in the atmosphere, it is necessary to collect a sufficient analyte mass for subsequent GC–MS analysis. However, the low sample flow rates inherent in the conventional cylindrical denuder (i.e., a maximum of a few liters per minute) require extremely long sampling times (e.g., months). The problem of low sampling flow can be partially reduced by passing the gas sample through an annular or parallel plate denuder (*29*,*30*), by using a large number of cylinder tubes in parallel (*31*), or by using a multiple channel denuder such as the honeycomb denuder and the multiple parallel plate denuder (*32*,*33*). Here, we used 12 individual cylinder tubes placed in a circle in parallel to compensate for the low sampling flow rate. The total flow through the system was 14.4 L min^{-1} (1.2 L min^{-1} for each tube), and the sampling time was reduced to several tens of days. This approach is applicable for long-lived $^{129}I_2$ measurement; but limited by the lifetime of radioactive decay for other short-lived molecular iodine (e.g., ^{131}I, $t_{1/2}$ = 8 days; ^{125}I, $t_{1/2}$ = 59 days). However, it can be expected that the sampling time would be reduced further if the α-CD/$^{127}I^-$ coatings are applied to a high-throughput denuder, e.g., honeycomb-like and multiple parallel plate denuder to which a higher flow rate can be introduced (for example 250 L min^{-1} (*33*)). In addition, a higher sensitivity can be expected if a radiometric method with a gamma detector instead of the GC–MS method is used for the direct measurement of the analyte collected in the denuder tube (*34*). In that case, also the determination of short-lived molecular iodine could be possible.

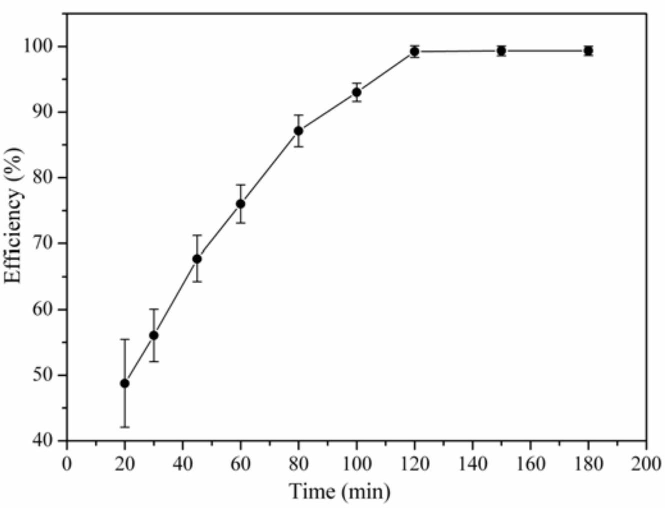

FIGURE 4. The time-dependent I_2 releasing profile from α-CD following addition of *N,N*-dimethylaniline and 2-iodosobenzoate. The points represent mean values of three measurements.

Evaluation of Laboratory and Field Measurements. The method showed sufficient accuracy at an I_2 concentration of ppbv (*22*). However, it is noted that the ambient $^{127}I_2$ concentrations in the coastal marine boundary layer are typically at pptv level. Therefore, we further tested the method accuracy at the concentration levels down to pptv. The results tested at a flow rate of 500 mL min^{-1} for 10–45 min were compared with the data obtained by calculating the outputs of the gas source and the dilution ratios (what is part of the Supporting Information, shown in Figure S3). A high correlation coefficient (R^2 = 0.9992) indicates the excellent accuracy of the present method. The slope (0.9892) is evidence of the absence of an analytical bias, being very close to unity. Furthermore, the performance of the denuder was demonstrated to be independent of the relative humidity of the sampled air. This feature can be attributed to the assistance of H_2O molecules to the inclusion complex formation as described above. The complex of α-CD with iodine in solid state is very stable (*35*). In general, no significant iodine lost was found, at least over a 2-month period of sample storage in refrigeration (around -15 ^{o}C). In addition, it is noted that the increases of either sampling duration or gas flow rate might be necessary for field measurement, especially for ambient $^{129}I_2$ determination. Additional experiments were then performed by sampling 49.2 pptv I_2 at a flow rate of 1.2 L min^{-1} for 14 days. The collection efficiency obtained was 81.2%, which is somewhat lower than the maximum value shown in Table 1 due to the increase of sampling flow. The LOD (S/N = 3) of the GC–MS under SIM mode was 0.51 pg for 4-I-DMA. Thus, the LOD is calculated to be 0.17 pptv for $^{127}I_2$ (sampling time 30 min at 500 mL min^{-1}) and 1.63×10^7 molecule m^{-3} for $^{129}I_2$ (sampling time 46 days at 14.4 L min^{-1}), respectively, which is much lower than the respective ambient concentration measured in this work.

TABLE 2. Determination of $^{127}I_2$ in the Marine Boundary Layer and $^{129}I_2$ in the Urban Atmosphere

sample	sampling time	$^{127}I_2$ (pptv)[a, c]	$^{129}I_2$ ($\times 10^8$ molecule m^{-3})[b, c]
070830-02	12:10–14:10	44.71 ± 1.56	nd
070830-04	23:10–01:10	108.55 ± 2.17	nd
070901-02	12:00–15:00	25.73 ± 1.11	nd
070902-02	00:00–00:30	69.74 ± 1.28	nd
080523-01	23 May–08 July	nd	2.33 ± 0.32

[a] $^{127}I_2$ samples were taken at low tide at Mweenish bay, Ireland. [b] $^{129}I_2$ samples were taken at Mainz, Germany. [c] mean ± S.D. (*n* = 3, referring to triplicate runs of the same sample). nd, not detected.

Based on the results above, which confirm the reliable collection of gaseous I_2 by α-CD/I^--coated denuder, we further investigated the potential interference of other iodine species in the I_2 measurements presented below. In view of the gaseous constituents in the atmosphere, potential species which can be entrapped into the α-CD interior cavity and subsequently afford the same iodination process as I_2 could be the interhalogens (e.g., ICl and IBr). However, these interhalogen species can be isolated by coupling a

1,3,5-trimethoxybenzene-coated denuder upstream of the α-CD/I^--coated denuder (*22*). The interaction of a fraction of α-CD with other gaseous constituents might occur during a long sampling period. However, the efficiency for molecular iodine collection could not significantly decrease since α-CD was presented in excess and the reaction towards iodine is very specific. The spiked iodide was also presented in excess. Even if a fraction of the spiked $^{129}I^-$ is consumed by other gaseous constituents, the consumption of the coexisted $^{127}I^-$ will be a factor of 0.17 of the consumed $^{129}I^-$, with the same $^{127}I^-/^{129}I^-$ isotopic ratio as in the spike standard (see the Postderivatization and Analysis section). Since the exact amount of the spiked $^{129}I^-$ which involves the complex formation of iodine–α-CD is determined by mass spectrometry after postderivatization, the exact mass of the spiked $^{127}I^-$ which involves the iodine–α-CD complex can be calculated based on the constant isotopic ratio of 0.17 and the sampled molecular iodine can be corrected by equation 1. In terms of field measurements in the coastal air another concern is the interference from iodine oxides (e.g., I_2O_5, I_4O_9) driven ultra-fine particles. Theoretical calculations from the Gormley–Kennedy equation (*36*) predict that more than 25% ultra-fine (≤ 5 nm) can diffuse to the inner wall of denuder. However, a major fraction of which will escape from the denuder with the gas stream since the coating material used here is not expected to be reactive towards particles. Furthermore, even if a small fraction of particles finally resides in the denuder they will not react with the derivatization agent during the postderivatization step and therefore will not interfere with the molecular iodine measurements. The same is true for the iodine oxides in gas phase (e.g., IO, OIO) (*22*). The exemplary measurements of ambient $^{127}I_2$ and $^{129}I_2$ concentrations are presented in Table 2. To the best of our knowledge it is the first time to measure ambient $^{129}I_2$. The $^{127}I_2$ mixing ratios measured during the campaign are somewhat higher than the reported average concentration by another “single-point” measurement technique BBCRDS at Mace Head (a nearby location) (*6*) due to higher biomass density at Mweenish Bay than at Mace Head, but are in general much higher compared with the data measured by LP-DOAS (e.g., (*7*)). An explanation for the discrepancy could be that the denuder technique provides “point” measurements on the foreshore; however, DOAS technique provides distance-averaged mixing ratio along the light-path of several kilometers extending over open sea, leading to potential underestimation of the concentration levels of I_2 in the intertidal zone. Still it should be noted that the duration of ambient $^{127}I_2$ sampling used in this work was in the range between 30 and 180 min, which does not allow the measurements of $^{127}I_2$ peak value. However, considering the limit of detection of the presented method as well as the concentration levels at the west coast of Ireland, we suggest a sampling time of 30–60 min for further field measurements in algae-rich coastal areas, so that a better time resolution and a more detailed study of the diurnal variation of ambient $^{127}I_2$ can be performed, and a better understanding of release mechanism and atmospheric impact of $^{127}I_2$ can be expected. Besides its application in I_2 quantitative analysis, α-CD/I^- can be expected to be used for immobilization of radioactive iodine from nuclear exhaust gases.

Acknowledgments

This work was supported by the German Research Foundation (Deutsche Forschungsgemeinschaft, DFG) within the Graduiertenkolleg 826 “Trace Analysis of Elemental Species: Method Developments and Applications”. We acknowledge additional financial support from the EU under the project: Marine Aerosol Production. We are also grateful to Uwe Parchatka (Atmospheric Chemistry Department of the Max Planck Institute for Chemistry in Mainz) for his assistance in organizing the $^{129}I_2$ sampling in Mainz.

Supporting Information Available

The synthesis procedure of 4-iodo-*N*,*N*-dimethylaniline and three figures as noted in the text. This material is available free of charge via the Internet at http://pubs.acs.org.

The synthesis procedure of 4-iodo-*N*,*N*-dimethylaniline

To 15 mL of 0.2 mol L^{-1} *N*,*N*-dimethylaniline aqueous solution, 381 mg of finely powdered I_2 was added. After the mixture was stirred at 50 °C for a few minutes, the active oxidant, a 30% aqueous solution of H_2O_2 (1.8 mmol) and a drop of 40% H_2SO_4 used as catalyst were introduced. The reaction mixture was stirred at 50 °C until all the iodine was visually observed to be consumed. The product was extracted with 30-mL CH_2Cl_2, washed with an aqueous solution of $Na_2S_2O_3$ (5%, 40 mL) and dried over anhydrous $MgSO_4$. Pure products were isolated by SiO_2 column chromatography using CH_2Cl_2 as mobile phase.

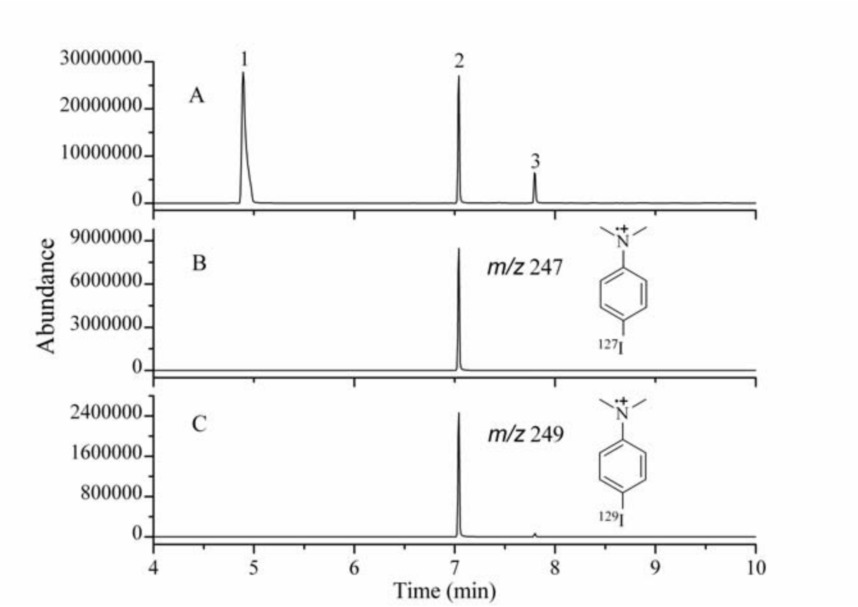

FIGURE S1. Total ion chromatogram of gaseous $^{127}I_2$ analysis obtained by GC–MS (A), and the extracted chromatogram for *m/z* 247 (B) and *m/z* 249 (C). Peak assignments: (1) DMA, (2) 4-I-DMA, and (3) 2,4,6-TBA (internal standard).

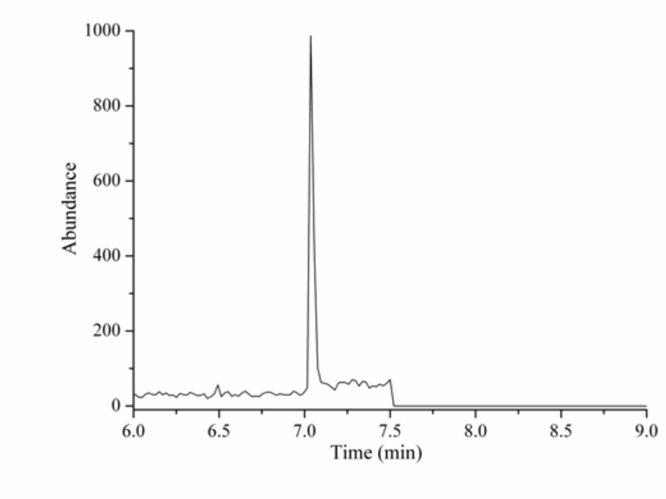

FIGURE S2. Extracted chromatogram for m/z 249 under the selected ion monitoring (SIM) mode for gaseous $^{129}I_2$ measurement.

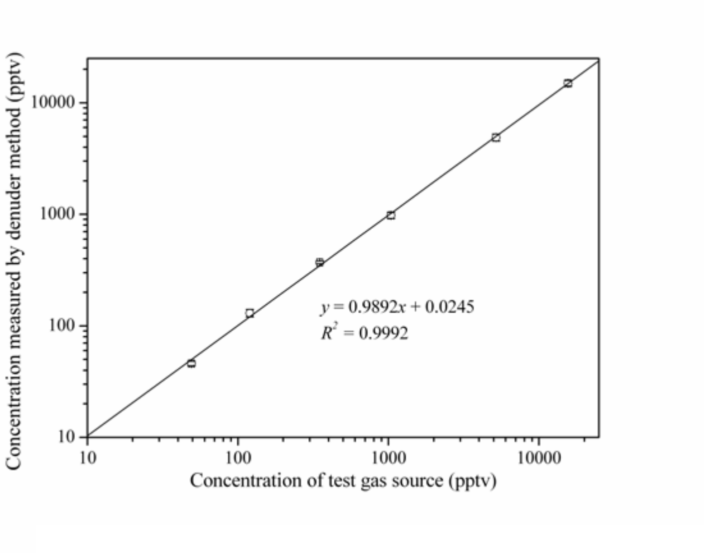

FIGURE S3. Plot of concentration measured by denuder *versus* concentration of the test gas source of gaseous I_2.

Literature Cited

(1) Carpenter, L. J. Iodine in the marine boundary layer. *Chem. Rev.* **2003**, *103*, 4953–4962.

(2) Carpenter, L. J.; Hopkins, J. R.; Jones, C. E.; Lewis, A. C.; Parthipan, R.; Wevill, D. J.; Poissant, L.; Pilote, M.; Constant, P. Abiotic source of reactive organic halogens in the sub-arctic atmosphere? *Environ. Sci. Technol.* **2005**, *39*, 8812–8816.

(3) Simpson, W. R.; von Glasow, R.; Riedel, K.; Anderson, P.; Ariya, P.; Bottenheim, J.; Burrows, J.; Carpenter, L. J.; Friess, U.; Goodsite, M. E.; Heard, D.; Hutterli, M.; Jacobi, H.-W.; Kaleschke, L.; Neff, B.; Plane, J.; Platt, U.; Richter, A.; Roscoe, H.; Sander, R.; Shepson, P.; Sodeau, J.; Steffen, A.; Wagner, T.; Wolff, E. Halogens and their role in polar boundary-layer ozone depletion. *Atmos. Chem. Phys.* **2007**, *7*, 4375–4418.

(4) McFiggans, G.; Plane, J. M. C.; Allan, B. J.; Carpenter, L. J.; Coe, H.; O'Dowd, C. D. A modeling study of iodine chemistry in the marine boundary layer. *J. Geophys. Res.* **2000**, *105*, 14371–14385.

(5) Saiz-Lopez, A.; Mahajan, A. S.; Salmon, R. A. Bauguitte, S. J.-B.; Jones, A. E.; Roscoe, H. K.; Plane, J. M. C. Boundary layer halogens in coastal Antarctica. *Science* **2007**, *317*, 348–351.

(6) Saiz-Lopez, A.; Plane, J. M. C.; McFiggans, G.; Williams, P. I.; Ball, S. M.; Bitter, M.; Jones, R. L.; Hongwei, C.; Hoffmann, T. Modelling molecular iodine emissions in a coastal marine environment: the link to new particle formation. *Atmos. Chem. Phys.* **2006**, *6*, 883–895.

(7) Peters, C.; Pechtl, S.; Stutz, J.; Hebestreit, K.; Hönninger, G.; Heumann, K. G.; Schwarz, A.; Winterlik, J.; Platt, U. Reactive and organic halogen species in three different European coastal environments. *Atmos. Chem. Phys.* **2005**, *5*, 3357–3375.

(8) Hoffmann, T.; O'Dowd, C. D.; Seinfeld, J. H. Iodine oxide homogeneous nucleation: an explanation for coastal new particle production. *Geophys. Res. Lett.* **2001**, *28*, 1949–1952.

(9) O'Dowd, C. D.; Jimenez, J. L.; Bahreini, R.; Flagan, R. C.; Seinfeld, J. H.; Hämer, K.; Pirjola, L.; Kulmala, M.; Jennings, S. G.; Hoffmann, T. Marine aerosol formation from biogenic iodine emissions. *Nature* **2002**, *417*, 632–636.

(10) McFiggans, G.; Coe, H.; Burgess, R.; Allan, J.; Cubison, M.; Alfarra, M. R.; Saunders, R.; Saiz-Lopez, A.; Plane, J. M. C.; Wevill, D. J.; Carpenter, L. J.; Rickard, A. R.; Monks, P. S. Direct evidence for coastal iodine particles from Laminaria macroalgae-linkage to emissions of molecular iodine. *Atmos. Chem. Phys.* **2004**, *4*, 701–713.

(11) Von Glasow, R. Seaweed, iodine, new particles and atmospheric chemistry-the current state of play. *Environ. Chem.* **2005**, *2*, 243–244.

(12) Küpper, F. C.; Carpenter, L. J.; McFiggans, G. B.; Palmer, C. J.; Waite, T. J.; Boneberg, E. M.; Woitsch, S.; Weiller, M.; Abela, R.; Grolimund, D.; Potin, P.; Butler, A.; Luther, G. W.; Kroneck, P. M. H.; Meyer-Klaucke, W.; Feiters, M. C. Iodide accumulation provides kelp with an inorganic antioxidant impacting atmospheric chemistry. *Proc. Natl. Acad. Sci.*

U.S.A. **2008**, *105*, 6954–6958.

(13) Burkholder, J. B.; Curtius, J.; Ravishankara, A. R.; Lovejoy, E. R. Laboratory studies of the homogeneous nucleation of iodine oxides. *Atmos. Chem. Phys.* **2004**, *4*, 19–34.

(14) Santschi, P. H.; Schwehr, K. A. ^{129}I/^{127}I as a new environmental tracer of geochronometer for biogeochemical or hydrodynamic processes in the hydrosphere and geosphere: the central role of organo-iodine. *Sci. Total. Environ.* **2004**, *321*, 257–271.

(15) Lopez-Gutierrez, J. M.; Garcia-Leon, M.; Schnabel, C.; Schmidt, A.; Michel, R.; Synal, Suter, M. Determination of ^{129}I in atmospheric samples by accelerator mass spectrometry. *Appl. Radiat. Isot.* **1999**, *51*, 315–322.

(16) Hou, X. L.; Aldahan, A.; Nielsen, S. P.; Possnert, G.; Nies, H.; Hedfors, J. Speciation of ^{129}I and ^{127}I in seawater and implications for sources and transport pathways in the north sea. *Environ. Sci. Technol.* **2007**, *41*, 5993–5999.

(17) Hou, X. L.; Dahlgaard, H.; Nielsen, S. P. Iodine-129 time series in Danish, Norwegian and Northwest Greenland coast and the Baltic Sea by seaweed. *Estuar. Coast. Shelf S.* **2000**, *51*, 571–584.

(18) Gallagher, D.; Mcgee, E. J.; Mitchell, P. I.; Alfimov, V.; Aldahan, A.; Possnert, G. Retrospective search for evidence of the 1957 windscale fire in NE Ireland using ^{129}I and other long-lived nuclides. *Environ. Sci. Technol.* **2005**, *39*, 2927–2935.

(19) Palmer, C. J.; Anders, T. L.; Carpenter, L. J.; Küpper, F. C.; McFiggans, G. B. Iodine and halocarbon response of Laminaria digitata to oxidative stress and links to atmospheric new particle production. *Environ. Chem.* **2005**, *2*, 282–290.

(20) Lengyel, I.; Epstein, I. R.; Kustin, K. Kinetics of iodine hydrolysis. *Inorg. Chem.* **1993**, *32*, 5880–5882.

(21) Vaughan, S.; Gherman, T.; Ruth, A. A.; Orphal, J. Incoherent broad-band cavity-enhanced absorption spectroscopy of the marine boundary layer species I_2, IO and OIO, *Phys. Chem. Chem. Phys.* **2008**, *10*, 4471–4477.

(22) Huang, R. J.; Hoffmann, T. Development of a coupled diffusion denuder system combined with gas chromatography/mass spectrometry for the separation and quantification of molecular iodine and the activated iodine compounds iodine monochloride and hypoiodous acid in the marine atmosphere, *Anal. Chem.* **2009,** *81*, 1777–1783.

(23) Martin, J. W.; Mabury, S. A.; Wong, C. S.; Noventa, F.; Solomon, K. R.; Alaee, M.; Muir, D. C. G. Airborne haloacetic acid. *Environ. Sci. Technol.* **2003**, *37*, 2889–2897.

(24) Zehavi, D.; Seiber, J. N. An analytical method for trifluoroacetic acid in water and air samples using headspace gas chromatographic determination of the methyl ester. *Anal. Chem.* **1996**, *68*, 3450–3459.

(25) Bettinetti, G.; Novak, C.; Sorrenti, M. Thermal and structural characterization of commercial α-, β- and γ-cyclodextrins. *J. Therm. Anal. Calorim.* **2002**, *68*, 517–529.

(26) Minns, J. W.; Khan, A. α-cyclodextrin-I_3^- host-gust complex in aqueous solution: theoretical and experimental studies. *J. Phys. Chem. A* **2002**, *106*, 6421–6425.

(27) Das, P.; Gupta, M.; Jain, A.; Verma, K. K. Single drop microextraction or solid phase microextraction-gas chromatography-mass spectrometry for the determination of iodine in pharmaceuticals, iodized salt, milk powder and vegetables involving conversion into 4-iodo-*N,N*-dimethylaniline. *J. Chromatogr. A* **2004**, *1023*, 33–39.

(28) Platzner, I. T. *Modern isotope ratio mass spectrometry*; Wiley: New York, 1997; pp 310–311.

(29) Temime, B.; Healy, R. M.; Wenger, J. C. A denuder-filter sampling technique for the detection of gas and particle phase carbonyl compounds. *Environ. Sci. Technol.* **2007**, *41*, 6514–6520.

(30) Ruiz, P. A.; Lawrence, J. E.; Ferguson, S. T.; Wolfson, J. M.; Koutrakis, P. A conuter-current parallel-plate membrane denuder for the non-specific removal of trace gases. *Environ. Sci. Technol.* **2006**, *40*, 5058–5063.

(31) Lewin, E. E.; Hansen, K. A. Diffusion denuder assembly for collection and determination of gases in air. *Anal. Chem.* **1984**, *56*, 842–845.

(32) Koutrakis, P.; Sioutas, C.; Ferguson, S. T.; Wolfson, J. M.; Mulik, J. D.; Burton, R. M. Development and evaluation of a glass honeycomb denuder/filter pack system to collect atmospheric gases and particles. *Environ. Sci. Technol.* **1993**, *27*, 2497–2501.

(33) Tang, H.; Lewis, E. A.; Eatough, D. J.; Burton, R. M.; Farber, R. J. Determination of the particle-size distribution and chemical-composition of semivolatile organic-compounds in atmospheric fine particles with a diffusion denuder sampling system. *Atmos. Environ.* **1994**, *28*, 939–947.

(34) Hou, X. L.; Ross, P. Critical comparison of radiometric and mass spectrometric methods for the determination of radionuclides in environmental, biological and nuclear waste samples. *Anal. Chim. Acta* **2008**, *608*, 105–139.

(35) Neoh, T.; Noda, Y.; Yoshii, H.; Furuta, T. Release characteristics of iodine encapsulated in cyclodextrins. *J. Inclus. Phenom. Mol.* **2006**, *56*, 117–123.

(36) Gormley, P. G.; Kennedy, M. Diffusion from a stream flowing through a cylindrical tube. *Proc. R. Ir. Acad. Sect. A* **1949,** *52*, 163–169.

analytical chemistry

Subscriber access provided by UNIV MAINZ

Article

Development of a Coupled Diffusion Denuder System Combined with Gas Chromatography/Mass Spectrometry for the Separation and Quantification of Molecular Iodine and the Activated Iodine Compounds Iodine Monochloride and Hypoiodous Acid in the Marine Atmosphere

Ru-Jin Huang, and Thorsten Hoffmann

Anal. Chem., **2009**, 81 (5), 1777-1783• DOI: 10.1021/ac801839v • Publication Date (Web): 06 February 2009

2.4 Development of a Coupled Diffusion Denuder System Combined with Gas Chromatography/Mass Spectrometry for the Separation and Quantification of Molecular Iodine and Activated Iodine Compounds Iodine Monochloride and Hypoiodous Acid in the Marine Atmosphere

Ru-Jin Huang, Thorsten Hoffmann*

Institute of Inorganic and Analytical Chemistry, Johannes Gutenberg-University of Mainz, Duesbergweg 10-14, D-55128 Mainz, Germany

Status: Published in Analytical Chemistry

This study concerns the development of a coupled diffusion denuder system capable of separating and quantifying gaseous molecular iodine (I_2) and two other highly reactive iodine species, ICl and HOI, which are collectively named activated iodine compounds (AIC). Both I_2 and AIC are key species in the atmospheric chemistry of iodine. 1,3,5-trimethoxybenzene (1,3,5-TMB) and α-cyclodextrin/$^{129}I^-$ (α-CD/$^{129}I^-$) coated denuders proved to be suitable for the collection of gaseous AIC and I_2, respectively. The experimental collection efficiencies for AIC (tested as ICl) and I_2 agreed well with the theoretical values for gas flow rates in the range between 300 and 1800 mL min^{-1}. The coupled denuder system (1,3,5-TMB-coated denuder as front-denuder coupled upstream of an α-CD/$^{129}I^-$-coated denuder) was applied successfully to separate test gas mixtures of ICl and I_2 at various mixing ratios in the laboratory. The operation of both denuder systems was demonstrated to be independent of

relative humidity (0–100%) and storage period (at least 2 weeks prior to and after sampling). Detection limits were achieved at sub parts-per-trillion-by-volume (sub-pptv) level. The presented method provides a reliable and practical approach for the speciation of gaseous iodine compounds. In addition, we report for the first time ambient air measurements of AIC mixing ratios, carried out at the atmospheric research station in Mace Head, Ireland. A maximum concentration of AIC of 30.2 pptv was observed for nighttime measurements and 6.0 pptv for daytime measurements. A similar diurnal pattern was found for I_2 with an average concentration level of 23.2 pptv during daytime and 85.1 pptv during nighttime, indicating a strong correlation with AIC.

Iodine is know as an essential element in the biosphere for centuries.[1] Within the past 2 decades also the impact of iodine on atmospheric chemistry received increasing attention and became a growing active research field.[2–7] Numerous tropospheric field measurements and modeling studies have been realized, especially in the marine boundary layer (MBL). Most of these studies investigated the impact of iodine on gas phase chemistry, such as the catalytic destruction of ozone via reaction with iodine atoms released by the photolysis of alky iodides or molecular iodine,[8,9] therefore affecting the atmospheric photooxidation budget.[9,10] Recently, gaseous iodine precursors have also been proposed to be involved in the enrichment of iodine in marine aerosols, the formation of new particles in the MBL and their evolution to form cloud condensation nuclei.[4,11–13] Although some progress has been made, a number of uncertainties about the sources, sinks, kinetic parameters and the recycling of iodine remain and the identification and quantification of reactive key species are still a challenging analytical problem.

Interest in iodine atmospheric chemistry has been greatly stimulated in the last few years by the suggestion that molecular iodine (I_2) rather than biogenic iodocarbons (e.g., CH_3I, CH_2I_2, CH_2ClI, and C_3H_7I) is the most important precursor for new particle formation and also the dominant source of coastal reactive iodine in the MBL.[14–16] When I_2 is released into the atmosphere it will rapidly be photolysed to I atoms during daytime, which then will react with ozone to yield iodine oxide. Self-reaction of IO is thought to result in the formation of higher iodine oxides,[11] which finally nucleate and form new particles. Other key iodine compounds can also be formed within theses reaction cycles, such as hypoiodous acid (HOI). Uptake of HOI on sea-salt aerosol has been proposed to enhance chlorine and bromine activation by the reaction of HOI with Cl^- and Br^-.[8,17] The subsequent products, ICl and IBr, can be released from the sea salt particles and enhance ozone depletion. However, the exact underlying chemical mechanisms leading to the different iodine species are still not understood, mostly due to the lack of analytical techniques to accurately measure certain key species, such as I_2, HOI or ICl. For this paper we collectively name HOI and ICl activated iodine compounds (activated in respect to their reactivity towards organic substrates), since in both molecules the iodine atom is positively polarized, which enhances its electrophilic reactivity towards organic molecules.

The most widely used method for the sampling of gaseous iodine species, especially radioactive iodine in the atmosphere, typically involves a front-filter to remove particulate iodine followed by an impregnated filter or alternative aqueous solution that captures gaseous iodine.[18–20] Unfortunately, during collection the filter-adsorbent technique is subjected to many artifacts resulting from particle-to-gas and gas-to-particle conversion reactions as well as the retention of gaseous iodine compounds on the pre-filter either directly on the filter material or on concurrently collected particulate matter. More recently, differential optical absorption spectroscopy (DOAS) has been successfully used to directly measure gaseous molecular iodine.[14,15] However, this approach has a relatively high detection limit (~20 ppt) and provides just distance-averaged concentrations without resolution along the light-path. In addition, unfavorable weather condition can affect the instrument performance. Nevertheless, single "point" in situ measurements of gaseous iodine species are frequently required in field measurements and laboratory studies. Yang and co-workers[21] have developed a convenient and novel optical sensor for gaseous iodine detection; however, the limit of detection (60 ppb) of the approach would not be sufficient for the measurement of gaseous iodine in the MBL (concentrations at ppt level). Obviously, a convenient, selective, sensitive and weather-independent approach would be beneficial for the measurement of atmospheric iodine species. To the best of our knowledge compounds like HOI or ICl have never been measured in the MBL, although models predict both molecules to be actively involved in atmospheric chemistry of iodine.[17,22]

Diffusion denuders are capable of gas–particle differentiation[23] and they have often successfully been used for the separation and enrichment of analytes in air.[24–29] This technique avoids the artifacts that may otherwise occur with filter-based methods. However, little attention was paid up to now to atmospheric iodine species. Starch-coated denuders in connection with inductively coupled plasma mass spectrometry (ICPMS) have been used before for I_2 measurements;[30] however, speciation of different gaseous iodine compounds is not possible with this denuder technique and ICPMS measurements are instrumentally demanding. Here, we report a coupled denuder system which consists of a 1,3,5-trimethoxybenzene (1,3,5-TMB)-coated cylindrical tube as front-denuder coupled upstream of an α-cyclodextrin/$^{129}I^-$ (α-CD/$^{129}I^-$)-coated tube for the separation and quantitative collection of gaseous AIC and I_2 in combination with a gas chromatography ion trap mass spectrometry (GC/MS) method. It should be noted that the generation of a stable gaseous HOI test gas atmosphere is a very difficult task.[31–34] However, HOI possesses a positively polarized iodine atom which enhances its electrophilic character and makes the molecule very reactive towards organic materials.[35–38] The same is true for ICl which is commercially available and much easier to handle in the laboratory. Therefore, in this work we used ICl as a surrogate for AIC, and all experiments described below were performed with this compound. We also report the results of the first application of the coupled denuder technique for field measurements at the coastal research station in Mace Head, Ireland.

EXPERIMENTAL

Chemicals. Iodine, iodine monochloride, 1,3-dimethoxybenzene, 1,4-dimethoxybenzene, 1,3,5-TMB, 2,4,6-tribromoanisole, and 4-iodoanisole were purchased from Aldrich (Steinheim, Germany). *N*,*N*-Dimethylaniline (DMA), 2,4,6-tribromoaniline, and α-CD were purchased from Acros Organics (Geel, Belgium). Anisole and ethyl acetate were obtained from Fluka (Steinheim, Germany). Cyclohexane was obtained from Fisher (Loughborough, UK). H_2O_2 aqeous solution (30%, wt.%) was obtained from Sigma-Aldrich (Steinheim, Germany). Iodide-129 standard solution (SRM 4949C) was purchased from NIST. The solution consists of 14.4% ^{127}I and 85.6% ^{129}I, corresponding to a constant $^{127}I/^{129}I$ ratio of 0.17.[39] (Safety note: as ^{129}I is long-lived radioactive isotope, solution was diluted and used in concentration lower than 100 µg L^{-1}, which refers to an radioactivity lower than 0.65 Bq g^{-1}). All other chemicals were of analytical reagent grade. Deionized water (18 MΩ cm) was used for preparation of all aqueous solutions.

Preparation of Standards. Both 4-iodo-*N*,*N*-dimethylaniline (4-iodo-DMA) and 1-iodo-2,4,6-trimethoxybenzene (1-iodo-2,4,6-TMB) are not commercially available and have been synthesized[40] for the purpose of quantification. To 15-mL of 0.2 mol L^{-1} DMA (or 1,3,5-TMB) aqueous solution, 381 mg of finely powdered I_2 was added. After the mixture was stirred at 50 °C for a few minutes, the active oxidant, a 30% aqueous solution of H_2O_2 (1.8 mmol) and a drop of 40% H_2SO_4 used as catalyst were introduced. The reaction mixture was stirred at 50 °C until all the iodine was visually observed to be consumed. The product was extracted with 30-mL CH_2Cl_2, washed with an aqueous solution of $Na_2S_2O_3$ (5%, 40 mL) and dried over anhydrous $MgSO_4$. Pure products were isolated by SiO_2 column chromatography using CH_2Cl_2 as mobile phase. The purity of 4-iodo-DMA and 1-iodo-2,4,6-TMB was 98.9% and 99.3%, respectively (GC–MS determinations). The concentration of stock standard solution of 4-iodo-DMA and 1-iodo-2,4,6-TMB was 2.5 mg mL^{-1} and 4.0 mg mL^{-1}, respectively. A series of working standard solutions was prepared by sequential dilution of the stock standard solutions.

Laboratory Experiments. *Installation of the Gas Calibration Sources.* I_2 and ICl test gas in nitrogen were generated from home-made gas sources based on the controlled evaporation of the compounds (Figure 1). The temperature of the vapor generator devices, which affects the vapor pressure and therefore the evaporation of I_2 (solid) and ICl (liquid), was set to 25 °C using a thermostat. To obtain low concentration levels of the test gas, a deactivated fused silica capillary (530 µm i.d., CS-Chromatographie Service GmbH, Langerwehe, Germany) was mounted on top of the glass vessel. This capillary acts as a diffusion barrier and therefore reduces the output of the test gas source. The length of the capillary was 2 cm for the I_2 source and 15.3 cm for the ICl source. However, due to the high evaporation rate of ICl the output of this chemical was still too high and a split valve was, therefore, connected to the outlet of the ICl source. Thus, only a fraction of the gaseous ICl leaving the test gas source was finally transferred into the dilution chamber (see Figure 1). Both sources were then connected with a 500 mL five-neck round bottom flask in which another nitrogen flow was introduced to get the diluted gas mixture of I_2 and ICl in the concentration range needed. The ratio of I_2 and ICl in the mixture was controlled by the split/needle valve of the ICl source. Two impingers with deionized water were used for the humidification of the test gas. Water drops in the nitrogen flow were trapped in a third impinger packed with glass wool. The relative humidity of the gas source system was measured by a humidity meter (Endress+Hauser GmbH, Maulburg, Germany). All joints were made of glass or Teflon material. The whole experimental system was protected from any adventitious light by aluminium foil to avoid photolytic degradation of I_2 or ICl.

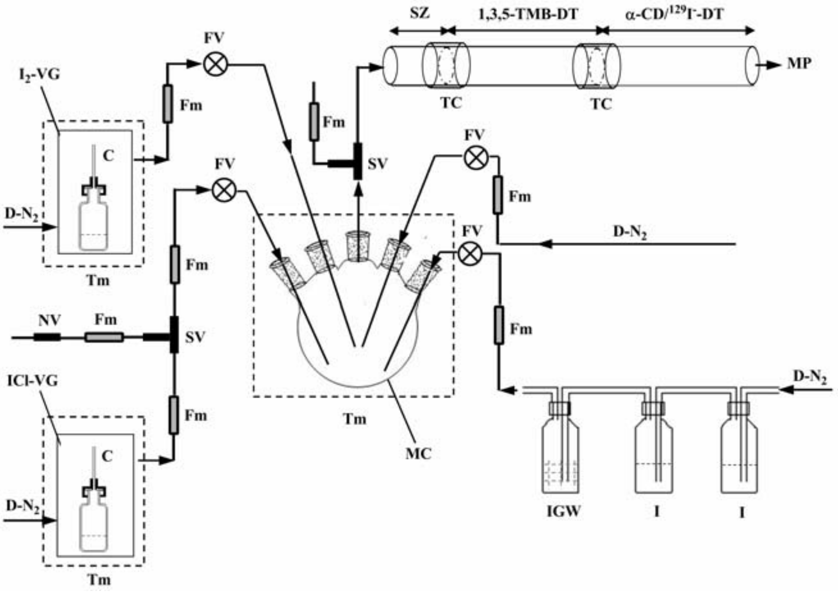

Figure 1. Schematic diagram of the gas generation and separation system: ICl-VG, ICl vapor generator; I_2-VG, I_2 vapor generator; C, deactivated capillary; Tm, thermostat; Fm, flow meter; FV, flow valve; SV, split valve; NV, needle valve; MC, mixing chamber; I, impinger with deionized water; IGW, impinger with glass wool; D-N_2, dry N_2 gas; SZ, inlet subduction zone; 1,3,5-TMB-DT, 1,3,5-TMB-coated denuder tube; α-CD/$^{129}I^-$-DT, α-CD/$^{129}I^-$-coated denuder tube; TC, Teflon connector; MP, membrane pump.

Denuder Preparation and Test Gas Sampling. The denuder tubes were made of brown borosilicate glass (50 cm length × 6 mm i.d.). DMA (1.5 mmol L^{-1}), anisole (1.5 mmol L^{-1}), 1,4-dimethoxybenzene (1.5 mmol L^{-1}), 1,3-dimethoxybenzene (1.5 mmol L^{-1}), 1,3,5-TMB (1.5 mmol L^{-1}), and α-CD (2.5 mg mL^{-1}) in methanol were used as coating solutions. The 2.5 mg mL^{-1} coating solution containing α-CD was used because of difficulties to feed more concentrated solutions into the denuder. To obtain denuders coated uniformly with the reagents, five (nine for coating solution with α-CD) 0.5 mL aliquots of individual coating solution were slowly pipetted into the openings of the glass tube which was held at an angle of about 10^{o} relative to the horizontal plane. During the coating procedure the tubes were rotated and flushed with nitrogen for drying (flow rate 0.5 L min^{-1}). Afterwards, the coated denuders were sealed with polypropylene (PP) end-caps and stored under refrigeration until sampling. Untreated glass tubes of specific length (3–18 cm) with the same diameter as the denuder tubes were coupled to the denuder inlet for different sampling flow rates, used as a subduction zone to adjust the laminar flow of the sampled gas into the denuder.[41] The test gas was sucked into the denuder by a membrane pump located downstream of the denuder with a sampling flow in the range between 300 and 1800 mL min^{-1}, typically for 10–45 min.

Denuder Performance. The collection efficiency of individual denuders with different coatings was determined by two different methods: (a) calculating the ratio between analyte amount found in the denuder elution and its known amount entering into the denuder and (b) connecting two identical denuders in series, measuring the relative amounts collected in each and thereby determining the fraction collected.[42] Both methods yielded essentially the same results and are not separately reported here. In addition, the collection efficiency of the denuders was investigated as a function of sampling flow rate between 300 and 1800 mL min^{-1}. The long-term stability of the coated denuders (stored prior to sampling) and the stability of the derivatives formed in the denuders after sampling were also investigated. In both sets of experiments the denuders were stored at -4 ^{o}C for 2 weeks.

Field Sampling. Ambient AIC and I_2 in the MBL were measured at the Mace Head Atmospheric Research Station (MHARS) located at the west coast of Ireland in

August–September 2007. Samples were taken by sampling ambient air through the coupled denuder system for 30–180 min at a flow rate of 500 mL min^{-1}, during low tide at both daytime and nighttime. The denuders were set vertically to eliminate particle deposition due to gravitational settling. Once the sampling was completed, the open ends of the tubes were again sealed with PP end-caps and kept under refrigeration.

Sample Preparation. The iodine species collected by different denuder methods were extracted applying different procedures. The samples collected with α-CD were eluted with five 2.0 mL aliquots of deionized water into a 25-mL calibrated flask. 500 μL of phosphate buffer (pH 6.4), 100 μL of 2,4,6-tribromoaniline (2.5 mg L^{-1}, internal standard), 400 μL of 2-iodosobenzoate (4.0 g L^{-1}) and 300 μL of DMA (0.2 g L^{-1}) were then added. The solution was diluted to about 23 mL with deionized water and subsequently shaken in a mechanical shaker at room temperature for about 120 min. 2.0 mL of sodium acetate solution (20%, m/m) was then introduced and the flask was filled to the calibrated mark with deionized water. Finally, the solution was extracted with 100 μL of cyclohexane. For the denuder tubes with other coatings than α-CD, the coatings were eluted with five 2.0 mL aliquots of ethanol/ethyl acetate (1:1, v/v). Then 100 μL of 2,4,6-tribromoanisole (6.0 mg L^{-1} in ethyl acetate) was added as an internal standard. The mixture was concentrated almost to dryness with a gentle stream of purified nitrogen and dissolved in 100 μL of ethyl acetate. For both sample preparation procedures no detectable derivatives in the sixth elution were found. Therefore, the five-time eluting procedure was applied in all cases.

GC/MS Analysis. The samples were analyzed using a GC/MS system (Trace GC/PolarisQ, Thermo Finnigan Italia S.p.A, Rodano, Italy). A fused-silica capillary column (Rtx®-5MS, Restek Co., Bad Homburg, Germany), 30 m × 0.25 mm and 0.25 μm film thickness, was used for separation. High-purity helium (99.999%) was used as a carrier gas at a constant flow of 1.0 mL min^{-1}. The temperature of the injector was set to 250 ^{o}C and the temperature of the transfer line was set to 300 ^{o}C. The GC oven temperature was held at 50 ^{o}C for 3 min and then increased with a rate of 30 ^{o}C min^{-1} to 220 ^{o}C and hold there for another 3 min. A 1 μL aliquot of the sample extract or standard was injected by an autosampler (AS 3000, Thermo

Finnigan). Ionization was carried out by electron ionization (EI, 70-eV). Data acquisition was performed in the full scan mode (*m/z* range 45–450) for mass spectrometric identification and characterization of the derivatives and in selected ion monitoring (SIM) mode for quantification. Table S1 (Supporting Information) shows retention time information as well as the mass-to-charge (*m/z*) ratios seleceted for quantification and confirmation of the target molecules.

RESULTS AND DISCUSSION

Stability of the Calibration Test Gas Sources. The exact output of the I_2 and ICl test gas sources was calculated from the weight loss of the test gas vials and the time period between weighting. After 2 weeks of initial equilibrium time a stable output was observed and the mean output from the test gas source was 61 ng min^{-1} and 1609 ng min^{-1} of I_2 and ICl, respectively. The test gas source stability was assessed by repeated output measuements. The relative standard deviation (RSD) of the I_2 output was 4.3% ($n = 9$) and that for ICl was 2.8% ($n = 20$).

Coating Evaluation. The efficiencies of different denuder coatings were investigated for the sampling of I_2 and ICl. In theory, the gas to be analyzed can be selectively removed by diffusion to the wall without significant deposition of the particulate material as a result of the much higher diffusion coefficient of gas-phase compounds than that of typical aerosol particles.[42] If the surface represents a perfect sink for the gaseous analyte and the flow is within certain limits (see below) the collection efficiency is close to 100%. In practice, however, especially the precondition of the coating acting as a perfect sink is difficult to reach and in these cases the collection efficiencies are consequently lower than 100%. The first coating material tested was DMA. DMA was selected because it is an activated molecule in respect to the electrophilic attack of iodine compounds (electrophilic aromatic substitution). The dimethylamine moiety of this substrate with its unshared pair of electrons is strongly activating and directs the entering iodine to the ortho and para positions. Although DMA has one para and two ortho positions available for substitutions, iodination occurs only at the para position since the substrate is present in excess and the substitution at the two ortho positions is sterically hindered by the large dimethylamino substituent. For the same reason this chemical has been used for the derivatization of elemental iodine in aqueous solution.[43] However, the collection efficiencies of DMA-coated denuders are much lower than the theoretically calculated efficiencies for both I_2 and ICl (Table 1). This behaviour is probably due to a still too small reaction rate constant for the reaction between gaseous I_2/ICl and DMA. Obviously, just a small amount of the analyte molecules did react with the coating material and most of the analyte molecules finally escaped from the denuder tube with the gas flow. Table 1 also shows that ICl is collected with about 5 times greater efficiency than I_2. This can be easily explained by the positive polarization of the iodine atom in the interhalogen, which provides a more electrophilic iodine moiety.

Since methoxy substituents are also strong activating substituents for electrophilic aromatic substitution, the next chemicals tested as coating materials were methoxy-, dimethoxy-, and trimethoxybenzenes. Due to the higher reactivity of the interhalogen these experiments were focused on ICl. As can be seen in Table 1, anisole (methoxybenzene) and 1,4-dimethoxybenzene showed no significant improvement in their collection efficiencies (less than 10%), even with a large excess of the coating material. 1,3-dimethoxybenzene showed a much better collection efficiency as coating material with a total efficiency up to 94%. However, the coating formed a liquid film at the inner wall of the denuder and therefore the denuders were difficult to be operated and stored. Furthermore, also the diiodo derivative was formed, certainly a disadvantage for the quantification procedure. Consequently, 1,3,5-TMB, the most activated toward electrophilic substitution among the methoxy-substituted benzene derivatives, was finally also tested as coating material. Satisfactory collection efficiencies for ICl were obtained and the values are very close to the expected theoretically values. On the basis of these results, 1,3,5-TMB was selected as most suited coating material for iodine sampling and tested further.

Table 1. The Coated Absorption Mediums Examined for the Gaseous Iodine and Iodine Monochloride[a]

coating	derivative	collection efficiency (%)	
		ICl	I_2
DMA	4-iodo-DMA	2.1	0.4
anisole	4-iodoanisole	1.6	N.D.[b]
1,4-dimethoxybenzene	1-iodo-2,5-dimethoxybenzene	5.5	N.D.
1,3-dimethoxybenzene	1-iodo-2,4-dimethoxybenzene	62.2	N.D.
	1,5-diiodo-2,4-dimethoxybenzene	32.2[c]	
1,3,5-TMB	1-iodo-2,4,6-TMB	99.4	1.2
α-CD	4-iodo-DMA	N.D.	45.1
α-CD/$^{129}I^-$	4-iodo-DMA	29.1	98.2

[a] gas flow rate: 350 mL min^{-1}. [b] Not Detected. [c] given as the difference between total collection efficiency and collection efficiency based on monoiodo derivative.

It is well known that cyclodextrins (CDs), especially α-CD,[44] form inclusion complexes with elemental iodine that can be displaced/extracted by other reagents under certain conditions. However, the collection efficiency obtained was less than 50% when just pure α-CD was used as coating material for gaseous I_2 collection. When small amounts of $^{129}I^-$ ($^{129}I^-/I_2 \geq 1:3$, mol/mol) were added to the α-CD coating solution, the efficiency could be increased to 98.2 %. This behaviour is similar to the formation of iodine complexes with starch in aqueous solution, for which the need of iodide ions has been emphasized recently.[45] From the experiments performed here, it is evident that the iodide ions are also beneficial for a stable complexation of iodine by α-CD, most likely due to the formation of I_3^- ions. As a consequence of the addition of $^{129}I^-$ to the coating material and the fact that the heavy iodine isotope contains a certain amount of ^{127}I (see the Experimental Section), the results for gaseous I_2 measurements have to be corrected based on constant isotope ratio of the $^{129}I^-$ spike in the coating material.

Effect of Gas Flow Rate. Obviously, the efficiency of the denuder to quantitatively retain gaseous analytes is a crucial factor for its analytical performance and one critical factor influencing the efficiency is the gas flow through the denuder. Therefore, the collection efficiencies for I_2 and ICl as a function of the gas flow rate were tested and compared with the theoretical (maximal) values. The diffusion coefficients (0.0924 cm^2 s^{-1} for I_2 and 0.102

cm^2 s^{-1} for ICl, respectively, at 25 °C) were calculated according to the FSG/LaBas Method.[46] The collection efficiency was then calculated from the Gormley–Kennedy equation.[41] Figure 2 shows the comparison of the theoretical efficiencies with the experimental ones. It can be seen from the figure that the experimental values of the collection efficiency for ICl are very close to the theoretical predictions within the gas flow range between 300 and 1800 mL min^{-1}. The experimental results for I_2 are slightly lower than the theoretical expectations, especially at higher flow rates. The reasons for the slightly smaller efficiencies can be manifold, e.g., a slightly slow reaction rate for the formation of the iodine-α-CD inclusion complexes or the incomplete reaction between iodine and DMA during the postderivatization step (~97.5% efficiency).

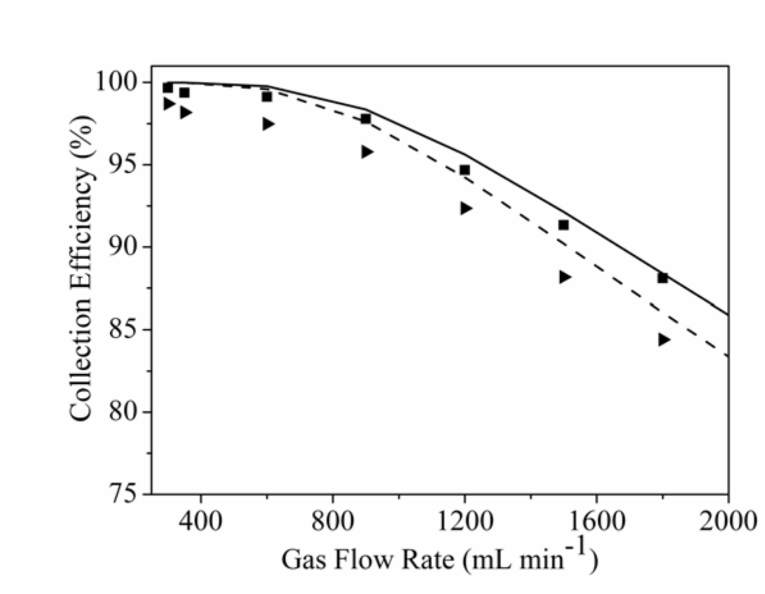

Figure 2. Collection efficiency for I_2 and ICl as a function of gas flow rate: solid line, theoretical collection efficiency curve of ICl; dashed line, theoretical collection efficiency curve of I_2; squares, experimental collection efficiency for ICl; triangles, experimental collection efficiency for I_2.

Separation of Gaseous ICl and I_2 Mixture. A remarkable result revealed from the data in Table 1 is that 1,3,5-TMB coating is suitable for the collection of gaseous ICl in the denuder with a very satisfactory efficiency but a very poor sink for gaseous I_2 collection (efficiency less than 1.2% at the flow rate of 350 mL min^{-1}). On the other hand, the α-CD/$^{129}I^-$ coating is a very efficient coating material for gaseous I_2 collection but less efficient for ICl collection (29.1% efficiency at 350 mL min^{-1} gas flow rate). Thus, it is possible to differentiate between

ICl and I_2 by a selective collection in different denuder tubes, employing a 1,3,5-TMB-denuder and a α-CD/$^{129}I^-$-denuder connected in series by a short Teflon tube. To minimize the interferences from each other, the 1,3,5-TMB-coated denuder was used as the front-denuder to collect ICl. The second denuder was coated with α-CD/$^{129}I^-$ to retain gaseous I_2. The results shown in Figure 3 (also see Table S2, Supporting Information) indicate that the coupled separation system established is reliable and practical for the differentiation of gas mixture of I_2 and ICl. The precision (1.8%–7.9% RSD), can be considered to be very satisfactory in view of other sources of error (not only denuder operation) that contributed to total RSD values, e.g., error of the GC–MS detection (RSD = 2.5% and 2.9% for 1-iodo-2,4,6-TMB and 4-iodo-DMA, respectively), fluctuation of vapour generated (RSD = 2.8%–4.3%) and nitrogen flow. The measured I_2 and ICl data for different mixture ratio are in close agreement with their respective calibrated values, with differences ranging from 1.5% to 6.8%.

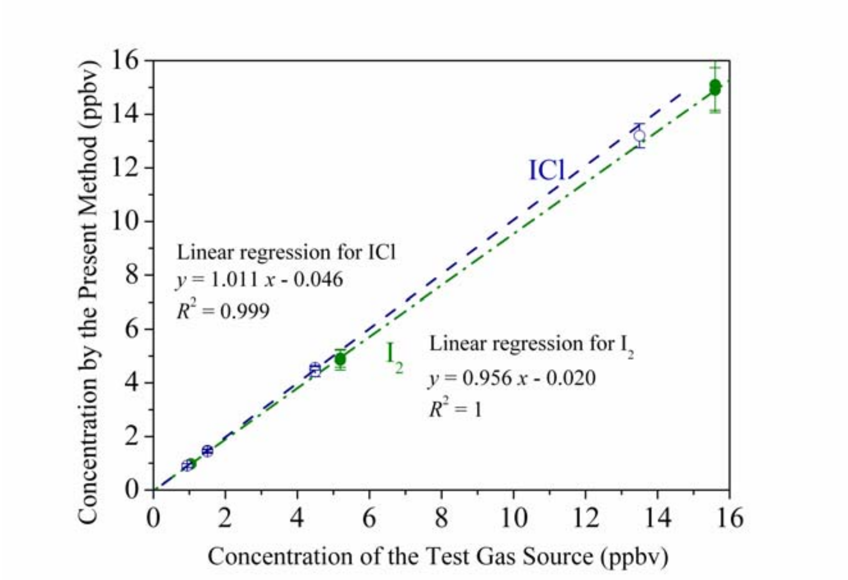

Figure 3. Plot of concentration measured by denuder vs the concentration of gaseous mixtures of ICl and I_2.

Evaluation of Operation Conditions of the Denuder. For practical reason it is more favourable if a batch of denuders can be prepared and stored several days prior to and after field sampling. Therefore, the stability for pre-prepared denuder tubes stored in a refrigerator for 2 weeks before and after sampling was investigated. In contrast to the collection efficiency obtained by use of freshly prepared denuders (99.2% for ICl and 97.8% for I_2, respectively, at a gas flow rate 500 mL min^{-1}), the respective collection efficiency of denuder stored prior to and after sampling test gas was slightly smaller, i.e., 97.9% and 95.1% for ICl, and 94.3% and 96.9% for I_2. According to the Student's significance test there was no difference at the 5% level between the stored and non-stored tubes for both I_2 and ICl. The differences of the collection efficiencies of denuders operated over a relative humidity ranging from 0 to 100% were less than 8.6% for ICl and less than 5.7% for I_2, respectively (Table S3, Supporting Information). It is noted that the concentrations of iodine species tested here could be somewhat higher than the typical ambient concentration levels. Thus, for field measurements, the extension of sampling time could be necessary to collect a sufficient analyte mass for subsequent GC/MS analysis. Therefore, additional experiments were performed by increasing the sampling time to 180 min at a flow rate of 500 mL min^{-1}. The differences of collection efficiencies were less than 4.8%. These results are not surprising because the coating materials are present in excess and highly reactive towards the target analytes. The instrument detection limit (IDL), based on a signal/noise (S/N) ratio of 10 under SIM mode, was 0.31 pg for 1-iodo-2,4,6-TMB and 1.72 pg for 4-iodo-DMA, respectively. Such low IDLs permit low sample volumes and short sampling times, which enabled us to increase the time resolution and study the diurnal variation of the atmospheric concentrations of both AIC and I_2. On the basis of 90 L sample volume, the LOD obtained in this work was 28.6 parts-per-quadrillion-by-volume (ppqv) for AIC and 94.6 ppqv for I_2, respectively.

Field Measurements. To further demonstrate the analytical performance of the developed method, the coupled denuder system was used for the measurement of AIC and I_2 in the remote MBL. The samples were taken at low tide during a field campaign at the Mace Head Research Station at the west coast of Ireland, where abundant atmospheric events such as ozone depletion and coastal new particle formation with regard to iodine chemistry were observed recently.

It is worthwhile to consider which other gaseous iodine species besides I_2, HOI, and ICl, can be present in the MBL and therefore potentially contribute tosor interfere withsthe AIC and I_2

measurements presented below. These are IBr, volatile organohalogens (e.g., iodomethane, diiodomethane), IO, and OIO. IBr proved to be converted into bromination derivative in the 1,3,5-TMB-coated denuder in our laboratory and therefore will not interfere with the AIC measurements presented here. Also the organohalogens will not contribute to the AIC values since the organohalogens contain a negatively polarized iodine atom (therefore even less reactive toward 1,3,5-TMB than I_2) or to the I_2 values since even if they would be collected within the α-CD-coated denuder (what is actually not expected) they will not react with the derivatization agent (DMA) during the subsequent sample preparation step. Similarly, the iodine oxides can be excluded to contribute to the AIC values because both molecules will not react with the TMB by an iodine substitution mechanism. Furthermore, Maguin et al.[47] observed that even at low pressure (~0.2 kPa) the self-reaction of iodine oxides is much faster than the reactions of iodine oxides with a series of hydrocarbons. It can be expected that the self-reaction of iodine oxides is significantly elevated at ambient pressure (101.3 kPa). In addition, typical concentrations of iodine oxides in the atmosphere are lower than those of the iodine species investigated here. Therefore, significant interferences from iodine oxides are also not expected.

Table 2. Determination of AIC and I_2 in the Remote Marine Boundary Layer (Mace Head, Ireland)

sample	sampling time	tidal height[a] (m)	AIC[b] (pptv)	I_2[b] (pptv)
070829-01	12:30–15:30	0.4 at 11:42	5.8 ± 0.6	23.6 ± 1.9
070830-01	23:30–00:30	0.1 at 00:03	30.2 ± 0.6	140.7 ± 5.6
070830-02	13:27–15:27	0.3 at 12:19	6.0 ± 0.5	29.1 ± 1.0
070831-01	23:10–01:10	0.1 at 00:40	10.3 ± 0.8	72.2 ± 3.4
070901-01	12:50–15:50	0.5 at 13:35	3.6 ± 0.2	16.8 ± 0.6
070902-01	00:00–03:00	0.6 at 01:58	7.4 ± 0.3	42.3 ± 1.2

[a] data are obtained on the Word Wide Web at URL: http://easytide.ukho.gov.uk. [b] Mean ± SD ($n = 5$).

Table 2 shows the results of the first application of the method for field measurements. Both AIC and I_2 were observed during daytime and nighttime within a 5 day period. A maximum I_2 mixing ratio of 140.7 pptv was measured at night and 29.1 pptv during the day, probably due to the rapid photolysis of I_2.[14] The respective daytime and nighttime average level of I_2 were 23.2 and 85.1 pptv. I_2 is expected to be released from marine macroalgae or kelp at low tide when these plants are exposed to air.[16,30] Therefore, the denuder method described here, which provides in situ point measurements of gaseous I_2, can be used to better identify the potential sources of molecular iodine. The mixing ratios of AIC during the period of 5 days were correlated with the levels of I_2 with a maximum value up to 30.2 pptv at night and 6.0 pptv during the day. As mentioned above the formation pathways and concentrations of AIC are not well known up to now. HOI is believed to be formed by the reaction of I atoms and HO_2 radicals; hence, HOI is expected to be present during the day. The formation of gaseous interhalogens including ICl are currently believed to be linked to the release from sea salt particles following uptake and heterogeneous chemistry of HOI[8,17] or, under appropriate conditions, freezing processes of sea salt solutions.[48] Obviously, a separate identification of HOI and ICl would be useful; however, a very similar chemistry of both species can be expected (positively polarized iodine atom), and therefore a cumulative concentration as measured here is still highly interesting. On the basis of the formation mechanisms we assume that HOI contributes to the AIC values especially during the day and ICl especially during the night. Given their high reactivity toward organic materials (Table 1), HOI and ICl could be an additional source for organic iodine[35] in marine aerosol where organic fractions account for 15–63% of submicrometer aerosol mass.[49,50] Certainly, further modeling exercises and especially field measurements are required to clarify the origin and atmospheric significance of I_2 and AIC since these species are critical for an understanding of the chemistry of halogen activation, ozone depletion, and particle formation in the MBL.[22,51]

CONCLUSIONS

This study demonstrates that 1,3,5-TMB-denuder coupled to α-CD/$^{129}I^-$-denuder is an efficient sampling system for the separation of gaseous AIC (ICl and HOI) and I_2, with satisfactory collection efficiencies (99.4% for AIC (tested as ICl) and 98.2% for I_2, respectively) and minimized interferences from each other. The analytical performances of the coupled system have been evaluated thoroughly. The precision and accuracy ranged from 1.8% to 7.9% and from 1.5% to 6.8%, respectively. The operation of both 1,3,5-TMB- and α-CD/$^{129}I^-$-denuder was independent of relative humidity and storage periods. Detection limits at ppqv level were achieved. In general, a coupled denuder system with specific coatings has a great potential in the speciation of different compounds in the atmosphere.

In addition, the coupled denuder system developed here has been applied to the measurements of AIC and I_2 in the remote marine boundary layer. For the first time, ambient AIC mixing ratios were measured with a maximum concentration of 30.2 pptv at night and 6.0 pptv during day at the atmospheric research station in Mace Head, Ireland. The average level of I_2 was 23.2 pptv during daytime and 85.1 pptv during nighttime. The coupled sampling system provides a practical, reliable and convenient approach for iodine species analysis in atmospheric domains such as coastal areas, the open sea, and polar regions.

ACKNOWLEDGMENT

We acknowledge the financial support from the German Research Foundation (Deutsche Forschungsgemeinschaft, DFG) within the graduate program 826 “Trace Analysis of Elemental Species: Development of Methods and Applications”. We also acknowledge the financial support from the European Union under the project: Marine Aerosol Production (MAP).

SUPPORTING INFORMATION AVAILABLE

More information in Tables S1, S2, and S3. This material is available free of charge via the Internet at http://pubs.acs.org.

The reason why *N*,*N*-dimethylaniline was selected as test coating material

N,*N*-dimethylaniline (DMA) was selected as coating material because it is an activated molecule in respect to the electrophilic attack of iodine compounds (electrophilic aromatic substitution). The dimethylamine moiety of this substrate with its unshared pair of electrons is strongly activating and directs the entering iodine to the *ortho* and *para* positions. Although DMA has one *para* and two *ortho* positions available for substitutions, iodination occurs only at the *para* position since the substrate is present in excess and the substitution at the two *ortho* positions is sterically hindered by the large dimethylamino substituent. For the same reason this chemical has been used for the derivatisation of elemental iodine in aqueous solution.

Table S1. SIM Conditions for Quantitative Analysis of AIC and I_2

AIC sample					I_2 sample				
R.T.[a] window (min)	R.T. (min)	compound	quant.[b] *m/z*	qual.[c] *m/z*	R.T. window (min)	R.T. (min)	compound	quant.[b] *m/z*	qual.[c] *m/z*
6.0–7.8	7.49	1,3,5-TMB	168	139	5.0–7.0	5.82	DMA	121	77
7.8–9.0	8.44	2,4,6-tribromoanisole	344	329, 346	7.0–8.3	8.04	4-iodo-DMA	247	119
9.0–11.6	9.17	1-iodo-2,4,6-TMB	294	139	8.3–11.6	8.79	2,4,6-tribromoaniline	329	250, 331

[a] R.T.: retention time in the chromatogram. [b] *m/z* ratio used for quantification. [c] m/z ratio used for confirmation.

Table S2. The Performance of the Separation System: Results from the Analysis of Gas Mixture (300 mL min^{-1})

concentration of the test gas source (ppbv)		concentration by the present method[a] (ppbv)		RSD (%)		differences between test gas concentration and measured data (%)	
I_2	ICl	I_2	ICl	I_2	ICl	I_2	ICl
15.6	13.5	14.9	13.2	5.6	3.4	4.6	2.2
15.6	4.49	15.1	4.56	6.3	1.8	3.3	1.5
5.19	4.49	4.92	4.42	6.8	4.2	5.3	1.6
5.19	1.5	4.85	1.47	7.6	3.7	6.8	2.1
1.04	1.5	0.98	1.44	6.5	4.5	5.9	3.9
1.04	0.94	0.97	0.91	7.1	7.9	6.5	3.3

[a] mean of three replicates.

Table S3. Effect of Relative Humidity on the Collection Efficiency

relative humidity (%)	collection efficiency[a] (%)		Differences (%)	
	I_2	ICl	I_2	ICl
~0	97.9 ± 1.3	99.2 ± 0.5	2.5	4.3
30	98.5 ± 1.6	98.7 ± 1.1	3.1	3.9
70	95.6 ± 3.7	95.4 ± 2.9	0.1	0.1
100	90.6 ± 4.3	88.5 ± 3.4	5.7	8.6

[a] mean ± SD (n = 3).

References:

(1) Dasgupta, P. K.; Liu, Y.; Dyke, J. V. *Environ. Sci. Technol.* **2008**, *42*, 1315–1323.

(2) Fabian, P.; Singh, O. N. *The Handbook of Environmental Chemistry, 4E: Reactive Halogen Compounds in the Atmosphere*; Springer-Verlag: Berlin and Heidelberg, 1999.

(3) Chameides, W. L.; Davis, D. D. *J. Geophys. Res.* **1980**, *85*, 7383–7398.

(4) O'Dowd, C. D.; Jimenez, J. L.; Bahreini, R.; Flagan, R. C.; Seinfeld, J. H.;Hämer, K.; Pirjola, L.; Kulmala, M.; Jennings, S. G.; Hoffmann, T. *Nature* **2002**, *417*, 632–636.

(5) O'Dowd, C. D.; Hoffmann, T. *Environ. Chem.* **2005**, *2*, 245–255.

(6) Kolb, C. E. *Nature* **2002**, *417*, 597–598.

(7) Carpenter, L. J. *Chem. Rev.* **2003**, *103*, 4953–4962.

(8) Vogt, R.; Sander, R.; von Glasow, R.; Crutzen, P. J. *J. Atmos. Chem.* **1999**, *32*, 375–395.

(9) McFiggans, G.; Plane, J. M. C.; Allan, B. J.; Carpenter, L. J.; Coe, H.; O'Dowd, C. D. *J. Geophys. Res.* **2000**, *105*, 14371–14385.

(10) Bloss, W. J.; Lee, J. D.; Johnson, G. P.; Sommariva, R.; Heard, D. E.; Saiz-Lopez, A.; Plane, J. M. C.; McFiggans, G.; Coe, H.; Flynn, M.; Williams, P.; Rickard, A. R.; Fleming, Z. *Geophys. Res. Lett.* **2005**, *32*, L06814.

(11) Hoffmann, T.; O'Dowd, C. D.; Seinfeld, J. H. *Geophys. Res. Lett.* **2001**, *28*, 1949–1952.

(12) Pechtl, S.; Lovejoy, E. R.; Burkholder, J. B.; von Glasow, R. *Atmos. Chem. Phys.* **2006**, *6*, 505–523.

(13) Pirjola, L.; O'Dowd, C. D.; Yoon, Y. J.; Sellegri, K. *Environ. Chem.* **2005**, *2*, 271–281.

(14) Saiz-Lopez, A.; Plane, J. M. C. *Geophys. Res. Lett.* **2004**, *31*, L04112.

(15) Peters, C.; Pechtl, S.; Stutz, J.; Hebestreit, K.; Hönninger, G.; Heumann, K. G.; Schwarz, A.; Winterlik, J.; Platt, U. *Atmos. Chem. Phys.* **2005**, *5*, 3357–3375.

(16) McFiggans, G.; Coe, H.; Burgess, R.; Allan, J.; Cubison, M.; Alfarra, M. R.; Saunders, R.; Saiz-Lopez, A.; Plane, J. M. C.; Wevill, D. J.; Carpenter, L. J.; Rickard, A. R.; Monks, P. S. *Atmos. Chem. Phys.* **2004**, *4*, 701–713.

(17) McFiggans, G.; Cox, R. A.; Mössinger, J. C.; Allan, B. J.; Plane, J. M. C. *J. Geophys. Res.* **2002**, *107*, D154271.

(18) Rahn, K. A.; Borys, R. D.; Duce, R. A. *Science* **1976**, *192*, 549–550.

(19) Yoshida, S.; Muramatsu, Y. *J. Radioanal. Nucl. Chem.* **1995**, *196*, 295–302.

(20) Fritz, B. G.; Patton, G. W. *J. Environ. Radioact.* **2006**, *86*, 64–77.

(21) Yang, L.; Saavedra, S. S.; Armstrong, N. R. *Anal. Chem.* **1996**, *68*, 1834–1841.

(22) von Glasow, R.; Crutzen, P. J. In *Treatise on Geochemistry Update 1*; Holland, H. D.,

Turekian, K. K., Eds.; Eleviser: Amsterdam, The Netherlands, 2007; Vol. 4.02, pp 1–67.

(23) Dasgupta, P. K. In *Sampling and Sample Preparation Techniques in Field and Laboratory*; Pawliszyn, J., Ed.; Elsevier:Amsterdam, The Netherlands, 2002; pp 97–160.

(24) Kloskowski, A.; Pilarczyk, M.; Namiesnik, J. *Crit. Rev. Anal. Chem.* **2002**, *32*, 301–335.

(25) Eatough, D. J.; White, V. F.; Hansen, L. D.; Eatough, N. L.; Ellis, E. C. *Anal. Chem.* **1985**, *57*, 743–748.

(26) Fisseha, R.; Dommen, J.; Sax, M.; Paulsen, D.; Kalberer, M.; Maurer, R.; Hofler, F.; Weingartner, E.; Baltensperger, U. *Anal. Chem.* **2004**, *76*, 6535–6540.

(27) Takeuchi, M.; Li, J.; Morris, K. J.; Dasgupta, P. K. *Anal. Chem.* **2004**, *76*, 1204–1210.

(28) Sheu, G.-R.; Mason, R. P. *Environ. Sci. Technol.* **2001**, *35*, 1209–1216.

(29) Landis, M. S.; Stevens, R. K.; Schaedlich, F.; Prestbo, E. M. *Environ. Sci Technol.* **2002**, *36*, 3000–3009.

(30) Sellegri, K.; Yoon, Y. J.; Jennings, S. G.; O'Dowd, C. D.; Pirjola, L.; Cautenet, S.; Chen, H.; Hoffmann, T. *Environ. Chem.* **2005**, *2*, 260–270.

(31) Barnes, I.; Becker, K. H.; Starcke, J. *Chem. Phys. Lett.* **1992**, *196*, 578–582.

(32) Gilles, M. K.; Turnipseed, A. A.; Talukdar, R. K.; Rudich, Y.; Villalta, P. W.; Huey, L. G.; Burkholder, J. B.; Ravishankara, A. R. *J. Phys. Chem.* **1996**, *100*, 14005–14015.

(33) Rowley, D. M.; Mössinger, J. C.; Cox, R. A.; Jones, R. L. *J. Atmos. Chem.* **1999**, *34*, 137–151.

(34) Holmes, N. S.; Adams, J. W.; Crowley, J. N. *Phys. Chem. Chem. Phys.* **2001**, *3*, 1679–1687.

(35) Baker, A. R. *Environ. Chem.* **2005**, *2*, 295–298.

(36) Pechtl, S.; Schmitz, G.; von Glasow, R. *Atmos. Chem. Phys.* **2007**, *7*, 1381–1393.

(37) Carpenter, L. J.; Hopkins, J. R.; Jones, C. E.; Lewis, A. C.; Parthipan, R.; Wevill, D. J.; Poissant, L.; Pilote, M.; Constant, P. *Environ. Sci. Technol.* **2005**, *39*, 8812–8816.

(38) Bichsel, Y.; von Gunten, U. *Environ. Sci. Technol.* **1999**, *33*, 4040–4045.

(39) Platzner, I. T. *Modern isotope ratio mass spectrometry*; Wiley: New York, 1997; pp 310–311.

(40) Jereb, M.; Zupan, M.; Stavber, S. *Chem. Commun.* **2004**, *22*, 2614–2615.

(41) Ali, Z.; Thomas, C. L. P.; Alder, J. F. *Analyst* **1989**, *114*, 759–769.

(42) Dasgupta, P. K.; Dong, S.; Hwang, H.; Yang, H.-C.; Zhang, G. *Atmos. Environ.* **1988**, *22*, 949–963.

(43) Mishra, S.; Singh, V.; Jain, A.; Verma, K. K. *Analyst* **2000**, *125*, 459–464.

(44) Neoh, T.; Noda, Y.; Yoshii, H.; Furuta, T. *J. Inclusion Phenom. Macrocyclic Chem.* **2006**, *56*, 117–123.

(45) Rendleman, J. A., Jr. *Carbohydr. Polym.* **2003**, *51*, 191–202.

(46) Lyman W. J.; Reehl W. F.; Rosenblatt D. H. *Handbook of Chemical Property Estimation Methods*; American Chemical Society: Washington, DC, 1993.

(47) Maguin, F.; Mellouki, A.; Laverdet, G.; Poulet, G.; Le Bras, G. *Int. J. Chem. Kinet.* **1991***, 23,* 237–245.

(48) O'Driscoll, P.; Lang, K.; Minogue, N.; Sodeau, J. *J. Phys. Chem. A* **2006**, *110*, 4615–4618.

(49) Cavalli, F.; Facchini, M. C.; Decesari, S.; Mircea, M.; Emblico, L.; Fuzzi, S.; Ceburnis, D.; Yoon, Y. J.; O'Dowd, C. D.; Putaud, J. P.; Dell'Acqua, A. *J. Geophys. Res.* **2004**, *109*, D24215.

(50) O'Dowd, C. D.; Facchini, M. C.; Cavalli, F.; Ceburnis, D.; Mircea, M.; Decesari, S.; Fuzzi, S.; Yoon, Y. J.; Putaud, J. P. *Nature* **2004**, *431*, 676–680.

(51) Simpson, W. R.; von Glasow, R.; Riedel, K.; Anderson, P.; Ariya, P.; Bottenheim, J.; Burrows, J.; Carpenter, L. J.; Friess, U.; Goodsite, M. E.; Heard, D.; Hutterli, M.; Jacobi, H.-W.; Kaleschke, L.; Neff, B.; Plane, J.; Platt, U.; Richter, A.; Roscoe, H.; Sander, R.; Shepson, P.; Sodeau, J.; Steffen, A.; Wagner, T.; Wolff, E. *Atmos. Chem. Phys.* **2007**, *7*, 4375–4418.

Chapter 3

Field Measurements

3.1 Observations of high concentrations of I_2 and IO in coastal air supporting iodine-oxide driven coastal new particle formation

R.-J. Huang,[1] K. Seitz,[3] C. D. O'Dowd,[2] U. Platt,[3] and T. Hoffmann[1]

[1]Institute of Inorganic and Analytical Chemistry, Johannes Gutenberg University of Mainz, D-55128 Mainz, Germany (t.hoffmann@uni-mainz.de)
[2]School of Physics and Centre for Climate and Air Pollution Studies, Environmental Change Institute, National University of Ireland, Galway, Ireland
[3]Institute of Environmental Physics, University of Heidelberg, Im Neuenheimer Feld 229, D-69120 Heidelberg, Germany

Status: Accepted by Geophysical Research Letters

Theoretical studies have predicted that concentrations of gaseous I_2 and IO of the order of 80–100 ppt and 40–50 ppt, respectively, are required in coastal air to account for photochemically-driven coastal new-particle formation events to occur. However, measurements reported to date (i.e., ~20 ppt I_2, ≤10 ppt IO) have not supported the required model predictions. Here, we present measurements of high concentrations of I_2 and IO in N.E. Atlantic marine air on the west coast of Ireland. The maximum mixing ratios of daytime I_2 and IO over the seaweed beds during low tide were 302 ppt and 35 ppt, respectively. The I_2 distribution was rather inhomogeneous, even at the inter-tidal zone, but closely related to the macroalgae biomass abundance. New particle formation bursts were frequently observed during daytime hours with the concentrations up to 4.5×10^5 particles cm^{-3} during low-tide conditions, and the concentrations of ultra-fine particles were positively correlated with the IO concentrations. Considering the constraints set out in theoretical studies for new particle

formation *via* condensation of condensable iodine oxide vapours, the results reported here clearly demonstrate that the molecular iodine and iodine monoxide concentrations in coastal air are sufficient to meet the theoretical precursor concentrations required to drive intensive coastal new-particle formation from higher order condensable iodine oxides.

1. Introduction

The impact of iodine chemistry in the lower troposphere is presently a subject of considerable interest. Numerous studies [e.g., von Glasow and Crutzen, 2007] have concentrated on the potential of reactive iodine to affect the oxidising capacity of the marine boundary layer (MBL) in a variety of ways: catalytic destruction of O_3, altering the partitioning of NO_x (NO_2/NO) and HO_x (HO_2/OH), and activating chlorine and bromine from sea-salt aerosol. Iodine may also play an important role in O_3 and Hg depletion episodes in the polar boundary layer. Recent field measurements and modeling studies indicate that these atmospheric processes could be enhanced with elevated tropospheric iodine level [Saiz-Lopez et al., 2008; Read et al., 2008].

Since molecular iodine (I_2) was suggested to be the dominant source of coastal reactive iodine in the MBL during the 2002 NAMBLEX field campaign at Mace Head (Ireland) [Saiz-Lopez and Plane, 2004], it has become well-established by laboratory studies that the emission of this molecular iodine from low tidal macroalgal exposure is indeed a most important process responsible for the observed tropospheric iodine level [McFiggans et al., 2004; Küpper et al., 2008]. Significant levels of molecular iodine have been observed at Mace Head and nearby sites (~100 parts per trillion (ppt)) [Saiz-Lopez and Plane, 2004; Saiz-Lopez et al., 2006; Peters et al., 2005], and at La Jolla, California (~8 ppt) [Finley and Saltzman, 2008]. Although large-scale I_2 observations have not been realized so far due to the lack of analytical techniques to accurately measure this species, the measurements of iodine monoxide (IO) radicals, an unambiguous product of iodine atom reaction with ozone, have been carried out at various coastal sites and the polar regions by ground-based approaches and satellite [e.g., Peters et al., 2005; Whalley et al., 2007; Schönhardt et al., 2008].

The formation of ultra-fine particles in the coastal atmosphere has been observed frequently [O'Dowd et al., 1998; O'Dowd et al., 2002; O'Dowd and Hoffmann, 2005]. Positive correlations between seaweed mass, I_2 emissions and the resulting particle concentrations have been elucidated from chamber experiments [Sellegri et al., 2005]. Also the role of iodine oxides in driving coastal ultra-fine particle formation has been widely investigated [e.g., Hoffmann et al., 2001; McFiggans et al., 2004]. This formation process is thought to involve the production of IO via the reaction of O_3 with iodine atoms that are generated by photolysis of I_2 and the self-reaction of IO to yield higher oxides (I_2O_y, where y = 2–5), which finally nucleate and form new particles. Therefore, the presence of IO in the atmosphere points to the possibility of new particle formation. However, model calculations [Burkholder et al., 2004] demonstrate that IO concentrations reported in recent field measurements using long-path differential optical absorption spectroscopy (LP-DOAS) are not sufficient to account for the significant aerosol production observed in the coastal MBL, mostly because the data derived from DOAS measurements are calculated assuming a constant concentration along the light path of several kilometers which consequently can not reveal the true concentration level in the inter-tidal zone of a fraction of a kilometer. The same is true for I_2 measurements which were mostly carried out by LP-DOAS, leading to potential underestimation of the concentration levels of I_2 in the inter-tidal zone. Although broadband cavity ring-down spectrometer (BBCRDS) can provide "single-point" in situ measurements of I_2 [Saiz-Lopez et al., 2006], the limits of detection of these spectrometric methods are in general relatively high, which makes the accurate quantification of daytime I_2 still difficult and therefore obscures our understanding on the atmospheric processes of iodine, since models have predicted that even very small amount of I_2 under daytime conditions could strongly affect the marine atmosphere [Peters et al., 2005].

While most of the above studies have been located at Mace Head, it should be noted that Mace Head possesses perhaps the lowest algal biomass in the region as most of the shore is characterized by bare rocks rather than notable kelp beds. This study extends the studies at Mace Head to simultaneous measurements in a nearby algal biomass hotspot, Mweenish Bay. During a campaign in August and September, 2007, elevated concentration levels of I_2 and

IO were observed, particularly over the exposed seaweed beds. This result provides substantial support to the strong iodine-containing new particle burst observed in the coastal MBL.

2. Field Measurements

The field measurements of I_2 and IO were made at the Mace Head Atmospheric Research Station (53.25^o N, 9.80^o W) and Mweenish Bay (53.32^o N, 9.73^o W), in N.E. Atlantic. The later is located about 7 km southeast of the Mace Head research station.

Molecular iodine was measured by a diffusion denuder system in combination with a gas chromatography–mass spectrometry (GC–MS) method, which provides "single-point" in situ concentrations of I_2 at the sampling site. Details of this recently developed denuder/GC–MS method are given by Huang and Hoffmann [2009] and therefore it is only briefly described here. Ambient I_2 samples were taken by brown denuder tubes (6 mm i.d. × 50 cm length) which were uniformly coated with 11.25 mg α-cyclodextrin (α-CD) and trace $^{129}I^-$, at a flow rate of 500 mL min^{-1} for 60–180 min. The interference iodine species such as ICl and HOI were isolated by coupling a 1,3,5-trimethoxybenzene-coated denuder upstream of the α-CD/$^{129}I^-$-coated denuder (data not shown here). After sampling, the open ends of the denuders were again sealed with PP end-caps and kept under refrigeration until subsequent laboratory measurements. In the laboratory, the samples were eluted with five 2.0 mL-portions of ultrapure water into a 25-mL flask in which amounts of 500 µL of phosphate buffer (pH 6.4), 100 µL of 2,4,6-tribromoaniline (2.5 mg L^{-1}, internal standard), 400 µL of sodium 2-iodosobenzoate, and 300 µL of *N*,*N*-dimethylaniline was added. Subsequently, the solution was shaken at room temperature for about 120 min, leading to a complete derivatization of I_2 into 4-iodo-*N*,*N*-dimethylaniline. Finally, the solution was extracted with 100 µL of cyclohexane. 1.0 µL of the extraction solution was injected into a GC–MS system (Trace GC/PolarisQ, Thermo Finnigan, Italy). A Rtx-5MS fused-silica capillary column (Restek Co., Bad Homburg, Germany) was used for chromatographic separation, and the MS was run in the selected ion monitoring (SIM) mode to enhance the sensitivity of measurements. The detection limit of the method is below 0.1 ppt for 90 L sample volume, and the collection efficiency is greater than 98%.

IO was measured by two active LP-DOAS systems [Platt and Stutz 2008]. Details are found in Seitz et al. [2009], thus only a brief description will be given here. The almost parallel light beam of a high pressure Xe-arc lamp (type: XBO 500, Osram), was sent through the open atmosphere to an array of quartz prism retro-reflectors (63 mm diameter each) and then reflected back to the receiving optics of the telescope. At Mace Head the light-path (6.8 km, one-way, 13.6 km total length) crossed Roundstone Bay to Roundstone, about 5–10 m above sea level at high tide, where the reflector consisting of 76 quartz prisms was located. At Mweenish Bay a light-path (2.0 km, one-way, 39 quartz prisms) crossing Mweenish Bay to Finish Island was established. This light-path crossed the sea at about 5–10 m above sea level at high tide. The reflected light was analyzed by a spectrometer (Acton Spectra Pro 300, f = 4.1 equipped with a 1900 gr mm^{-1} grating and Acton Spectra Pro 500, f = 6.9, 600 gr mm^{-1} grating for the measurements at Mace Head and Mweenish Bay, respectively). In both cases the detector used was a 1024 pixel photodiode array (type: S3904-1024, Hamamatsu). Spectra of the atmospheric light beam, scattered sunlight, and the Xe-arc lamp, were recorded. For each wavelength range an atmospheric measurement spectrum with a time resolution of 30 sec and signal integration of about 15 min (a maximum of 30 co-added spectra) was taken. IO was measured in the 430 ± 40 nm wavelength regions. For the analysis of the LP-DOAS data the software DOASIS was used to simultaneously fit the different references to the atmospheric spectrum using a non-linear least-squares method (for details see Platt and Stutz [2008]). The spectra were analyzed for IO absorption structures in the wavelength range between 416 and 439 nm including references of NO_2 and H_2O in the fitting procedure. The averaged IO detection limits are 0.6 ppt at Mace Head and 2.1 ppt at Mweenish Bay.

At Mweenish Bay, particle measurements were carried out by a nano scanning mobility particle sizer (nano-SMPS), covering sizes from 3 nm to 20 nm, and a standard SMPS, covering sizes from 10 nm to 100 nm. Both the nano-SMPS and SMPS were standard Thermo Systems Inc. (TSI) systems [Wang and Flagan, 1990], with the nano-SMPS using the

TSI 3025a condensation particle counter (CPC) as a detector and the SMPS using a TSI 3010 CPC as a detector. The instruments were located about 150 m away from the low tide region and sampling was conducted down a 3 m long, ¼” stainless steel inlet. Size resolved concentrations were corrected for diffusional losses, which were calculated based on tube diameter and residence time in sample tube. Equations were taken from Seifeld and Pandis [2006].

3. Results and Discussion

“Single-point” in situ measurements of littoral I_2 were made by a coupled denuder system [Huang and Hoffmann, 2009]. Compared to our previous starch-coated denuder system [Sellegri et al., 2005; Saiz-Lopez et al., 2006] this newly developed method provides better collection efficiency by the use of more effective coating materials and better accuracy by minimizing the interference iodine species. However, it should still be noted that the sampling time of denuder used in this work is relatively long (ranged from 60 to 180 min) which does not allow measurements at the time scales at which the photolysis of I_2 occurs. Therefore, the peak values of I_2 might actually be larger than those reported here.

At Mweenish Bay, the daytime in situ measurements taken exactly over the central zone of seaweed beds during low tide show very high mixing ratios of I_2, ranging from 110.3 to 301.8 ppt with an average of 186.3 ppt. Since the inlet of the denuder was set up very close to the seaweed beds (~5 cm) during sampling it is reasonable to treat these data as local source strength. When the measurements were carried out downwind of the seaweed beds with a distance of about 100–150 m, the daytime concentration decreased to about 36.7 ppt (ranging from 14.9 to 87.2 ppt, also partly shown in Figure 1a). This significant decrease of I_2 mixing ratio observed downwind of (i.e., further away from) the seaweed beds could be attributed to the rapid photolysis of I_2 that has a photolytic lifetime of 10 s [Saiz-Lopez et al., 2006], which is further supported by the large particle plumes observed during the advection crossing 100–150 m, and to the concentration dilution effect during the air mass transport from seaweed beds to the sampling site. Note that during these measurements the wind (from sea direction) passed over the seaweed beds with a speed of 5.4–7.7 m s^{-1} corresponding to a transport time of about 14–28 seconds. However, the averaged night-time I_2 mixing ratio downwind of the seaweed beds (~124 ppt) is comparable to the levels found directly above the seaweed beds (source strength) although the values drop to around 30 ppt in several episodes. This result indicates that I_2 mixing ratio will reach a steady state in the coastal air at night, which could be responsible for the pulse of IO that typically occurred after dawn [Saiz-Lopez and Plane, 2004].

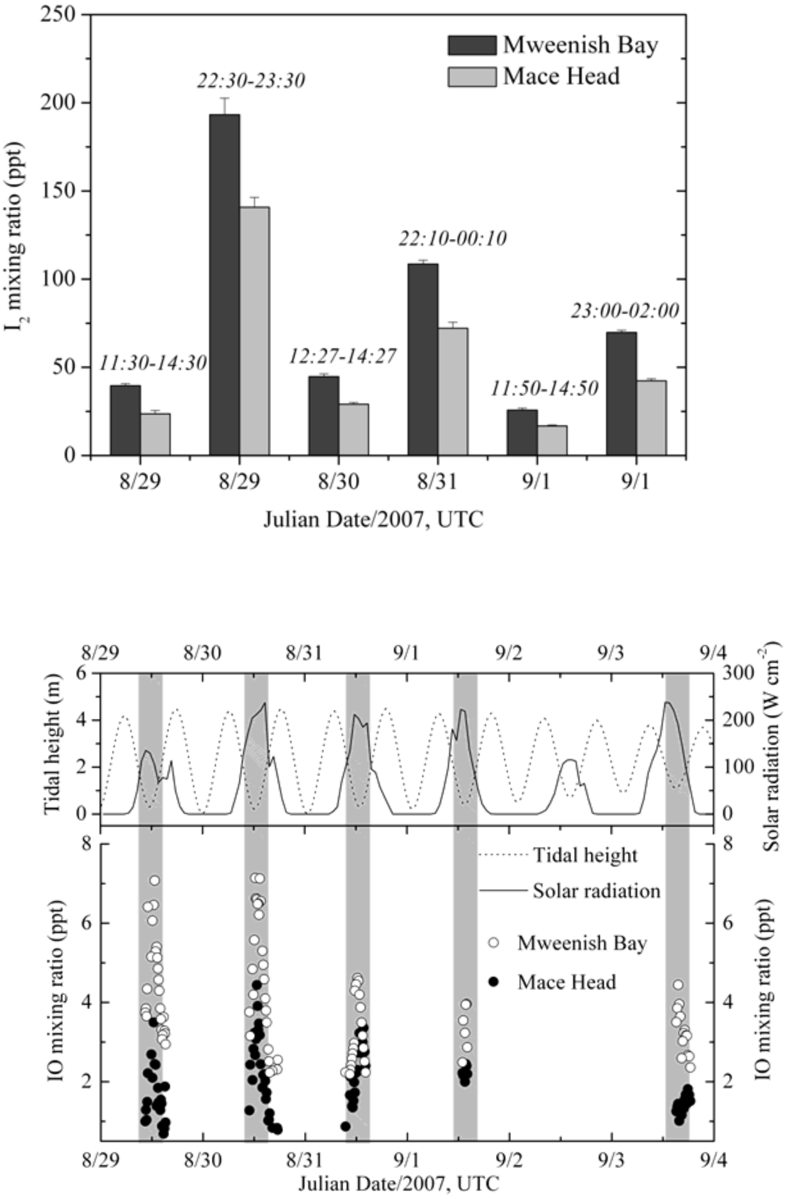

Figure 1. Comparison measurements of littoral I_2 (a) and spatial IO (b) between Mweenish Bay and Mace Head. Note that I_2 samples were simultaneously taken in the intertidal zone

about 100–150 m away from the algae beds during daytime and night-time low tide in both locations. The time (UTC) present above the column indicates the sampling period of each sample and the error bars refer to triplicate measurements of the same sample by GC–MS. Also note that only the IO values above the individual detection limits are presented here. The averaged detection limits are 0.6 ppt at Mace Head and 2.1 ppt at Mweenish Bay, respectively. Elevated IO levels were observed during low tide with intense solar irradiation. Also the IO mixing ratios were positively correlated to the concentrations of I_2.

I_2 measurements were also simultaneously carried out at Mace Head. The selected sampling site was about 100–150 m away from the seaweed beds. The averaged daytime I_2 mixing ratio (~23 ppt) is comparable to the reported average concentration (~26 ppt) by BBCRDS at the same site [Saiz-Lopez et al., 2006]. However, the mixing ratios during both daytime and night-time are significantly lower at Mace Head than at Mweenish Bay (see Figure 1a). This difference could be attributed to the higher biomass density at Mweenish Bay than at Mace Head and the difference in algal species composition at these two sites, i.e., dominated by *Laminaria digitata*, *Laminaria hyperborean*, *Himanthalia elongata*, *Palmaria palmata* and *Alaria esculenta* at Mace Head and *Ascophyllum nodosum* and *Fucus vesiculosus* at Mweenish bay [Irish Seaweed Centre, 2001], since chamber experiments showed that the emissions of I_2 are related to the seaweed species and biomass [Sellegri et al., 2005].

Comparison measurements of IO were made between Mweenish Bay and Mace Head by LP-DOAS. At Mace Head, the mixing ratios of IO observed are consistent with previous measurements taken during the 1998 PARFORCE [Carpenter et al., 2001] and 2002 NAMBLEX field campaigns [Saiz-Lopez and Plane., 2004]. At Mweenish Bay, IO was measured for the first time, and the mixing ratios observed were strikingly higher when compared to that at Mace Head. As shown in Figure 1b, the maximum IO mixing ratios occur at low tide during the period of high solar irradiation, and the daily IO maximum decreases gradually with the increase of the minimum in tidal height (correlation coefficient $r^2 = 0.68$). This diurnal profile is well consistent with the characteristics of I_2 emission at the local shoreline. When elevated I_2 concentrations occurred on August 29 and 30, higher IO mixing ratios were observed correspondingly (see Figure 1a and b). Obviously, enhanced algal exposure leads to elevated I_2 emissions and consequently higher concentrations of IO. This result is further supported by additional measurements at Mweenish Bay where IO mixing ratios of up to 35.0 ± 7.7 ppt were observed by a very short DOAS light-path (500 m, one-way) which covered exclusively the exposed seaweed beds at low tide [Seitz et al., 2009]. It is noted that this maximum IO concentration is very close to the littoral level (27.6 ± 3.2 ppt) at Roscoff (Brittany, France) measured by the "sing-point" in situ technique of cavity ring-down spectroscopy [Wada et al., 2007] and laser induced fluorescence spectroscopy [Whalley et al., 2007]. It may therefore be inferred that the actual IO concentration could be 5–10 times higher than that reported from LP-DOAS measurements of several kilometers extending over open sea in the coastal atmosphere at Mweenish Bay and nearby locations.

The elevated concentration levels of I_2 and IO are clearly correlated to the observation of strong new-particle bursts in 14 out of 23 days of measurements (17th August–8th September) at Mweenish Bay. Figure 2a illustrates the particle size distribution spectrum measured on 30th August. The ultra-fine particle bursts take place during daytime low tide and last for about 4–6 h, which is closely related to the diurnal variation of the seaweed exposure period. The concentrations of ultra-fine particles ($D < 7$ nm) can be as high as 4.5×10^5 particles cm^{-3} during the lowest water (spring tide) and are positively correlated to the measured IO column density, as shown in Figure 2b. Note, in the correlation presented, the IO time scale is shifted by ~15 minutes to allow advection time. Although the shift may be excessive for a transit of 150 m, it was the minimum time scale that could be shifted due to instrument temporal resolution. The correlation coefficient $r^2 = 0.66$, suggesting a significant dependency of particle concentration less than 7 nm on IO vapour concentrations.

In summary, the present work shows that elevated concentration of I_2 can occur over the seaweed beds during low tide under atmospheric conditions. The source strength is closely related to the seaweed species and their biomass. Shortly beyond the seaweed beds I_2 concentrations decrease significantly during daytime, indicating rather inhomogeneous I_2 distributions even in the inter-tidal zone. Elevated IO mixing ratios are also observed over the seaweed beds, which drives the enhanced new particle bursts at the concentration level of ~10^5 particles cm^{-3}. These results clearly demonstrate that the concentration levels of I_2 and

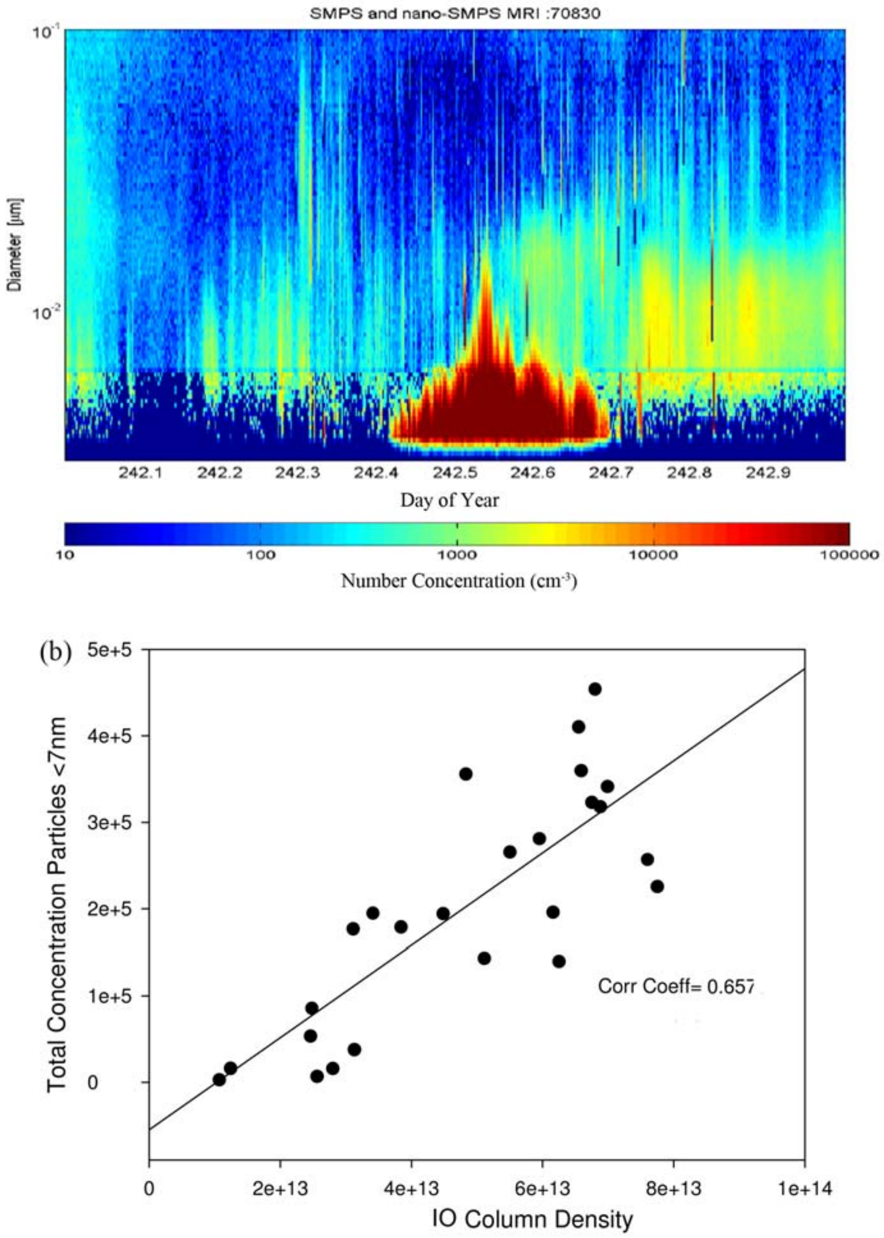

Figure 2. (a) The particle size distribution of 30th September observed at Mweenish Bay, and (b) the correlation between ultra-fine particle concentrations and IO column density during the period of particle bursts (spring low tide). Note that the IO time scale is shifted by ~15 minutes to compensate for the advection time.

IO in coastal air are sufficient to meet the theoretical precursor concentrations required to drive intensive coastal new-particle formation from higher order condensable iodine oxides. From the correlations established in the current work in combination with previous observations of new particle bursts at the west coastline of Ireland [Sellegri et al., 2005; O'Dowd et al., 2007] and at Brittany (France) [Whitehead et al., 2009] as well as with the laboratory studies [O'Dowd et al., 2002; McFiggans et al., 2004; Küpper et al., 2008], it may be inferred that tidally driven new particle formation events could be widespread over the algae-rich coastline.

Acknowledgements. This study was supported by the European Union under the FP6 project (Contract No. 018332): Marine Aerosol Production (MAP) and the German Research Foundation (Deutsche Forschungsgemeinschaft, DFG) within the graduate program 826 "Trace Analysis of Elemental Species: Development of Methods and Applications". The authors are grateful to the Martin Ryan Institute, especially Richard Fitzgerald, for the support during the field measurements.

References

Burkholder, J. B., J. Curtius, A. R. Ravishankara, and E. R. Lovejoy (2004), Laboratory studies of the homogeneous nucleation of iodine oxides, *Atmos. Chem. Phys.*, *4*, 19–34.

Carpenter, L. J., K. Hebestreit, U. Platt, and P. S. Liss (2001), Coastal zone production of IO precursors: a 2-dimensional study, *Atmos. Chem. Phys.*, *1*, 9–18.

Finley, B. D., and E. S. Saltzman (2008), Observations of Cl_2, Br_2 and I_2 in coastal marine air, *Geophys. Res. Lett.*, *113*, D21301, doi:10.1029/2008JD010269.

von Glasow, R., and P. J. Crutzen (2007), Tropospheric halogen chemistry, in: *Treatise on Geochemistry Update 1*, edited by H. D. Holland and K. K. Turekian, vol. 4.02, pp. 1–67, Eleviser, Amsterdam, The Netherlands.

Hoffmann, T., C. D. O'Dowd, and J. H. Seinfeld (2001), Iodine oxide homogeneous nucleation: An explanation for coastal new particle production, *Geophys. Res. Lett.*, *28*(10), 1949–1952.

Huang, R.-J., and T. Hoffmann (2009), Development of a coupled diffusion denuder system combined with gas chromatography/mass spectrometry for the separation and quantification of molecular iodine and the activated iodine compounds iodine monochloride and hypoiodous acid in the marine atmosphere, *Anal. Chem.*, *81*, 1777–1783.

Irish Seaweed Centre (2001), Connemara seaweed survey, an assessment of the commercially valuable seaweed species of connemara, 44 pp., National University of Ireland, Galway, Ireland.

Küpper, F. C., et al. (2008), Iodide accumulation provides kelp with an inorganic antioxidant impacting atmospheric chemistry, *Proc. Natl. Acad. Sci. U.S.A.*, *105*(19), 6954–6958.

McFiggans, G., et al. (2004), Direct evidence for coastal iodine particles from Laminaria macroalgae–linkage to emissions of molecular iodine, *Atmos. Chem. Phys.*, *4*, 701–713.

O'Dowd, C. D., M. Geever, M. K. Hill, M. H. Smith, and S. G. Jennings (1998), New particle formation: Nucleation rates and spatial scales in the clean marine coastal environment, *Geophys. Res. Letts.*, *25*(10), 1661–1664.

O'Dowd, C. D., J. L. Jimenez, R. Bahreini, R. C. Flagan, J. H. Seinfeld, K. Hämeri, L. Pirjola, M. Kulmala, S. G. Jennings, and T. Hoffmann (2002), Marine aerosol formation from biogenic iodine emissions, *Nature*, *417*, 632–636.

O'Dowd, C. D., and T. Hoffmann (2005), Coastal new particle formation: A review of the current state-of-the-art, *Environ. Chem.*, *2*, 245–255.

O'Dowd, C. D., Y. J. Yoon, W. Junkerman, P. Aalto, M. Kulmala, H. Lihavainen, and Y. Viisanen (2007), Airborne measurements of nucleation mode particles I: coastal nucleation and growth rates, *Atmos. Chem. Phys.*, *7*, 1491–1501.

Peters, C., S. Pechtl, J. Stutz, K. Hebestreit, G. Hönninger, K. G. Heumann, A. Schwarz, J. Winterlik, and U. Platt (2005), Reactive and organic halogen species in three different European coastal environments, *Atmos. Chem. Phys.*, *5*, 3357–3375.

Platt, U., and J. Stutz (Eds.) (2008), *Differential optical absorption spectroscopy, Principles and Applications*, in Physics of Earth and Space Environments, 597 pp., Springer, Heidelberg.

Read, K. A., et al. (2008), Extensive halogen-mediated ozone destruction over the tropical Atlantic Ocean, *Nature*, *453*(7199), 1232–1235.

Saiz-Lopez, A., and J. M. C. Plane (2004), Novel iodine chemistry in the marine boundary layer, *Geophys. Res. Lett.*, *31*, L04112, doi:10.1029/2003GL019215.

Saiz-Lopez, A., J. M. C. Plane, G. McFiggans, P. I. Williams, S. M. Ball, R. L. Jones, C. Hongwei, and T. Hoffmann (2006), Modelling molecular iodine emissions in a coastal marine environment: the link to new particle formation, *Atmos. Chem. Phys.*, *6*, 883–895.

Saiz-Lopez, A., et al. (2008), On the vertical distribution of boundary layer halogens over coastal Antarctica: implications for O_3, HO_x, NO_x and the Hg lifetime, *Atmos. Chem. Phys.*, *8*, 887–900.

Schönhardt, A., A. Richter, F. Wittrock, H. Kirk, H. Oetjen, H. K. Roscoe, and J. P. Burrows (2008), Observations of iodine monoxide columns from satellite, *Atmos. Chem. Phys.*, *8*, 637–653.

Seinfeld, J. H., and S. N. Pandis (2006), Atmospheric Chemistry and Physics, ISBN 0-471-72018-6, John Wiley & Sons.

Seitz, K., J. Buxmann, D. Pöhler, T. Sommer, J. Tschritter, C. D. O'Dowd, and U. Platt (2009), The spatial distribution of the reactive iodine species IO from simultaneous active and passive DOAS observations, *Atmos. Chem. Phys. Discuss.*, *9*, 1–28.

Sellegri, K., Y. J. Yoon, S. G. Jennings, C. D. O'Dowd, L. Pirjola, S. Cautenet, H. Chen, and T. Hoffmann (2005), Quantification of coastal new ultra-fine particles formation from in situ and chamber measurements during the BIOFLUX campaign, *Environ. Chem.*, *2*, 260–270.

Wada, R., J. M. Beames, and A. J. Orr-Ewing (2007), Measurement of IO radical concentrations in the marine boundary layer using a cavity ring-down spectrometer, *J. Atmos. Chem.*, *58*, 69–87.

Wang, S. C., and R. C. Flagan(1990), Scanning electrical mobility spectrometer, *Aerosol Sci. Tech.*, *13*(2), 230–240.

Whalley, L. K., K. L. Furneaux, T. Gravestock, H. M. Atkinson, C. S. E. Bale, T. Ingham, W. J. Bloss, and D. E. Heard. (2007), Detection of iodine monoxide radicals in the marine boundary layer using laser induced fluorescence spectroscopy, *J. Atmos. Chem.*, *58*, 19–39.

Whitehead, J. D., G. B. McFiggans, M. W. Gallagher, and M. J. Flynn (2009), Direct linkage between tidally driven coastal ozone deposition fluxes, particle emission fluxes, and subsequent CCN formation, *Geophys. Res. Lett.*, 36, L04806, doi:10.1029/2008GL035969.

3.2 In situ measurements of molecular iodine in the marine boundary layer: the link to macroalgae and the implications for O_3, IO, OIO and NO_x

R.-J. Huang[1], K. Seitz[2], J. Buxmann[2], D. Poehler[2], K. E. Hornsby[3], L. J. Carpenter[3], U. Platt[2], and T. Hoffmann[1]

[1]Institute for Inorganic and Analytical Chemistry, Johannes Gutenberg-University of Mainz, Duesbergweg 10-14, D-55128 Mainz, Germany

[2]Institute for Environmental Physics, University of Heidelberg, Im Neuenheimer Feld 229, D-69120 Heidelberg, Germany

[3]Department of Chemistry, University of York, Heslington, York YO10 5DD, UK

Status: Accepted by Atmospheric Chemistry and Physics, published online in ACPD.

Abstract. "Single-point" in situ measurements of molecular iodine (I_2) were carried out in the coastal marine boundary layer (MBL) using diffusion denuders in combination with a gas chromatography–mass spectrometry (GC–MS) method. Comparison measurements were taken at Mace Head and Mweenish Bay, on the West Coast of Ireland. The observed mixing ratios of I_2 at Mweenish Bay are much higher than that at Mace Head, which is consistent with differences in local algal biomass density and algal species composition. The concentration levels of I_2 were found to correlate inversely with tidal height and correlate positively with the concentration levels of O_3 in the surrounding air. However, the released I_2 can also lead to O_3 destruction via the reaction of O_3 with iodine atoms that are formed by the photolysis of I_2 during the day and via the reaction of I_2 with NO_x at night. IO and OIO were measured by long-path differential optical absorption spectroscopy (LP-DOAS). The results show that the concentrations of both daytime and nighttime IO are correlated with the mixing ratios of I_2. In addition, I_2 was measured simultaneously by the LP-DOAS technique and compared with the "single-point" in situ measurement. The results suggest that the local algae sources dominate the inorganic iodine chemistry at Mace Head and Mweenish Bay.

1 Introduction

The role of iodine chemistry in ozone depletion events and marine aerosol formation has received considerable attention in the past few years (Saiz-Lopez et al., 2007; Read et al., 2008; O'Dowd et al., 2002; Vogt et al., 1999). The precusors for these iodine-related atmospheric processes have been proposed, from early studies, to be iodocarbons such as CH_3I, CH_2I_2, CH_2ClI, CH_2BrI, C_2H_5I, C_3H_7I, or C_4H_9I (Carpenter et al., 1999). However, recent field measurements show that molecular iodine (I_2) is probably the dominant source of atmospheric iodine in certain coastal regions. A maximum I_2 mixing ratio of 93 parts per trillion by volume (pptv) at night and of 25 pptv during the day was observed during the North Atlantic Marine Boundary Layer Experiment (NAMBLEX) field campaign at Mace Head, Ireland in summer 2002 using a long-path differential optical absorption spectroscopy (LP-DOAS) (Saiz-Lopez and Plane, 2004). During periods of daylight, I_2 molecules in the atmosphere photolyze to I atoms which then react with O_3 to yield iodine oxide (IO). A clear anti-correlation between IO and tidal height and a correlation between IO and solar irradiation were also observed at Mace Head (Carpenter et al., 2001; Saiz-Lopez et al., 2006a). The self-reaction of IO is thought to result in the formation of higher iodine oxides like OIO or I_2O_4 and finally leads to new particle formation (Hoffmann et al., 2001; O'Dowd and Hoffmann, 2005; Pirjola et al., 2005). Also, IO radicals play a key role in a number of other important tropospheric processes, including NO_x and HO_x chemistry.

Biogenic emission of I_2 by macroalgae has been suggested to be one of the most important processes responsible for the observed tropospheric iodine levels in coastal locations (McFiggans et al., 2004; Pirjola et al., 2005; Palmer et al., 2005). A recent study shows that iodine is accumulated in macroalgae (e.g., *Laminaria digitata*) in the form of iodide, which can react with O_3 when the plants are exposed to the ambient air at low tide, leading to the direct release of I_2 into the atmosphere (Küpper et al., 2008). However, the correlations between I_2 emissions and algal species are still poorly understood, especially under realistic ambient conditions, so that the impacts of biogenic emission of I_2 on tropospheric photochemistry on regional and global scales remain an open question.

Currently, data on ambient I_2 are still quite scarce, and most of the measurements were carried out by long-path differential optical absorption spectroscopy (LP-DOAS) (Saiz-Lopez and Plane, 2004; Saiz-Lopez et al., 2006a; Peters et al., 2005). This technique provides spatial average concentrations along the DOAS light-path (usually several kilometres in length), thus is incapable of resolving inhomogeneous distributions of I_2. However, it has been proposed that the spatial variability of the sources of reactive iodine leads to significant spatial variations in the concentrations of iodine species. Thus, the DOAS measurements can lead to ambiguity in the identification of the source of the iodine species (Peters et al., 2005; von Glasow and Crutzen, 2007). Therefore, "point" in situ measurements of gaseous I_2 are highly desirable to better identify the potential source of molecular iodine. A broadband cavity ring-down spectrometer (BBCRDS) was deployed during the NAMBLEX campaign, and the application of this system to "point" in situ measurements of ambient I_2 has been demonstrated (Bitter et al., 2005). Recently, incoherent broadband cavity-enhanced absorption spectroscopy (IBBCEAS) has been developed in the laboratory for gaseous I_2 measurements (Vaughan et al., 2008). However, the detection limits of these spectrometric methods are relatively high (~20 ppt), which makes the clear identification of daytime I_2 still difficult. In addition, the initial concentrations from direct I_2 emissions are not accessible by the spectrometric methods since the light-path runs mostly at a height of several meters above the ground and the rapid photolysis of I_2 during daytime causes a vertical concentration gradient. However, model studies have predicted that even very low concentrations of I_2 under daytime conditions could strongly affect the marine atmosphere (Peters et al., 2005).

In this paper, we present the results of a 5-week field campaign carried out at Mace Head and Mweenish Bay located at the West Coast of Ireland in August/September 2007. Ambient I_2 mixing ratios were measured by a diffusion denuder system combined with a gas chromatography–mass spectrometry (GC–MS) with precolumn derivatization method and by the DOAS technique for comparison. The correlation between I_2 concentrations at different measurement sites, ozone concentrations, tidal height, and occurance of different algal species were investigated. Also the impact of iodine on nighttime chemistry was studied.

2 Experimental

2.1 Diffusion denuder sampling in combination with GC–MS measurements

Ambient I_2 samples were taken by diffusion denuder tubes (6 mm i.d. × 50 cm length) (Huang and Hoffmann, 2009). The collection of I_2 is based on the rapid formation of inclusion complexes of I_2 with the combined coatings α-cyclodextrin (α-CD) and iodide (I^-). To obtain denuders coated uniformly with the coating reagents, nine 0.5 mL aliquots of coating solution (2.5 mg mL^{-1} α-CD and trace $^{129}I^-$ in methanol) were slowly pipetted into the openings of the brown denuder tube which was held at an angle of about 10^o relative to the horizontal plane. During the coating procedure the tubes were rotated and flushed with nitrogen for drying (flow rate 0.5 L min^{-1}). Afterward, the coated denuders were sealed with polypropylene (PP) end-caps and stored under refrigeration until sampling. At the sampling site, the denuders were set vertically to eliminate particle deposition due to gravitational settling. The interference iodine species were isolated by coupling a 1,3,5-trimethoxybenzene-coated denuder upstream of the α-CD/I^--coated denuder (Huang and Hoffmann, 2009), and an untreated glass tube of specific length (15 cm) with the same diameter as the denuder tube was coupled to the denuder inlet, used as a subduction zone to adjust the laminar flow of the sampled air into the denuder. Ambient air was sampled through the denuder system by a membrane pump located downstream of the denuder for 30–180 min at a flow rate of 500 mL min^{-1}. Once the sampling was completed, the open ends of the tubes were again sealed with PP end-caps and kept under refrigeration until subsequent laboratory measurements.

In the laboratory, the samples were eluted with five 2.0 mL-portions of ultrapure water into a 25-mL calibrated flask. Amounts of 500 μL of phosphate buffer (pH 6.4), 100 μL of 2,4,6-tribromoaniline (2.5 mg L^{-1}, internal standard), 400 μL of sodium 2-iodosobenzoate, and 300 μL of *N*,*N*-dimethylaniline were then added. The solution was diluted to about 23 mL with ultrapure water and subsequently shaken at room temperature for about 120 min. 2.0 mL of sodium acetate solution (20% m/v) was then introduced, and the solution was diluted to the mark with ultrapure water. Finally, the solution was extracted with 100 μL of cyclohexane. 1.0 μL of the solution was injected into a gas chromatography with an ion-trap mass spectrometer (Trace GC/PolarisQ, Thermo Finnigan Italia S.p.A., Rodano, Italy). A fused-silica capillary column (30 m × 0.25 mm i.d., d_f: 0.25 μm, Rtx-5MS, Restek Co., Bad Homburg, Germany) was used for chromatographic separation. High-purity helium (99.999%) was used as a carrier gas at a constant flow of 1.0 mL min^{-1}. The temperature of the injector was set to 250 ^oC and the transfer line was 300 ^oC. The temperature of the GC oven was programmed as follows: initial temperature 50 ^oC (hold 3 min), 30 ^oC min^{-1} to 220 ^oC (hold 3 min). The MS was operated in the electron impact (EI) ionization mode with an acceleration energy of 70 eV. A solvent delay of 4.5 min preceded the MS spectra acquisition in the selected ion monitoring (SIM) mode in the following sequence: 4.50–6.00 min, *m/z*: 77, 121; 6.00–7.50 min, *m/z*: 119, 247; 7.50–11.67 min, *m/z*: 250, 329, 331. The blanks were estimated by measuring the unsampled denuders which were sealed throughout the campaign and were found to be within the ranges of the limit of detection (0.17 pptv).

2.2 DOAS measurements

DOAS is a well established technique to identify and quantify trace gases by their narrow band absorption structures (Platt and Stutz, 2008). In this study, two active LP-DOAS instruments were used. The setup of the LP-DOAS systems used was a further development of the coaxial mirror system introduced by Axelson et al. (1990). The light beam was sent through the open atmosphere to an array of quartz prism retro-reflectors (63 mm diameter each). For the measurements at Mace Head the light-path (6.8 km, one-way) crossed Roundstone Bay to Roundstone about 10 m above sea level at high tide, where the reflector (consisting of 76 quartz prisms) was located. At Mweenish Bay, a light path (2.0 km, one-way, 39 quartz prisms) was established crossing Mweenish Bay at about 5 m above sea level at high tide. For both instruments the reflected light was analyzed by a spectrometer (Acton Spectra Pro 300, f= 4.1, 1900 gr mm^{-1} and an Acton Spectra Pro 500, f= 6.9, 600 gr mm^{-1} grating for the measurements at Mace Head and Mweenish Bay, respectively). The detector used was a 1024 pixel photodiode array detector (type: S3904-1024, Hamamatsu). O_3 was measured in 320 ± 40 nm, IO in 430 ± 40 nm, I_2 and OIO in 550 ± 40 nm, and NO_3 in 630 ±

40 nm. For the analysis of the LP-DOAS data the software DOASIS (Kraus, 2005) was used to simultaneously fit the different references to the atmospheric spectrum using a non-linear least-squares method (e.g., Stutz and Platt, 1996). In addition, a polynomial was included to account for broad band structures due to scattering in the atmosphere. IO was analyzed in the wavelength range between 416 and 439 nm. The IO cross section (Spietz et al., 2005) as well as references of NO_2 (Voigt et al., 2002) and H_2O (Rothmann et al., 2005) were included in the IO fitting procedure. The evaluation of I_2 was performed in the wavelength range between 530 and 567 nm and the cross sections of I_2 (Saiz-Lopez et al., 2004), references of OIO (Bloss et al, 2001), NO_2, O_4 (Greenblatt et al., 1990) and H_2O were considered during the fit. O_3 was analyzed between 315 and 342.5 nm (Mweenish Bay) and 332.5 and 343.75 nm (Mace Head) and the cross sections of O_3 (Voigt et al., 2001), BrO (Wilmouth et al., 1999), SO_2 (Vandaele et al., 1994), HCHO (Meller and Moortgat, 2000), NO_2, O_4 and HONO (Stutz et al., 2000) were included in the fitting procedure. NO_3 was analyzed between 618 and 626 nm and 657 and 664 nm and fitted using NO_3 (Yokelson et al., 1994) and H_2O cross sections.

2.3 Online GC–MS measurements

CH_3I, C_2H_5I, CH_2BrI, CH_2ICl and CH_2I_2 were analysed automatically from 3 L of dried air using a Perkin Elmer (USA) Turbomass GC–MS system connected to a Perkin Elmer Automated Thermal Desorption unit (ATD). Air samples were measured every 45 minutes during 5 days of measurement between the 29th of August and the 11th of September 2007. Analytes were trapped onto a 3-stage carbon-based adsorbent micro trap (Air monitoring trap, Perkin Elmer, UK) held at -30 °C. The micro trap was then flash heated to 360 °C, injected onto a 60 m DB5 GC column (Supelco), then analysed by the MS in single ion mode. The GC–MS was calibrated against a gas standard prepared in-house containing low-pptv mixing ratios of the target halocarbons in zero grade nitrogen (BOC, UK) at 100 bar in an Aculife cylinder (10 L, CK Gases). This gas standard was quantified in our laboratory against a permeation tube system (Wevill and Carpenter, 2004) immediately after the campaign. The method is discussed in more detail in Hornsby et al. (2009).

2.4 Sampling sites

The denuder sampling systems and LP-DOAS instruments were positioned at the Mace Head Atmospheric Research Station (53.25° N, 9.80° W) and the Mweenish Bay (53.32° N, 9.73° W) (see Fig. 1). Also, at Mace Head, in situ measurements of reactive iodine species were carried out by the online GC–MS system. The Mace Head site is well known for atmospheric events with regard to iodine chemistry. A detailed description of this measurement site can be found elsewhere (Carpenter et al., 2001). Mweenish Bay is located about 7 km southeast of the Mace Head research station in an area of large seaweed beds. The algae species present differ from those at Mace Head, with brown species *Ascophyllum nodosum* and *Fucus vesiculosus* being dominant. (Irish Seaweed Centre, 2001). In addition, Mweenish Bay has a higher seaweed density. Denuder sampling was carried out in the intertidal zone at Mweenish Bay-II for consecutive 30 days (6 August–4 September, 2007) and at Mace Head for consecutive 6 days (28 August–2 September, 2007). To explore the concentration levels of I_2 from direct biogenic emissions, several samples were taken by denuder during low tide in the central zone of algae beds (Mweenish Bay-I). The distance between Mweenish Bay-I and Mweenish Bay-II is about 100–150 m.

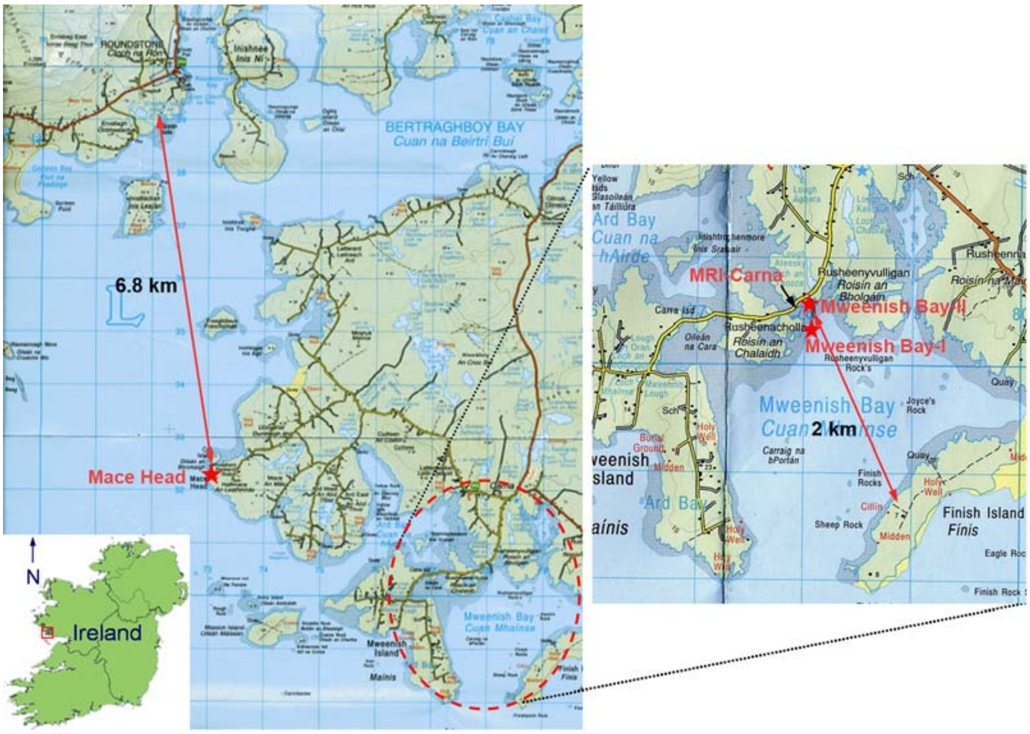

Fig. 1. The denuder sampling sites (★) and the light paths of the LP-DOAS measurements at Mace Head and Mweenish Bay, Ireland.

3 Results and Discussion

3.1 Iodine emissions from macroalgae

Although laboratory-based studies have observed the direct emissions of I_2 from macroalgae (e.g., *Laminaria*) (Sellegri et al., 2005; Küpper et al., 2008; Dixneuf et al., 2009), the levels of I_2 emissions under atmospheric conditions have not been clarified so far. To address this question we used diffusion denuders which can provide “single-point” in situ measurements of I_2 to collect samples at the central zone of algae beds (Mweenish Bay-I) during low tide. Since I_2 is rapidly photolyzed to iodine atoms during daytime, the denuder tubes were set up exactly above the algae beds with a very short vertical distance of around 5 cm between the seaweed and the denuder inlet to minimize the potential influence of photolysis. Fig. 2(A) shows the results of 5-day measurements within a period of 21 days, at a fixed sampling site. The mixing ratios of I_2 were observed to fluctuate with a range between 110 and 302 ppt. This fluctuation could be attributed to algae themselves and the surrounding atmosphere. In the literature, Küpper et al. (1998) reported that young plantlets of seaweed have larger capacity of iodine uptake than adult plants. Thus, within these 21 days the changes of physiological conditions of algae can lead to the differences of iodine level accumulated in the seaweed and thereby the emission level of I_2 into the air. Certainly, other factors such as solar radiation, temperature, and ozone concentration may also contribute to the observed fluctuation of I_2 emission. A plot of the I_2 mixing ratio observed at Mweenish Bay-I against the measured O_3 (Fig. 2(B)) shows that the emissions of I_2 increase with increasing O_3 mixing ratio. This finding (although the data set is very limited) is in close agreement with the result from a chamber experiment (Palmer et al., 2005) as well as the recently suggested mechanism in which I_2 emissions are supposed to be regulated by the ozone-scavenging reaction of the accumulated iodide on the algae surfaces (Küpper et al., 2008).

Given the short atmospheric lifetime of I_2 and the dilution effect during air transport (Saiz-Lopez et al., 2004; Saiz-Lopez et al., 2006b; Palmer et al., 2005), I_2 mixing ratio downwind of the seaweed beds could be lower. As expected, the mixing ratios of I_2 observed at Mweenish Bay-II (i.e., further far away from the seaweed beds) decreased significantly compared to the enhanced levels observed at Mweenish Bay-I (Fig. 2(A)). These comparison results were associated with northwesterly/southwesterly winds which passed over the algae beds with low speeds (<7.7 m s^{-1}). When the wind came from northeasterly (land) direction the levels of I_2 measured at Mweenish Bay-II decreased further to around 5 ppt, which indicates further that local algae is really an unambiguous emission source of I_2 under the ambient conditions in the coastal area.

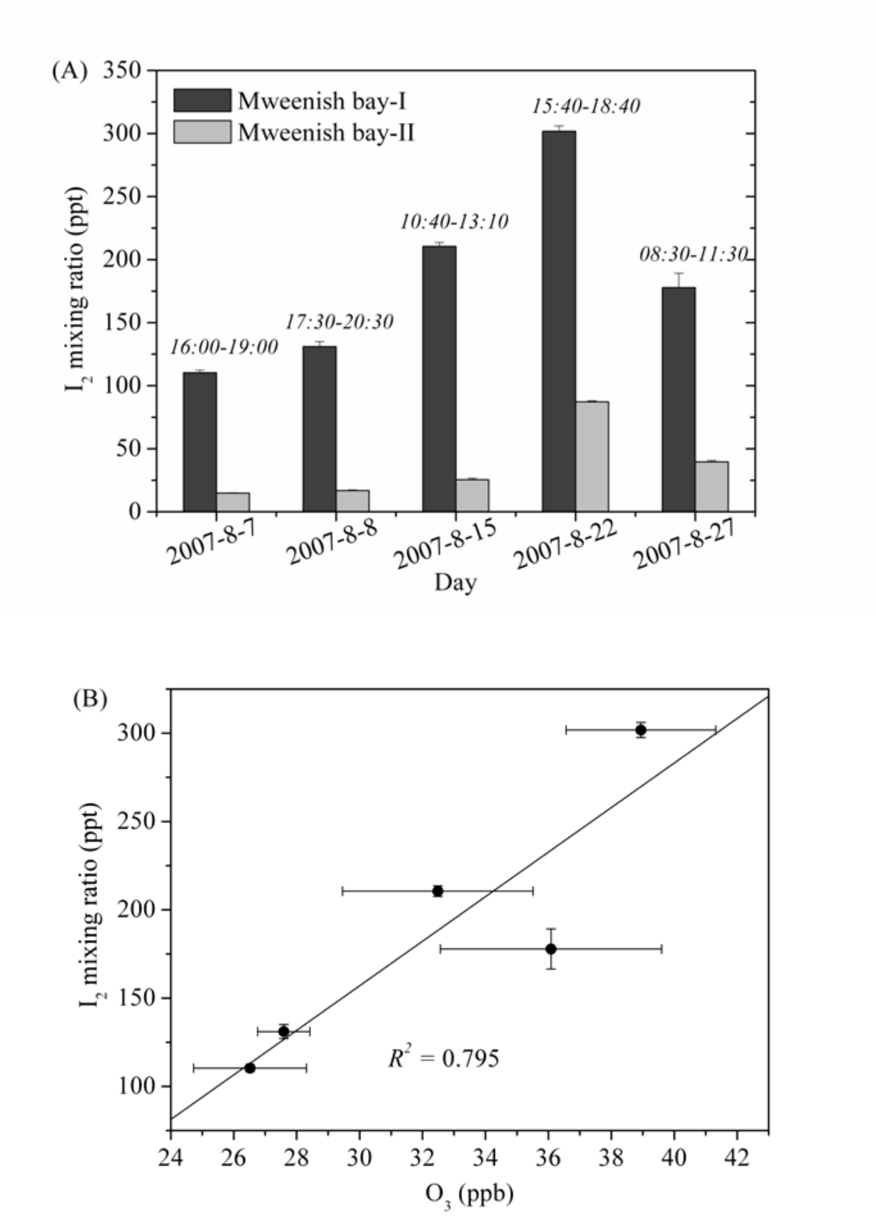

Fig. 2. Comparison of the mixing ratio of I_2 between Mweenish Bay-I and Mweenish Bay-II **(A)**, and the correlation between the emission of I_2 and the concentration of O_3 in the surrounding air at Mweenish Bay-I **(B)**.

Over the course of this study the concentration levels of I_2 observed at Mace Head were significantly lower than that at Mweenish Bay-II. The maximum mixing ratios for daytime and nighttime measurements at Mace Head were 29 ppt and 141 ppt, respectively, and the values at Mweenish Bay-II were 87 ppt and 193 ppt, respectively. The discrepancies of I_2 levels between Mace Head and Mweenish Bay could be attributed to the higher biomass density at Mweenish Bay than at Mace Head and the difference on algae species composition present at these two locations (Irish Seaweed Centre, 2001). It suggests that Mweenish Bay is a "hot spot" of iodine atmospheric chemistry.

Since algae is an important source of ambient I_2 and the biomass of algae exposed to air is related to the tidal height, the tidal effects on I_2 emissions were investigated during daytime and nighttime throughout the campaign at Mweenish Bay-II. A plot of I_2 mixing ratio as a function of tide height exhibits a clear anticorrelation (Fig. 3), which is in agreement with the recent observations at Mace Head (Bale et al., 2008; Saiz-Lopez et al., 2006a). It is apparent that the levels of I_2 are higher at low tide during nighttime due to its accumulation in the absence of solar photolysis. Nevertheless, we also observed that I_2 mixing ratios at Mweenish Bay-II were maintained at levels of around 15–18 ppt when strong westerly winds occurred (>10.8 m s^{-1}, from sea direction). The locally emitted I_2 certainly will dilute in an evolving air plume during air mass transport. However, this interesting episode occurred irrespective of the state of tide as well as day or night. Given that a certain amount of macroalgae at the nearby rocky upper littoral zone was still exposed to the atmosphere whenever the high tide occurred, these values (15–18 ppt) could represent the background level of I_2 at the coastline.

The concentrations of reactive organic iodine species measured at Mace Head by an online GC–MS technique are compared to I_2 observed by the denuder/GC–MS method in Fig. 4. Clearly, the concentration of I_2 is much higher than that of the iodocarbons for both daytime and nighttime measurements. Therefore, it is clear that I_2 is the predominant iodine precursor at Mace Head. However, like the emissions of I_2, the biogenic emissions of iodocarbons are also algae species dependent, and high concentration levels of iodocarbons have been reported at Brittany, a French Atlantic Coast (Peters et al., 2005). Therefore, it is difficult to tell whether I_2 is the predominant source of iodine in coastal areas other than Mace Head.

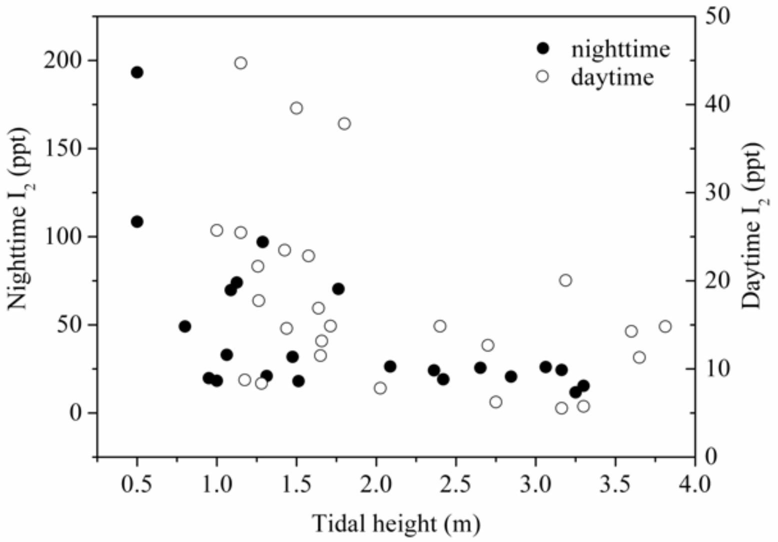

Fig. 3. The mixing ratio of I_2 as a function of tidal height at the sampling site Mweenish Bay-II. Note that I_2 was measured by denuder/GC-MS.

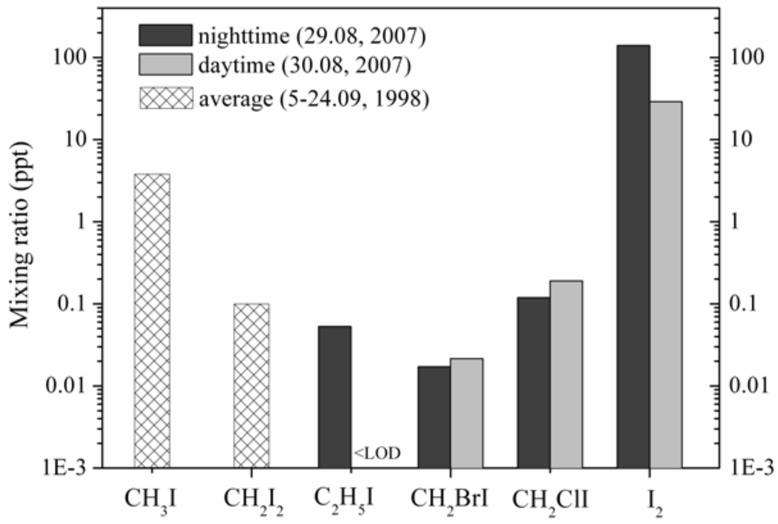

Fig. 4. Typical mixing ratios of reactive organic iodine species and I_2 at Mace Head. The average CH_3I and CH_2I_2 mixing ratios during the 1998 PARFORCE campaign at Mace Head (also given in Carpenter, et al., 2003) are included since these two species were not measured during the campaign in 2007. The limits of detection (LODs) for CH_3I, C_2H_5I, CH_2BrI and CH_2ICl are 0.2, 0.1, 0.02 and 0.04 ppt, respectively. The bar is missing if the mixing ratio is below the LOD. Note the logarithmic scale.

3.2 Implications for O_3, IO, OIO and NO_x

IO mixing ratios were measured by LP-DOAS at both Mweenish Bay and Mace Head during the campaign. The average and maximum values of daytime IO were 3.4 ± 1.0 and 9.5 ± 0.8 ppt for consecutive 30-day measurements at Mweenish Bay, and 1.1 ± 0.3 and 4.4 ± 0.6 ppt for consecutive 9-day measurements at Mace Head, respectively. Note that the maximum mixing ratios were observed around noon. A plot of three sets of data measured at Mweenish Bay indicates that daytime IO concentration levels increase with the increase of I_2 concentrations and of the solar irradiation, as shown in Fig. 5. A similar trend was also observed at Mace Head by Commane et al. (2008) during this campaign. These provide good evidence for the photochemical production of IO from coastal emissions of I_2. Fig. 5 also shows that I_2 concentrations increase with enhanced solar irradiation. Since enhanced biological activity and biogenic emissions of iodine species have been suggested to correlate with solar irradiation together with warmer temperature (Carpenter et al., 1999), I_2 emissions can be expected to be more elevated when low tide periods coincide with maximum solar irradiation exposure.

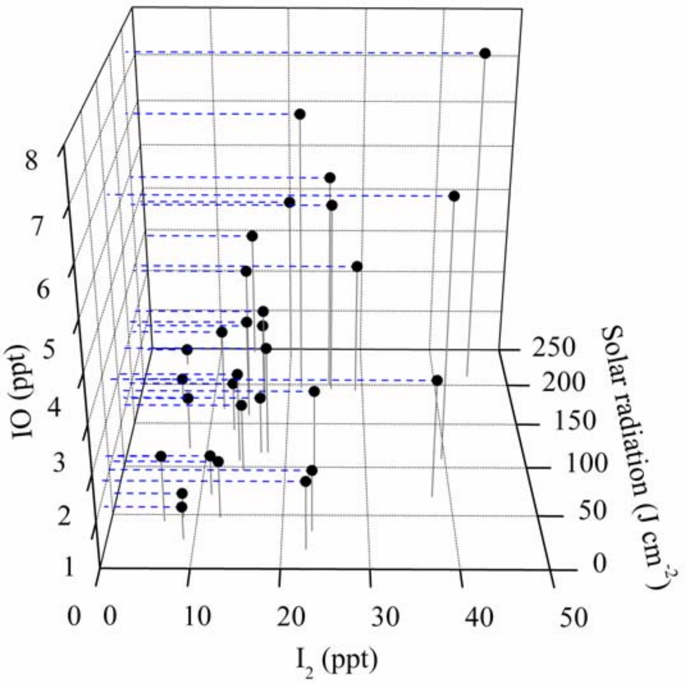

Fig. 5. The observed daytime IO as a function of the solar radiation and the concentration of I_2. Measurements were taken at Mweenish Bay. IO and I_2 were measured by LP-DOAS and denuder/GC-MS, respectively.

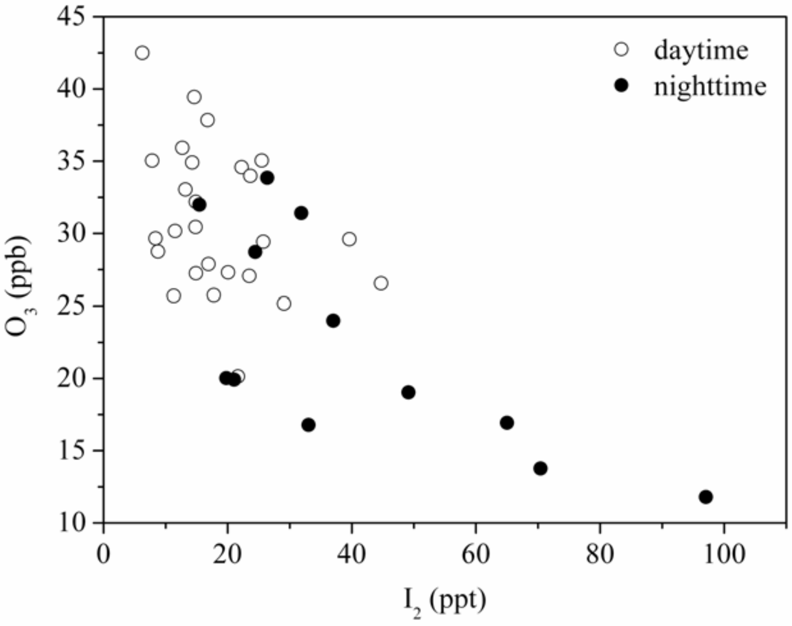

Fig. 6. Plot of O_3 versus I_2 during ozone destruction events at Mweenish Bay. Note that O_3 was measured by LP-DOAS, and I_2 by denuder/GC-MS.

Recent models predict that bromine- and iodine-induced ozone destruction can also occur in the troposphere (Vogt et al., 1999; von Glasow et al., 2004). Most recently, extensive halogen-mediated ozone destruction over the tropical Atlantic Ocean has been suggested (Read et al., 2008). However, reduction in the tropospheric ozone burden through iodine emitted from coastal marine sources has not been verified by observations so far. During the 5-week field observations at Mweenish Bay the mixing ratios of ozone decreased in several days from the normal levels of ~40 ppt down to as low as 12 ppt. Since the measurements by denuders did not cover all these ozone destruction events observed by LP-DOAS and the time resolution of the two techniques was different, we use the mean O_3 concentrations observed at the timescales of I_2 measurements to investigate the correlations between these two ambient constituents. The results show that O_3 concentration decreases in general with the increase of I_2 concentration for daytime observations (Fig. 6), which is consistent with the observations shown in Fig. 5 and strongly supports the viewpoint that photochemical production of daytime IO is related to concentration levels of O_3. For nighttime observations, a clear anti-correlation of O_3 with I_2 was observed, as shown in Fig. 6. Surprisingly, the O_3 concentrations dropped significantly to around 15 ppb when a high level of I_2 mixing ratio was observed around midnight. Here, it should be noted that the correlation between O_3 and

I_2 shown in Fig. 6 is opposite to that shown in Fig. 2(B). This can be attributed to the difference on the observation condition. The positive correlation presented in Fig 2(B) was measured exactly above the algae beds, therefore, can be the consequence of the ozone-scavenging reaction of iodide on the algae surfaces at low tide (i.e., $I^- + O_3 \rightarrow I_2$) (Küpper et al., 2008). However, the negative correlation presented in Fig 6 was measured in the intertidal zone about 150 m from the algae beds. In this case, the emitted I_2 will mix up and react with other atmospheric constituents, leading to the O_3 destruction.

The nighttime iodine chemistry is still not quite clear. The gas-phase reaction of I_2 with O_3 is too slow (Vikis and Macfarlane, 1985) to lead to significant O_3 destruction. A suggested reaction (Chambers et al., 1992; Saiz-Lopez et al., 2006a) for the formation of atomic iodine (R1) at night is

$$I_2 + NO_3 \rightarrow I + IONO_2 \qquad \text{(R1)}$$

Based on quantum chemical calculations this reaction has recently been proposed to be the major source of iodine oxides at night (Kaltsoyannis and Plane, 2008). The resulting atomic iodine will then react rapidly with O_3 to form IO (R2). The IO produced can react with NO_3 (R3) with a rate coefficient of 9×10^{-12} cm^3 $molecule^{-1}$ s^{-1} (Dillon et al., 2008), which will lead to additional NO_3 consumption and will compete with IO + IO for nighttime OIO formation.

$$I + O_3 \rightarrow IO + O_2 \qquad \text{(R2)}$$

$$IO + NO_3 \rightarrow OIO + NO_2 \qquad \text{(R3)}$$

Our observations during nighttime at Mweenish Bay show that, with the increase of I_2 concentrations, the NO_3 concentrations decrease (Fig. 7). The results indicate the importance of nitrate radicals on the nighttime iodine chemistry in the coastal marine boundary layer (MBL). However, it should be noted that the lower O_3 levels at higher I_2 levels would also indicate a lower source of NO_3 given the production pathway of NO_3 (R4).

$$NO_2 + O_3 \rightarrow NO_3 + O_2 \qquad \text{(R4)}$$

It also should be noted that the observed O_3 loss rate for both daytime and nighttime measurements (Fig. 6) is much higher than the value predicted by model simulations by

Saiz-Lopez et al. (2006a; 2006b). A possible explanation could be that other halogen compounds which have the similar diurnal pattern as I_2 also contribute to the O_3 loss. Indeed, the activated iodine compounds, ICl and HOI, showed a strong correlation with I_2 (Huang and Hoffmann, 2009).

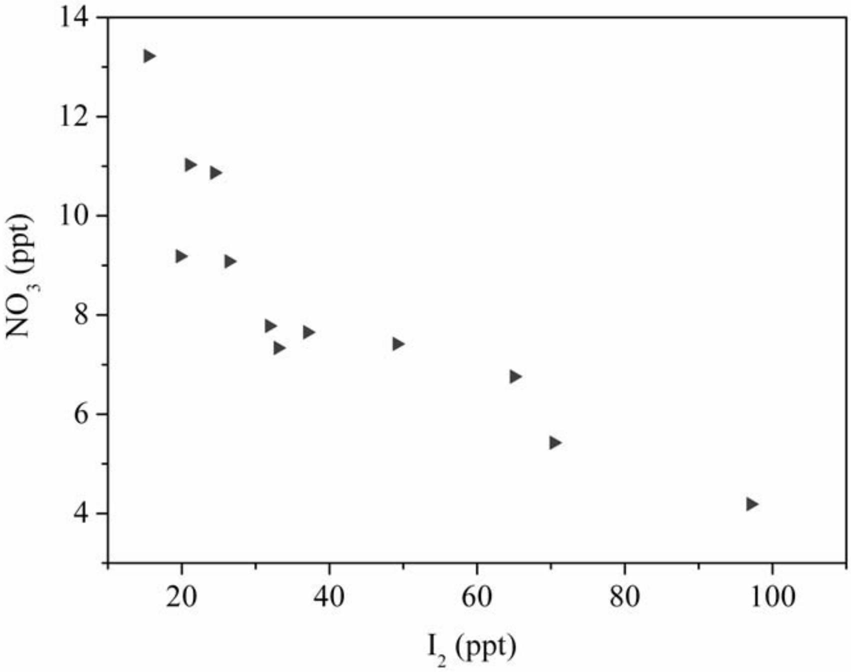

Fig. 7. NO_3 as a function of I_2 at night at Mweenish Bay. Note that NO_3 were measured by LP-DOAS, and I_2 was measured by denuder/GC-MS.

During the campaign OIO was also measured at Mweenish Bay and Mace Head. Unambiguous identification of the absorption structure of OIO was not realized although it was observed several times above the detection limit (average, 12.5 ppt at Mweenish Bay and 3.3 ppt at Mace Head, respectively). The measurement of OIO in the spectral region of 500–600 nm has some principal problems (Peters et al., 2005), leading to high residual structures and therefore high errors and high limit of detection. To date the only unambiguous daytime OIO measurements is made in the Gulf of Maine (Stutz et al., 2007). At Mace Head (Peters et al., 2005; Saiz-Lopez et al., 2006a), Cape Grim (Allan et al., 2001), and Roscoff (Mahajan et al., 2009), OIO has been observed during the nighttime but never in the daytime.

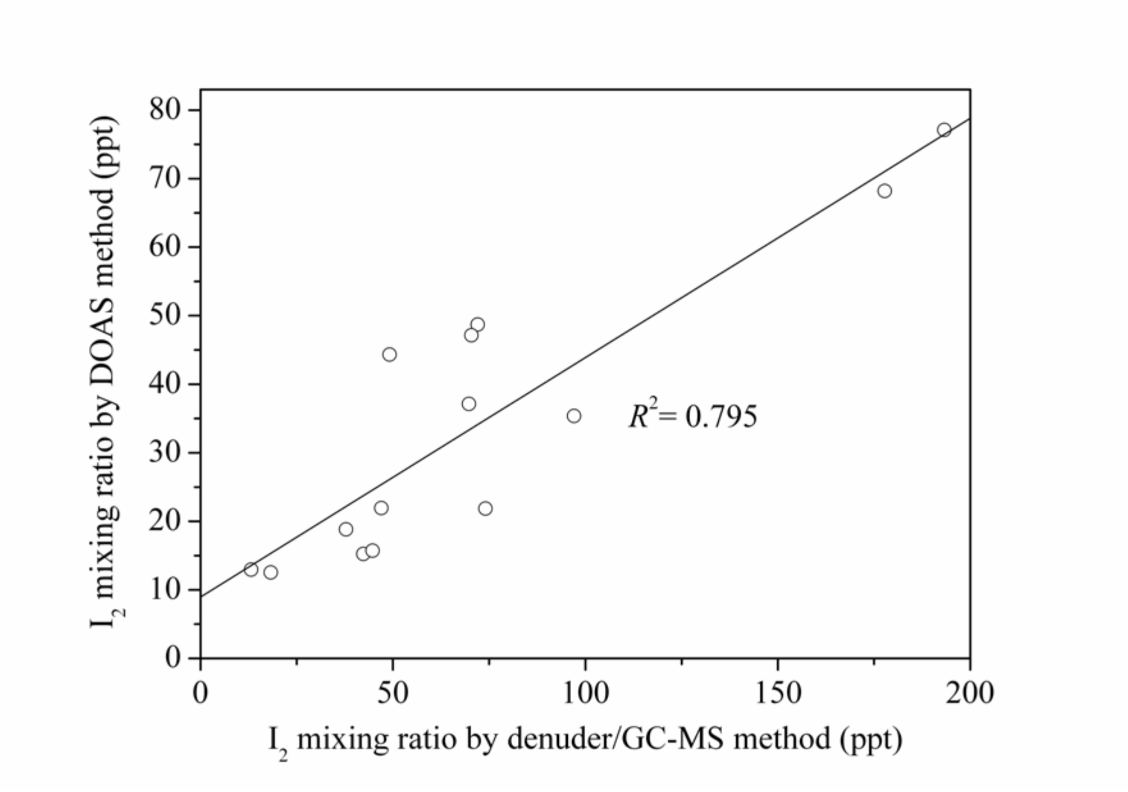

Fig. 8. Comparison measurements of I_2 between denuder/GC–MS and LP-DOAS.

3.3 Data evaluation

Gas-phase reactive inorganic iodine species (I_2, IO, and OIO) have been observed at Mace Head previously (Table 1). A maximum mixing ratio of I_2 of 93 ppt at night and 25 ppt during the day was observed by LP-DOAS during the NAMBLEX campaign (Saiz-Lopez and Plane, 2004). Exemplary in situ measurements of daytime I_2 were also performed at Mace Head using BBCRDS (Bitter et al., 2005) and at a nearby location (Mweenish bridge) using denuder tubes in combination with ICP–MS analysis (Saiz-Lopez et al., 2006b), which reported much higher mixing ratios of daytime I_2 compared to the LP-DOAS measurements (see Table 1). A more comprehensive comparison between "single-point" in situ and LP-DOAS measurements was carried out at both Mace Head and Mweenish Bay during the campaign. Note that average values of LP-DOAS measurements within the same sampling period of denuder measurements at Mweenish Bay-II and Mace Head were used for comparison because of the different time resolution of the two techniques. As shown in Fig. 8, the denuder method recorded much higher concentrations of I_2 than the LP-DOAS method, for both daytime and nighttime measurements. This can be attributed to the facts that denuder method provides "single-point" in situ measurements in the intertidal zone; however, LP-DOAS technique provides distance-average mixing ratios of a rather inhomogeneous distribution along the light-path (i.e., 4–14 km). As described above, the local algae sources dominate the inorganic iodine chemistry at Mace Head and Mweenish Bay. However, under the conditions of Mace Head and Mweenish Bay, the seaweeds extend only over a short distance of the DOAS light-path and most of the light-path extended over the open sea. In addition, a vertical I_2 concentration gradient caused by its rapid photolysis during daytime and by diffusion at night is expected. The vertical distance between the denuder inlets and the sea level is shorter than that between the DOAS light-path and sea level. Thus, the inhomogeneous spatial distribution of I_2 can be responsible for the observed discrepancies of I_2 mixing ratios.

The maximum mixing ratios of daytime IO measured by LP-DOAS at Mace Head are consistent with previous observations. However, the levels of this iodine species observed at Mweenish Bay are significantly higher than that at Mace Head. These results suggest that Mweenish Bay is a biological “hot spot” of iodine atmospheric chemistry. It should be noted that the time resolution of both LP-DOAS measurement and denuder sampling is greater than tens of minutes. This does not allow measurements at the timescales at which the iodine species (I_2, IO, and OIO) are produced. Therefore, it can be expected that the actual peak values of these three iodine species could be higher than those reported here. This is supported by comparison results of IO measurements by LP-DOAS and laser-induced fluorescence (LIF) spectroscopy at Mace Head (Commane et al., 2008). Since the LIF technique provides “point” in situ measurements with higher time resolution (10 s–5 min), the maximum mixing ratios of IO observed by LIF are significantly higher than that measured by LP-DOAS, with a maximum value of 34 ppt reported. Considering the limit of detection of the denuder/GC–MS method (0.17 ppt for a sampling duration of 30 min at 500 mL min^{-1}) as well as the concentration levels at the West Coast of Ireland, we suggest a shorter sampling time for example 10–30 min for further field measurements in algae-rich coastal areas. This would help to obtain a better time resolution and to get a more detailed study of the diurnal variation of ambient I_2 and a better understanding of the release mechanism and atmospheric impact of I_2.

Table 1. Observations of reactive inorganic iodine species (I_2, IO, and OIO) at Mace Head and Mweenish Bay, Ireland, by different techniques

Species	Location, year	Technique	Spatiality	Max. conc. (ppt)		Reference
				Daytime	Nighttime	
I_2	Mace Head, 1998	LP-DOAS	14.4 km	–	61.3 ± 12	Peters et al. (2005)
	Mace Head, 2002	LP-DOAS	8.4 km	25	93 ± 3	Saiz-Lopez and Plane (2004)
	Mace Head, 2002	BBCRDS	“point” in situ	94 ± 20	–	Bitter et al. (2005)
	Mweenish bridge, 2003	Denuder/ICP–MS	“point” in situ	115	–	Saiz-Lopez et al. (2006b)
	Mace Head, 2007	Denuder/GC–MS	“point” in situ	29.1 ± 1.0	140.7 ± 5.6	this work
	Mace Head, 2007	LP-DOAS	13.6 km	–	94.4	this work
	Mweenish Bay-I, 2007	Denuder/GC–MS	“point” in situ	301.8 ± 4.3	–	this work
	Mweenish Bay-II, 2007	Denuder/GC–MS	“point” in situ	87.2 ± 1.8	193.3 ± 9.3	this work
	Mweenish Bay, 2007	LP-DOAS	4.0 km	–	–	this work
IO	Mace Head, 1997	LP-DOAS	14.4 km	6.7 ± 0.5	–	Alicke et al. (1999)
	Mace Head, 1998	LP-DOAS	14.4 km	7.2 ± 0.3	–	Hebestreit (2001)
	Mace Head, 2002	LP-DOAS	8.4 km	7.0 ± 0.5	3	Saiz-Lopez and Plane (2004)
	Mace Head, 2007	LIF	“point” in situ	33.8 ± 3.3	–	Commane et al. (2008)
	Mace Head, 2007	LP-DOAS	13.6 km	4.4 ± 0.6	–	this work
	Mweenish Bay, 2007	LP-DOAS	4.0 km	9.5 ± 0.8	–	this work
OIO	Mace Head, 1998	LP-DOAS	14.4 km	–	9.2 ± 3.3	Peters et al. (2005)
	Mace Head, 2002	LP-DOAS	8.4 km	< 4	10.8	Saiz-Lopez et al. (2006a)
	Mace Head, 2002	BBCRDS	“point” in situ	–	13 ± 4	Bitter et al. (2005)
	Mace Head, 2007	LP-DOAS	13.6 km	–	–	this work
	Mweenish Bay	LP-DOAS	4.0 km	–	–	this work

4 Conclusions

A diffusion denuder in combination with a GC–MS method has been used for “single-point” in situ measurements of I_2 at the West Coast of Ireland. The observations show that the emissions of I_2 from macroalgae are correlated with the surrounding O_3 concentration levels. Comparison of I_2 measurements was carried out at Mace Head and Mweenish Bay, and the results indicate that the mixing ratios of I_2 are correlated with species and biomass of local algae and that Mweenish Bay is a biological "hot spot" of iodine atmospheric chemistry. An anticorrelation between I_2 concentration levels and tidal height was observed for both daytime and nighttime measurements. In addition, the mixing ratios of I_2 were also measured by LP-DOAS and compared to the denuder/GC–MS measurements. The results show that local coastal emissions are the main source of ambient I_2 and that the denuder/GC–MS method can be used to better identify the potential source of I_2.

The levels of I_2 and the intensity of solar irradiation affect significantly the mixing ratios of daytime IO and O_3. However, during nighttime the involvement of NOx in the reaction cycles of I_2 are found to be responsible for the enhanced O_3 destruction. Certainly, more laboratory-based studies and field measurements are required to clarify the importance of the nighttime atmospheric chemistry of iodine.

Acknowledgements. This work was supported by the European Union under the FP6 project (Contract No. 018332): Marine Aerosol Production (MAP), the German Research Foundation (Deutsche Forschungsgemeinschaft, DFG) within the graduate program 826 "Trace Analysis of Elemental Species: Development of Methods and Applications", the European Science Foundation INTROP exchange scheme and the European Community EUSAAR Infrastructure fund, as well as NERC grant NE/D006538/1. The authors are grateful to Colin O'Dowd (NUI, Galway) for leading the field campaign and to the Martin Ryan Institute, especially Richard Fitzgerald, for the support during the field measurements. KEH acknowledges NERC for award of a studentship.

References

Alicke, B., Hebestreit, K., Stutz, J., and Platt, U.: Iodine oxide in the marine boundary layer, Nature, 397, 572–573, 1999.

Allan, B. J., Plane, J. M. C., McFiggans, G.: Observations of OIO in the remote marine boundary layer, Geophys. Res. Lett. 28, 1945–1948, 2001.

Axelson, H., Galle, B., Gustavson, K., Ragnarsson, P., and Rudin, M.: A transmitting/receiving telescope for DOAS-measurements using retroreflektor technique., Techn. Dig. Ser., 4, 641–644, 1990.

Bale, C. S. E., Ingham, T., Commane, R., Head, D. E., and Bloss, W. J.: Novel measurements of atmospheric iodine species by resonance fluorescence, J. Atmos. Chem., 60, 51–70, 2008.

Bitter, M., Ball, S. M., Povey, I. M., and Jones, R. L.: A broadband cavity ringdown spectrometer for in-situ measurements of atmospheric trace gases, Atmos. Chem. Phys., 5, 2547–2560, 2005, www.atmos-chem-phys.org/acp/5/2547/.

Bloss, W. J., Rowley, D. M., Cox, R. A., and Jones, R. L.: Kinetics and products of the IO self-reaction, J. Phys. Chem. A, 105, 7840–7854, 2001.

Carpenter, L. J.: Iodine in the marine boundary layer, Chem. Rev., 103, 4953–4962, 2003.

Carpenter, L. J., Hebestreit, K., Platt, U., and Liss, P. S.: Coastal zone production of IO precursors: a 2-dimensional study, Atmos. Chem. Phys., 1, 9–18, 2001, www.atmos-chem-phys.org/acp/1/9/.

Carpenter, L. J., Liss, P. S., and Penkett, S. A.: Marine organohalogens in the atmosphere over the Atlantic and Southern Oceans, J. Geophys. Res., 108(D9), 4256, doi: 10.1029/2002JD002769, 2003.

Carpenter, L. J., Sturges, W. T., Penkett, S. A., Liss, P. S., Alicke, B., Hebestreit, K., and Platt, U.: Short-lived alkyl iodides and bromides at Mace Head, Ireland: Links to biogenic sources and halogen oxide production, J. Geophys. Res.-Atmos, 104, 1679–1689, 1999.

Chambers, R. M., Heard, A. C., and Wayne, R. P.: Inorganic gas-phase reactions of the nitrate radical: I_2+NO_3 and I+NO_3, J. Phys. Chem., 96, 3321–3331, 1992.

Commane, R., Bale, C. S. E., Furneaux, K. L., Ingham, T., Whalley, L. K., Heard, D. E., and Bloss, W. J.: Iodine monoxide in the marine boundary layer, EGU General Assembly, Vienna, Austria, 13–18 April 2008, EGU2008-A-04243, 2008.

Dixneuf, S., Ruth, A. A., Vaughan, S., Varma, R. M., and Orphal, J.: The time dependence of molecular iodine emission from *Laminaria digitata*, Atmos. Chem. Phys., 9, 823–829, 2009, www.atmos-chem-phys.net/9/823/2009/.

Dillon, T. J., Tucceri, M. E., Sander, R., Crowley, J. N.: LIF studies of iodine oxide chemistry, Part 3. Reactions $IO + NO_3 \rightarrow OIO + NO_2$, $I + NO_3 \rightarrow IO + NO_2$, and $CH_2I + O_2 \rightarrow$ (products): implications for the chemistry of the marine atmosphere at night, Phys. Chem. Chem. Phys., 10, 1540–1554, 2008.

von Glasow, R., and Crutzen, P. J.: Tropospheric halogen chemistry, in: Treatise on Geochemistry Update 1, edited by: Holland, H. D., Turekian, K. K., Eleviser, Amsterdam, The Netherlands, Vol. 4.02, pp 1–67, 2007.

von Glasow, R., von Kuhlmann, R., Lawrence, M. G., Platt, U., and Crutzen, P. J.: Impact of reactive bromine chemistry in the troposphere, Atmos. Chem. Phys., 4, 2481–2497, 2004, www.atmos-chem-phys.org/acpd/4/4877/.

Greenblatt, G. D., Orlando, J. J., Burkholder, J. B., and Ravishankara, A. R.: Absorption-measurements of oxygen between 330 nm and 1140 nm, J. Geophys. Res.-Atmos., 95, 18577–18582, 1990.

Hebestreit, K.: Halogen oxides in the mid-latitudinal planetary boundary layer, Institute for Umweltphysik, University of Heidelberg, PhD thesis, 2001.

Hoffmann, T., O'Dowd, C. D., and Seinfeld, J. H.: Iodine oxide homogeneous nucleation: An explanation for coastal new particle production, Geophys. Res. Lett., 28, 1949–1952, 2001.

Hornsby, K. Flynn, M., Dorsey, J., Gallagher, M., Chance, R., Jones, C., and Carpenter, L.: A relaxed accumulation (REA)-GC/MS system for the determination of halocarbon fluxes, Atmos. Meas. Tech. Discuss., 2, 951–980, 2009.

Huang, R.-J., and Hoffmann, T.: Development of a coupled diffusion denuder system combined with gas chromatography/mass spectrometry for the separation and quantification of molecular iodine and the activated iodine compounds iodine monochloride and hypoiodous acid in the marine atmosphere, Anal. Chem., 81, 1777–1783, 2009.

Irish Seaweed Centre: Connemara seaweed survey, an assessment of the commercially valuable seaweed species of connemara, National University of Ireland, Galway, pp. 1– 44, 2001.

Kaltsoyannis, N., and Plane, J. M. C.: Quantum chemical calculations on a selection of iodine-containing species (IO, OIO, INO_3, $(IO)_2$, I_2O_3, I_2O_4 and I_2O_5) of importance in the atmosphere, Phys. Chem. Chem. Phys., 10, 1723–1733, 2008.

Kraus, S.: DOASIS–a framework design for DOAS, Combined Faculties for Mathematics and for Computer Science, University of Mannheim, PhD thesis, 2005.

Küpper, F. C., Carpenter, L. J., McFiggans, G. B., Palmer, C. J., Waite, T. J., Boneberg, E. M., Woitsch, S., Weiller, M., Abela, R., Grolimund, D., Potin, P., Butler, A., Luther, G. W., Kroneck, P. M. H., Meyer-Klaucke, W., and Feiters, M. C.: Iodide accumulation provides kelp with an inorganic antioxidant impacting atmospheric chemistry, Proc. Natl. Acad. Sci. U.S.A., 105, 6954–6958, 2008.

Küpper, F. C., Schweigert, N., Ar Gall, E., Legendre, J. M., Vilter, H., and Kloareg, B.: Iodine uptake in Laminariales involves extracellular, haloperoxidase-mediated oxidation of iodide, Planta, 207, 163–171, 1998.

Mahajan, A. S., Oetjen, H., Saiz-Lopez, A., Lee, J. D., McFiggans, G. B., Plane, J. M. C.: Reactive iodine species in a semi-polluted environment, Geophys. Res. Lett., 36, L16803, dio:10.1029/2009GL038018, 2009.

McFiggans, G., Coe, H., Burgess, R., Allan, J., Cubison, M., Alfarra, M. R., Saunders, R., Saiz-Lopez, A., Plane, J. M. C., Wevill, D. J., Carpenter, L. J., Rickard, A. R., and Monks, P. S.: Direct evidence for coastal iodine particles from Laminaria macroalgae–linkage to emissions of molecular iodine, Atmos. Chem. Phys., 4, 701–713, 2004, www.atmos-chem-phys.org/acp/4/701/.

Meller, R., and Moortgat, G. .K.: Temperature dependence of the absorbtion cross section of formaldehyde between 223 and 323 K in the wavelength range 225–375 nm, J. Geophys. Res.,105, 7089–7101, 2000.

O'Dowd, C. D., and Hoffmann, T.: Coastal new particle formation: a review of the current state-of-the-art, Environ. Chem., 2, 245–255, 2005.

O'Dowd, C. D., Jimenez, J. L., Bahreini, R., Flagan, R. C., Seinfeld, J. H., Hämeri, K., Pirjola, L., Kulmala, M., Jennings, S. G., and Hoffmann, T.: Marine aerosol formation from biogenic iodine emissions, Nature, 417, 632–636, 2002.

Palmer, C. J., Anders, T. L., Carpenter, L. J., Küpper, F. C., and McFiggans, G. B.: Iodine and halocarbon response of Laminaria digitata to oxidative stress and links to atmospheric new particle production, Environ. Chem., 2, 282–290, 2005.

Peters, C., Pechtl, S., Stutz, J., Hebestreit, K., Hönninger, G., Heumann, K. G., Schwarz, A., Winterlik, J., and Platt, U.: Reactive and organic halogen species in three different European coastal environments, Atmos. Chem. Phys., 5, 3357–3375, 2005, www.atmos-chem-phys.org/acp/5/3357/.

Pirjola, L., O'Dowd, C. D., Yoon, Y. J., and Sellegri, K.: Modelling iodine particle formation and growth from seaweed in a chamber, Enivron. Chem., 2, 271–281, 2005.

Platt, U., and Stutz, J. (Eds.): Differential optical absorption spectroscopy: Principles and applications, in: Physics of earth and space environments, Springer-Verlag Berlin Heidelberg, 2008.

Read, K. A., Mahajan, A. S., Carpenter, L. J., Evans, M. J., Faria, B. V. E., Heard, D. E., Hopkins, J. R., Lee, J. D., Moller, S. J., Lewis, A. C., Mendes, L., McQuaid, J. B., Oetjen, H., Saiz-Lopez, A., Pilling, M. J., and Plane, J. M. C.: Extensive halogen-mediated ozone destruction over the tropical Atlantic Ocean, Nature, 453, 1232–1235, 2008.

Rothman, L. S., Jacquemart, D., Barbe, A., Benner, D. C., Birk, M., Brown, L. R., Carleer, M. R., Chackerian, C. J., Chance, K., Coudert, L. H., Dana, V., Devi, V. M., Flaud, J. M., Gamache, R. R., Goldman, A., Hartmann, J. M., Jucks, K. W., Maki, A. G., Mandin, J. Y., Massie, S. T., Orphal, J., Perrin, A., Rinsland, C. P., Smith, M. A. H., Tennyson, J., Tolchenov, R. N., Toth, R. A., Auwera, J. V., Varanasi, P., and Wagner, G.: The HITRAN 2004 molecular spectroscopic database, J. Quant. Spectrosc. Ra., 96, 139–204, 2005.

Saiz-Lopez, A., Mahajan, A. S., Salmon, R. A., Bauguitte, S. J.-B., Jones, A. E., Roscoe, H. K., and Plane, J. M. C.: Boundary layer halogens in coastal antarctica, Science, 317, 348–351, 2007.

Saiz-Lopez, A., and Plane, J. M. C.: Novel iodine chemistry in the marine boundary layer, Geophys. Res. Lett., 31, L04112, doi:10.1029/2003GL019215, 2004.

Saiz-Lopez, A., Plane, J. M. C., McFiggans, G., Williams, P. I., Ball, S., M., Bitter, M., Jones,

R. L., Hongwei, C., and Hoffmann, T.: Modelling molecular iodine emission in a coastal marine environment: the link to new particle formation, Atmos. Chem. Phys., 6, 883–895, 2006b, www.atmos-chem-phys.net/6/883/2006/.

Saiz-Lopez, A., Saunders, R. W., Joseph, D. W., Ashworth, S. H., and Plane, J. M. C: Absolute absorption cross-section and photolysis rate of I_2, Atmos. Chem. Phys., 4, 1443–1450, 2004, www.atmos-chem-phys.org/acp/4/1443/.

Saiz-Lopez, A., Shillito, J. A., Coe, H., and Plane, J. M. C.: Measurements and modelling of I_2, IO, OIO, BrO and NO_3 in the mid-latitude marine boundary layer, Atmos. Chem. Phys., 6, 1513–1528, 2006a, www.atmos-chem-phys.net/6/1513/2006/.

Sellegri, K., Yoon, Y. J., Jennings, S. G., O'Dowd, C. D., Pirjola, L., Cautenet, S., Chen, H., and Hoffmann, T.: Quantification of coastal new ultra-fine particles formation from in situ and chamber measurements during the BIOFLUX campaign, Environ. Chem. 2, 260–270, 2005.

Spietz, P., Martin, J. C. G., and Burrows, J. P.: Spectroscopic studies of the I_2/O_3 photochemistry: Part 2. Improved spectra of iodine oxides and analysis of the IO absorption spectrum, J. Photoch. Photobio. A, 176, 50–67, 2005.

Stutz, J., Kim, E. S., Platt, U., Bruno, P., Perrino, C., and Febo, A.: UV-visible absorption cross section of nitrous acid, J. Geophys. Res., 105, 14585–14592, 2000.

Stutz, J., Pikelnaya, O., Hurlock, S. C., Trick, S., Pechtl, S., and von Glasow, R.: Daytime OIO in the Gulf of Maine, Geophys. Res. Lett., 34, L22816, dio: 10.1029/2007GL031332, 2007.

Stutz, J., and Platt, U.: Numerical analysis and estimation of the statistical error of differential optical absorption spectroscopy measurements with least-squares methods, Appl. Opt., 35, 6041–6053, 1996.

Vaughan, S., Gherman, T., Ruth, A. A., and Orphal, J.: Incoherent broad-band cavity-enhanced absorption spectroscopy of the marine boundary layer species I_2, IO and OIO, Phys. Chem. Chem. Phys., 10, 4471–4477, 2008.

Vandaele, A. C., Simon, P. C., Guilmot, J. M., Carleer, M., and Colin, R.: SO_2 absorption cross-section measurement in the UV using a fourier-transform spectrometer, J. Geophys. Res.-Atmos., 99, 25599–25605, 1994.

Vikis, A. C., and MacFarlane, R.: Reaction of iodine with ozone in the gas phase, J. Phys. Chem., 89, 812–815, 1985.

Vogt, R., Sander, R., von Glasow, R., and Crutzen, P. J.: Iodine chemistry and its role in halogen activation and ozone loss in the marine boundary layer: A model study, J. Atmos. Chem., 32, 375–395, 1999.

Voigt, S., Orphal, J., Bogumil, K., and Burrows, J. P.: The temperature dependence (203-293 K) of the absorption cross sections of O_3 in the 230-850 nm region measured by Fourier-transform spectroscopy, J. Photoch. Photobio. A, 143, 1–9, 2001.

Voigt, S., Orphal, J., and Burrows, J. P.: The temperature and pressure dependence of the absorption cross-sections of NO_2 in the 250-800 nm region measured by Fourier-transform spectroscopy, J. Photoch. Photobio. A, 149, 1–7, 2002.

Wevill, D. J., and Carpenter, L. J.: Automated measurement and calibration of reactive volatile halogenated organic compounds in the atmosphere, Analyst, 129, 634–638, 2004.

Wilmouth, D. M., Hanisco, T. F., Donahue, N. M., and Anderson, J. G.: Fourier transform untraviolet spectroscopy of the $A\ ^2\Pi_{3/2} \leftarrow X\ ^2\Pi_{3/2}$ transition of BrO, J. Phys. Chem. A, 103, 8935–8945, 1999.

Yokelson, R. J., Burkholder, J. B., Fox, R. W., Talukdar, R. K., and Ravishankara, A. R.: Temperature dependence of the NO_3 absorption spectrum, J. Phys. Chem. 98, 13144–13150, 1994.